

**HIV-1 SUBTYPE B DETERMINANTS OF NEUROPATHOGENESIS: VIRAL  
CHARACTERISTICS ASSOCIATED WITH DEMENTIA**

Gretja Lea Schnell

A dissertation submitted to the faculty of the University of North Carolina at Chapel Hill in partial fulfillment of the requirements for the degree of Doctor of Philosophy in the Department of Microbiology and Immunology (Virology).

Chapel Hill  
2010

Approved By:

Advisor: Ronald Swanstrom, Ph.D.

Reader: Blossom Damania, Ph.D.

Reader: Mark Heise, Ph.D.

Reader: Kevin Robertson, Ph.D.

Reader: Lishan Su, Ph.D.

## **ABSTRACT**

Gretja L. Schnell

### **HIV-1 SUBTYPE B DETERMINANTS OF NEUROPATHOGENESIS: VIRAL CHARACTERISTICS ASSOCIATED WITH DEMENTIA**

(Under the direction of Dr. Ronald Swanstrom)

Human immunodeficiency virus type 1 (HIV-1)-associated dementia (HAD) is a severe neurological disease resulting from HIV-1 infection of cells in the central nervous system (CNS). Significant genetic compartmentalization has been detected between virus in the periphery and virus in the cerebrospinal fluid (CSF)/CNS in subjects with dementia. Although progress has been made over the past thirty years in understanding HIV-1-associated dementia, the mechanisms leading to the development of neurological disease during HIV-1 infection remain unclear. In this dissertation, I examine the neuropathogenesis of HIV-1 over the course of infection by determining the viral characteristics associated with the development of dementia in HIV-1-infected adults. Compartmentalization between the periphery and the CNS has not been previously described for subjects with primary HIV-1 infection. I detected compartmentalized HIV-1 variants in the CSF of a subset of primary infection subjects, and using longitudinal analyses I found that compartmentalization in the CSF can be resolved during primary infection.

Compartmentalized HIV-1 variants in the CNS/CSF of subjects with dementia are thought to replicate in long-lived perivascular macrophages and/or microglia in the CNS. I examined the source of compartmentalized HIV-1 in the CSF of subjects with neurological disease and in neurologically-asymptomatic subjects who were initiating antiretroviral

therapy. In subjects with neurological disease, I found that rapid decay of CSF-compartmentalized variants was associated with high CSF pleocytosis, whereas slow decay measured for CSF-compartmentalized variants in subjects with neurological disease was correlated with low peripheral CD4 cell count and reduced CSF pleocytosis. The longer half-lives I detected suggest that compartmentalized HIV-1 in the CSF of some HAD subjects may be originating from a long-lived cell type in the brain. I also examined the viral genotypes and phenotypes associated with the CSF-compartmentalized variants with differential decay rates. I detected significant compartmentalization in the CSF HIV-1 population for subjects with neurological disease, and the envelope phenotype characterization revealed two distinct classes of viral encephalitis associated with extensive genetic compartmentalization and the clinical diagnosis of dementia. These results will form the basis of future studies to decipher the biology underlying viral evolution and enhanced HIV-1 replication in the CNS.

To my parents, Charlyce and David, thanks for your endless encouragement and support.

To my husband Ryan, thanks for your understanding, patience, and love of adventure.

## ACKNOWLEDGEMENTS

The studies presented in this dissertation were carried out under the supervision of Dr. Ronald Swanstrom. I am extremely grateful for his guidance, critical thinking, and patience during my graduate career. I also want to thank both Dr. Swanstrom and the training grant in sexually transmitted diseases and AIDS for providing the funding for these studies. I have had the opportunity to travel around the world to many conferences during my stint as a graduate student, and I am extremely thankful for those opportunities. I also want to thank all of my committee members: Blossom Damania, Mark Heise, Kevin Robertson, and Lishan Su. They provided scientific guidance and discussions for the work presented in this dissertation. To my collaborators at UCSF, Richard W. Price and Serena Spudich, these studies would not have been possible without your expertise and the clinical samples that you provided. I am extremely thankful for all of your scientific guidance, fruitful discussions, and critical input on manuscripts.

I want to thank Dr. Annelies Vanrie and the UNC office of global health for providing funding for me to participate in the Malawi-Carolina summer public health institute and a clinical research project in Blantyre, Malawi during the summer of 2009. My experiences that summer were both educational and amazing. Finally, to the Swanstrom lab, thanks for the many years of entertainment and help with experiments. I especially want to thank Dr. Jeffrey Anderson for all of his helpful assistance and fun anecdotes, and Elizabeth Pollom for the many laughs shared in our corner of the Swanstrom lab.

## TABLE OF CONTENTS

|   |     |
|---|-----|
| LIST OF TABLES .....  | ix  |
| LIST OF FIGURES .....   | x   |
| LIST OF ABBREVIATIONS.....  | xii |
| CHAPTER   |     |
| I. INTRODUCTION .....   | 1   |
| HIV-1 REPLICATION AND PATHOGENESIS .....  | 2   |
| HIV-1 genome organization and replication strategy.....   | 2   |
| The path to AIDS .....  | 4   |
| HIV-1 NEUROPATHOGENESIS.....  | 5   |
| HIV-1-associated dementia.....  | 5   |
| Patterns of neuropathogenesis for other neurovirulent viruses.....  | 7   |
| HIV-1 BIOLOGY AND NEUROVIRULENCE .....  | 10  |
| Crossing the blood-brain barrier: neuroinvasion by HIV .....  | 10  |
| HIV-1 envelope: cellular attachment and entry in the CNS .....  | 14  |
| Virological and immunological markers of HIV-1<br>neuropathogenesis.....  | 17  |
| HIV-1 COMPARTMENTALIZATION IN THE CNS .....   | 19  |
| Compartmentalization of HIV-1 between the periphery and the<br>central nervous system is associated with dementia ..... | 19  |
| The source of compartmentalized HIV-1 in the CNS.....   | 21  |

|      |   |    |
|------|---|----|
|      | NEUROPATHOLOGICAL DAMAGE IN THE CNS DURING HIV-1 INFECTION .....  | 24 |
|      | Neurotoxic HIV-1 proteins in the CNS .....  | 25 |
|      | Inflammation in the CNS .....   | 25 |
|      | SIGNIFICANCE AND OBJECTIVES.....  | 27 |
| II.  | COMPARTMENTALIZATION AND CLONAL AMPLIFICATION OF HIV-1 VARIANTS IN THE CEREBROSPINAL FLUID DURING PRIMARY INFECTION .....                   | 29 |
|      | Abstract.....   | 30 |
|      | Introduction.....   | 31 |
|      | Materials and Methods.....  | 33 |
|      | Results.....  | 37 |
|      | Discussion.....   | 44 |
|      | Acknowledgements.....   | 49 |
|      | Tables.....   | 50 |
|      | Figures.....  | 53 |
| III. | COMPARTMENTALIZED HUMAN IMMUNODEFICIENCY VIRUS TYPE 1 ORIGINATES FROM LONG-LIVED CELLS IN SOME SUBJECTS WITH HIV-1-ASSOCIATED DEMENTIA..... | 64 |
|      | Abstract.....   | 65 |
|      | Author Summary.....   | 66 |
|      | Introduction.....   | 67 |
|      | Results.....  | 70 |
|      | Discussion.....   | 78 |
|      | Materials and Methods.....  | 85 |
|      | Acknowledgements.....   | 87 |

|  |     |
|--|-----|
| Tables .....   | 88  |
| Figures.....   | 91  |
| IV.   DISTINCT CELLULAR ORIGINS OF COMPARTMENTALIZED HIV-1 IN<br>THE CSF OF SUBJECTS WITH HIV-1-ASSOCIATED DEMENTIA DEFINE<br>TWO CLASSES OF VIRAL ENCEPHALITIS..... | 100 |
| Abstract.....  | 101 |
| Introduction.....  | 102 |
| Materials and Methods.....   | 104 |
| Results.....   | 110 |
| Discussion.....  | 117 |
| Acknowledgements.....  | 124 |
| Tables.....  | 125 |
| Figures.....   | 128 |
| V.    DISCUSSION AND FUTURE DIRECTIONS.....  | 142 |
| APPENDIX: IDENTIFICATION AND RECOVERY OF MINOR HIV-1 VARIANTS<br>USING THE HETERODUPLEX TRACKING ASSAY AND BIOTINYLATED<br>PROBES .....                              | 156 |
| Abstract.....  | 157 |
| Introduction.....  | 158 |
| Materials and Methods.....   | 160 |
| Results.....   | 165 |
| Discussion.....  | 171 |
| Acknowledgements.....  | 174 |
| Figures.....   | 175 |
| REFERENCES .....   | 179 |

## LIST OF TABLES

|           |   |     |
|-----------|---|-----|
| Table 2.1 | Subject population characteristics and inflammatory markers .....     | 50  |
| Table 2.2 | Single genome amplification results.....                              | 52  |
| Table 3.1 | Sample characteristics.....   | 88  |
| Table 3.2 | HIV-1 variant decay.....  | 89  |
| Table 4.1 | Subject characteristics and CSF compartmentalization.....             | 125 |
| Table 4.2 | Cellular tropism characteristics of envelope-pseudotyped viruses..... | 126 |

## LIST OF FIGURES

|            |   |     |
|------------|---|-----|
| Figure 2.1 | Cross-sectional and longitudinal HTA analysis of HIV-1 in the blood plasma and CSF of primary infection subjects..... | 53  |
| Figure 2.2 | Phylogenetic analysis of plasma and CSF HIV-1 populations.....  | 54  |
| Figure 2.3 | Phylogenetic and sequence analyses of plasma and CSF HIV-1 populations at 198 dpi for subject 9018.....               | 56  |
| Figure 2.4 | Phylogenetic and sequence analyses of subject 7146 HIV-1 populations in the plasma and CSF at 156 dpi.....            | 58  |
| Figure 2.5 | Phylogenetic analysis of subject 7146 HIV-1 populations at days 177 and 203 post-infection.....                       | 60  |
| Figure 2.6 | Longitudinal phylogenetic analysis of subject 7146 HIV-1 populations.....   | 62  |
| Figure 3.1 | Longitudinal HTA analysis and HIV-1 decay in the blood plasma and CSF of asymptomatic subjects.....                   | 91  |
| Figure 3.2 | Longitudinal HTA analysis and HIV-1 decay in blood plasma and CSF of neurologically symptomatic subjects.....         | 93  |
| Figure 3.3 | Summary of HIV-1 half-lives from asymptomatic and neurologically symptomatic subjects.....                            | 95  |
| Figure 3.4 | Examination of the V3 region of <i>env</i> using the biotin-V3 HTA.....   | 96  |
| Figure 3.5 | Model of HIV-1 infection in the central nervous system.....   | 98  |
| Figure 4.1 | Phylogenetic analysis of plasma and CSF HIV-1 populations for neurologically asymptomatic subjects.....               | 128 |
| Figure 4.2 | Phylogenetic analysis of plasma and CSF HIV-1 populations for neurologically symptomatic subjects.....                | 130 |
| Figure 4.3 | Longitudinal phylogenetic analysis of subject 7036 HIV-1 populations.....   | 132 |
| Figure 4.4 | Longitudinal phylogenetic analysis of subject 7115 HIV-1 populations.....   | 133 |
| Figure 4.5 | Coreceptor tropism of HIV-1 envelope-pseudotyped reporter viruses.....  | 134 |

|            |  |     |
|------------|--|-----|
| Figure 4.6 | HIV-1 envelopes from the plasma and CSF of all subjects efficiently infect cells with a high CD4 surface expression .....                                      | 136 |
| Figure 4.7 | HIV-1 envelopes from the plasma and CSF of neurologically asymptomatic subjects do not infect cells with a low CD4 surface expression .....                    | 137 |
| Figure 4.8 | HIV-1 envelopes from the plasma and CSF of neurologically symptomatic subjects differ in their ability to infect cells with a low CD4 surface expression ..... | 138 |
| Figure 4.9 | Lysine at position 170 in the HIV-1 envelope is associated with the ability to enter cells with a low CD4 surface expression.....                              | 140 |
| Figure 5.1 | Model of HIV-1 in the CNS during class 1 and class 2 viral encephalitis .....  | 155 |
| Figure A.1 | The biotin-HTA strategy.....   | 175 |
| Figure A.2 | Identification and recovery of minor V3 variants using a biotinylated-V3 HTA .....   | 176 |
| Figure A.3 | Examination of the sensitivity of the biotin-V3 HTA .....  | 177 |
| Figure A.4 | Detection of minor protease inhibitor resistance mutations using a biotinylated-protease HTA.....  | 178 |

## LIST OF ABBREVIATIONS

|            |  |
|------------|--|
| AIDS       | Acquired immune deficiency syndrome                        |
| BBB        | Blood-brain barrier  |
| CD4        | Main cellular receptor used by HIV-1 to enter target cells |
| CCR5       | CC-chemokine receptor 5; coreceptor used by HIV-1          |
| CNS        | Central nervous system                                     |
| CSF        | Cerebrospinal fluid  |
| CXCR4      | CXC-chemokine receptor 4; coreceptor used by HIV-1         |
| DPI        | Days post-infection  |
| <i>env</i> | HIV-1 envelope gene  |
| Env        | HIV-1 envelope protein                                     |
| gp120      | HIV-1 envelope glycoprotein surface subunit                |
| gp41       | HIV-1 envelope glycoprotein transmembrane subunit          |
| HAART      | Highly active antiretroviral therapy                       |
| HAD        | HIV-1-associated dementia                                  |
| HIV-1      | Human immunodeficiency virus type 1                        |
| HIVE       | HIV-1 encephalitis   |
| HTA        | Heteroduplex tracking assay                                |
| PCR        | Polymerase chain reaction                                  |
| PSSM       | Position-specific scoring matrix                           |
| MCMD       | Minor cognitive motor disorder                             |
| SGA        | Single genome amplification                                |
| SIV        | Simian immunodeficiency virus                              |

|           |  |
|-----------|--|
| R5-tropic | HIV-1 envelope which uses the coreceptor CCR5      |
| X4-tropic | HIV-1 envelope which uses the coreceptor CXCR4     |
| V1-V5     | Hyper-variable regions 1-5 of the envelope protein |

## **CHAPTER ONE**

### **INTRODUCTION**

## **HIV-1 REPLICATION AND PATHOGENESIS**

### *HIV-1 genome organization and replication strategy*

Human immunodeficiency virus type 1 (HIV-1) belongs to the *Lentivirus* genus within the family *Retroviridae*. HIV-1 has a single-stranded positive-sense RNA genome, and two copies of the genome are encapsulated per virion. The HIV-1 DNA, the provirus, is approximately 9.7 kilobases in length, and the genome consists of ten genes that are flanked on the 5' and 3' ends by the HIV-1 long terminal repeats (LTRs). The HIV-1 genes encode the structural proteins Gag (a polyprotein precursor that includes the matrix protein, capsid protein, and nucleocapsid) and Env, the non-structural enzymes Pro and Pol (a polyprotein precursor containing the reverse transcriptase and integrase), the accessory proteins (Vif, Vpr, Vpu, and Nef), and the regulatory proteins (Tat, Rev) (88).

In a mature HIV-1 virion, the full-length dimeric RNA genome is associated with the nucleocapsid protein (NC). NC relies on a short packaging signal located near the 5' end of the viral RNA to target the unspliced RNA genome into virions (88, 102). In the mature virion the NC-RNA complex is surrounded by the capsid protein (CA) arranged in a conical structure. Several copies of the protease (PR), integrase (IN), and reverse transcriptase (RT) enzymes are also encapsulated in the virion, with RT and IN activities needed for infection of new cells (106). This core structure is encircled with a spherical layer of the matrix protein (MA) that resides immediately below the viral envelope. The envelope is a lipid bilayer acquired during viral budding from an infected cell, and contains both cellular proteins and a few trimers of the HIV-1 envelope protein (106).

The HIV-1 lifecycle begins with attachment to the main cellular receptor CD4, and the coreceptors CCR5 or CXCR4. The viral envelope protein mediates both receptor attachment and viral membrane fusion with the target cell. The viral core is then internalized into the cytoplasm of the cell where RT converts the genomic RNA to double-stranded DNA. The viral DNA moves into the nucleus and is integrated into the host chromosome by the viral integrase, forming the provirus. The integration step has been reported to occur more frequently in areas of active gene transcription where the chromatin structure is in an open conformation (273).

Cellular transcription factors interact with specific domains located in the HIV-1 5' LTR and drive the initial round of transcription from the provirus (230). Production of the Tat protein during this process increases the level of transcription from the provirus by over several hundred-fold (102, 187). Tat binds to the transactivation response region (TAR) located on the transcribing viral RNA and stimulates transcription elongation of RNA polymerase II (178). Another HIV-1 regulatory protein, Rev, is important for nuclear export of unspliced or partially spliced viral mRNAs (102). Rev binds to the Rev-responsive element (RRE) located in the viral mRNA and brings the RNA together with the nuclear export protein CRM1 (44). Translation of the viral RNAs then generates viral precursor polyproteins, and viral assembly and budding occurs at the plasma membrane. Maturation of immature virions happens during or immediately after budding when the polyproteins are cleaved by the viral protease (106, 150). The HIV-1 accessory proteins (Vif, Vpr, Vpu, and Nef) serve various functions during viral replication, including evasion of cellular restriction factors (192, 323).

### *The path to AIDS*

The course of HIV-1 infection in a person can be divided into three main stages: primary infection, chronic infection, and acquired immune deficiency syndrome (AIDS) (77). During all stages of HIV-1 infection, the main target cells for productive infection include activated memory CD4<sup>+</sup> T cells and monocytes/macrophages, although naïve CD4<sup>+</sup> T cells can be infected by CXCR4-tropic viruses (X4) which generally evolve later during the course of infection (39). Primary HIV-1 infection includes the acute and early phases of infection during which peak plasma viremia often occurs and a viral ‘set point’ may be reached (45, 179). Shortly after HIV-1 infection the memory CD4<sup>+</sup> T cell population declines drastically, including the substantial depletion of CD4<sup>+</sup> T cells in the gut-associated lymphoid tissue (6). Several weeks post-infection the HIV-1 load decreases in response to the generation of virus-specific CD8<sup>+</sup> cytolytic T lymphocytes (CTL) (15, 221). The humoral immune response to HIV-1 infection occurs at the end of the primary stage of infection, coinciding with a partial rebound in peripheral CD4<sup>+</sup> T cell counts.

The chronic phase of infection is a long asymptomatic period that can last for years. This period is characterized by persistent viral replication and evolution, and a steady loss of peripheral CD4<sup>+</sup> T cells leading to immune exhaustion and immunodeficiency (54). Leading up to the clinical onset of AIDS there is a drop in CD4<sup>+</sup> T cell counts and increased viral replication (38). The clinical diagnosis of AIDS occurs with the appearance of an AIDS-defining illness or when CD4<sup>+</sup> T cell counts fall below 200 cells/ $\mu$ l, and this leads to the development of opportunistic infections and cancers associated with HIV-1 infection (14). Early clinical symptoms of immunodeficiency include the appearance of candidiasis and shingles, while more severe AIDS-defining illnesses include HIV-associated dementia (14),

histoplasmosis, cryptococcosis, pneumonia caused by *Pneumocystis carinii*, tuberculosis, *Toxoplasma gondii* infection of the brain, lymphomas, and Kaposi's sarcoma (54).

Eventually, HIV-1 infection weakens the immune system to a point of no return, and the HIV-1-infected individual succumbs to an opportunistic infection during the final stage of disease.

## **HIV-1 NEUROPATHOGENESIS**

### *HIV-1-associated dementia*

Neurological dysfunction is an important complication of HIV-1 infection of cells in the central nervous system (CNS), and neurological problems associated with HIV-1 infection have been well described in the literature since the epidemic first began (149, 208, 209). HIV-1-infected individuals can develop mild to severe neurological symptoms associated with HIV-1 infection, including the development of HIV-1-associated dementia (HAD) (14, 107). HAD is characterized by severe neurological dysfunction, and affected individuals have greatly impaired cognitive and motor functions, including extensive behavioral changes (209). Prior to the advent of highly active antiretroviral therapy (HAART), 20-30% of HIV-1-infected adults developed dementia (107, 261), and upwards of 50% of affected children developed neurological impairment and encephalitis (202). Widespread use of HAART has decreased the prevalence of dementia to around 10% of HIV-1-infected adults, although minor neurological problems are still common (107).

Diagnosis of neurological disease resulting from HIV-1 infection is conducted according to the AIDS dementia complex (ADC) stages (245). An ADC stage number of zero is assigned to subjects with clinically normal mental and motor function. The diagnosis of minor cognitive motor disorder (MCMD) is assigned an ADC stage 1, and indicates that the HIV-1-infected subject has decreases in memory and computational intellectual skills and/or mild motor impairment (210). ADC staging of 2-4 includes mild to severe dementia resulting from HIV-1 infection. Even during the less severe stages, individuals diagnosed with dementia have substantial motor disabilities and intellectual impairment such that they cannot maintain a job or provide basic care for themselves (210).

Some HAD subjects are also diagnosed with HIV-1 encephalitis (HIVE); however, not all subjects with HIV-1-associated neuro-impairment suffer from physiological brain damage. HIVE is characterized by neurological impairment coupled with HIV-specific neuropathology evident in brain tissue obtained from either a brain biopsy or post-mortem autopsy (24). Histopathological changes in brain tissue are the hallmarks of HIVE diagnosis, especially the presence of multinucleated giant cells of the macrophage/microglia origin (22, 23, 208). HIVE brain lesions exist as foci and are generally widespread (24), and the foci are associated with inflammatory changes including reactive astrocytes and increased macrophage infiltrates (24, 208).

The incidence of HAD and MCMD has decreased due to the widespread use of HAART; however, these disorders continue to affect a substantial proportion of the HIV-1-infected population (14, 107). The insufficient CNS penetration of some antiretroviral drugs may allow HIV-1 to persist in the CNS during the course of therapy (103, 107, 239, 272). In addition, higher prevalence of HAART has led to an increased lifespan and an older

demographic of HIV-infected subjects, and these subjects in particular have an increased risk of developing HAD due to their enhanced age (11, 146). Minor neurological problems associated with HIV-1 infection, including MCMD and peripheral neuropathies, are also on the rise (4, 107), indicating that neurological disorders will remain a problem for HIV-1-infected subjects in the future.

#### *Patterns of neuropathogenesis for other neurovirulent viruses*

Several DNA and RNA viruses are able to infect and replicate within cells of the central nervous system (CNS). Infections of the CNS are particularly difficult to eliminate due to the immune-privileged nature of the CNS and the longevity of cells that comprise the nervous system. RNA virus infection of the CNS results in either viral clearance, long-term persistence, or death of the infected individual (110). DNA viruses have both lytic and latent stages during viral infection, and the viral genome is maintained in the nucleus of the infected cell either by integration into the host chromosome, or by a viral episome (110). Viral latency generally causes persistent infection of the CNS due to viral evasion of immune detection, and many DNA virus infections are reactivated when the host becomes immune compromised.

Proper CNS function is maintained by five important cell types located in the brain parenchyma, all of which are targets for viral infection. Astrocytes regulate CNS homeostasis by maintaining blood-brain barrier (BBB) function and regulating the levels of neurotransmitters and toxic materials to provide an optimal extracellular environment for neurons (2). Microglia are brain-resident macrophages located within the brain parenchyma, while perivascular macrophages reside in close proximity to blood vessels. Perivascular

macrophages and microglia play important roles in immune responses to CNS injury and infection. Neurons use electrical impulses to control both cognitive and motor function, while oligodendrocytes produce the myelin sheath surrounding the axons of neurons, which promotes efficient transfer of neuronal signals (107, 110).

Viruses have been shown to infect all cell types present in the brain parenchyma, and neurotropic viruses gain access to target cells by invading CNS tissue in very disparate ways. Human herpesvirus 6 and JC virus both infect oligodendrocytes, while HIV-1 targets perivascular macrophages/microglia and human T lymphotropic virus I infects astrocytes (110). However, neurons are the most common target cell for viral infection of the CNS, and are targets for viruses like rabies, West Nile, and mosquito-borne alphaviruses. As an example, rabies virus (RV) is neurotropic and the causative agent of the neurological disease rabies (58). Transmission of RV occurs through the bite of an infected animal by inoculation of infectious virus in the saliva (58). Infectious virions invade neurons at the site of inoculation, and travel via retrograde axonal transport to the central nervous system (CNS) where the virus continues to replicate and spread (58, 79). Wild-type RV does not kill infected neurons, and it is thought that neuron impairment is responsible for the death of infected individuals (58). Other neurotropic viruses invade the CNS by directly infecting brain endothelial cells that comprise the BBB (41), while others enter via diapedesis (movement of blood cells through intact capillary walls) of infected monocytes and lymphocytes (85, 121).

Innate and adaptive immune responses are required for RNA virus clearance from CNS tissue. Interferon (IFN)- $\alpha/\beta$  production in response to viral infection induces the expression of pro-inflammatory cytokines and chemokines, which stimulates the migration of

immune cells to the site of viral infection, and promotes the development of an adaptive immune response (95, 144). In the CNS, resident cells that can respond to IFN- $\alpha/\beta$  include astrocytes, neurons, microglia, and endothelial cells (110, 225, 226). Astrocytes (regulators of brain homeostasis) and microglia (resident brain macrophages) are both activated in response to neuronal insult, and can rapidly produce a vast array of cytokines and chemokines (IL-6, TNF, MIP-1 $\beta$ , MCP-1, RANTES, and more) (75, 110, 193, 303). Production of IFN- $\alpha/\beta$  and other pro-inflammatory molecules in the CNS induces: 1) activation of neighboring cells, 2) amplification of local innate immune responses, 3) up-regulation of MHC molecule expression, 4) increased expression of adhesion molecules on endothelial cells, 5) modification of BBB permeability, and 6) attraction of circulating immune cells into the CNS (75, 95, 110, 303).

The production of IFN- $\alpha/\beta$  is important for host survival during a viral infection of the CNS. Accordingly, many viruses have evolved mechanisms for subverting the interferon response in the CNS. West Nile virus (WNV) encodes several non-structural proteins that attenuate the IFN response, and studies in mice have shown that WNV virulence is determined largely by resistance to IFN- $\alpha/\beta$  induction (156, 184, 263). *In vitro* studies found that WNV fails to activate interferon regulatory factor (IRF)-3 (87) and the nonstructural protein 1 was found to inhibit signal transduction from Toll-like receptor 3 (318). Rabies virus P protein was also identified as an antagonist of the type I interferon system by interfering with STAT1 (21, 304, 305) and IRF-3 (20) function.

Adaptive immune responses are necessary for RNA virus clearance from infected cells in the CNS. Viral clearance from neurons generally requires antibody-secreting B cell migration into the CNS (128, 300), although the exact mechanism by which antibodies

inhibit viral replication within neurons is not understood. Studies using rabies virus (141) and Sindbis virus (176) in mice have found that the local detection of B cells and production of virus-neutralizing antibodies in the CNS are required for the clearance of RV. Migration of T cells into the CNS is also known to be important in the clearance of RNA virus infections in the CNS from both neurons and glial cells (110). Trafficking CD4<sup>+</sup> and CD8<sup>+</sup> T cells have been reported in the CNS during infection of rabies (74, 235, 258) and Sindbis virus (12) infection. Additionally, it has been reported that T cell-mediated clearance of mouse hepatitis virus (strain JHM) is cell-type specific (110). Mouse hepatitis virus clearance from oligodendrocytes requires IFN- $\gamma$  (223), but CD8<sup>+</sup> T cells are needed for clearance from microglia (290). In the absence of an appropriate adaptive immune response, failure to clear a viral infection in the CNS ultimately leads to death of the infected individual through neuron dysfunction by direct viral insult (ex. rabies) or persistent immune activation (ex. HIV-1).

## **HIV-1 BIOLOGY AND NEUROVIRULENCE**

### *Crossing the blood-brain barrier: neuroinvasion by HIV*

The blood-brain barrier (BBB) is a specialized barrier that regulates brain homeostasis, and restricts the movement of molecules and cells between the peripheral blood and the brain parenchyma (1, 2, 127, 157). The BBB is formed by tight junctions between endothelial cells that line capillaries in the brain (1, 2, 201). The brain microvascular endothelial cells are surrounded by astrocyte foot processes, and many studies have shown

that astrocytes regulate BBB permeability through the secretion of compounds that alter tight junction proteins and adherens junctions proteins (1, 2, 75, 174, 193, 247, 252, 274). In addition, the close proximity of pericytes (cells present around the outer surface of capillaries), microglia, and neurons to endothelial cells has prompted studies evaluating their roles in BBB regulation (2). Molecules known to affect BBB permeability include MCP-1 (287, 288), TNF- $\alpha$  (86), apolipoprotein E (90, 99, 171, 200), many of the interleukins (1, 2, 157), and steroids (47). BBB permeability is also increased during periods of inflammation, including HIV-1 infection (57).

HIV-1 infection of the CNS occurs shortly after peripheral infection, most likely through the trafficking of infected lymphocytes and monocytes across the blood-brain barrier (BBB) (168, 186, 197, 216). Due to the selective permeability of the BBB, HIV-1 may persist in the CNS during therapy due to the insufficient CNS penetration of some antiretroviral drugs (103, 107, 239, 272). Several mechanisms have been proposed for HIV-1 infection of the CNS. The first two theories focus on HIV-1 interactions with the brain microvascular endothelial cells. One hypothesis is that HIV-1 may directly infect the endothelial cells; however *in vitro* studies have shown that HIV-1 infection of endothelial cells is highly restricted and non-productive (204, 237). The second hypothesis focuses on the transcytosis of HIV-1 by the endothelial cells, and several studies have reported the internalization of HIV-1 pseudovirions (10) or SIV particles (227) by brain endothelial cells. However, this model of HIV infection of the CNS is not widely supported, and no studies have shown how the internalized virus leaves the endothelial cell to replicate in the parenchyma.

The most widely supported theory is the “Trojan horse” hypothesis which proposes that HIV-1 enters the CNS through the trafficking of infected monocytes and lymphocytes across the BBB. This idea was first proposed by Peluso *et al.* (121, 228) using visna virus to examine the spread of lentiviruses into the CNS of sheep. A small number of leukocytes are known to cross the BBB during normal physiological conditions to carry out immune surveillance of the CNS, and this process is highly regulated and requires cell-specific interactions with endothelial cells. Leukocyte transmigration across the BBB involves rolling of leukocytes across the brain endothelial cells, activation, leukocyte adhesion to the endothelial cells, and subsequent diapedesis (248). Lymphocyte homing to the CNS is determined by both the expression of adhesion molecules (ICAM-1, VCAM-1) on brain endothelial cells (110, 248), and the expression of chemoattractant cytokines and chemokines in the brain parenchyma and perivascular spaces (248, 288).

CNS inflammation caused by viral infection can induce the migration of lymphocytes from the periphery into the CNS through the production of homing chemokines (72, 248). The key determinants for B cell migration are not well defined, but some chemokines (CXCL10, MCP-1, MIP-1 $\alpha$ ) are known to attract B cells to the CNS (198). In addition, T cell migration into the CNS is assisted by ICAM-1 and VCAM-1 (72, 73, 110), and studies found increased expression of the ICAM-1 ligand LFA-1 on HIV-1-infected PBMCs (167, 214). The adhesion molecule VCAM-1 was also found to be upregulated on endothelial cells in the brains of macaques with SIV encephalitis (265). MCP-1 is also a strong chemoattractant for monocytes and activated T cells. Previous studies have reported that MCP-1 induces the transmigration of leukocytes across a model of the human BBB (89, 312), and MCP-1 is known to be elevated in the CSF of HIV-1-infected subjects with

dementia (33, 155, 276). Additional studies have also reported that HIV-1-infected monocytes/macrophages secrete higher levels of MIP-1 $\alpha$  and MIP-1 $\beta$  (16, 268), TNF- $\alpha$  and IL-1 $\beta$  (101, 215), and matrix metalloproteinase (MMP)-9 (55, 167) compared to uninfected monocytes/macrophages. The increased levels of these chemokines serve to induce high levels of adhesion molecules on brain endothelial cells for altered attachment and transmigration of HIV-1-infected cells across the BBB (56).

In addition to crossing the BBB, HIV-1-infected cells can enter the CNS via two other routes from the peripheral blood. The first alternative pathway of leukocyte migration is from the blood to the CSF across the choroid plexus, a cellular membrane that produces CSF. The choroid plexus is comprised of choroid plexus epithelial cells, a central stroma, and an endothelial lumen (248). The choroid plexus epithelial cells are linked with tight junctions to prevent the passive transfer of molecules from the blood to the CSF. Leukocytes can be detected in the CSF of healthy individuals at low levels, and this process seems to be highly regulated due to the skewed ratios of leukocytes in the CSF compared to the plasma (137, 294). Leukocytes in the CSF are mostly T cells, with an increased ratio of CD4<sup>+</sup> central memory cells (137, 160, 294). The blood-CSF route of leukocyte migration most likely contributes to viral burden and entry into the CNS during HIV-1 infection. Subjects with HAD have higher HIV-1 RNA concentrations in the CSF compared to the peripheral blood (70, 71, 307), and increased CSF white blood cell counts are correlated with CSF HIV-1 RNA concentrations (195, 286). The final pathway of leukocyte migration is from the peripheral blood to the subarachnoid space, although not much is known about this route of entry into the brain.

After crossing the BBB HIV-1 comes in contact with resident cells in the brain parenchyma, including perivascular macrophages, microglia, astrocytes, oligodendrocytes, and neurons (107). Perivascular macrophages and brain-resident microglia are known to sustain productive HIV-1 infection (40, 97, 107, 232, 295, 315), although astrocytes may be non-productively infected by HIV-1 (97, 107, 232, 260). Perivascular macrophages are located in the brain parenchyma adjacent to capillaries, and it has been estimated that around 30% of the cell population is replaced in 2-3 months (135) by infiltrating monocytes (134). Parenchymal microglia are resident macrophages of the brain that are populated during fetal development, and the repopulation rate is thought to be extremely slow with only a small percentage of cells replaced over the course of several years (135, 172, 302). In addition to being targets for HIV-1 infection, macrophages and microglia constitute the immunoregulatory cells of the brain and can become activated in response to HIV-1 in the CNS.

#### *HIV-1 envelope: cellular attachment and entry in the CNS*

The HIV-1 envelope glycoprotein (Env) is produced as a 160 kilo-dalton polyprotein precursor (gp160) that is heavily glycosylated during translation (88). Translation of the gp160 polyprotein is initiated in the cytoplasm, and the first translated amino acids include a signal peptide that targets the protein to the rough endoplasmic reticulum (ER) (106). Translation is completed in the rough ER where the signal peptide is removed, and the newly synthesized gp160 polyprotein interacts with host chaperones for proper folding and oligomerization into trimers (66, 316). The gp160 polyproteins then move to the trans-Golgi network where gp160 is cleaved by a cellular furin-like protease into the gp120 surface and

gp41 transmembrane subunits (205). After cleavage the gp120 and gp41 subunits remain non-covalently associated, and this forms the functional envelope trimer of heterodimers that is transported to the cell membrane. A substantial amount of gp120 is shed from the surface of HIV-infected cells due to the weak interaction between gp120 and gp41 (88, 102).

The main functions of the HIV-1 Env protein include receptor and coreceptor binding, which determines the cellular tropism of HIV-1 variants, and membrane fusion with the target cell. Due to the exposure of gp120 (and to a lesser degree gp41) on the surface of the virion, epitopes in the glycoprotein are the main targets of neutralizing antibodies in response to HIV infection. The surface gp120 subunit has interspersed conserved (C1-C5) and variable (V1-V5) domains, and the V1-V5 domains are surface-exposed and evolve rapidly in response to antibody selection, serving as a protective shield for the conserved regions (297). In addition, some studies have reported a neurotoxic effect of gp120 in neuronal cultures (61, 136, 181, 267), which is discussed in a later section.

The major cellular surface receptor for HIV-1 is CD4 (46), a member of the immunoglobulin family that is highly expressed on CD4<sup>+</sup> T cells and expressed at low levels on the surface of macrophages (42, 173). In order to enter target cells, HIV-1 gp120 also interacts with the coreceptors CCR5 (31, 53) or CXCR4 (78). Crystal structures of the gp120 monomer lacking some of the variable domains have shown that the CD4 binding site on gp120 is located in a deep binding pocket that is thought to be protected from antibodies by the glycosylated variable loops (142, 165, 166). Specific residues in both CD4 (Phe-43) and gp120 (C3 and C4 domains, and others) are important for this interaction (88).

CD4 binding induces conformational changes in gp120 and gp41, which is required for envelope fusogenicity (266) and exposes epitopes on gp120 that are required for

coreceptor binding by the V3 loop (35) and other structures (166, 255). One crystal structure of gp120 bound to CD4 revealed that the V3 loop extends away from the gp120 core structure to enhance coreceptor binding after CD4 has been engaged (142). Coreceptor binding to gp120 completes viral attachment to the target cell and induces a new conformational change which stimulates insertion of the gp41 fusion peptide into the target cell membrane. The gp41 trimer then rearranges to form a six-helix bundle (91) which brings the viral and cellular membranes together to facilitate fusion.

Perivascular macrophages and brain-resident microglia are the two main cell types in the CNS that are known to sustain productive HIV-1 infection (40, 97, 107, 232, 295, 315). Perivascular macrophages and microglia in the CNS express low receptor densities of CD4, CCR5 and CXCR4, similar to other macrophage populations (112). Studies examining the characteristics of CNS variants have reported that brain-derived HIV-1 envelopes from subjects with HIVE have increased macrophage tropism and low CD4 dependence compared to envelopes obtained from lymph node tissue (63, 109, 233, 256, 298). The majority of macrophage-tropic envelopes use the CCR5 coreceptor for infection of macrophages and microglia (92); however, a study by Gorry *et al.* (108) reported that some HIV-1 variants can enter macrophages and microglia using the CXCR4 coreceptor.

HIV-1 infection has been reported in microglia (40) and perivascular macrophages (82, 161, 295, 315) using *in situ* hybridization and immunohistochemistry techniques. It is generally accepted that the main reservoir of HIV-1-infected cells in the CNS is the perivascular macrophage population, while infection of parenchymal microglia is more controversial. HIV-1 isolates have been shown to productively infect primary human microglia *in vitro* (278, 292, 310). However, studies of brains from HIVE subjects have

shown significant increases in the number of infiltrating perivascular macrophages (81, 82, 105, 322), whereas these cells are mostly absent from the brain tissue of asymptomatic subjects. In addition, multinucleated giant cells found in the brains of subjects with HIVE express the CD14 and CD45 antigens, which indicate the presence of perivascular macrophage instead of microglia (80, 82, 107). SIV studies in macaques have also reported SIV infection of macrophage/microglia in the CNS (158, 317) and the amplification of SIV DNA from brain tissue (34, 259).

#### *Virological and immunological markers of HIV-1 neuropathogenesis*

In general, subjects with severe neurological complications resulting from HIV-1 infection have higher viral burden in the CSF compared to the peripheral blood, including subjects with HIV-1-associated dementia (HAD) (70, 71, 307). Substantial HIV-1 genetic compartmentalization has also been reported between the blood and the cerebrospinal fluid (CSF) of subjects with HAD (126, 236, 254, 291). In addition, previous studies have reported that neurotropic HIV-1 variants can infect macrophages (108, 109, 233, 298). The association of viral compartmentalization with dementia is described in detail in the next section.

Specific amino acid substitutions in the Env protein have been reported to be associated with macrophage tropism and dementia. One study by Dunfee *et al.* (64) reported that the HIV Env variant N283 was found more frequently in brain-derived *env* sequences, and was associated with HIV-associated dementia. This study also found that N283 enhances viral entry in macrophages and microglia by contributing to low CD4 dependence (64). However, a more recent study reported that the N283 variant is not the only

determinant of macrophage tropism, and identified amino acid residues on the CD4 binding loop flanks and residues in the V3 loop that conferred macrophage tropism to HIV-1 envelopes (62). A separate report found an HIV variant in the V4 region of Env, D386, that occurs more frequently in subjects with HAD (65). This Env variant was thought to change cell tropism by eliminating an N-linked glycosylation site at position 386 in the envelope protein, and reportedly enhances HIV entry in macrophages but not microglia (65). Other studies have shown that the V1/V2 and V3 regions of gp120 from brain-derived envelopes contribute to reduced CD4 dependence and enhanced fusogenicity associated with macrophage tropism (108, 243, 256, 298).

In addition to viral features associated with dementia, immunological markers of neuropathogenesis have been reported for HIV-1-infected individuals. The levels of CSF neopterin, a pteridine produced by activated macrophages and associated with intrathecal immunoactivation (18, 104), and CSF light-chain neurofilament protein (NFL), a biomarker of CNS injury (3, 104, 199), are significantly elevated in subjects with HIV-1-associated dementia. The levels of the chemokines interferon- $\gamma$ -inducible protein 10 (IP-10) and monocyte chemoattractant protein-1 (MCP-1) have also been detected at elevated levels in the CSF of HAD subjects compared to asymptomatic subjects (32, 33, 155, 276). In addition, a more recent study reported that plasma lipopolysaccharide levels, an indicator of microbial translocation across the gut membrane and known to activate monocytes, are elevated in HAD subjects compared to controls (5).

One easily measured marker of inflammation in the CNS is pleocytosis, the presence of white blood cells (WBC) in the CSF. Lymphocytes are not commonly present in the CNS, and clinical studies have defined CSF pleocytosis as CSF WBC >5 cells/ $\mu$ l (194, 286).

Although pleocytosis can occur at any stage of neurological disease, increased CSF WBC counts are correlated with CSF HIV-1 RNA concentrations (195, 286). The levels of some chemokines associated with inflammation have also been correlated with CSF pleocytosis, including CSF IP-10 concentrations (32) and CSF MCP-1 concentrations (203). Coinciding with reports of increased CNS inflammation associated with the development of HAD, several studies have reported an increase in the total number of brain perivascular macrophages in subjects with HIVE (81, 82, 105). A more general feature of neurological disease progression is the constitutive activation of the immune system (32, 33, 104, 155, 276). Ultimately, a complete understanding of neuropathogenesis will need to integrate all of these genetic and pathological features.

## **HIV-1 COMPARTMENTALIZATION IN THE CNS**

*Compartmentalization of HIV-1 between the periphery and the central nervous system is associated with dementia*

Compartmentalized HIV-1 variants have been detected in the brains of HAD subjects at autopsy, and these brain-derived variants are genetically distinct from virus detected in the periphery (64, 65, 109, 218, 242, 256, 298). Viral genetic compartmentalization has also been reported between the blood and the cerebrospinal fluid (CSF) of HAD subjects later during the course of infection (126, 236, 254, 291). Previous studies have reported increased HIV-1 compartmentalization in the CNS/CSF of subjects with neurological disease (126, 213, 254, 272, 289). However, compartmentalized viral variants have also been detected in

the CSF of asymptomatic subjects, indicating that the simple detection of CSF-compartmentalized variants is not related to the degree of neurological disease (126, 254). A separate study found that in subjects without severe neurological disease CSF pleocytosis was associated with viral population mixing between the periphery and CSF, resulting in decreased CSF compartmentalization (283).

Studies conducted by Ritola *et al.* (254) and Harrington *et al.* (126) examined HIV-1 *env* compartmentalization between the blood plasma and CSF using the heteroduplex tracking assay (HTA) (51, 52) to distinguish between HIV-1 genetic variants in the CSF that were either compartmentalized in the CSF or equilibrated with the peripheral blood. These studies reported that the fraction of compartmentalized virus in the CSF is significantly higher in HAD subjects compared to both asymptomatic or MCMD subjects (126, 254). In addition, Harrington *et al.* reported that increased *env* compartmentalization in HAD subjects was not simply a function of low CD4 counts in HAD subjects (126).

Another group of studies, most originating from Dana Gabuzda's group, have focused on examining the biological characteristics of HIV-1 envelopes obtained from autopsy brain and lymph node tissue of subjects with varying degrees of neurological impairment and encephalitis. These studies have reported that brain-derived HIV-1 envelopes from subjects with encephalitis have increased macrophage tropism and low CD4 dependence compared to envelopes obtained from lymph node tissue (63, 109, 233, 256, 298). Due to the enhanced capacity to use low CD4 levels, it is thought that macrophage-tropic envelopes have a more exposed CD4 binding pocket to allow efficient gp120-receptor interactions. Studies by Dunfee *et al.* (63) and Peters *et al.* (233) reported that macrophage-tropic envelopes have increased sensitivity to CD4 binding site antibodies. In addition, neutralizing antibody titers

are much lower in the CNS compared to the plasma, providing an immune-isolated anatomical site for macrophage-tropic HIV-1 variants to evolve.

Compartmentalization between the periphery and the CSF has also been reported in macaques infected with simian immunodeficiency virus (SIV) (123). In a small pilot study, Harrington *et al.* (123) reported that discordance between SIV populations in the blood and CSF was associated with elevated CSF MCP-1 levels and increased numbers of infiltrating perivascular macrophages. Other studies using SIV-infected macaques have reported SIV infection of macrophage/microglia in the CNS (158, 317) and the amplification of SIV DNA from brain tissue (34, 259), indicating that SIV infection of local cells in the CNS occurs during the course of infection.

Extensive compartmentalization between the periphery and the CNS has been reported in subjects with HAD; however, it is not yet known when compartmentalization occurs during the course of HIV-1 infection. Studies examining compartmentalization in the CNS during primary HIV-1 infection have been limited, and compartmentalization has not been detected in the CSF of primary infection subjects (126, 253). Determining whether compartmentalization in the CSF begins during the primary stage of HIV-1 infection could have major implications for antiretroviral treatment regimens, including the timing of CNS-penetrating drugs.

#### *The source of compartmentalized HIV-1 in the CNS*

HIV-1 invades the CNS shortly after infection, and after crossing the BBB it comes in contact with resident cells in the brain parenchyma, including perivascular macrophages, microglia, astrocytes, oligodendrocytes, and neurons (107). Perivascular macrophages and

brain-resident microglia are the two cell types in the CNS that are known to sustain productive HIV-1 infection (40, 97, 107, 232, 295, 315), although non-productive infection may occur in astrocytes (97, 107, 232, 260). Perivascular macrophages and microglia in the CNS also express low receptor densities of CD4, CCR5, and CXCR4, and previous studies have reported that neurotropic HIV-1 variants can infect macrophages (108, 109, 161, 256, 298).

The population dynamics of HIV-1 replication have been studied extensively in the periphery (139, 231, 311), but the extent of viral replication in specific cell types in the CNS over the course of disease is not yet known. The use of antiretroviral drugs to prevent HIV-1 infection of uninfected cells can be used as a tool to examine the rate of decay for cell-free virus and virally-infected cells. Previous studies have reported that HIV-1 decay in the peripheral blood after the initiation of HAART occurs in at least two phases (139, 311). The first phase of decay is rapid and represents the turnover of cell-free virions and productively infected CD4<sup>+</sup> T cells (139, 231, 281, 311). The second phase is slower and may reflect the decay of long-lived infected cells, possibly cells of the monocyte lineage and latently infected resting CD4<sup>+</sup> T cells (139, 279, 281, 311). A more recent study using the integrase inhibitor raltegravir, which targets a later step in the HIV-1 lifecycle than HAART, reported altered HIV-1 decay kinetics and a reduction of the second viral decay phase (207). The reduction in the second phase of HIV-1 decay suggests that integration is a rate-limiting step in a subset of infected cells, and may indicate that longer-lived HIV-1-infected cells contribute less to total viral load than previously thought (207, 275). However, the results from this study do not negate the possibility that the second phase of HIV-1 decay may reflect the turnover of long-lived cells

One problem with studying viral population dynamics in the CNS is that human brain tissue samples are difficult to obtain. In order to examine viral evolution in the CNS over the course of HIV-1 infection, most studies have examined viral populations in the CSF, which reflects virus originating from both local CNS tissue and the peripheral blood (69, 70, 96, 119). Several studies examining viral decay rates in the CSF of HIV-1-infected subjects reported similar viral decay kinetics in both CSF and plasma for most individuals; however, some subjects displayed a slower clearance of virus from the CSF (68, 69, 246, 289). Additionally, slower clearance of HIV-1 from the CSF has been associated with the presence of neurological disease (68, 69, 246, 289). A study conducted by Harrington *et al.* (124) examined the cellular sources of HIV-1 in the CNS by utilizing the HTA to measure viral decay rates in HIV-1-infected subjects initiating antiretroviral therapy (124). This study reported that the subset of compartmentalized virus detected in the CSF of four asymptomatic subjects decayed rapidly after the initiation of therapy, suggesting that the compartmentalized virus is coming from a short-lived cell type, such as CD4<sup>+</sup> T cells (124).

HIV-1 persistence in the CNS can be described by two pathways based on previous studies (289). The first pathway is based on the continuous trafficking of short-lived infected CD4<sup>+</sup> T cells into the CNS. Virus in the CNS is constantly replenished from the periphery, resulting in similar HIV-1 populations in both the periphery and the CSF (254, 289). In this model, virus in both the CSF and plasma should decay rapidly upon the initiation of HAART. This type of CNS infection has been described in previous studies involving asymptomatic HIV-1-infected subjects (124, 289).

The second pathway is based on HIV-1 infection of long-lived perivascular macrophages and microglia in the CNS. Here, virus originates from local CNS tissue

resulting in large differences in HIV-1 populations in the CSF and periphery (126, 254). The second model predicts that virus in the CSF will have slower decay kinetics compared to the periphery due to the much slower turnover time of macrophages and microglia (135, 172, 302). Previous studies involving subjects with severe neurological disease that are initiating HAART have described strong compartmentalization between the CSF and plasma (126, 254), and slower elimination of HIV-1 from the CSF (68, 69, 246, 289), suggesting a longer-lived cell as the source of this virus. However, the exact cellular origin of compartmentalized HIV-1 detected in the CSF has not been established.

## **NEUROPATHOLOGICAL DAMAGE IN THE CNS DURING HIV-1 INFECTION**

HIV-1 infection and replication in cells of the CNS can lead to tissue damage in the brains of some subjects with HAD, a disorder known as HIV encephalitis (HIVE). During HIVE, productively infected macrophages and microglia fuse together to form multinucleated giant cells (22, 23, 208), microgliosis and astrogliosis also occur (26, 208), and neuron loss has been observed (25, 26, 314). Two mechanisms have been proposed to explain neurodegeneration in the CNS resulting from HIV-1 infection: 1) direct injury resulting from neurotoxic viral proteins, and 2) bystander inflammation due to activation of CNS immune cells and astrocytes (107). Activation of glial cells in the CNS is thought to result from both direct viral infection (activation of infected cells) and secreted inflammatory products (activation of uninfected cells).

### *Neurotoxic HIV-1 proteins in the CNS*

The HIV-1 proteins gp120, Tat, and Vpr have demonstrated neurotoxicity *in vitro*. As mentioned previously, gp120 is shed from the surface of infected cells and virions due to a weak non-covalent interaction with gp41 (61, 153). *In vitro* studies have reported gp120-induced neuron death resulting from interactions with the viral coreceptors expressed on neurons (8, 133, 321). Other studies have shown that gp120 interacts with the *N*-methyl-D-aspartate (NMDA) receptor on neurons to induce neuronal cell death (320). Neuronal cell death is thought to occur via disruption of the intracellular calcium environment, which induces neuron apoptosis (61, 169). The neurotoxic effects of Tat have been studied extensively due to the finding that Tat is secreted in high amounts *in vitro* (28). Tat has been found to directly interact with the NMDA receptor on neurons, leading to neuronal apoptosis (129, 285); however, most of the neurotoxic effects of Tat are a result of toxic products released from infected macrophages/microglia (238, 301). Finally, some studies have reported that soluble Vpr induces neuron apoptosis in culture (224). The actual extracellular concentrations of gp120, Tat, and Vpr in the CNS are not known, which prompts the caveat that the neurotoxic data generated *in vitro* from these proteins may not translate to what actually occurs in the CNS. The interaction of immune cells in the CNS with extracellular viral proteins would also activate inflammatory responses.

### *Inflammation in the CNS*

The most widely accepted mechanism of neurodegeneration during HIV-1 infection is the induction of inflammation due to the presence of viral antigen in the CNS. The persistence of HIV-1 cell-free virus and virus-infected cells in the CNS stimulates a state of

constitutive immune-activation in the CNS. Increases in CSF viral load generally correlate with increased levels of inflammatory markers in the CSF of HAD subjects (195, 286). Inflammation in the CNS disrupts the homeostatic environment of the CNS and leads to activation of glial cells, including perivascular macrophages, microglia and astrocytes. Activated glial cells are known to secrete pro-inflammatory cytokines, chemokines and other toxic products, which activate other uninfected cells and stimulates the migration of additional lymphocytes and monocytes into the CNS (98).

Inflammation-induced neurological disease is amplified in subjects with HAD. Multiple pro-inflammatory cytokines and chemokines are amplified in the CSF of HAD subjects compared to subjects without neurological symptoms, including IP-10 and MCP-1 (32, 33, 155, 276), IL-1 $\beta$  (17, 94), TNF- $\alpha$  (111, 319), and M-CSF levels are increased in the CSF of HIV-1-infected subjects (93, 219). Markers of macrophage and microglia activation have also been detected in subjects with HAD. HIV-1 infection induces macrophages to secrete quinolinic acid (114, 322), which is also produced in response to stimulation by TNF- $\alpha$  and IFN- $\gamma$  (229, 322). Quinolinic acid also stimulates secretion of MCP-1 from astrocytes (113). Activated macrophages also secrete platelet activating factor, an arachidonic acid metabolite that contributes to neurotoxicity in HAD subjects (100, 101). In addition, activated microglia and astrocytes have increased levels of inducible nitric-oxide synthase, an enzyme that generates the free radical nitric oxide (NO) from L-arginine (322). Previous studies have reported that NO production from activated glial cells contributes to neurodegeneration in HAD subjects (185, 217). Astrocyte activation results in the production of inflammatory cytokines and disrupts the glutamate regulatory pathway (107). Increased concentrations of glutamate in the extracellular environment cause neuron death

due to uninhibited calcium entry into neuronal cells (84). In general, all of these inflammatory molecules (and others) contribute to immune activation and neurodegeneration in the CNS, eventually leading to the development of dementia in a subset of HIV-1-infected individuals.

## **SIGNIFICANCE AND OBJECTIVES**

HIV-1-associated dementia occurs in a subset of infected individuals, and results in significant neurological dysfunction. The incidence of HAD is higher in countries with limited access to antiretroviral drugs and in older HIV-infected subjects. In individuals that develop neurological disease, HIV-1 found in the CNS can include viral variants that are distinct from variants in the peripheral blood (64, 65, 126, 218, 236, 242, 254, 256, 291). However, it is currently unknown why a subset of HIV-1-infected individuals develop HAD or MCMD, nor is it known to what extent independent replication of HIV-1 in the CNS is a factor in CNS pathogenesis. Previous research in our laboratory has shown that distinct compartmentalized HIV-1 variants are associated with HAD and neurological disease. The degree of CSF-compartmentalization also seems to be associated with HAD, such that subjects with HAD have an increased abundance of compartmentalized HIV-1 variants in their CSF (126, 254). Due to the lack of predictive markers for HAD, treatment with CNS-penetrating drugs is not usually started until neurodegeneration is apparent.

The main objective of this dissertation is to characterize viral genetic determinants associated with CNS compartmentalization and the development of neurological disease in

HIV-1-infected adults. Genetic differences in compartmentalized virus could arise via two pathways: a founder effect or adaptation to enhanced replication in the CNS. I hypothesize that immunodeficiency allows viral replication to occur in the CNS, which can lead to viral genetic adaptation. In addition, viral adaptation to the CNS environment leads to compartmentalization and preferential replication in the CNS, resulting directly or indirectly (through an inflammatory response) in CNS damage and the development of neurological disease. The projects outlined in this dissertation focus on characterizing HIV-1 genetic compartmentalization over the course of HIV-1 infection, examining the genotypic and phenotypic differences between compartmentalized and non-compartmentalized HIV-1 variants in subjects with HAD or no neurological symptoms, and defining the cellular origin of compartmentalized HIV-1 variants. The discovery of specific viral genetic determinants associated with the development of HAD will establish why a subset of HIV-1-infected individuals develop HAD. In addition, viral determinants that are detectable prior to the onset of dementia could be used as a screening tool for the diagnosis of HAD.

## CHAPTER TWO

### COMPARTMENTALIZATION AND CLONAL AMPLIFICATION OF HIV-1 VARIANTS IN THE CEREBROSPINAL FLUID DURING PRIMARY INFECTION

Reprinted from: Schnell, G., R.W. Price, R. Swanstrom, and S. Spudich. 2010.

Compartmentalization and Clonal Amplification of HIV-1 Variants in the Cerebrospinal  
Fluid during Primary Infection. *J Virol* 84:2395-407.

Reproduced/amended with permission from American Society for Microbiology.

## ABSTRACT

Human immunodeficiency virus type 1 (HIV-1)-associated dementia (HAD) is a severe neurological disease that affects a subset of HIV-1-infected individuals. Increased compartmentalization has been reported between blood and cerebrospinal fluid (CSF) HIV-1 populations in subjects with HAD, but it is still not known when compartmentalization arises during the course of infection. To assess HIV-1 genetic compartmentalization early during infection, we compared HIV-1 populations between the peripheral blood and CSF in 11 primary infection subjects, with analysis of longitudinal samples over the first 18 months for a subset of subjects. We used heteroduplex tracking assays targeting the variable regions of *env*, and single genome amplification and sequence analysis of the full length *env* gene, to identify CSF-compartmentalized variants and examine viral genotypes within the compartmentalized populations. Most subjects had equilibrated HIV-1 populations between the blood and CSF compartments. However, compartmentalized HIV-1 populations were detected in the CSF of three primary infection subjects, and longitudinal analysis of one subject revealed that compartmentalization during primary HIV-1 infection was resolved. Clonal amplification of specific HIV-1 variants was identified in the CSF population of one primary infection subject. Our data show that compartmentalization can occur in the CNS of subjects in primary HIV-1 infection in part through persistence of the putative transmitted parental variant, or via viral genetic adaptation to the CNS environment. The presence of distinct HIV-1 populations in the CSF indicates that independent HIV-1 replication can occur in the CNS, even early after HIV-1 transmission.

## INTRODUCTION

Human immunodeficiency virus type 1 (HIV-1) infection of the central nervous system (CNS) can lead to neurological disease in a subset of HIV-1-infected individuals, including the development of HIV-1-associated dementia (HAD) (14, 107). HAD is characterized by severe neurological dysfunction, and affected individuals generally have impaired cognitive and motor functions. HIV-1 enters the CNS during primary infection, most likely via the migration of infected monocytes and lymphocytes across the blood-brain barrier (168, 186, 216). The main cell types in the CNS that HIV-1 can productively infect are the perivascular macrophages and microglial cells, which express low receptor densities of CD4, CCR5, and CXCR4 (40, 107, 295, 315). Previous studies have also reported that neurotropic HIV-1 variants are generally macrophage-tropic (108, 109, 161, 233, 256, 298). Although cells in the CNS may be infected with HIV-1 during the course of disease, it is still unclear whether productive HIV-1 replication occurs in the CNS early during infection.

Genetically compartmentalized HIV-1 variants have been detected in the brains of HAD subjects at autopsy (64, 65, 218, 242, 256), and in the cerebrospinal fluid (CSF) of HAD subjects sampled over the course of infection (126, 236, 254, 291). Extensive compartmentalization between the periphery and the CNS has been reported in subjects with HAD; however, it is not yet known when compartmentalization occurs during the course of HIV-1 infection. Primary HIV-1 infection refers to the acute and early phases of infection during which peak plasma viremia often occurs and a viral ‘set point’ may be reached (45, 179), within up to the first year after HIV exposure (324). Studies examining compartmentalization between the blood plasma and CSF during primary infection have been

limited, and extensive compartmentalization has not been detected in primary infection subjects (126, 253).

In this study we examined HIV-1 genetic compartmentalization between the peripheral blood and CSF during primary HIV-1 infection. Cross-sectional and longitudinal blood plasma and CSF samples were analyzed for viral compartmentalization using the heteroduplex tracking assay (HTA) and single genome amplification (SGA). We used the HTA to differentiate between HIV-1 variants in the CSF that were either compartmentalized to the CSF or equilibrated with the peripheral blood. Previous studies have used the HTA to separate HIV-1 genetic variants in different anatomical compartments (50, 124, 131, 254), and to follow HIV-1 evolutionary variants over the course of infection (49, 125, 159, 212, 251, 253). We also conducted SGA on a subset of subjects to further examine viral genetic compartmentalization during primary infection. Here we report the detection of compartmentalized and clonally amplified HIV-1 variants in the CSF of subjects in the primary stage of HIV-1 infection. Our results suggest that minor to extensive HIV-1 genetic compartmentalization can occur between the periphery and the CNS during primary HIV-1 infection, and that viral compartmentalization, as measured in the CSF, is transient in some subjects.

## **MATERIALS AND METHODS**

### **Subject population.**

Study subjects were individuals enrolled in a neurological study of acute and early HIV-1 infection at the University of California at San Francisco. Diagnosis of primary HIV-1 infection at enrollment followed the previously described Serologic Testing Algorithm for Recent HIV Seroconversion (STARHS) (206). In brief, subjects had positive HIV-1 nucleic acid testing and either had negative antibody tests in the past 12 months, or had a less-sensitive EIA result supportive of infection within the previous six months. Further estimation of days since HIV-1 exposure (days post infection, dpi) was based upon either the presence of symptoms of an acute seroconversion reaction or taken as the halfway point between last negative and first positive antibody test (180, 182). Serial blood plasma and cerebrospinal fluid (CSF) samples were collected for study purposes as early as possible after initial diagnosis and at varying intervals thereafter. Plasma and CSF HIV-1 RNA concentrations were determined using the Amplicor HIV Monitor kit (Roche). The study was approved by the Committee for Human Research at the University of California at San Francisco, and all subjects provided written informed consent for the collection of samples.

### **Markers of inflammation.**

Entry blood and CSF determinations including cell counts, differential, protein, and albumin were performed by the San Francisco General Hospital Clinical Laboratories. CSF neopterin was assayed using a commercially available ELISA assay according to the vendor's methods (Henning Berlin GMBH, Berlin, Germany).

### **Viral RNA isolation, RT-PCR, HTA, and PhosphorImager analysis.**

Procedures for viral RNA isolation, RT-PCR, and HTA have been previously described (51, 52, 124, 159, 212, 251). HIV-1 RNA was isolated from blood plasma and CSF samples (140  $\mu$ l) using the QIAmp Viral RNA kit (Qiagen). All CSF samples were centrifuged at 1,000 x g for 5 minutes prior to RNA isolation to remove contaminating cellular debris. To increase template number, samples with viral RNA levels less than 10,000 copies/ml were pelleted (0.5-1.0 ml) by centrifugation at 25,000 x g for 1.5 hours prior to RNA isolation. Reverse transcription and PCR amplification of the V1/V2 and V4/V5 regions of *env* were conducted with 5  $\mu$ l of purified RNA (from 60  $\mu$ l column elution volume) using the Qiagen One-Step RT-PCR kit (Qiagen) as per manufacturer's instructions, and using previously described primers for V1/V2 (159, 251) and V4/V5 (251).

The heteroduplex annealing reactions have been previously described (159, 212). Heteroduplexes were separated by 6% native polyacrylamide gel electrophoresis for V1/V2 and V4/V5 HTA (124, 159). The HTA probes used in these studies include the V1/V2 Ba-L probe (159, 251), V1/V2 JRFL probe (159, 251), V4/V5 NL4-3 probe (124), and the V4/V5 YU2 probe (251). The HTA gels were dried under vacuum, and bands were visualized by autoradiography. The dried HTA gels were exposed to a PhosphorImager screen, and the relative abundance of each detected viral variant (heteroduplex) was calculated using ImageQuant software (Molecular Dynamics). The variant RNA concentration was calculated by multiplying the relative abundance of each individual variant by the total HIV-1 RNA concentration for that sample. Template sampling was validated by analyzing duplicate RT-PCR products by HTA for each sample. For any time point where the HTA patterns between the two replicates differed significantly (>20%), the samples were not used in data analysis.

Percent difference values between plasma and CSF viral populations were calculated as previously described (159, 251).

### **Single genome amplification (SGA).**

HIV-1 RNA was isolated as described in the previous section. Viral RNA was reverse transcribed using the Superscript III Reverse Transcriptase (Invitrogen) and oligo(dT) as per manufacturer's instructions. SGA of the full-length HIV-1 *env* gene through the 3' U3 region was conducted as previously described (154, 220, 262). Briefly, cDNA was endpoint diluted and nested PCR (67, 280) was conducted using the Platinum *Taq* High Fidelity polymerase (Invitrogen) as described by Salazar-Gonzalez *et al.* (262). The primers B5853 UP0 (5'- TAGAGCCCTGGAAGCATCCAGGAAG-3') and LTR DN1 (5'- GACTCTCGAGAAGCACTCAAGGCAAGCTTTATTGAG-3') were used for the first round of PCR. The primers B5957 UP1 (5'- GATCAAGCTTTAGGCATCTCCTATGGCAGGAAGAAG-3') and LTR DN1 were used for the second round of PCR. The SGA amplicons were then sequenced from the start of V1 through the ectodomain of gp41 [Hxb2 numbering of positions 6600-8000].

### **Phylogenetic and compartmentalization analyses.**

Nucleotide sequences of the *env* genes were aligned using Clustal W (30, 299) or MAFFT software (152). Maximum likelihood phylogenetic trees were generated using PhyML (116) with the following parameters: HKY85 nucleotide substitution model, four substitution rate categories, estimation of the transition/transversion rate ratio, estimation of the proportion of invariant sites, and estimation of the gamma distribution parameter (115).

All sequences were subjected to quality control analysis to ensure that sequences from different subjects were not mislabeled.

Variants in the CSF were considered compartmentalized by HTA if they were either unique to the CSF or if they had a substantially higher copy number in the CSF compared to the plasma. Compartmentalization of CSF viral populations by sequence was determined using the Slatkin-Maddison test for compartmentalization (282) implemented in the HyPhy software (240) and using 10,000 permutations.

#### **Nucleotide sequence accession numbers.**

Nucleotide sequences determined in this study have been deposited in GenBank under the accession numbers GQ49667 to GQ497076 and GU206564 to GU206786.

## RESULTS

### **Study population characteristics and inflammatory markers.**

Our study included 17 subjects enrolled in a neurological primary HIV-1 infection cohort for which we attempted to examine CNS compartmentalization during primary infection (see Table 2.1 for clinical and laboratory characteristics). Eleven subjects had sufficient viral RNA loads in both the plasma and CSF compartments for HTA and SGA analyses of the viral populations. All subjects in this study had higher HIV-1 RNA concentrations in the plasma than in the CSF, and a substantial proportion (35%, 6 of 17) of the subjects had extremely low CSF HIV-1 RNA concentrations at study entry (mean=232 copies/ml,  $\pm$  197), in contrast to the other 11 subjects (mean=22,986 copies/ml,  $\pm$  49,492). Viral population characteristics were not analyzed for six subjects with low CSF viral load at entry (subjects 9003, 9010, 9012, 9014, 9016, 9017).

We measured inflammation and cell migration into the CNS for each subject through several indirect analyses, including CSF/plasma albumin ratios, CSF white blood cell (WBC) counts, and CSF neopterin levels. The CSF/plasma albumin ratios were calculated as a measure of blood-brain barrier (BBB) disruption, while CSF WBC levels were measured as a simple marker of inflammation and inflammatory cell migration into the CNS. Additionally, the level of CSF neopterin, a pteridine produced by activated macrophages and associated with intrathecal immunoactivation, is elevated in HIV-infected subjects and characteristically particularly high (>22 nmol/L) in those with HIV-1-associated dementia (18, 104). All 17 subjects were enrolled within the first year of infection, with a median dpi at baseline of 143 (interquartile range 58-165 days). Subjects were naïve to antiretroviral treatment at

enrollment, and only one subject started treatment during the study intervals reported here (subject 7146, after 11/10/03).

Based on published normal values of CSF WBC (0-5 cells/ $\mu$ l) (83) and CSF/albumin ratio (< 6.8) (13), most subjects had mild to moderate CNS inflammation and blood brain barrier disruption during this early stage of infection. Subject 7146 was symptomatic at the time of enrollment with clinical meningitis that was presumed secondary to HIV-1 seroconversion (extensive laboratory evaluation for standard bacteria, tuberculosis, spirochetes, and fungal organisms was negative), and had the highest levels of CSF WBC, CSF/plasma albumin ratio, and CSF neopterin in the group (see Table 2.1). All other subjects with HTA or SGA performed were neurologically asymptomatic at study enrollment.

### **Compartmentalization of HIV-1 variants in the CSF during primary infection.**

The heteroduplex tracking assay (HTA) is a useful tool for resolving and quantifying complex viral populations based on their genotype, and is able to detect minor variants within the viral population. We utilized HTAs targeting the hypervariable regions V1/V2 and V4/V5 of the *env* gene to detect and distinguish between compartmentalized and non-compartmentalized HIV-1 variants in the CSF and plasma of primary infection subjects. Cross-sectional HTA analyses were conducted on 7 primary infection subjects, and we were able to classify the relationship between the blood and CSF viral populations into two groups. Five subjects (9001, 9002, 9006, 9007, and 9019; see Figure 2.1A) showed concordance (% difference between blood and CSF >20%) between the blood plasma and CSF viral populations at the earliest time point sampled.

The second group (subjects 9018, 7146) had evidence of compartmentalization when comparing the blood and CSF viral populations at study entry (Figure 2.1B). In this small study, the two subjects with compartmentalized variants in the CSF had higher CSF viral loads compared to subjects with concordant populations in the plasma and CSF (Table 2.1). HIV-1 populations in the plasma and CSF were also discordant in subjects with CSF-compartmentalized variants as measured by percent difference (9018 = 29.2% different at 198 dpi; 7146 = 23.9% different at 156 dpi). In this group, subject 9018 had only mild CNS inflammation, while subject 7146 had evidence of significant inflammation in the CNS (see Table 2.1). These results show that HIV-1 compartmentalization in the CSF can occur during primary infection, and as early as 5 months after HIV-1 transmission.

### **Compartmentalization during primary HIV-1 infection can be transient.**

Longitudinal HTA analyses were conducted to examine compartmentalization in the CSF over the course of primary HIV-1 infection (subjects 9001, 9002, 9006, 9007, and 7146). HIV-1 populations in the plasma and CSF were concordant over time for subjects 9001, 9002, 9006, and 9007, with some minor variations (see Table 2.1 for percent difference values). In subject 9001, viral populations between the plasma and CSF were concordant at each time point; however, the viral population underwent substantial divergence between time points, demonstrating equilibration between these compartments even as the virus was evolving in the periphery. Conversely, HTA analysis of subject 9002 revealed concordance between the plasma and CSF populations over time, with only a small amount of viral diversification detected at 597 dpi. Results for subjects 9006 and 9007 are summarized in Figure 2.1 and Table 2.1. We conclude that for these subjects most of the virus detected in

the CSF was recently imported from the periphery and underwent little independent replication in the CNS.

Longitudinal HTA analysis of subject 7146 revealed one viral variant that was compartmentalized in the CSF at 156 and 177 dpi, although by 177 dpi this variant comprised a small minority of the total CSF viral population. We also noticed that a new viral variant was significantly enriched in the CSF viral population at day 203 post-infection (Figure 2.1B). However, the plasma and CSF viral populations had equilibrated again by 530 dpi. At this time point, the CSF variant that was enriched at 203 dpi still seemed to be slightly enriched in the CSF compared to the plasma population, although this difference was now minor. These results indicate that when compartmentalization occurs during primary HIV-1 infection it can be transient, and the CSF viral population can change substantially over the course of primary HIV-1 infection.

**Single genome amplification confirms compartmentalization and identifies clonal amplification of HIV-1 variants in the CSF of primary infection subjects.**

We examined the genetically compartmentalized viral variants in more detail by conducting single genome amplification (SGA) on plasma and CSF samples from subjects with detectable compartmentalization in the CSF by HTA (subjects 9018, 7146). We also conducted SGA on two subjects (9002 and 9007) with equilibrated HIV-1 populations between the plasma and CSF, and on an additional 4 subjects that were not analyzed by HTA (9025, 9037, 9039, 9040; see Figure 2.2 and Table 2.2). The structure of the phylogenetic trees and limited *env* sequence diversity suggest that subjects 9002, 9007, 9025, 9037, and 9039 were each infected with a single HIV-1 variant during transmission. We found that

plasma and CSF *env* sequences for subjects 9002, 9025, 9037, and 9039 mixed together throughout their respective phylogenetic trees, indicating that the two compartments were well equilibrated for each subject (Figure 2.2A). In addition, the CSF *env* sequences for these subjects were not considered compartmentalized using the Slatkin-Maddison test (9002  $p=0.56$ ; 9025  $p=0.84$ ; 9037  $p=0.057$ ; 9039  $p=0.97$ ). Subject 9007 had plasma and CSF HIV-1 populations that were well equilibrated at 149 dpi (Slatkin-Maddison test,  $p=0.6928$ ), although the viral populations were somewhat discordant 406 dpi (see Figure 2.2B; Slatkin-Maddison test,  $p=0.0397$ ). These data confirm the HTA analysis showing that the plasma and CSF can be fully equilibrated.

SGA was also conducted on the cross-sectional plasma and CSF samples for subject 9018, which had one compartmentalized variant detected by HTA, and subject 9040. We detected significant compartmentalization between the blood plasma and CSF HIV-1 populations for subject 9040 (see Figure 2.2C; Slatkin-Maddison test,  $p<0.0001$ ), and further sequence analysis demonstrated that all of the compartmentalized variants encoded a common V169R amino acid substitution in the V1/V2 stem region of the Env protein. Similarly, phylogenetic analysis of subject 9018 revealed a subset of *env* sequences derived from the CSF that branched separately from the rest of the sequences in the tree (Figure 2.3A). In addition, the compartmentalized population in the CSF had a unique Q170R amino acid substitution in the V1/V2 stem of envelope. However, the CSF viral population was not considered compartmentalized by the Slatkin-Maddison test ( $p=0.1078$ ). Even though the entire CSF viral population was not considered compartmentalized, a small HIV-1 population in the CSF appears compartmentalized based on the phylogenetic tree structure and good bootstrap support for this node (Figure 2.3A).

Based on the sequence and phylogenetic data, subject 9018 was likely infected with at least two viral variants during transmission. The two sequences that are likely closest to the parental viruses are 9018 C 13 / 9018 P 1 and 9018 C 14 (Figure 2.3B), and recombination between the transmitted viruses appears to account for much of the *env* genetic diversity detected in both the plasma and CSF populations. This interpretation also leads to the conclusion that one of the putative transmitted sequences was underrepresented in the periphery and maintained in the CNS.

Longitudinal SGA analysis for subject 7146 revealed transient compartmentalization and clonal amplification in the CSF HIV-1 population. Based on the phylogenetic tree structure and *env* sequence diversity at the first time point sampled (156 dpi), we believe that subject 7146 was infected with two HIV-1 variants during the transmission event (Figure 2.4A). The viral variants that appear to be most closely related to the parental viruses are 7146 1P 1 and 7146 1C 1 (Figure 2.4B), and extensive recombination between the two transmitted viruses can account for most of the variants. Similar to what we detected in the phylogenetic analysis of subject 9018, one of the transmitted variants was maintained in the CSF but largely absent from the plasma viral population.

Phylogenetic analysis of the first time point for subject 7146 (156 dpi) revealed compartmentalization between the plasma and CSF viral populations (Figure 2.4A), and this was associated with increased inflammation in the CNS (see Table 2.1). In particular, one HIV-1 variant was clonally amplified in the CSF population (see bracket in Figure 2.4A). Compartmentalization was confirmed using the Slatkin-Maddison test ( $p=0.0047$ ), and the CSF population was still considered compartmentalized when the clonally amplified viral variants were removed from the analysis ( $p=0.0437$ ). The plasma and CSF populations in

subject 7146 were equilibrated by 177 dpi (Figure 2.5A; Slatkin-Maddison test,  $p=0.2964$ ), coincident with elevated measures of BBB disruption (Table 2.1). The CSF viral population was considered compartmentalized again at 203 dpi based on phylogenetic analysis (Figure 2.5B; Slatkin-Maddison test,  $p=0.0048$ ) and in the setting of a reduced CSF/plasma albumin ratio. We also detected a small cluster of clonally amplified sequences in the CSF-compartmentalized population at 203 dpi, although the viral populations were equilibrated again by 530 dpi (data not shown; Slatkin-Maddison test,  $p=0.877$ ).

A phylogenetic tree containing representative data from all four time points sampled for subject 7146 revealed that the clonally amplified variants in the CSF at 156 dpi had died out of the CSF population by 177 dpi, and did not give rise to any additional CSF viral variants (noted with a bracket in Figure 2.6). In addition, HIV-1 variants in the CSF that were compartmentalized at 203 dpi (noted with arrows) arose from one main branch in the phylogenetic tree, and these variants were lost by 530 dpi. Clonally amplified variants detected in the CSF at 203 dpi were also lost from the viral population by 530 dpi. We noticed that CSF sequences compartmentalized at 203 dpi branched with sequences detected in the CSF at 156 and 177 dpi, even though no compartmentalized variants were detected in the CSF at 177 dpi. This indicates that CSF variants detected at entry were maintained over the course of several months in the CNS of this subject. These data suggest that compartmentalization during primary infection can be resolved and recur later during infection. Additionally, transient clonal amplification can occur in the CSF-compartmentalized viral population.

## **DISCUSSION**

Extensive HIV-1 genetic compartmentalization between the periphery and the CNS has been reported in subjects with HAD (64, 65, 126, 218, 236, 242, 254, 256, 291). Compartmentalized viral variants present in the CSF of HAD subjects are thought to originate from long-lived cells in the CNS (271), and are maintained in the population by independent viral replication in the brain. The time that compartmentalization occurs during the course of HIV-1 infection has been a subject of debate, and the absence of CSF-compartmentalized variants during primary infection has supported the idea that compartmentalization occurs later during chronic infection (126, 254). The goal of our current work was to determine whether compartmentalized HIV-1 variants are present in the CSF of primary infection subjects, and to examine the evolution of CSF variants over the course of early HIV-1 infection.

In this study, we used heteroduplex tracking assays (HTAs) and single genome amplification (SGA) to identify CSF-compartmentalized variants and examine the compartmentalized viral populations. Cross-sectional HTA analysis revealed several examples of compartmentalized HIV-1 variants in the CSF early during HIV-1 infection. We also observed that compartmentalization during primary HIV-1 infection could be transient, and the compartmentalized variants in the CSF changed over time. Our SGA analyses confirmed the detection of compartmentalized variants in the CSF and identified clonal amplification of CSF variants in one subject with primary infection (subject 7146).

A proportion of the primary infection subjects enrolled in our study had low baseline CSF viral loads, even though the plasma viral loads were high. One explanation is that

plasma virus is not efficiently entering the CNS in these subjects, while another possibility is that HIV-1 that enters the CSF/CNS is being rapidly cleared. In either case, our data suggests that substantial autonomous viral replication is not occurring in the CNS of this subset of primary infection subjects. This is consistent with our finding that the majority of primary infection subjects in our study had concordant viral populations between the plasma and CSF compartments. The detection of equilibrated viral populations in the CSF early during HIV-1 infection indicates that the CSF compartment is accessible to most of the peripheral HIV-1 variants, and supports an absence of sustained viral replication in the CNS, although independent viral replication in the CNS may be occurring at a level below our limit of detection.

Three of the primary infection subjects that we analyzed had compartmentalized HIV-1 variants present in their CSF viral population, indicating that local viral replication can occur in the CNS at this stage. Subjects 9018 and 7146 had a multiple variant transmission event based on our sequence and phylogenetic data, where one HIV-1 lineage was detected in both the plasma and CSF, while a second transmitted virus lineage was only detected in the CSF virus population (Figure 2.3 and Figure 2.4). These data suggest that some CSF variants have properties that permit enhanced replication in the CNS, even early after viral transmission.

Phylogenetic and sequence analysis from subject 9040 revealed a V169R single amino acid substitution in the V1/V2 stem region of Env for CSF variants that were compartmentalized, and this change was not detected in any of the plasma *env* sequences. The compartmentalized HIV-1 variants in the CSF of subject 9018 had a similar Q170R substitution to a basic amino acid in the same region of the Env protein, and HIV-1 variants

in the plasma and CSF of 7146 had an R/K170 genotype. This suggests that perhaps basic amino acid substitutions in the V1/V2 stem of Env enhance viral replication in the CNS environment. One possibility is that additional basic amino acids in the V1/V2 stem could enhance the binding and entry of these viral variants to cells with low receptor densities on the surface, such as perivascular macrophages and microglia in the CNS. However, basic amino acid substitutions in the V1/V2 stem do not completely explain compartmentalization during primary infection since several subjects without compartmentalized variants in the CSF have additional basic amino acid substitutions within their plasma and CSF HIV-1 populations (data not shown).

Studies examining viral populations in the CSF of primary HIV-1 infection subjects have been limited; however, a small study by Harrington *et al.* (2007) examined the population dynamics of SIVsm E660 in the blood and CSF of macaques over the course of infection (123). A comparison of the blood and CSF viral populations revealed two distinct patterns of evolution: viral genetic concordance between the blood and CSF populations in two macaques, and discordance in the blood/CSF populations in a third macaque (123). Notably, the blood/CSF population discordance that was detected in animal C002 arose early after transmission (day 27) and persisted over the course of infection (123). Similarly, we detected concordance between the blood plasma and CSF viral populations for eight of the primary infection subjects in our study. Three subjects in our study showed discordance and compartmentalization in the CSF viral population, and this disturbance was apparent early after transmission (5 months). Additionally, Harrington *et. al* (2007) reported increased levels of CSF monocyte chemoattractant protein-1 (MCP-1) and statistically significant numbers of infiltrating CD68<sup>+</sup> macrophages in brain sections of macaque C002 compared to

other animals in the study (123). Human studies have also shown that the levels of chemokines such as interferon- $\gamma$ -inducible protein 10 (IP-10) and MCP-1 are elevated in the CSF of HAD subjects compared to asymptomatic subjects (32, 33, 155, 276). Although our measures of CNS inflammation differ from the macaque study, we detected elevated levels of CSF neopterin and pleocytosis in one subject with moderate CSF compartmentalization.

One easily measured marker of inflammation in the CNS is pleocytosis, defined as CSF WBC  $>5$  cells/ $\mu$ l (194, 286). Although pleocytosis can occur at any stage of neurological disease, during chronic infection increased CSF WBC counts are correlated with CSF HIV-1 RNA concentrations (195, 286). Subject 7146 had elevations in CSF WBC, as well as CSF neopterin and albumin ratio prior to initiation of antiretroviral therapy (see Table 2.1). We believe this inflammatory environment in the CNS resulted from both independent HIV-1 replication and the correlated meningitis detected at entry in subject 7146. The detection of BBB disruption also suggests an increased ability of lymphocytes to traverse the BBB and move into the CNS. Subjects 9018 and 9040 also had evidence of compartmentalization of CSF variants; however, CSF WBC, CSF neopterin, and albumin ratio levels were not distinct from those in subjects without compartmentalization. Thus, marked inflammation at a given time point is not necessary for the production or maintenance of compartmentalized variants.

One specific viral lineage in subject 7146 was clonally amplified in the CSF viral population at 156 dpi, and our longitudinal SGA analysis determined that this viral lineage died out in both the CSF and plasma populations by 177 dpi. We believe that an influx of inflammatory cells may have resulted in the clonal amplification of specific CSF viral variants at entry. Monocytes and CD4<sup>+</sup> T cells migrating into the CNS would provide a

larger target cell population for HIV-1 infection, and may stimulate increased HIV-1 replication in the CNS. A small population of clonally amplified variants was also detected in the CSF at 203 dpi when CSF pleocytosis was still apparent. These data suggest that independent HIV-1 replication may occur in the CNS of primary infection subjects with detectable compartmentalized variants, and this viral replication may cause increased inflammation in the CNS that can result in the clonal expansion of CSF variants.

In conclusion, our study illustrates a complex pattern of HIV-1 evolution in the CNS during primary/early infection. The majority of subjects in the primary stage of HIV-1 infection have equilibrated HIV-1 populations between the blood plasma and CSF; however, we detected compartmentalized HIV-1 variants in the CSF populations of three primary infection subjects. Two subjects with compartmentalized variants in the CSF were asymptomatic and did not show elevated levels of inflammatory markers in the CSF, suggesting that compartmentalized virus in the CSF/CNS can occur during primary HIV-1 infection in the absence of overt neurological symptoms. Additionally, sequence data from *env* genes obtained from subject 9040 (165 dpi) suggest that HIV-1 can rapidly adapt to enhance viral entry and growth in the context of the CNS environment. Early detection of CSF-compartmentalized variants may identify subjects that will have HIV-associated neurological problems later during infection since similar compartmentalization late in infection likely indicates a loss of control of viral replication in the periphery and is associated with HAD ((126); unpublished observation). Our results demonstrate that compartmentalization in the CNS compartment can arise shortly after HIV-1 transmission, and suggests that subjects with compartmentalization of viral variants in the CSF during

early infection should be considered for early antiretroviral therapy to reduce viral replication in the CNS.

## **ACKNOWLEDGEMENTS**

We thank Evelyn Lee for coordinating the clinical studies and materials, and the subjects for their participation. G. Schnell was supported in part by the NIH training grant T32-AI07001. This work was supported by the NIH award R01-MH67751 (to R.S.), the UNC Center for AIDS Research (NIH award P30-AI50410), the Lineberger Cancer Center core grant (NIH award P30-CA16086), NIH award K23-MH074466 and R01-MH81772 (to S.S.), NIH award R01-NS37660 (to R.W.P.), and NIH award UL1RR024131 (to UCSF).

**Table 2.1. Subject population characteristics and inflammatory markers.**

| Subject ID <sup>a</sup> | Sample date | DPI <sup>b</sup> | CD4 <sup>c</sup> | CSF WBC <sup>d</sup> | Plasma HIV RNA <sup>e</sup> | CSF HIV RNA <sup>e</sup> | Albumin ratio <sup>f</sup> | CSF neopterin <sup>g</sup> | % Diff. <sup>h</sup> |
|-------------------------|-------------|------------------|------------------|----------------------|-----------------------------|--------------------------|----------------------------|----------------------------|----------------------|
| 9003                    | 3/1/06      | 78               | 1044             | 2                    | 26,400                      | 49                       | 3.38                       | 7.3                        |                      |
| 9010                    | 10/10/06    | 235              | 497              | 11                   | 1,030                       | 206                      | 5.55                       | 9.5                        |                      |
| 9012                    | 2/8/07      | 103              | 601              | 8                    | 74,131                      | 398                      | 11.09                      | 14.3                       |                      |
| 9014                    | 3/20/07     | 169              | 751              | 12                   | 35,481                      | 537                      | 4.13                       | 8.5                        |                      |
| 9016                    | 4/24/07     | 143              | 353              | 1                    | 776,247                     | 49                       | 5.44                       | 6.6                        |                      |
| 9017                    | 6/20/07     | 49               | 361              | 14                   | 17,378                      | 151                      | 4.51                       | 8.6                        |                      |
| 9001                    | 12/14/05    | 206              | 488              | 3                    | 153,000                     | 246                      | 4.55                       | 14.3                       | NR                   |
|                         | 3/22/06     | 305              | 573              | 4                    | 194,000                     | 1,180                    | 3.50                       | 19.0                       | 19.0                 |
|                         | 6/21/06     | 393              | 575              | 5                    | 74,800                      | 4,120                    | 4.33                       | 20.5                       | 10.4                 |
| 9002                    | 2/15/06     | 86               | 770              | 6                    | 7,670                       | 19                       | 6.47                       | 8.9                        | 0                    |
|                         | 4/6/06      | 137              | 686              | 2                    | 16,500                      | 208                      | 6.69                       | 11.3                       | 0                    |
|                         | 8/22/06     | 273              | 539              | 8                    | 44,800                      | 4,560                    | 7.35                       | 21.0                       | 0                    |
|                         | 9/26/06     | 306              | 542              | 14                   | 32,400                      | 4,630                    | 9.29                       | 21.3                       | 0                    |
|                         | 10/26/06    | 336              | 501              | 14                   | 37,200                      | 12,000                   | 9.61                       | 17.0                       | 0                    |
|                         | 12/14/06    | 384              | 640              | 12                   | 198,000                     | 8,130                    | 9.67                       | 15.1                       | 0                    |
|                         | 5/8/07      | 528              | 546              | 11                   | 13,800                      | 1,280                    | 9.79                       | 9.0                        | 0                    |
|                         | 7/17/07     | 597              | 459              | 2                    | 40,000                      | 515                      | 8.73                       | 10.1                       | 6.6                  |
| 9006                    | 9/14/06     | 150              | 435              | 8                    | 27,700                      | 1,300                    | 4.64                       | 12.9                       | 0                    |
|                         | 11/1/06     | 197              | 512              | 6                    | 29,000                      | 1,310                    | 4.31                       | n/a                        | 0                    |
|                         | 3/20/07     | 336              | 453              | 6                    | 65,600                      | 1,620                    | 3.75                       | n/a                        | 15.9                 |
| 9007                    | 9/18/06     | 149              | 256              | 4                    | 233,000                     | 426                      | 10.85                      | 33.1                       | NR                   |
|                         | 11/2/06     | 193              | 336              | 9                    | 183,000                     | 3,250                    | 7.88                       | 23.5                       | 14.4                 |
|                         | 6/5/07      | 406              | 292              | 4                    | 29,500                      | 3,900                    | 6.87                       | 22.9                       | 7.4                  |
| 9019                    | 8/13/07     | 58               | 750              | 13                   | 49,300                      | 1,390                    | 5.58                       | 13.9                       | 2.2                  |
| 9025                    | 4/21/08     | 50               | 752              | 7                    | 101,000                     | 15,200                   | 3.91                       | n/a                        | n/a                  |
| 9037                    | 5/14/09     | 46               | 884              | 26                   | 507,652                     | 2,682                    | 6.35                       | n/a                        | n/a                  |
| 9039                    | 6/1/09      | 36               | 539              | 53                   | 367,728                     | 19,911                   | 9.31                       | n/a                        | n/a                  |
| 9018                    | 8/2/07      | 198              | 350              | 11                   | 404,000                     | 37,500                   | 6.45                       | 11.6                       | 29.2                 |
| 9040                    | 6/15/09     | 165              | 705              | 4                    | 16,710                      | 6,176                    | 7.67                       | n/a                        | n/a                  |
| 7146                    | 9/23/03     | 156              | 552              | 86                   | 429,000                     | 168,000                  | 14.35                      | 56.6                       | 23.9                 |
|                         | 10/14/03    | 177              | 476              | 97                   | 217,000                     | 24,900                   | 14.35                      | 41.2                       | 19.1                 |
|                         | 11/10/03    | 203              | 310              | 53                   | 103,000                     | 26,000                   | 7.12                       | 23.5                       | 41.1                 |
|                         | 4/29/04     | 372              | 380              | 1                    | 13,399                      | 19                       | 4.39                       | 14.5                       | n/a                  |
|                         | 6/24/04     | 427              | 337              | 2                    | 225,000                     | 36                       | 7.31                       | n/a                        | n/a                  |
|                         | 10/7/04     | 530              | 305              | 2                    | 308,000                     | 2,630                    | 5.40                       | 20.0                       | 15.9                 |

<sup>a</sup>= Antibody data. Subject 9003: 1 band (p24) 12/20/05. Subject 9010: negative Ab 8/2005. Subject 9012: not known. Subject 9014: negative Ab on 8/4/06; positive Ab on 12/6/07. Subject 9016: positive HIV RNA, negative Ab 12/27/06. Subject 9017: not known. Subject 9001: negative Ab 5/25/05; 10 bands 11/1/05. Subject 9002: 10 bands 1/3/06. Subject 9006: 2 bands (p24, gp160) 5/5/06. Subject 9007: not known. Subject 9019: positive HIV RNA, negative Ab 6/2007. Subject 9025: negative HIV RNA 1/14/08; HIV RNA 10,000 cps/ml, negative Oraquick 3/13/08; positive Ab 3/20/08. Subject 9037: negative EIA with positive

ELISA 4/19/09. Subject 9039: not known. Subject 9018: last negative Ab 11/4/06. Subject 9040: negative Ab 11/4/08; negative Ab 2/24/09. Subject 7146: negative Ab 3/25/03.

<sup>b</sup>= estimated days post-infection

<sup>c</sup>= cells/ $\mu$ l

<sup>d</sup>= CSF white blood cell counts (cells/ $\mu$ l)

<sup>e</sup>= copies/ml

<sup>f</sup>= CSF/plasma albumin ratio

<sup>g</sup>= nmol/L; n/a=not applicable

<sup>h</sup> = Percent difference values between plasma and CSF viral populations as measured by HTA. Reported values are the average calculated from two independent HTA replicates (see refs. (159, 251) for methods). Percent difference values were not measured for subjects 9003, 9010, 9012, 9014, 9016, and 9017 due to low CSF HIV-1 RNA levels. n/a=not applicable; NR=not reported due to poor sampling

**Table 2.2. Single genome amplification results.**

| Subject ID | Sample date | DPI <sup>a</sup> | Plasma amplicons | CSF amplicons | CSF compartment <sup>b</sup> |
|------------|-------------|------------------|------------------|---------------|------------------------------|
| 9002       | 10/26/06    | 338              | 20               | 26            | Eq                           |
| 9007       | 9/18/06     | 149              | 29               | 15            | Eq                           |
|            | 6/5/07      | 406              | 20               | 28            | Uneq                         |
| 9018       | 8/2/07      | 198              | 29               | 22            | Comp                         |
| 9025       | 4/21/08     | 50               | 19               | 27            | Eq                           |
| 9037       | 5/14/09     | 46               | 37               | 29            | Eq                           |
| 9039       | 6/1/09      | 36               | 40               | 24            | Eq                           |
| 9040       | 6/15/09     | 165              | 23               | 24            | Comp                         |
| 7146       | 9/23/03     | 156              | 22               | 27            | Comp, Amp                    |
|            | 10/14/03    | 177              | 36               | 29            | Eq                           |
|            | 11/10/03    | 203              | 26               | 26            | Comp, Amp                    |
|            | 10/7/04     | 530              | 33               | 22            | Eq                           |

<sup>a</sup>= estimated days post-infection

<sup>b</sup>= HIV-1 population characteristics in the CSF compartment. Eq=equilibration with the blood plasma; Uneq=discordance between the CSF and blood plasma without substantial compartmentalization; Comp=compartmentalization in the CSF; Amp=clonal amplification of variants detected in the CSF

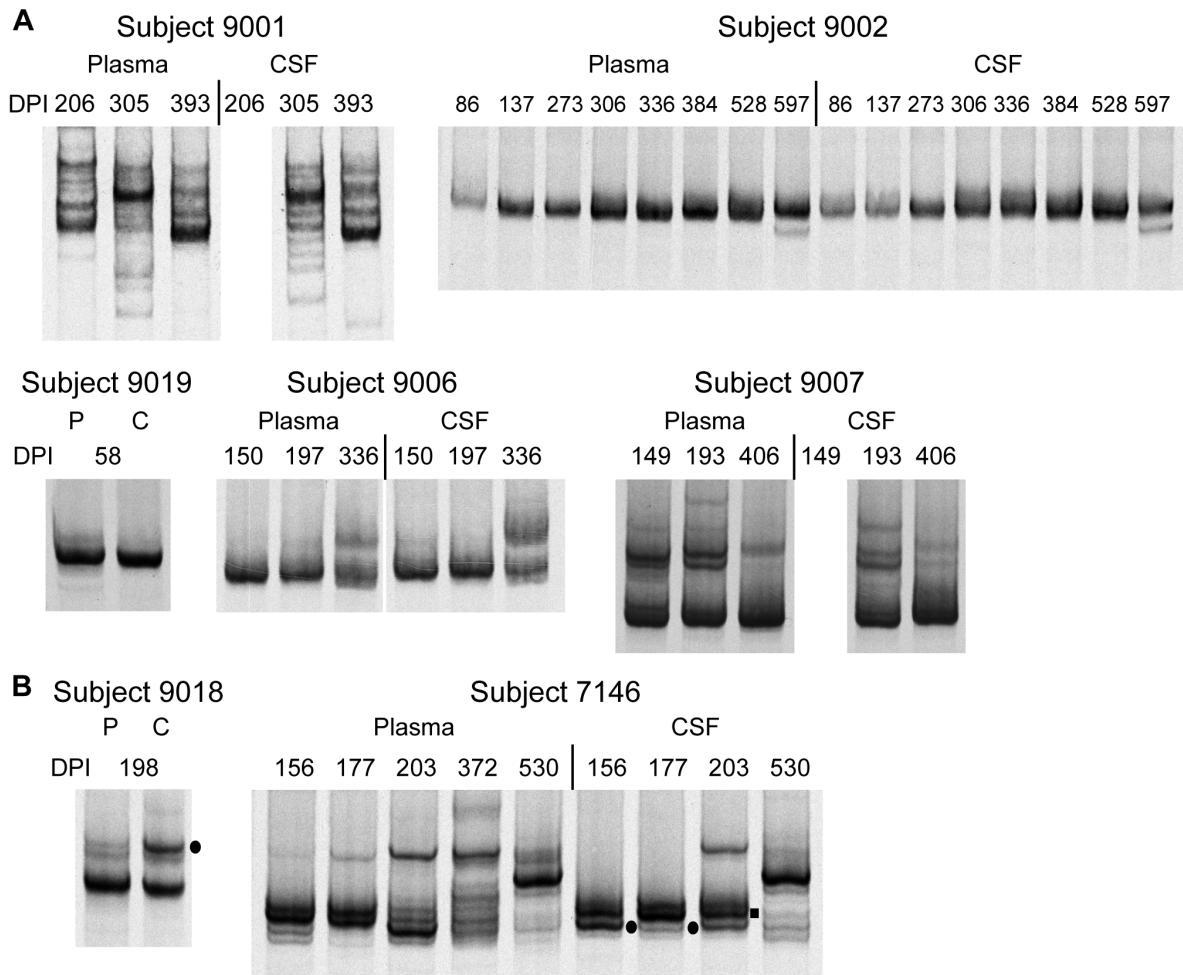


**Figure 2.1. Cross-sectional and longitudinal HTA analysis of HIV-1 in the blood plasma and CSF of primary infection subjects. (A)** Longitudinal V1/V2 or V4/V5 HTA analysis of HIV-1 using paired blood plasma and CSF samples from 5 subjects without compartmentalized CSF variants. The HTA shown for subject 9007 targeted the V1/V2 region of *env*, and the V4/V5 HTA is shown for all other subjects. Sample time points are listed above each HTA gel as days post-infection (DPI). The HTA gel images for the CSF viral population of subject 9001 at 206 dpi and subject 9007 at 149 dpi are not included in the figure because there was poor reproducibility between the HTA replicates due to low CSF viral load. **(B)** Longitudinal V4/V5 HTA analysis of HIV-1 using paired blood and CSF samples from 2 subjects with compartmentalized CSF variants. CSF-compartmentalized variants are indicated with a filled black circle next to the gel image. Variants that are enriched in the CSF are indicated with a filled black square next to the gel image.

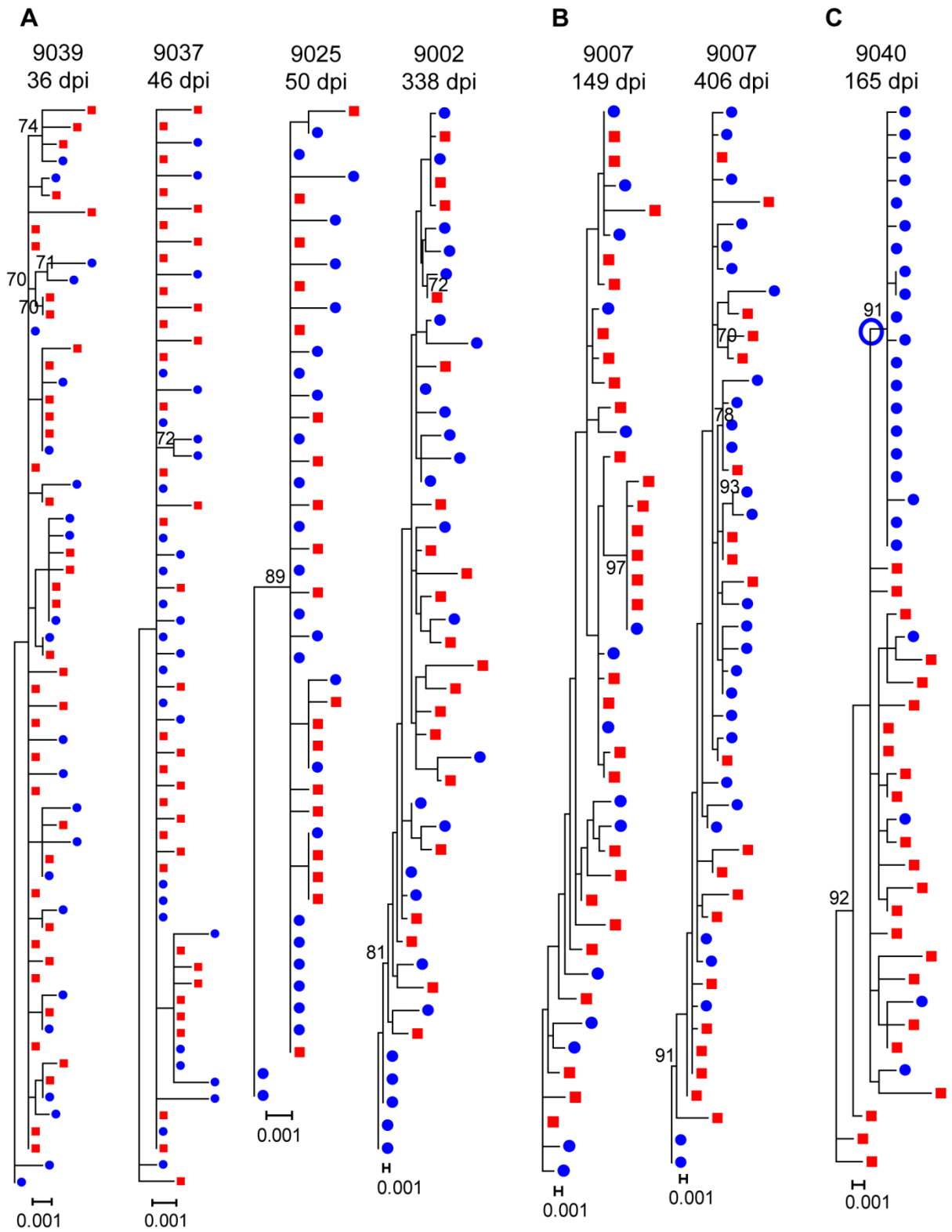


**Figure 2.2. Phylogenetic analysis of plasma and CSF HIV-1 populations. (A)** Phylogenetic trees of HIV-1 *env* sequences for subjects 9002, 9025, 9037, and 9039, which

display equilibration between blood plasma and CSF HIV-1 populations. **(B)** Phylogenetic trees of HIV-1 *env* sequences for subject 9007 at 149 dpi and 406 dpi. HIV-1 populations were equilibrated at 149 dpi, but became slightly discordant at 406 dpi. **(C)** Phylogenetic tree of HIV-1 *env* sequences for subject 9040, which displays significant compartmentalization in the CSF. The blue circle illustrates the node of divergence for the compartmentalized CSF sequences. SGA amplicons were first aligned, and a maximum-likelihood phylogenetic tree was constructed using PhyML. Bootstrap numbers  $\geq 70$  are indicated at the appropriate nodes. Sequences obtained from the CSF are labeled with solid blue circles, and plasma sequences are labeled with solid red rectangles on the tree. Genetic distance between sequences is indicated by the distance scale bar at the bottom of the tree.

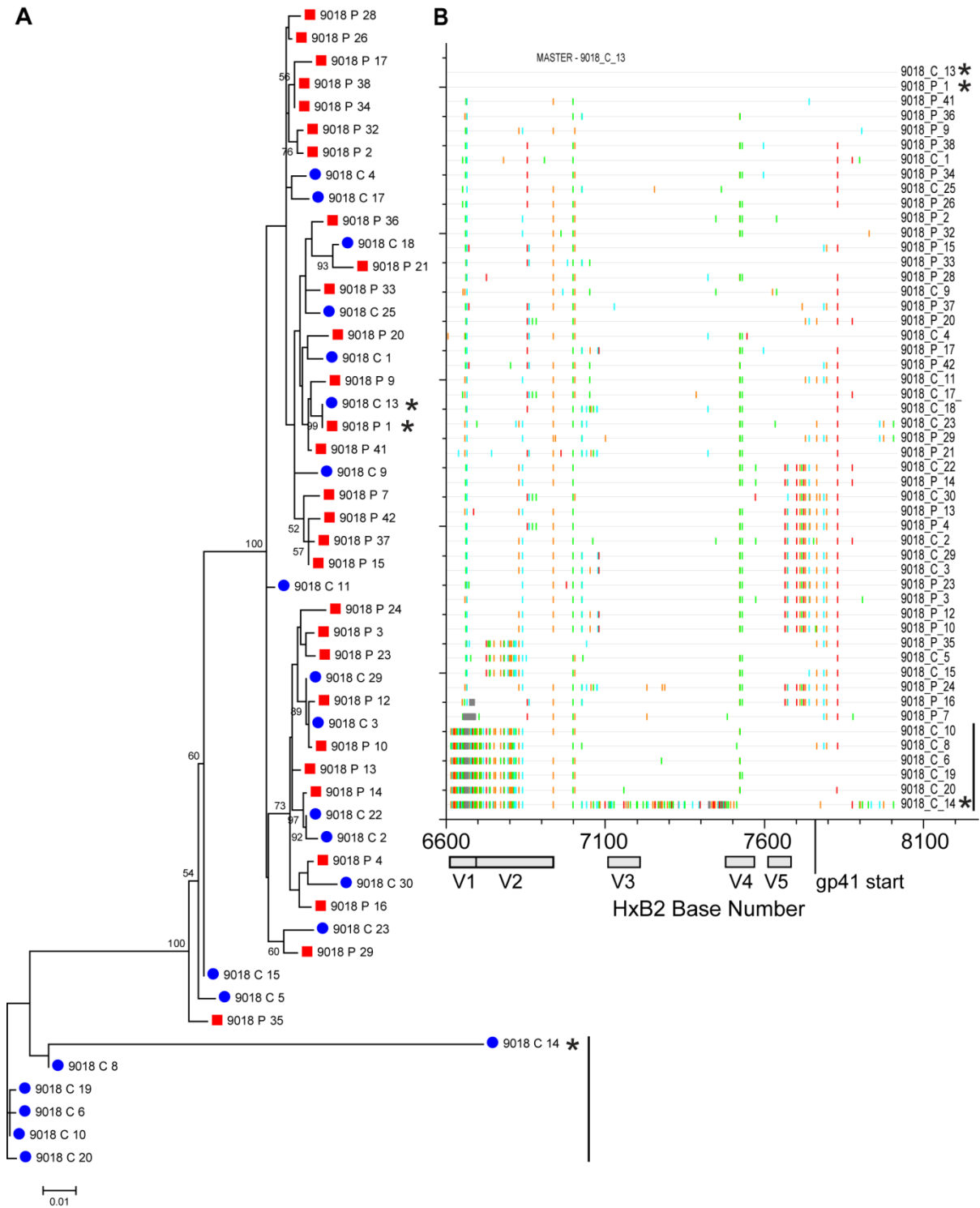


**Figure 2.3. Phylogenetic and sequence analyses of plasma and CSF HIV-1 populations at 198 dpi for subject 9018. (A) Maximum-likelihood phylogenetic tree. Sequences from the CSF (C) are labeled with solid blue circles, and plasma sequences (P) are labeled with solid red rectangles. Genetic distance between sequences is indicated by the scale bar**

located at the bottom of the tree. Bootstrap values >50 are labeled at the appropriate nodes. Putative transmitted viruses are labeled with asterisks, and CSF populations that were considered compartmentalized based on the phylogenetic analysis are indicated with a solid black line. **(B)** Highlighter plot of aligned *env* plasma and CSF sequences. The HXB2 base number is indicated on the x-axis, and the sequence ID is indicated on the y-axis. Base changes are indicated by the following ticks on the highlighter plot: A=green, T=red, G=orange, C=light blue, Gaps=gray.

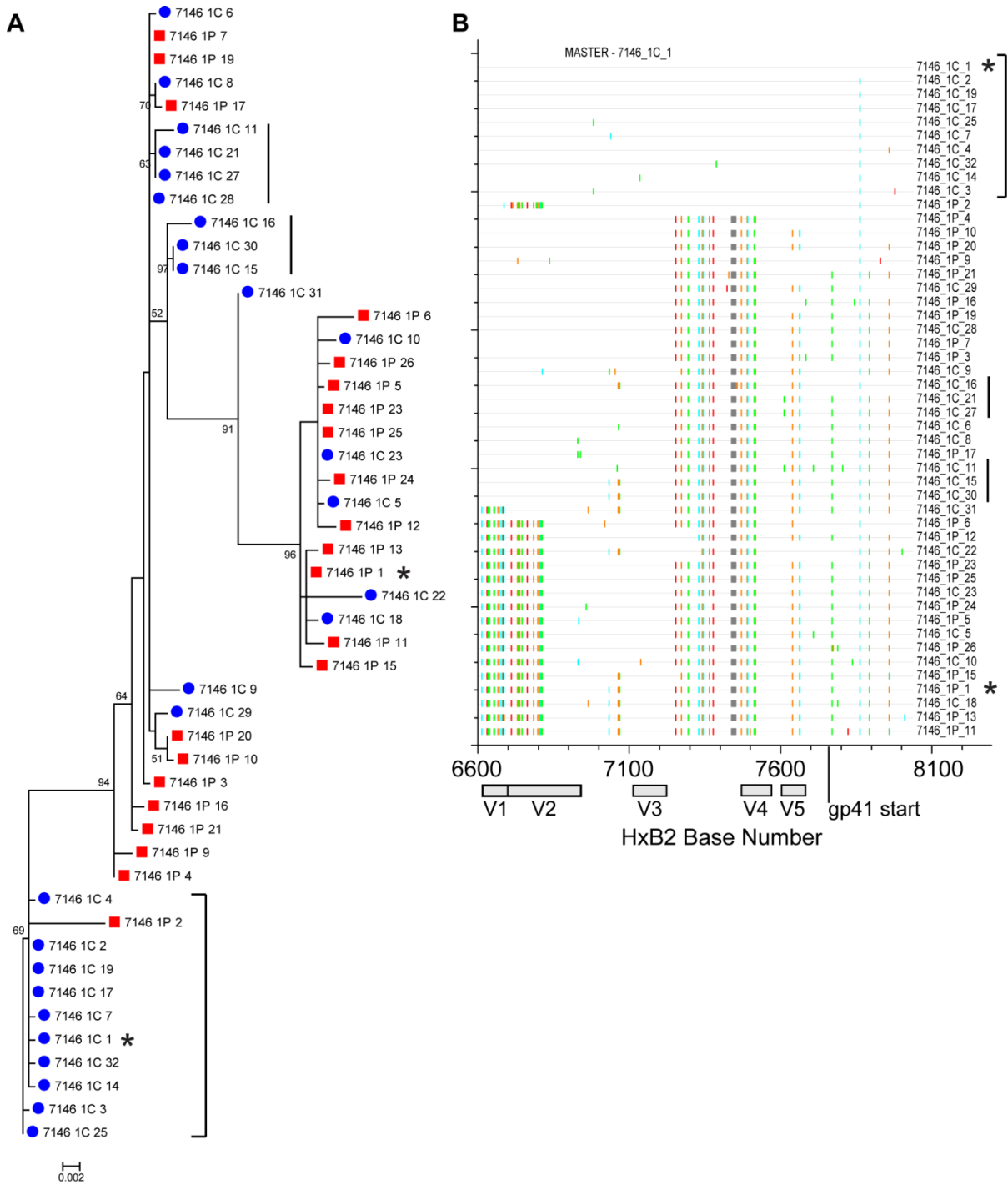


**Figure 2.4. Phylogenetic and sequence analyses of subject 7146 HIV-1 populations in the plasma and CSF at 156 dpi.** (A) Maximum-likelihood phylogenetic tree. Sequences from the CSF (C) are labeled with solid blue circles, and plasma sequences (P) are labeled with solid red rectangles. Bootstrap values >50 are labeled at the appropriate nodes. Genetic distance between sequences is indicated by the scale bar located at the bottom of the tree. The clonally amplified HIV-1 variants in the CSF population are indicated by the black

bracket. Putative transmitted viruses are labeled with asterisks, and CSF populations that were compartmentalized are indicated with a solid black line. **(B)** Highlighter plot of aligned plasma and CSF *env* sequences. The HXB2 base number is indicated on the x-axis, and the sequence ID is indicated on the y-axis. Base changes are indicated by the following ticks on the highlighter plot: A=green, T=red, G=orange, C=light blue, Gaps=gray.

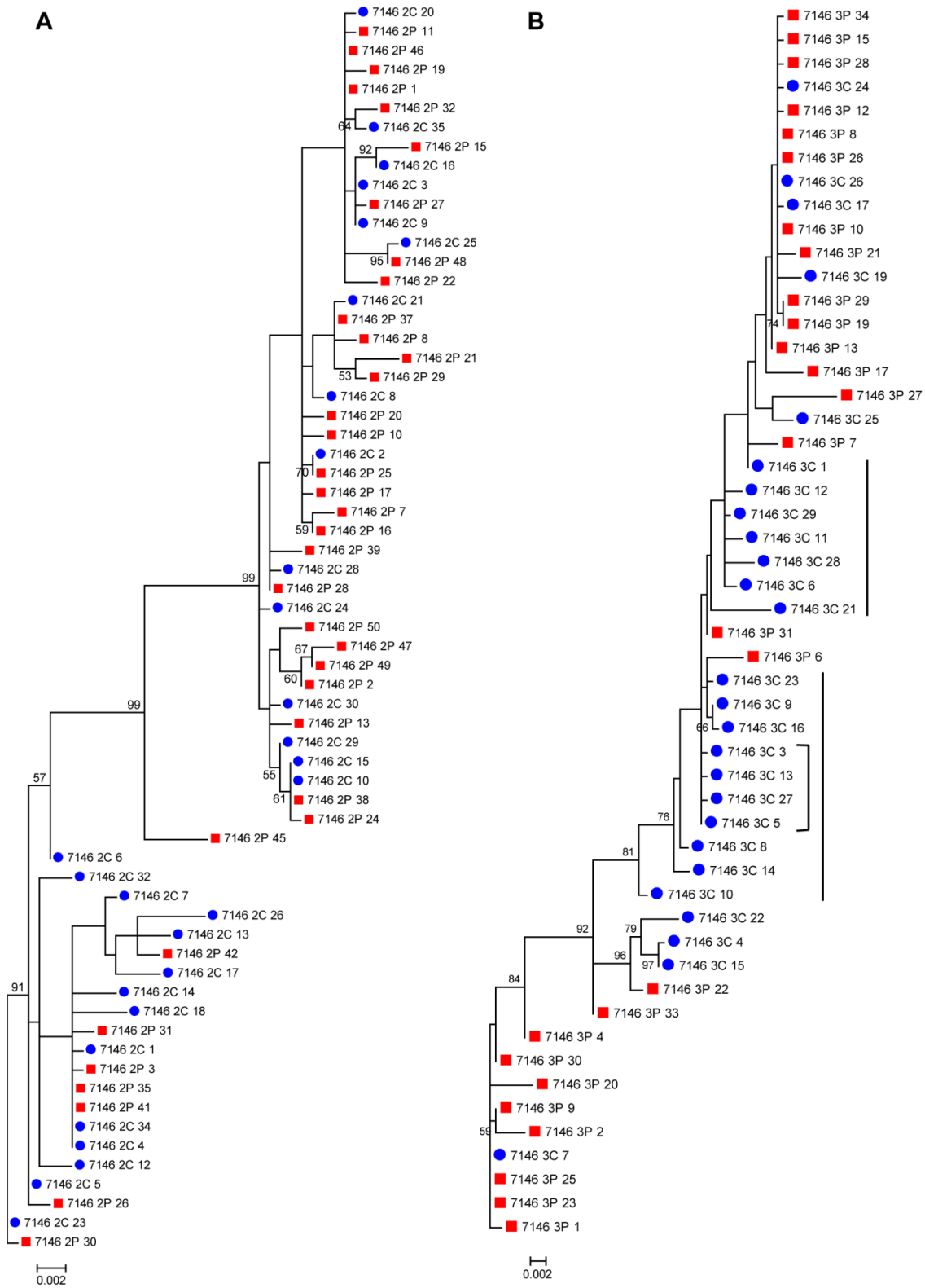


**Figure 2.5. Phylogenetic analysis of subject 7146 HIV-1 populations at days 177 and 203 post-infection. (A) Phylogenetic tree of plasma and CSF HIV-1 *env* sequences at 177**

dpi. **(B)** Phylogenetic tree of HIV-1 populations at 203 dpi. Sequences from the CSF (C) are labeled with solid blue circles, and plasma sequences (P) are labeled with solid red rectangles. The CSF sequences that were considered compartmentalized are indicated by the solid black lines. Clonally amplified HIV-1 variants in the CSF population are indicated by the black bracket. Bootstrap values  $>50$  are labeled at the appropriate nodes. Genetic distance between sequences is indicated by the scale bar located at the bottom of the tree.

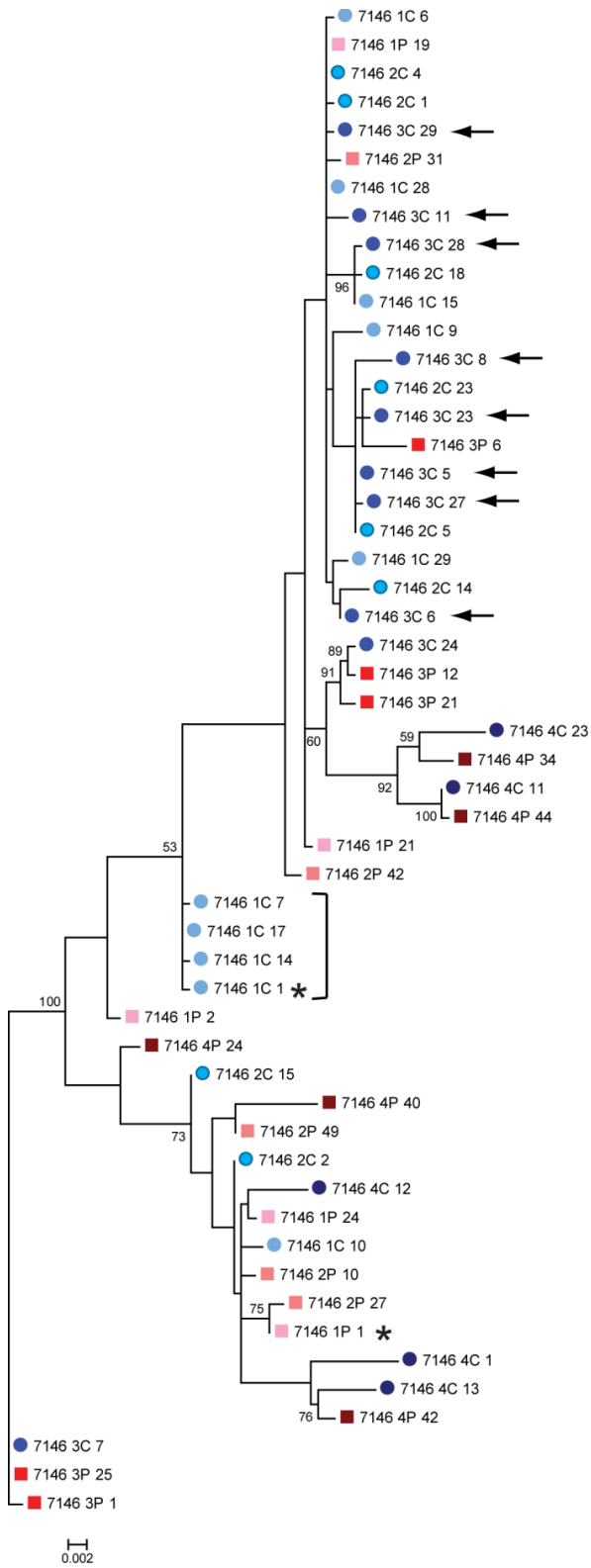


**Figure 2.6. Longitudinal phylogenetic analysis of subject 7146 HIV-1 populations.** Phylogenetic tree of a representative set of plasma and CSF HIV-1 sequences from 156 dpi

(1P=light pink square; 1C=light blue circle), 177 dpi (2P=dark pink square; 2C=bright blue circle with dark outline), 203 dpi (3P=bright red square; 3C=royal blue circle), and 530 dpi (4P=dark red-brown square; 4C=navy blue circle). CSF sequences that were clonally amplified at 156 dpi are indicated by the black bracket, and CSF sequences that were considered compartmentalized at 203 dpi are indicated with black arrows. The putative transmitted variants are labeled with asterisks. Bootstrap values >50 are labeled at the appropriate nodes. Genetic distance between sequences is indicated by the scale bar located at the bottom of the tree.

## **CHAPTER THREE**

### **COMPARTMENTALIZED HUMAN IMMUNODEFICIENCY VIRUS TYPE 1 ORIGINATES FROM LONG-LIVED CELLS IN SOME SUBJECTS WITH HIV-1- ASSOCIATED DEMENTIA**

Reprinted from: Schnell, G., S. Spudich, P. Harrington, R. W. Price, and R. Swanstrom.  
2009. Compartmentalized human immunodeficiency virus type 1 originates from long-lived  
cells in some subjects with HIV-1-associated dementia. PLoS Pathog 5:e1000395.

## ABSTRACT

Human immunodeficiency virus type 1 (HIV-1) invades the central nervous system (CNS) shortly after systemic infection, and can result in the subsequent development of HIV-1-associated dementia (HAD) in a subset of infected individuals. Genetically compartmentalized virus in the CNS is associated with HAD, suggesting autonomous viral replication as a factor in the disease process. We examined the source of compartmentalized HIV-1 in the CNS of subjects with HIV-1-associated neurological disease and in asymptomatic subjects who were initiating antiretroviral therapy. The heteroduplex tracking assay (HTA), targeting the variable regions of *env*, was used to determine which HIV-1 genetic variants in the cerebrospinal fluid (CSF) were compartmentalized and which variants were shared with the blood plasma. We then measured the viral decay kinetics of individual variants after the initiation of antiretroviral therapy. Compartmentalized HIV-1 variants in the CSF of asymptomatic subjects decayed rapidly after the initiation of antiretroviral therapy, with a mean half-life of 1.57 days. Rapid viral decay was also measured for CSF-compartmentalized variants in four HAD subjects ( $t_{1/2}$  mean = 2.27 days). However, slow viral decay was measured for CSF-compartmentalized variants from an additional four subjects with neurological disease ( $t_{1/2}$  range = 9.85 days to no initial decay). The slow decay detected for CSF-compartmentalized variants was not associated with poor CNS drug penetration, drug resistant virus in the CSF, or the presence of X4 virus genotypes. We found that the slow decay measured for CSF-compartmentalized variants in subjects with neurological disease was correlated with low peripheral CD4 cell count and reduced CSF pleocytosis. We propose a model in which infiltrating macrophages replace CD4<sup>+</sup> T cells as

the primary source of productive viral replication in the CNS to maintain high viral loads in the CSF in a substantial subset of subjects with HAD.

## **AUTHOR SUMMARY**

Infection of the central nervous system (CNS) with human immunodeficiency virus type 1 (HIV-1) can lead to the development of HIV-1-associated dementia, a severe neurological disease that results in cognitive and motor impairment. Individuals that are chronically infected with HIV-1 sometimes display unique viral variants in their cerebrospinal fluid (CSF) that are not detected in the blood virus population, termed CSF-compartmentalized variants. The cell type that produces CSF-compartmentalized virus throughout the course of infection has not been determined. We used a sensitive assay to detect compartmentalized variants in the CSF of subjects with and without neurological disease, and then measured the decay kinetics of compartmentalized virus when subjects were starting antiretroviral therapy. We found that compartmentalized virus decays rapidly in asymptomatic subjects. Additionally, we detected differential decay (i.e. rapid or slow) in subjects with neurological disease, and this was associated with the number of white blood cells in the CSF. Our data supports a model of HIV-1 infection in the CNS where compartmentalized virus is produced by a long-lived cell type (slow decay), and this virus can be amplified by short-lived cells (rapid decay) that traffic into the CNS, but is increasingly produced from long-lived cells in the immunodeficient state.

## INTRODUCTION

Human immunodeficiency virus type 1 (HIV-1)-associated dementia (HAD) is a severe neurological disease that affects a subset of HIV-1-infected individuals (14, 107). HIV-1 infection of the central nervous system (CNS) occurs shortly after peripheral infection, most likely through the trafficking of infected lymphocytes and monocytes across the blood-brain barrier (BBB) (197, 216). Once HIV-1 crosses the BBB it can infect perivascular macrophages and brain-resident microglia, and some studies have shown that neurotropic viruses preferentially infect macrophages (108, 161, 256, 298). HIV-1 may persist in the CNS during therapy due to the insufficient CNS penetration of some antiretroviral drugs (103, 107, 239, 272).

HIV-1 variants have been detected at autopsy in the brains of HAD subjects, and these brain-derived variants are genetically distinct from virus detected in the peripheral blood (64, 65, 218, 242, 256). A principal impediment to studying viral evolution in the CNS is that direct sampling of HIV-1 in brain tissue is usually possible only once, at biopsy or autopsy. To examine viral populations in the CNS over the course of HIV-1 infection we have relied upon repeated sampling of virus in the cerebrospinal fluid (CSF). Previous studies have shown that virus detected in the CSF originates from both local CNS tissue and the peripheral blood (69, 70, 96, 119), indicating that the CSF may act as a site of mixing of virus present in the brain and the periphery. In addition, genetic compartmentalization has been reported between blood plasma and CSF viral variants (126, 236, 254, 291). We previously examined the cellular sources of HIV-1 in the CNS by utilizing the heteroduplex tracking assay (HTA) to measure viral decay rates in HIV-1-infected subjects initiating

antiretroviral therapy (124). In this study we reported that the subset of compartmentalized virus detected in the CSF of four asymptomatic subjects decayed rapidly after the initiation of therapy, suggesting that the compartmentalized virus is coming from a short-lived cell type, such as CD4<sup>+</sup> T cells (124).

The population dynamics of systemic HIV-1 replication have been studied extensively (139, 231, 311), but the extent of viral replication in specific cell types in the CNS over the course of disease is not yet known. The use of antiretroviral drugs to prevent HIV-1 infection of uninfected cells provides a tool for “viewing” the rate of decay for cell-free virus and virally-infected cells. HIV-1 decay in peripheral blood after the initiation of highly active antiretroviral therapy (HAART) occurs in at least two phases (139, 311). The first phase of decay is rapid and has been proposed to represent the turnover of cell-free virions and productively infected CD4<sup>+</sup> T cells (139, 231, 281, 311). The second phase is slower and may reflect the decay of long-lived infected cells, possibly latently infected resting CD4<sup>+</sup> T cells and cells of the monocyte lineage (139, 279, 281, 311), and the release of virions from follicular dendritic cells (138, 281). Recently, a study using the integrase inhibitor raltegravir reported altered HIV-1 decay kinetics and a reduction of the second viral decay phase (207), suggesting integration as a rate limiting step of infection in a subset of cells. The implications of these data on measured viral decay rates remain to be clarified; however, the reduction in the second phase of HIV-1 decay may indicate that longer-lived HIV-1-infected cells contribute less to total viral load than previously thought, but it does not preclude the possibility that the second phase of HIV-1 decay may reflect the turnover of long-lived cells (207, 275).

In this study, we characterized the lifespan of the cellular source of compartmentalized HIV-1 in the CNS of subjects with and without symptomatic neurological disease by calculating viral decay rates during the initiation of antiretroviral therapy. The heteroduplex tracking assay (HTA) (51, 52) was used to distinguish between HIV-1 genetic variants in the CSF that were either compartmentalized to the CSF or equilibrated with the peripheral blood. HTA has been used in previous studies to differentiate between HIV-1 genetic variants in separate anatomical compartments (50, 124, 131, 254) and HIV-1 evolutionary variants (49, 125, 159, 212, 251, 253), including drug resistance mutations (151, 250). The HTA is a useful tool for resolving and quantifying complex viral populations based on their genotype, and is able to detect HIV-1 variants that comprise as little as 1-3% of the total viral population. We targeted the variable regions of the *env* gene for HTA analysis of our subject population in order to resolve multiple HIV-1 genetic variants. In this study we confirm rapid viral decay in the CSF of asymptomatic subjects initiating HAART, and we report reduced rates of viral decay of compartmentalized virus in the CSF in a subset of neurologically symptomatic subjects initiating antiretroviral therapy. These results suggest a shift in the cell type that produces the bulk of the virus in the CSF late in disease as part of the process of viral pathogenesis in the CNS.

## **RESULTS**

### **Subject population characteristics.**

Our analysis included 11 asymptomatic subjects (7 new subjects, 4 subjects reported in (124)), 1 subject with minor cognitive motor disorder (MCMD), and 7 subjects with HIV-1-associated dementia (HAD; see Table 3.1). In general, subjects with HAD have higher viral load in the CSF (70, 71, 307) and increased HIV-1 compartmentalization in the CSF (126, 254). To assess compartmentalization we measured the relative abundance of HIV-1 variants in the blood plasma and CSF as resolved by the heteroduplex tracking assay (HTA), then calculated the percent difference values between the two viral populations (see Table 3.2). We found that the CSF and plasma viral populations were different for subjects with HIV-associated neurological disease (average = 67% different; range = 36 – 88% different) compared to the asymptomatic subjects (average = 42% different; range = 10 – 78% different). This difference approached statistical significance in spite of the small sample size ( $p = 0.054$  using a two-tailed Mann-Whitney test), and this trend of increased viral compartmentalization in the CSF with HAD is consistent with the difference seen in a larger cross-sectional analysis (126). We next used the HTA to follow differential decay of shared and compartmentalized variants when subjects initiated therapy. In this study, the subjects had an average reduction of 91% of the virus in the blood, and 88% of the virus in the CSF, over the period of sampling for HTA analysis (Table 3.2).

### **Compartmentalized HIV-1 in the CSF of asymptomatic subjects decays rapidly.**

The HTA is a useful tool for sampling complex viral populations, and is sensitive enough to detect minor variants within the population. We utilized HTAs targeting the hyper-variable regions V1/V2 and V4/V5 of the *env* gene to detect and measure the decay of individual HIV-1 variants in the cerebrospinal fluid and plasma of subjects initiating HAART. The HTA that was the most reproducible (V1/V2 or V4/V5) was used for the final decay and half-life calculations. The half-lives for the different variants in the blood for four of these subjects have been reported previously (143).

The V1/V2 and V4/V5 HTA analyses for the seven new asymptomatic subjects revealed rapid HIV-1 decay for both compartmentalized and shared variants detected in the CSF (see Figure 3.1). The decay of individual variants was organized into two groups for half-life analysis: decay of CSF-compartmentalized variants and decay of variants shared between the blood and the CSF. The HTA gels for the longitudinal samples from the seven new asymptomatic subjects are shown in Figure 3.1A, and graphs representing the viral decay are shown in Figure 3.1B. In this analysis, viral variants that decay more slowly will make up an increasing percentage of the total viral population over the course of therapy. However, if all variants decay at the same rate then the relative percentages will remain the same over time. HIV-1 half-lives for plasma and CSF variants were calculated based on the slopes of the decay curves (summarized in Table 3.2). Based on data generated from the seven new asymptomatic subjects analyzed in this study, half-lives calculated for the total plasma viral load decay were short ( $t_{1/2}$  mean = 1.46 days;  $t_{1/2}$  range = 0.58 – 2.27 days), and total CSF viral load half-lives were short ( $t_{1/2}$  mean = 1.5 days;  $t_{1/2}$  range = 0.77 – 2.04 days). These half-lives are similar to the data reported for 4 asymptomatic subjects that were previously studied (124).

Although some asymptomatic subjects have large percent difference values between the blood and CSF viral populations, not all of the variants detected in the CSF met the criteria for compartmentalization. Viral variants in the CSF were considered compartmentalized if they were unique to the CSF or they were present in a substantially higher concentration in the CSF compared to the plasma. CSF-compartmentalized variants were detected in asymptomatic subjects 5005, 4014, and 4022. To increase our sample size we included the half-life data from the four asymptomatic subjects reported in ref. (124) in our analysis of CSF-compartmentalized decay. Including these additional four subjects (n=7 total asymptomatic subjects with some compartmentalized virus: 3 new subjects and 4 previously reported subjects), we found that the half-lives for CSF-compartmentalized variants in these subjects were short, with a mean of 1.57 days ( $t_{1/2}$  range = 0.75 – 2.75 days; see below). These data indicate that CSF-compartmentalized virus in asymptomatic subjects is most likely originating from a short-lived cell type, such as a CD4<sup>+</sup> T cell. The reported half-life of a productively infected CD4<sup>+</sup> T cell is approximately 2 days (281), which coincides with our average measured half-life of 1.57 days in these subjects.

**Differential decay of compartmentalized HIV-1 in the CSF of neurologically symptomatic subjects is correlated with immunodeficiency and CSF pleocytosis.**

We expanded our analysis of viral decay to HIV-1-infected subjects who were diagnosed with either MCMD or HAD to address the hypothesis that CSF-compartmentalized variants in these subjects originate from longer-lived cells. Viral decay in the CSF of eight subjects with neurological disease was analyzed using HTAs targeting the V1/V2 and V4/V5 regions of *env*. The HTA analyses for the eight subjects with HIV-

associated neurological disease showed either rapid or slow viral decay among the subjects. The longitudinal HTA gels for each neurologically symptomatic subject are shown in Figure 3.2A, and the graphs of viral decay are shown in Figure 3.2B and 3.2C. Similar to the asymptomatic subject decay analysis, individual variants were grouped as either CSF-compartmentalized variants or variants shared between the blood and the CSF for the decay analysis.

Total plasma viral load decay was rapid for all subjects with neurological disease, with a mean half-life of 2.11 days ( $t_{1/2}$  range = 1.42 – 2.91 days; summarized in Table 3.2 and Figure 3.3). We measured rapid viral decay for CSF-compartmentalized variants after the initiation of HAART for four subjects with HAD (4033, 5003, 7036, 4051;  $t_{1/2}$  mean = 2.27 days;  $t_{1/2}$  range = 1.23 – 3.67 days; Figure 3.2B and 3.3; summarized in Table 3.2), similar to asymptomatic subjects. In contrast, prolonged viral decay was measured for CSF-compartmentalized variants for the other four subjects with neurological disease (4013, 5002, 4059, 7115;  $t_{1/2}$  range = 9.85 days to no initial decay), with three subjects displaying biphasic decay. CSF-compartmentalized variants for subjects 4013, 5002, and 7115 displayed a biphasic decay (see Figure 3.2C), where the first phase of viral decay was slow (4013  $t_{1/2}$  = 28.5 days; 7115  $t_{1/2}$  = no initial decay; 5002  $t_{1/2}$  = no initial decay), and the second phase was faster (4013  $t_{1/2}$  = 3.9 days; 7115  $t_{1/2}$  = 6.4 days; 5002  $t_{1/2}$  = 4.24 days). Figure 3.3 and Table 3.2 report the half-lives calculated for both phases of decay. Subject 4059 displayed only a slower decay rate for the CSF-compartmentalized variants ( $t_{1/2}$  = 9.85 days). Total CSF viral load decay was similar to the decay rates measured for CSF-compartmentalized variants for all subjects with neurological disease. This is due to the fact that most of the virus in the CSF was compartmentalized in these HAD subjects. The decay of the small amounts of

shared variants fluctuated in these subjects from decreasing with a rate similar to the virus in plasma to decreasing with a slow rate similar to that of the CSF-compartmentalized variants (see Table 3.2).

For each CSF sample time point the CSF white blood cell (WBC) count was measured to determine if any subjects had CSF pleocytosis (defined as  $>5$  cells/ $\mu$ l; (194, 286)). We found that all four subjects with rapid CSF-compartmentalized variant decay either had high CSF WBC levels at entry (4033 = 28 cells/ $\mu$ l; 5003 = 46 cells/ $\mu$ l; 7036 = 240 cells/ $\mu$ l; 4051 = 12 cells/ $\mu$ l), or the CSF WBC levels increased while on therapy. Conversely, the four subjects with neurological disease that displayed slower CSF-compartmentalized variant decay either had extremely low levels of CSF WBCs at entry (4013 = 10 cells/ $\mu$ l; 5002 = 66 cells/ $\mu$ l; 4059 = 1 cells/ $\mu$ l; 7115 = 12 cells/ $\mu$ l), or the CSF WBC levels decreased to low levels after the initiation of antiretroviral therapy. We examined the CSF WBC levels of these two groups in more detail by calculating the CSF WBC average for each subject from baseline through the first 14 days of antiretroviral therapy. The subjects with rapid CSF-compartmentalized variant decay had higher CSF WBC averages, while subjects with slower or biphasic CSF-compartmentalized variant decay had lower CSF WBC averages (see Table 3.1), and this difference was statistically significant ( $p=0.029$  using a two-tailed Mann-Whitney test). It has been reported that HIV-1-infected subjects with CD4 counts below 50 cells/ $\mu$ l have reduced CSF pleocytosis (286). We also examined whether the viral decay rates measured by HTA were correlated with the degree of immunodeficiency by analyzing CD4 counts for each group of subjects. The four subjects with rapid CSF-compartmentalized variant decay had significantly higher baseline CD4 counts (see Table 3.1) compared to the four subjects with slower CSF-

compartmentalized variant decay ( $p=0.006$  using a two-tailed unpaired t-test). Thus, in subjects with HIV-1-associated neurological disease, viral decay rates are associated with the degree of immunodeficiency and CSF pleocytosis.

We did not detect an association between CSF pleocytosis and rapid viral decay in the CSF for asymptomatic subjects. The CSF WBC average was calculated for each subject as stated above, and the range extended from 0 cells/ $\mu$ l up to 20 cells/ $\mu$ l (Table 3.1). All variants detected in the CSF of asymptomatic subjects decayed rapidly upon the initiation of antiretroviral therapy; however, we found that the presence of CSF-compartmentalized variants was associated with higher average CSF WBC levels. All four of the asymptomatic subjects that did not have compartmentalized virus had low average CSF WBC counts (4012, 4030, 4023, 4021), while the three asymptomatic subjects that had detectable CSF-compartmentalized variants also had higher average CSF WBC levels (5005, 4022, 4014; see Table 3.1). Thus in the asymptomatic subjects the presence of pleocytosis may be associated with an early inflammatory response to increased levels of autonomously replicating virus.

**Slower decay in neurologically symptomatic subjects is not associated with CNS drug penetration, drug resistance mutations, or V3/X4 sequence differences.**

Some antiretroviral drugs have poor penetration into the CNS (175). In order to determine whether the differential decay we detected by HTA was associated with poor CNS drug penetration, we calculated the CNS Penetration Effectiveness (CPE) rank (175) for the drug regimens that each of the 15 subjects were receiving at the time of sample collection (see Table 3.1). Drugs that have poor penetration into the CNS were assigned a rank of 0, intermediate penetration was assigned a rank of 0.5, and high penetration was assigned a rank

of 1 (175). The four subjects that showed a longer viral half-life by HTA analysis had CPE ranks ranging from 2.0 to 2.5, while the other subjects that displayed rapid viral decay had CPE ranks from 1.5 (5 subjects) to 3.5 (1 subject). All subjects with neurological disease had CPE ranks above 2.0 except for subject 5003 (CPE rank = 1.5). A previous study reported that CPE ranks below 2.0 were associated with a significant (88%) increase in the ability to detect virus in the CSF, and higher CSF viral loads were associated with low CPE ranks (175). All of the subjects with longer viral half-lives had CPE ranks of 2.0 or above, suggesting that the slower HIV-1 decay we detected by HTA was not associated with poor CNS drug penetration. Alternatively, there could be infected cells located in parenchymal compartments that are less accessible to drugs, but this seems unlikely because the virus still has access to the CSF.

We also investigated the possibility that slower decay was a result of drug resistance mutations present in the viral population in the CSF. Drug resistance mutations were measured for CSF samples of subjects 4013, 5002, 4059, and 7115. The resistance test was conducted for time points after the initiation of drug selection to allow for enrichment of any potential drug resistant variants. Subjects 4013, 5002, and 4059 showed no evidence of resistance mutations in reverse transcriptase (RT) or protease that confers resistance to antiretroviral drugs (data not shown). Subject 7115 had the resistance mutation K103N in RT, which confers resistance to non-nucleoside RT inhibitors (NNRTI). However, at the time of this study, subject 7115 was not taking an NNRTI, and was instead on a drug regimen that included zidovudine, lamivudine, and lopinavir. Therefore, there is no evidence that drug resistance played a role in the slower viral decay detected by HTA in these four subjects.

Using the biotin-V3 HTA procedure, we also examined whether slower viral decay was associated with V3 sequence differences. The biotin-HTA is a modification of the original HTA method that incorporates a biotin tag into the probe to allow direct sequencing of the query strand isolated from the gel (269). This newly developed HTA procedure resolves minor variants in the gel, and then allows the recovery and sequence analysis of both major and minor HIV-1 V3 variants from complex viral populations (269). Following V3 PCR amplification and HTA analysis, we excised the gel fragments containing the V3 heteroduplexes, purified the query DNA strand using streptavidin-coated magnetic Dynabeads®, and directly sequenced the subsequent V3 PCR products (269). The migration patterns for the V3 heteroduplexes and the inferred V3 amino acid sequence obtained for the heteroduplex in each gel band are shown in Figure 3.4. The biotin-V3 HTA procedure was conducted on plasma samples from all subjects at the first time point collected, and CSF samples were analyzed for subjects with HIV-associated dementia. No significant V3 sequence differences were detected between asymptomatic and symptomatic subjects, or between subjects with rapid versus slow decay by HTA (Figure 3.4B). Only one subject (4014) had V3 sequences that were X4-like by the Position-Specific Scoring Matrix (PSSM) method (145) of predicting co-receptor usage based on genotype. We did note that two subjects with slower decay by HTA had compartmentalized V3 variants detected in the CSF viral population that were much more R5-like by sequence compared to the V3 sequence variants detected in the plasma viral population. However, R5-like V3 sequences were also detected in the CSF for HAD subjects with rapid viral decay, indicating that V3 sequence differences and co-receptor usage are not responsible for the differential decay detected by HTA.

## DISCUSSION

There are several lines of evidence that support the idea that HIV-1 can replicate in the central nervous system (CNS). HIV-1-infected macrophages and microglia have been detected in the brains of subjects with HIV-1-associated dementia (HAD) at autopsy (9, 161, 295). In addition, genetically distinct HIV-1 variants, different from those in the peripheral blood, are seen in the CNS of subjects with HAD (64, 65, 218, 242, 256). These inferences can be extended using CSF as a surrogate for the CNS where genetic compartmentalization can be detected when comparing blood and CSF viral variants (126, 236, 254, 291), and bulk virus in the CSF of subjects initiating HAART can decay with different kinetics compared to virus in the blood (68, 69, 119). Furthermore, it appears that this independent replication is relevant, if not causal, of HIV-associated neuropathogenesis. The extent of compartmentalization in the CSF, as measured by the heteroduplex tracking assay, increases in subjects with HAD, suggesting more sustained autonomous replication is associated with the neurological disease state (126, 254). Also, slow decay of virus in the CSF compared to the blood is associated with subjects with neurological disease, especially HAD subjects, suggestive of virus being produced from a different cellular source (68, 69, 119). In addition to viral genetic compartmentalization there are other markers of neuropathogenesis in HIV-1-infected individuals, such as CSF neopterin (18, 104), CSF light-chain neurofilament protein (3, 104, 199), and CSF chemokine levels (32, 33, 155, 203, 276). In the current work we have attempted to combine the observations of viral genetic compartmentalization and differential decay in subjects initiating HAART by comparing the rates of decay of variants shared between the CSF and the blood versus those variants that were compartmentalized in

the CSF. The goal of this work was to examine the link between compartmentalized virus as a marker for autonomous replication in the CNS and the production of virus in the CNS by long-lived cells.

We used heteroduplex tracking assays (HTAs) targeting the variable regions of *env* to identify CSF-compartmentalized variants and variants shared between the CSF and blood plasma, and then measured the viral decay kinetics of these two distinct classes of viral variants after the initiation of antiretroviral therapy for asymptomatic and neurologically symptomatic subjects. We found that plasma HIV-1 variants decayed rapidly for both neurologically asymptomatic and symptomatic subjects, indicating that short-lived cells, presumably activated CD4<sup>+</sup> T cells, are the predominant source of virus in the periphery during all disease stages. Additionally, shared and compartmentalized variants in the CSF of seven asymptomatic subjects decayed rapidly, with a mean half-life of 1.35 and 1.57 days, respectively. These decay rates are consistent with our previous study of four asymptomatic subjects (124). HIV-1 viral load decays in the peripheral blood with the same half-life as a productively infected CD4<sup>+</sup> T cell (approximately 2 days; (139, 281, 311)), so it is most likely that CSF-shared and compartmentalized virus in asymptomatic subjects is originating from a short-lived cell type, such as a CD4<sup>+</sup> T cell. The level of HIV-1 compartmentalization in the CSF in these asymptomatic subjects varied, and we noted that there was a trend of increased CSF pleocytosis in the asymptomatic subjects with greater compartmentalization.

We also examined HIV-1 decay in subjects with neurological disease that were starting HAART. Rapid viral decay was measured for CSF-compartmentalized variants after the initiation of HAART for four HAD subjects ( $t_{1/2}$  mean = 2.27 days), while slow viral decay was measured for CSF-compartmentalized variants from the other four subjects with

neurological disease ( $t_{1/2}$  range = 9.85 days to no initial decay). It is known that HIV-1 may persist in the CNS during antiretroviral therapy due to insufficient CNS penetration of some antiretroviral drugs (103, 107, 239, 272). We determined that the slow decay detected for CSF-compartmentalized variants was not associated with poor CNS drug penetration, the presence of drug resistant virus in the CSF, or the detection of X4-like virus genotypes. It has been suggested that HIV-1 produced by long-lived cell lineages such as macrophages, microglia, and resting CD4<sup>+</sup> T cells most likely decays with a half-life of 14 days or greater (279, 281, 311). The longer half-lives we detected suggest that compartmentalized HIV-1 in the CSF of some neurologically symptomatic subjects may be originating from a long-lived cell type.

While slower HIV-1 decay was detected for half of the subjects with neurological disease, compartmentalized variants in the CSF of some subjects decayed rapidly. Further analysis revealed that the differential decay measured for CSF-compartmentalized variants in subjects with neurological disease was correlated with the degree of CSF pleocytosis. Four of the eight subjects with HIV-associated neurological disease displayed rapid CSF-compartmentalized variant decay, and this was correlated with higher CSF WBC levels (moderate to severe pleocytosis). The compartmentalized variants detected in the CSF of the four other subjects showed slow or biphasic decay after the initiation of HAART, and this was associated with lower CSF WBC levels (no or mild pleocytosis). Additionally, the subjects with rapid CSF-compartmentalized variant decay had significantly higher CD4 counts than subjects with slow compartmentalized variant decay, indicating that subjects with slow decay of CSF-compartmentalized virus have increased immunodeficiency. We suggest that more profound immunodeficiency results in fewer lymphocytes trafficking into the CNS,

which is consistent with the decreased CSF WBC counts for the subjects with slow decay. HIV-1 infection can be associated with CSF pleocytosis in neurologically symptomatic subjects, asymptomatic subjects, and individuals lacking any CNS opportunistic infections (194). Additionally, some studies have shown that CSF WBC levels are correlated with CSF HIV-1 RNA concentrations (195, 246, 286), and CSF pleocytosis has been shown to decrease after the initiation of antiretroviral therapy (194). In this current study we found an association between the extent of immunodeficiency, CSF pleocytosis and rapid HIV-1 decay kinetics for compartmentalized variants in the CSF of neurologically symptomatic subjects, although the strength of the interpretation is somewhat limited by our small sample size.

Taken together, we have developed a model of HIV-1 infection in the CNS in the context of neurological disease (Figure 3.5). The model has several features that incorporate viral genetic compartmentalization, CSF pleocytosis, and viral decay rates in the CSF as a measure of the virus-producing cell. First, the majority of the virus detected in the CSF of a subset of asymptomatic subjects is imported from the peripheral blood (Figure 3.5A). HIV-1-infected CD4<sup>+</sup> T cells in the peripheral blood release virus that is detectable in the blood plasma and the CSF and that decays rapidly upon the start of antiretroviral therapy, representing the relatively fast turnover of uninfected CD4<sup>+</sup> T cells. HIV-1-infected CD4<sup>+</sup> T cells in the peripheral blood can migrate from the periphery into the CNS and secrete virus in the CNS that is genetically similar to virus in the peripheral blood. No or only mild pleocytosis was detected for this group of asymptomatic subjects, and we suggest this represents minimal inflammation in the CNS. It is possible that some CNS HIV-1 variants are independently replicating at a low level in these asymptomatic subjects, but we were not able to detect these genetic variants above the background of virus recently imported from

the periphery. In these subjects virus decays with the half life of peripheral T cells, the presumed source of the virus.

A second pattern exists for the other asymptomatic subjects and also for a subset of the neurologically symptomatic subjects. There is increased compartmentalization of HIV-1 in this subset of asymptomatic subjects, and the majority of virus detected in the CSF is compartmentalized in HIV-1-infected individuals with severe neurological disease. In addition, both of these groups have increased pleocytosis. We found that CSF-compartmentalized variants decayed rapidly upon the initiation of antiretroviral therapy in these remaining asymptomatic subjects and in this subset of four subjects with HIV-1-associated dementia. It is possible that compartmentalized variants detected in these subjects are produced by long-lived cells in the CNS; however the majority of the compartmentalized virus is produced by a short-lived cell type. We propose that compartmentalized virus may be maintained by long-lived cells in the CNS and that this virus is amplified by short-lived trafficking CD4<sup>+</sup> T cells to detectable levels in the CSF for asymptomatic subjects, and to high titers in the CSF of HAD subjects (Figure 3.5B). The elevated level of pleocytosis is indicative of an inflammatory response, most likely to the autonomously replicating virus. Increased levels of CSF white blood cells may account for the influx of T cells that could be the source of the short-lived cells that are amplifying the compartmentalized virus. We would expect that most of the infiltrating T cells are HIV-specific, although some lymphocytes may be migrating into the CNS due to a general inflammatory environment. The asymptomatic subjects in this group have the hallmarks of viral pathogenesis associated with neurological disease and may be at risk for transition to HAD.

Third, we detected slow decay of compartmentalized variants in the CSF for the four remaining subjects with neurological disease. These subjects shared the feature of viral genetic compartmentalization but did not show high levels of pleocytosis. Additionally, this subject group had the lowest blood CD4<sup>+</sup> T cell counts (Table 3.1), indicating a state of increased immunodeficiency. We suggest that these subjects have more profound immunodeficiency, which would allow even more extensive viral replication and compartmentalization in the CNS (Figure 3.5C). Increased immunodeficiency would result in reduced trafficking of CD4<sup>+</sup> T cells into the CNS, so these cells would no longer be present to amplify virus from local CNS tissue, consistent with the reduced pleocytosis in this group. The slow decay rate of virus in the CSF in the absence of inflammatory cells suggests that compartmentalized HIV-1 in the CNS of these HAD subjects is originating from a long-lived cell type, such as perivascular macrophages and/or microglia in the CNS. Virus is unlikely to be coming from T cells that are persisting in the absence of immune-mediated killing since there is still rapid viral decay in the peripheral blood. The CSF viral loads of all four subjects displaying slow decay were high, similar to subjects with rapid viral decay, suggesting that a large amount of compartmentalized virus is being produced by longer-lived cells in the CNS. This may suggest that peripheral, uninfected monocytes may migrate into the brain parenchyma and differentiate into perivascular macrophages to levels that can sustain high viral loads in the CSF. An influx of monocytes into the CNS could also allow the entrance of peripherally-infected monocytes, which would explain the slower decay we detected for shared variants in the CSF of these subjects.

Our studies support a model where increasing levels of autonomous viral replication in the CNS first induces an inflammatory state that then progresses to neurologic disease with

increasing immunodeficiency. More profound immunodeficiency ultimately reveals long-lived cells that are able to maintain independent replication of virus in the CNS. Several *env* gene markers have been described in viral sequences taken at autopsy and linked to the ability of HIV-1 to infect macrophages (64, 65). The CSF provides an alternative window on these viral sequences where the evolution of the virus and its properties can be followed over time and into the disease state. Viral genetic compartmentalization and other markers of CNS inflammation could also play an important role in defining subjects at risk of progression to neuropathogenesis in the absence of therapeutic intervention.

## **MATERIALS AND METHODS**

### **Ethics statement.**

This study was conducted according to the principles expressed in the Declaration of Helsinki. The study was approved by the Institutional Review Board of the University of California at San Francisco. All subjects provided written informed consent for the collection of samples and subsequent analysis.

### **Subject population and sampling.**

The samples from study subjects used for variant decay analysis were collected during previous studies carried out at the University of California at San Francisco. All subjects used in this study were HIV-1-infected subjects that were initiating highly-active antiretroviral therapy. Subjects 4012, 4013, 4014, 5002, 5003, and 5005 were recruited from a study examining antiretroviral therapy responses in the CSF, and are described in more detail in ref. (289). Serial blood plasma and cerebrospinal fluid (CSF) samples were collected at baseline prior to the start of therapy and at varying intervals thereafter. Plasma and CSF HIV-1 RNA concentrations were determined using the Amplicor HIV Monitor kit (Roche). CSF white blood cell counts were measured by routine methods in the San Francisco General Clinical Laboratory. Drug resistance mutations were analyzed for CSF samples of subjects 4013, 5002, 4059, and 7115 using the TRUGENE® HIV-1 Genotyping Test Resistance Report using GuideLines™ Rules 12.0 (Bayer HealthCare).

### **RNA isolation, RT-PCR, and HTA.**

Viral RNA isolation, RT-PCR, and HTA procedures were conducted as previously described (124, 159, 212, 251). Briefly, viral RNA was isolated from blood plasma and CSF samples (140  $\mu$ l) using the QIAmp Viral RNA kit (Qiagen). Prior to RNA isolation, all CSF samples were centrifuged at 2,500 rpm for 5 minutes to remove any contaminating cellular debris. Samples with viral RNA levels less than 10,000 copies/ml were pelleted (0.5-1.0 ml) by centrifugation at 25,000 x g for 1.5 hours prior to RNA isolation to increase template number and improve sampling. Reverse transcription and PCR amplification of the V1/V2, V3, and V4/V5 regions of *env* were conducted with 5  $\mu$ l of purified RNA (from 60  $\mu$ l column elution volume) using primers that have been previously described for V1/V2 (159, 251), V3 (269); and V4/V5 (251) and using the Qiagen One-Step RT-PCR kit (Qiagen) as per manufacturer's instructions.

Heteroduplex annealing reactions were conducted as previously described (159, 212). The heteroduplexes were separated by 6% native polyacrylamide gel electrophoresis for V1/V2 and V4/V5 HTA (124, 159), and by 12% PAGE for biotin-V3 HTA (269). The HTA probes used in these studies have been previously reported: V1/V2 Ba-L probe (159, 251), V1/V2 JRFL probe (159, 251), V4/V5 NL4-3 probe (124), V4/V5 YU2 probe (251), and the V3 Mut-1 probe (269). The HTA gels were dried under vacuum, and bands were visualized by autoradiography. For the biotin-V3 HTA procedure, the desired labeled bands were excised from the dried gels, the DNA was purified from the gel, and the V3 sequence was obtained as previously described (269). Duplicate RT-PCR products were analyzed by HTA for each sample to validate sampling and ensure reproducibility of the HTA pattern at each time point. Any time points where the HTA pattern between the two replicates differed

significantly (>20%) were not used in the data analysis. Percent difference values between plasma and CSF viral populations were calculated as previously described (159, 251).

### **Phosphorimager analysis and half-life calculations.**

The dried HTA gels were exposed to a PhosphorImager screen, and the relative abundance of each detected viral variant (heteroduplex) was calculated using ImageQuant software (Molecular Dynamics). The variant RNA concentration was calculated by multiplying the relative abundance of each individual variant by the total HIV-1 RNA concentration for that sample. Variants in the CSF were considered compartmentalized by HTA if they were either unique to the CSF or if they had a substantially higher copy number in the CSF compared to the plasma. Compartmentalized variant half-lives were calculated using the time points when the viral load initially dropped after the start of antiretroviral therapy.

### **ACKNOWLEDGMENTS**

We thank Evelyn Lee for coordinating the clinical studies and materials, and the subjects for their participation. GS was supported by the NIH training grant T32-AI07001, and PH by the NIH training grant T32-CA09156. This work was supported by the NIH award R01-MH67751 (to RS), the UNC Center for AIDS Research (NIH award P30-AI50410), the Lineberger Cancer Center core grant (NIH award P30-CA16086), NIH award K23-MH074466 to SS, NIH award R01-NS37660 to RWP, and NIH award UL1RR024131 to UCSF. The funders had no role in study design, data collection and analysis, decision to publish, or preparation of the manuscript.

**Table 3.1. Sample characteristics.**

| Subject ID | Cell counts (cells/ $\mu$ l) |                      | ADC Stage <sup>c</sup> | Drug Regimen            | CPE total <sup>d</sup> | HIV-1 RNA (log <sub>10</sub> copies/ml) <sup>a</sup> |      |
|------------|------------------------------|----------------------|------------------------|-------------------------|------------------------|--|------|
|            | CD4 <sup>a</sup>             | CSF WBC <sup>b</sup> |                        |                         |                        | Plasma   | CSF  |
| 4012       | 295                          | 13                   | 0                      | 3TC, NVP, NFV, AZT      | 2.5                    | 5.18   | 4.39 |
| 4014       | 1140                         | 20                   | 0                      | ddI, NVP, d4T           | 1.5                    | 4.41   | 4.42 |
| 4021       | 215                          | 2                    | 0                      | AZT, 3TC, NFV           | 1.5                    | 4.97   | 4.02 |
| 4022       | 372                          | 18                   | 0                      | 3TC, NFV, AZT           | 1.5                    | 4.58   | 4.77 |
| 4023       | 215                          | 0                    | 0                      | AZT, 3TC, NFV, EFV      | 2.0                    | 5.50   | 3.77 |
| 4030       | 239                          | 5                    | 0                      | d4T, 3TC, EFV           | 1.5                    | 4.86   | 4.06 |
| 5005       | 267                          | 19                   | 0                      | ABC, NVP, SGC, NFV      | 2.0                    | 5.30   | 4.99 |
| 4033       | 173                          | 28                   | 2                      | IDV, RTV, 3TC, ABC, NVP | 3.5                    | 4.83   | 5.23 |
| 4051       | 344                          | 26                   | 3                      | AZT, 3TC, EFV           | 2.0                    | 5.61   | 5.41 |
| 5003       | 234                          | 39                   | 3                      | NFV, d4T, ABC           | 1.5                    | 3.31   | 4.33 |
| 7036       | 267                          | 150                  | 2                      | AZT, 3TC, NVP           | 2.5                    | 5.12   | 5.37 |
| 4013       | 148                          | 6                    | 1                      | 3TC, NVP, NFV, d4T      | 2.0                    | 4.62   | 4.75 |
| 4059       | 53                           | 1                    | 3                      | AZT, 3TC, LPVr          | 2.5                    | 5.31   | 5.08 |
| 5002       | 59                           | 23                   | 3                      | 3TC, NVP, NFV, ABC      | 2.5                    | 4.24   | 5.32 |
| 7115       | 50                           | 9                    | 2                      | AZT, 3TC, LPVr          | 2.5                    | 5.87   | 4.85 |

<sup>a</sup> = Baseline samples

<sup>b</sup> = Average CSF white blood cell counts over the first 14 days of antiretroviral therapy.

<sup>c</sup> = ADC staging: (245).

<sup>d</sup> = CNS Penetration Effectiveness Rank total. The CPE ranks for each drug in the regimen were summed to get the CPE total.

**Table 3.2. HIV-1 variant decay.**

| Subject ID | % HIV-1 RNA decrease (days on HAART) |                       | Plasma Half-life (days) | CSF-Compartmentalized Variant Data |                               | CSF Shared Variant Data |                               | % Diff. <sup>c</sup> |
|------------|--------------------------------------|-----------------------|-------------------------|------------------------------------|-------------------------------|-------------------------|-------------------------------|----------------------|
|            | Plasma                               | CSF                   |                         | % CSF VL <sup>a</sup>              | Half-life (days) <sup>b</sup> | % CSF VL <sup>a</sup>   | Half-life (days) <sup>b</sup> |                      |
| 4012       | 96 (10)                              | 97 (10)               | 1.36                    | 0                                  | N/A                           | 100                     | 1.73                          | 29                   |
| 4014       | 92 (7)                               | 95 (7)                | 1.96                    | 83.6                               | 1.9                           | 16.4                    | 1.3                           | 37                   |
| 4021       | 90 (5)                               | 82 (5)                | 1.2                     | 7                                  | >1.59 <sup>f</sup>            | 93                      | 1.59                          | 36                   |
| 4022       | 87 (4)                               | 93 (4)                | 1.01                    | 37                                 | 0.75                          | 63                      | 0.79                          | 47                   |
| 4023       | 90 (3)                               | 79 (3)                | 0.58                    | 0                                  | N/A                           | 100                     | 0.88                          | 58                   |
| 4030       | 90 (3)                               | 90 (3)                | 1.81                    | 0                                  | N/A                           | 100                     | 1.83                          | 10                   |
| 5005       | 97 (10)                              | 98 (10)               | 2.27                    | 100                                | 2.04                          | 0                       | N/A                           | 78                   |
| 4033       | 92 (8)                               | 92 (8)                | 1.64                    | 77                                 | 1.44                          | 23                      | 2.44                          | 72                   |
| 4051       | 95 (10)                              | 94 (10)               | 2.32                    | 39                                 | 2.74                          | 61                      | 2.19                          | 36                   |
| 5003       | 54 (6)                               | 82 (6)                | 2.69 <sup>e</sup>       | 94                                 | 1.23                          | 6                       | 1.05                          | 88                   |
| 7036       | 99 (25)                              | 99 (25)               | 2.91                    | 82                                 | 3.67                          | 18                      | 2.95                          | 80                   |
| 4013       | 93 (15)                              | 20 (9)                | 2.32                    | 73                                 | 28.5                          | 27                      | 4.3                           | 78                   |
|            |                                      | 76 (15)               |                         |                                    | 3.9                           |                         | 2.0                           |                      |
| 4059       | 98 (14)                              | 62 (14)               | 2.35                    | 92                                 | 9.85                          | 8                       | 5.84                          | 46                   |
| 5002       | 98 (6)                               | Inc. (6) <sup>d</sup> | 1.42                    | 98                                 | No decay                      | 2                       | No decay                      | 72                   |
|            |                                      | 93 (28)               |                         |                                    | 4.24                          |                         | 1.76                          |                      |
| 7115       | 99 (10)                              | 40 (10)               | 1.25                    | 47                                 | No decay                      | 53                      | 4.88                          | 65                   |
|            |                                      | 95 (33)               |                         |                                    | 6.4                           |                         | 6.05                          |                      |

<sup>a</sup> = Based on the region of *env* (V1/V2 or V4/V5) that was the most reproducible by two independent HTA replicates.

<sup>b</sup> = Reported half-lives are the average calculated from decay analyses of two independent HTA replicates. N/A = not applicable.

<sup>c</sup> = Percent difference values between plasma and CSF viral populations as measured by HTA. Reported values are the average calculated from two independent HTA replicates (see refs. (159, 251) for methods).

<sup>d</sup> = Total CSF viral load increased initially for subject 5002.

<sup>e</sup> = Total plasma viral decay for subject 5003 was calculated for the drop in viral load from days 3 to 6 on HAART. There was a slight increase in plasma viral load from days 6 to 10 on HAART, which can be seen in Figure 3.2B, but this increase does not seem to be significant. Although the baseline samples were not available for analysis, we know that the baseline plasma viral load was 126,000 copies/ml, and this subject had undetectable viral loads in both plasma and CSF by 2 months post-HAART, so there was an overall good response to antiretroviral therapy. The small variation in plasma viral load from days 6 to 10 on therapy could be explained by a number of technical, pharmacological, and/or biological factors.

<sup>f</sup> = A compartmentalized variant was detected for subject 4021 in the day 5 CSF sample; however, the relative abundance of this variant was less than other bands detected that were not reproducible by HTA, indicating that the detection of this band may be due to inefficient sampling and low viral load. It is equally possible that this band represents a reproducible

compartmentalized variant that is decaying more slowly than the other variants detected by HTA. Therefore, the half-life for the CSF-compartmentalized variants is listed as >1.59 days (a half-life of 1.59 days was measured for CSF shared variants).

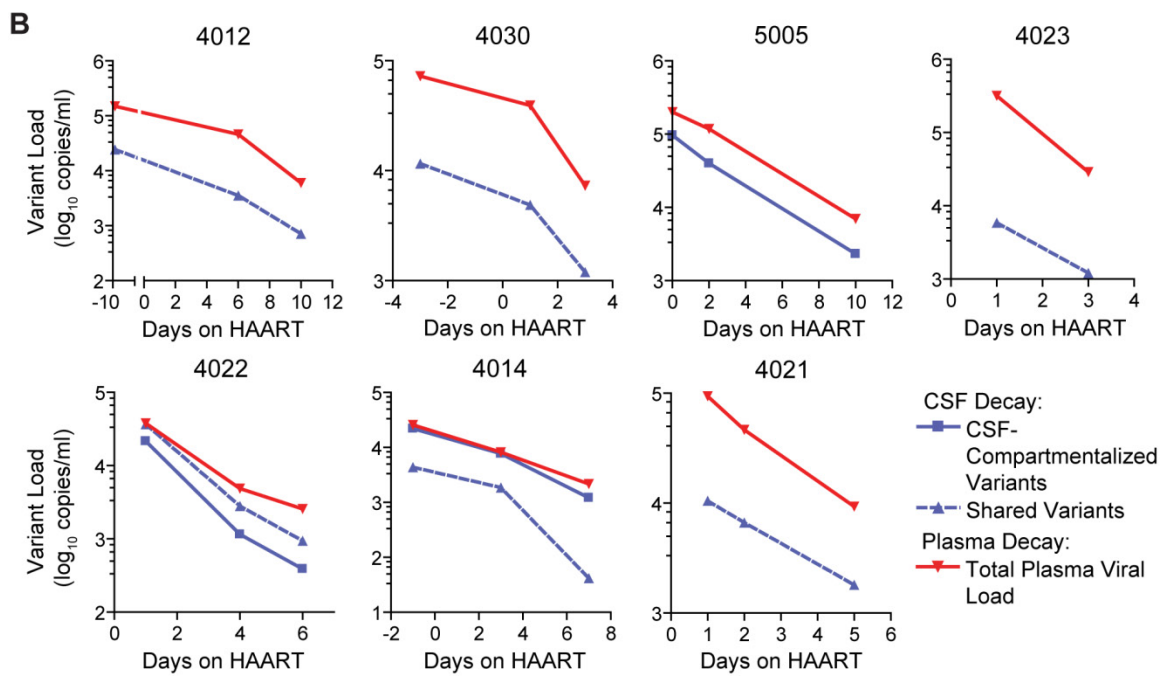
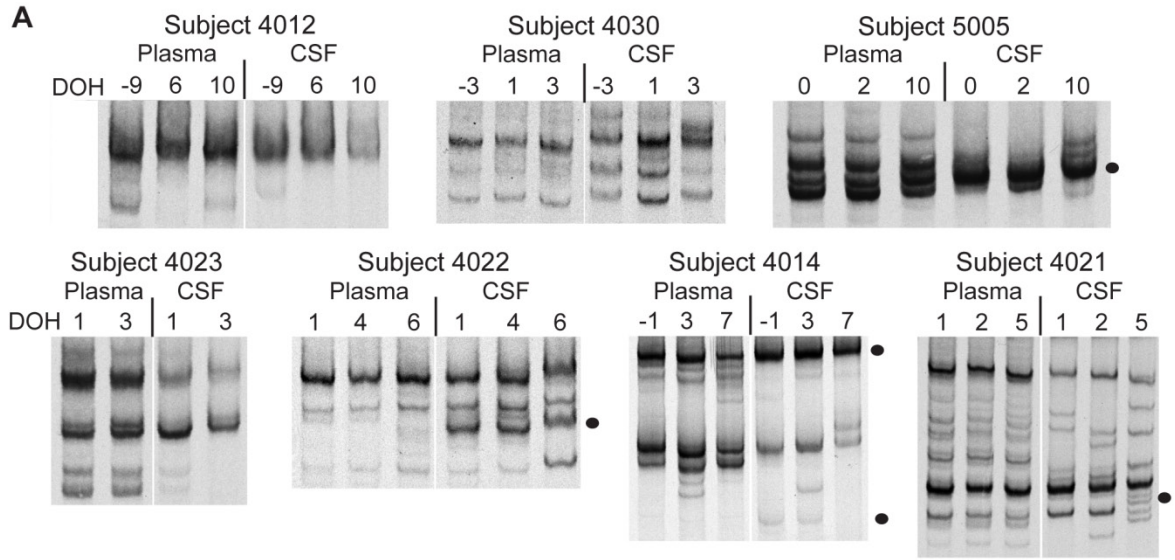


**Figure 3.1. Longitudinal HTA analysis and HIV-1 decay in the blood plasma and CSF of asymptomatic subjects.** (A) Longitudinal V1/V2 or V4/V5 HTA analysis of HIV-1 using paired blood plasma and CSF samples from 7 asymptomatic subjects that were initiating antiretroviral therapy. The HTA shown for subject 4014 targeted the V1/V2 region of *env*, and the V4/V5 HTA is shown for all other subjects. Sample time points are listed above each HTA gel as days on HAART (DOH) with day 0 indicating the day that antiretroviral therapy was started. CSF-compartmentalized variants are indicated with a filled black circle next to the gel image. The V4/V5 HTA analysis for subject 4021 revealed a compartmentalized variant in the day 5 CSF sample, not present in the blood plasma, that was reproducible by HTA; however, the relative abundance of this variant (3.6%) was less than that of other

bands detected in the same sample that were not reproducible by HTA, indicating that the detection of this band may be due to inefficient sampling and low viral load. Compartmentalized variants were not detected for three subjects. **(B)** HIV-1 decay kinetics in the blood plasma and CSF. Viral variants in the CSF were categorized as either compartmentalized or shared between the plasma and CSF for the decay analysis. Total plasma viral load decay is shown in red, CSF-compartmentalized variant decay is denoted by the solid blue line, and decay of variants shared between the plasma and CSF is shown by the dashed blue line. It should be noted that in our decay analysis for subject 4012 we assumed the viral load at day 0 would be similar to the viral load measured for the baseline samples at day -9.

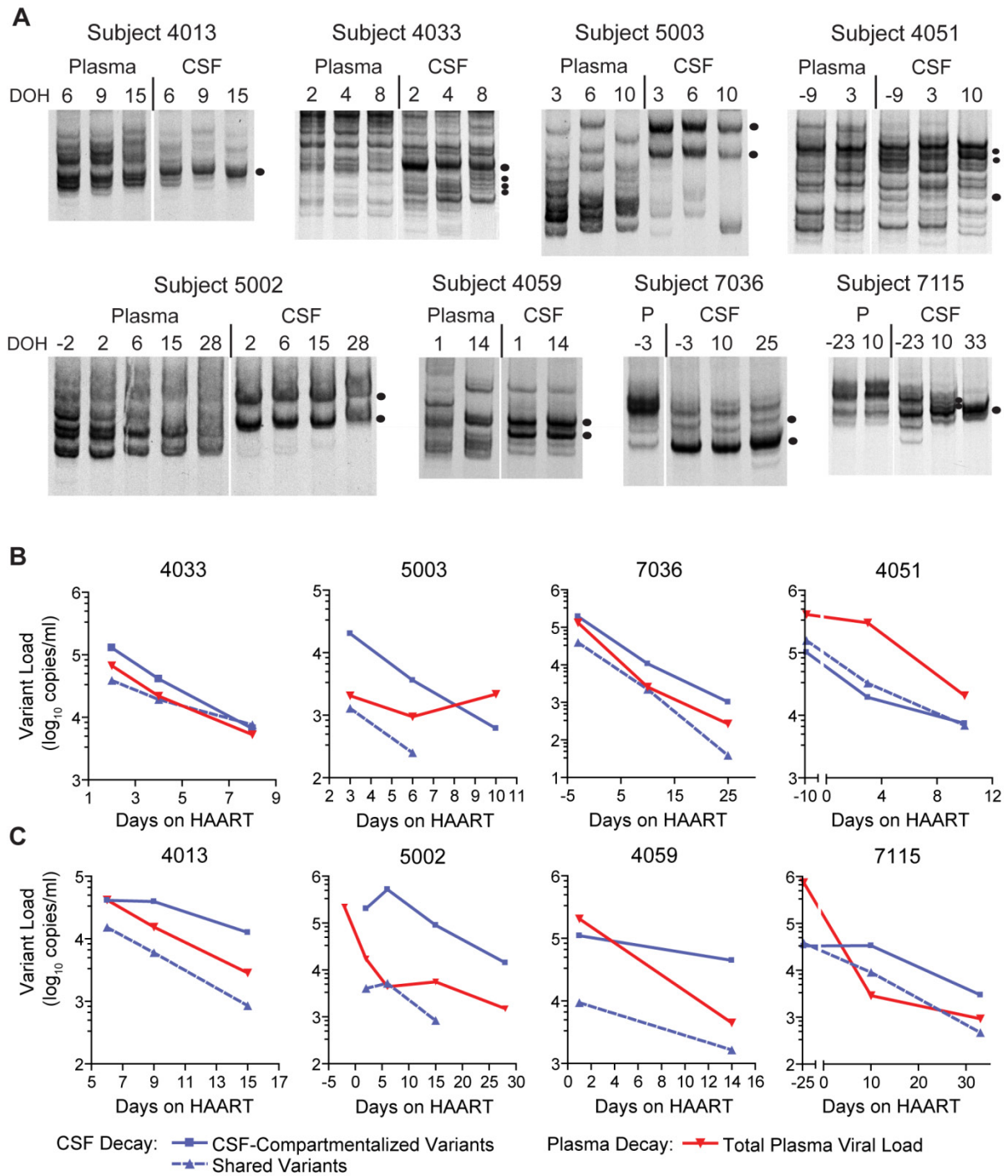


**Figure 3.2. Longitudinal HTA analysis and HIV-1 decay in blood plasma and CSF of neurologically symptomatic subjects.** (A) Longitudinal V4/V5 HTA analysis of HIV-1 in paired blood plasma and CSF samples from 1 subject with MCMD (subject 4013) and 7 subjects with HIV-associated dementia that were initiating HAART. Plasma (P) and CSF sample time points are listed above each HTA gel as days on HAART (DOH), and day 0 indicates the start of antiretroviral therapy. CSF-compartmentalized variants are indicated by

a filled black circle. **(B, C)** HIV-1 decay kinetics in the blood plasma and CSF viral populations. Viral variants in the CSF were categorized as either compartmentalized in the CSF or shared between the plasma and CSF. Total plasma viral load decay is shown in red, CSF-compartmentalized variant decay is denoted by the solid blue line, and decay of variants shared between the plasma and CSF is shown by the dashed blue line. Four subjects (4033, 5003, 7036, 4051) displayed rapid decay in their CSF-compartmentalized variant population (shown in panel B), while the other four subjects (4013, 5002, 4059, 7115) had slower decay of CSF-compartmentalized variants (shown in panel C). Subjects 4013, 5002, and 7115 showed differential decay of CSF-compartmentalized variants where initially the compartmentalized variant population decreased very slowly (4013) or increased (5002, 7115) after the start of therapy, and at subsequent time points began decreasing at a faster rate (panel C). In our decay analysis for subjects 4051 and 7115 we assumed that the viral load at day 0 would be similar to the viral load measured for the baseline samples at day -9 for subject 4051 and at day -25 for subject 7115. In this regard, subject 7115 was followed longitudinally for several years prior to the start of antiretroviral therapy, and the viral loads in both the plasma and CSF samples remained relatively constant over time (data not shown).

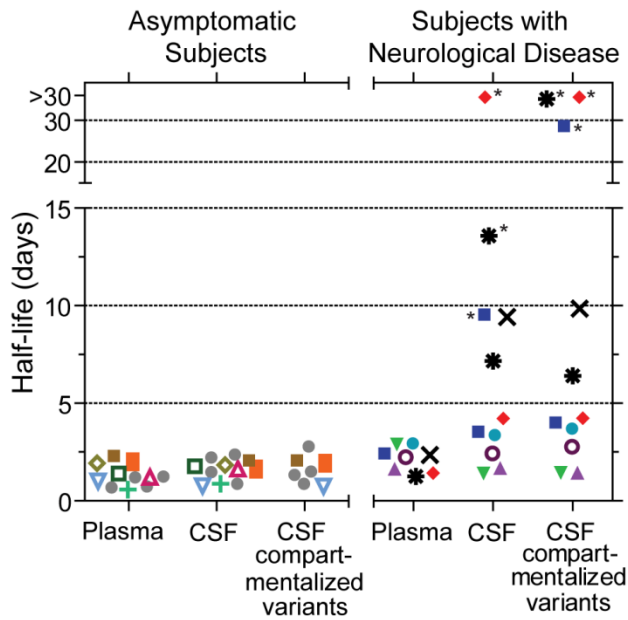


**Figure 3.3. Summary of HIV-1 half-lives from asymptomatic and neurologically symptomatic subjects.** Half-lives were calculated for total plasma viral load decay (Plasma), total CSF viral load decay (CSF), and CSF-compartmentalized variant decay (CSF compartmentalized variants). The half-lives were calculated using the time points when the variant load initially dropped after each subject initiated antiretroviral therapy. All half-lives listed in the figure are the average calculated from decay analyses of two independent HTA replicates. Half-lives are listed for the seven new asymptomatic subjects analyzed in this study plus four asymptomatic subjects (labeled as 4 Asy.) that were previously reported in ref. (124), 1 subject with MCMD (subject 4013), and 7 subjects with HIV-1-associated dementia. The asymptomatic subjects include: 4012 (open green square), 4030 (open yellow-green diamond), 5005 (brown square), 4023 (green plus symbol), 4022 (open, inverted blue triangle), 4014 (orange rectangle), 4021 (open fuchsia triangle), and 4 Asy. (gray circles). The subjects with HIV-associated neurological disease include: 4033 (purple triangle), 5003 (inverted green triangle), 7036 (teal circle), 4051 (open purple circle), 4013 (blue square), 5002 (red diamond), 4059 (black x symbol), and 7115 (black irregular circle). Two different half-lives are listed for subjects 4013, 5002, and 7115 for both total CSF viral load decay (CSF) and CSF-compartmentalized variant decay (CSF-compartmentalized variants). Each of these three subjects showed biphasic decay by HTA analysis, and the half-life data point denoted with the asterisk represents the phase 1 half-life (slower), while the half-life lacking the asterisk was calculated for phase 2 of decay (faster). The CSF-compartmentalized variant population increased initially for subjects 5002 and 7115, so there was no decay detected for these subjects during phase 1 and their half-lives are listed on the graph as >30 days. Similarly, the total CSF viral load increased for subject 5002 during phase 1 of decay and the half-life is listed on the graph as >30 days.

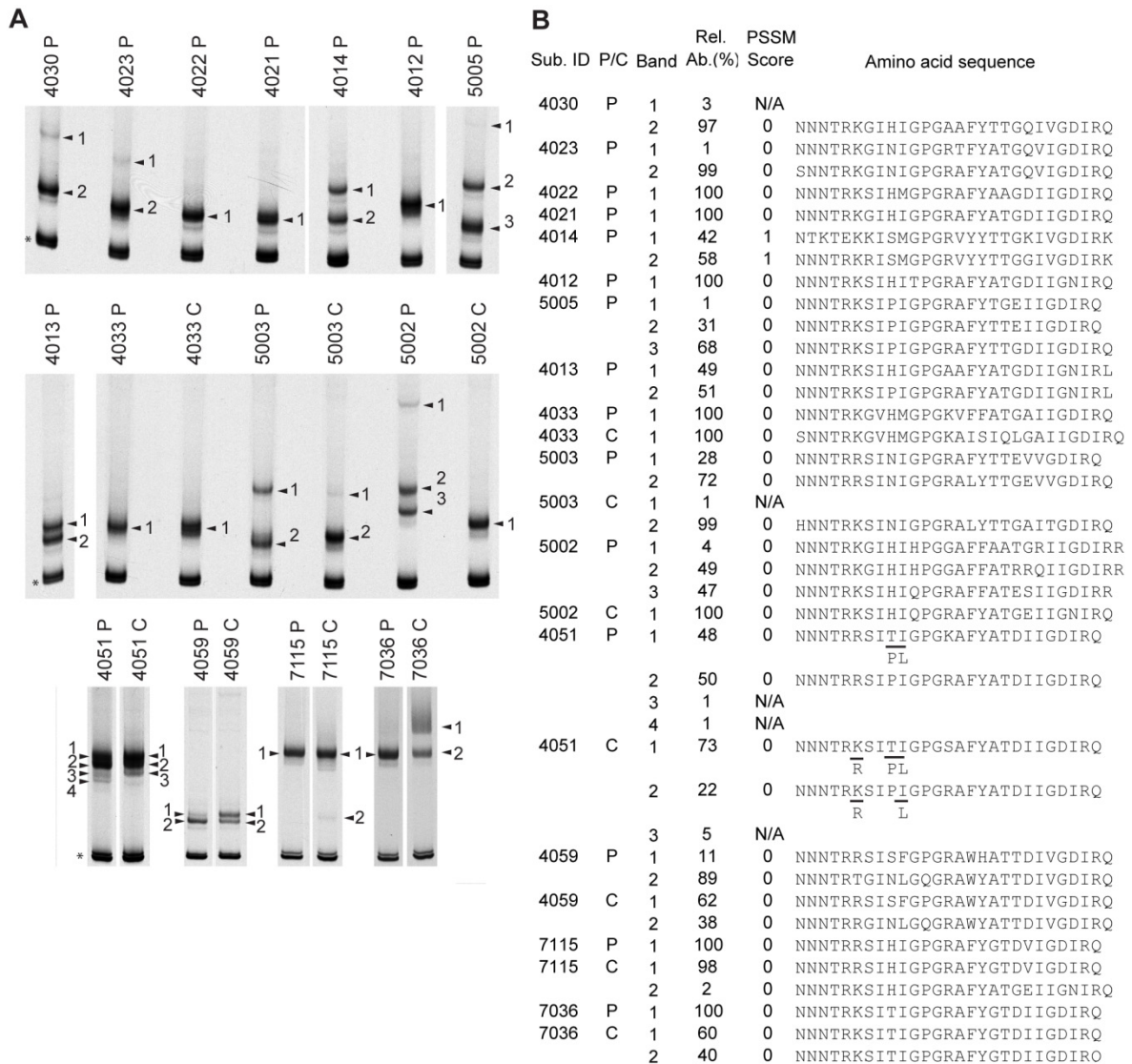


**Figure 3.4. Examination of the V3 region of *env* using the biotin-V3 HTA. (A)** Biotin-V3 HTA analysis of the baseline samples collected for asymptomatic and neurologically symptomatic subjects. Plasma samples (P) were analyzed for all subjects, and CSF samples (C) were analyzed for HAD subjects. The asterisk indicates the double-stranded probe band, and shifted heteroduplex bands are noted with arrowheads and numbers. **(B)** Summary table of the V3 sequence information obtained using the biotin-V3 HTA procedure. The desired V3 bands were excised from the dried gel, the query strand DNA was purified and PCR amplified, and the V3 PCR products from each band were sequenced. The sample type (P/C; P = plasma sample, C = CSF sample), relative abundance (Rel. Ab.), and PSSM score (0 = R5-like sequence, 1 = X4-like sequence, N/A = not applicable) for each sequence are listed in the table. Note: the V3 PCR primers used to amplify the V3 products extend into the first four and the last three amino acids of the V3 sequence. The V3 sequences provided do not include these amino acids; however, we added the JRFL consensus amino acid sequence to the beginning (CTR<sub>P</sub>) and end (AHC) of each V3 sequence to predict coreceptor usage using

PSSM. Mixtures in the sequence peaks were detected at specific positions in V3 bands from subject 4051 plasma and CSF samples, and these mixtures are noted in the reported amino acid sequences.

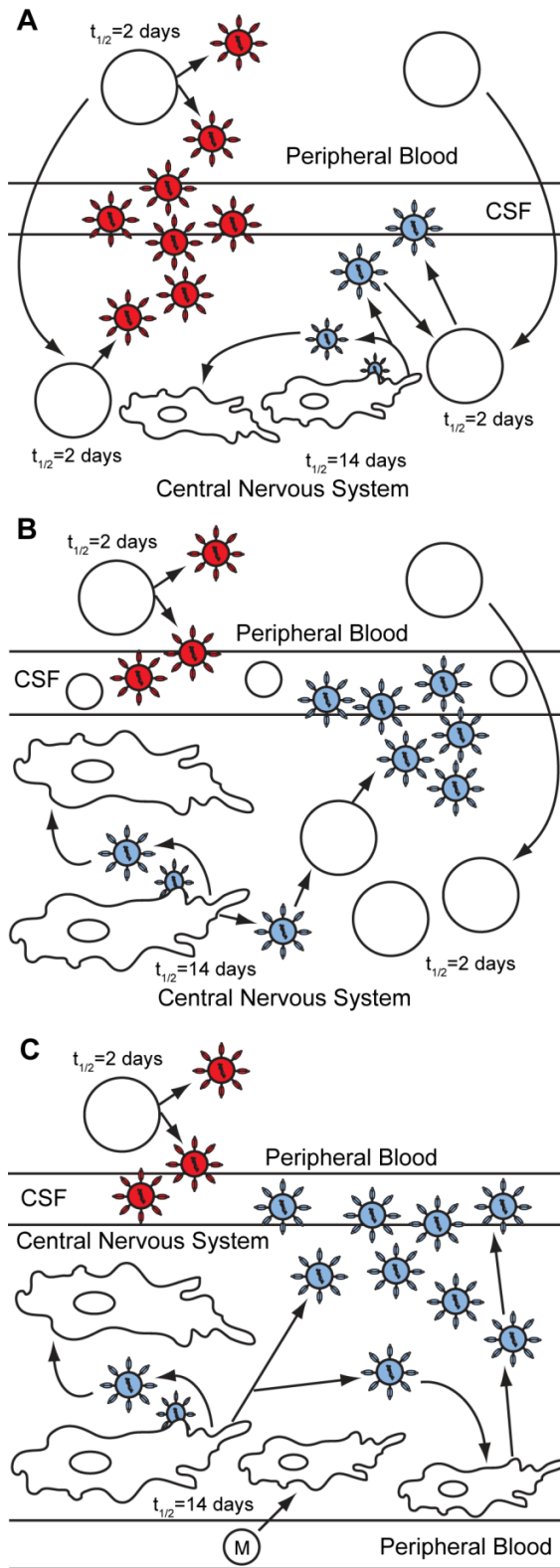


**Figure 3.5. Model of HIV-1 infection in the central nervous system.**  $CD4^+$  T cells are represented by open circles, macrophages are represented by the irregularly shaped cells,

monocytes are represented by open circles labeled with an M, blood plasma viral variants are represented by the red virus particles, and CNS compartmentalized viral variants are represented by the blue virus particles. **(A)** HIV-1 infection in the CNS of a subset of asymptomatic subjects without detectable compartmentalized virus or CSF pleocytosis. All HIV-1 detected in the CSF decays rapidly after the initiation of therapy, suggesting that CSF virus is coming from a short-lived cell type. **(B)** HIV-1 infection in the CNS of asymptomatic and neurologically symptomatic subjects with compartmentalization, high CSF pleocytosis and rapid viral decay. In this model, local CNS virus is able to replicate to higher titers during periods of immunodeficiency and stimulate an inflammatory response in the CNS. Uninfected CD4<sup>+</sup> T cells that migrate into the CNS can become infected by compartmentalized HIV-1 produced by macrophages and microglia in the CNS, and then amplify the local CNS-compartmentalized virus to higher concentrations. Thus, a rapid decay rate for compartmentalized virus is detected after the initiation of antiretroviral therapy. **(C)** HIV-1 infection in the CNS of neurologically symptomatic subjects with slow viral decay. Our data indicate that compartmentalized variants in the CSF of HAD subjects are originating from long-lived macrophages and microglia in the CNS, resulting in a slow decay rate for compartmentalized virus. We propose that periods of profound immunodeficiency allow compartmentalized virus in the CNS to replicate to high titers, and that in the absence of other lymphocytes (such as CD4<sup>+</sup> T cells) peripheral, uninfected monocytes may migrate into the brain parenchyma in large numbers and differentiate into perivascular macrophages. These macrophages can then become infected by compartmentalized HIV-1 variants in the CNS and support viral replication at detectable levels.

## CHAPTER FOUR

### DISTINCT CELLULAR ORIGINS OF COMPARTMENTALIZED HIV-1 IN THE CSF OF SUBJECTS WITH HIV-1-ASSOCIATED DEMENTIA DEFINE TWO CLASSES OF VIRAL ENCEPHALITIS

Gretja Schnell generated the HIV-1 *env* amplicons and clones, and conducted the phylogenetic analyses and phenotype experiments. Sarah Joseph established the 293-Affinofile cell line for the Swanstrom laboratory, and analyzed the CD4 and CCR5 receptor densities using flow cytometry. Richard W. Price and Serena Spudich designed the human study protocols and collected the human blood and cerebrospinal fluid samples. The data presented in this chapter are currently in preparation for submission to a peer-reviewed journal.

## **ABSTRACT**

Human immunodeficiency virus type 1 (HIV-1) infection of the central nervous system (CNS) can lead to the development of HIV-1-associated dementia (HAD). Viral genetic compartmentalization between the periphery and the CNS is associated with HAD, and HIV-1 variants isolated from the brain tissue of HAD subjects can infect macrophages. We examined the genotypic and phenotypic viral characteristics associated with compartmentalized HIV-1 variants in subjects with HIV-1-associated neurological disease and in asymptomatic subjects. Single genome amplification was used to examine HIV-1 populations in the cerebrospinal fluid (CSF) and the peripheral blood, and compartmentalized envelope phenotypes were defined by generating envelope-pseudotyped reporter viruses and testing for cellular tropism. Extensive genetic compartmentalization was detected in the CSF HIV-1 populations of subjects with neurological disease, and longitudinal analysis revealed that significant compartmentalization in the CSF viral population seems to arise concurrently with the development of neurological complications. We found that distinct cellular origins of compartmentalized HIV-1 in the CNS define two classes of viral encephalitis. Compartmentalized HIV-1 envelopes in three HAD subjects were dependent on high CD4 surface expression for infection (class 1). However, CSF-compartmentalized envelopes from an additional four subjects with neurological disease were able to mediate infection of cells with a low density of surface CD4 (class 2), and this was correlated with increased immunodeficiency. We propose that increased HIV-1 replication in the CNS/CSF compartment stimulates immune cell migration to the CNS, and the degree of immunodeficiency may define the cellular origin of the replicating compartmentalized virus.

## INTRODUCTION

Human immunodeficiency virus type 1 (HIV-1) can invade the central nervous system (CNS) shortly after peripheral infection through the migration of infected cells, including monocytes and lymphocytes, across the blood-brain barrier (BBB) (197, 216). After crossing the BBB, HIV-1 can infect local cells in the CNS and establish an autonomous replicating viral population (107, 234). A subset of HIV-1-infected individuals develops mild to severe neurological symptoms associated with HIV-1 infection, including the development of HIV-1-associated dementia (HAD) (14, 107, 244, 245). Compartmentalized HIV-1 variants have been detected in the cerebrospinal fluid (CSF) of HIV-1-infected individuals spanning all degrees of neurological disease. Studies examining HIV-1 evolution in the CSF using the heteroduplex tracking assay (HTA) found increased viral genetic compartmentalization in the CSF of HAD subjects (126, 254), and genetically distinct HIV-1 variants have been detected in the CNS of subjects with HAD (64, 65, 218, 242, 256), suggesting that autonomous viral replication is occurring in the CNS of subjects with more severe neurological disease.

Several mechanisms have been proposed for HIV-1 transport across the BBB, including direct infection of brain endothelial cells (204, 237), transcytosis by endothelial cells (10), and the most supported theory of HIV-1 entry via trafficking of HIV-1-infected monocytes and lymphocytes across the BBB (107). Perivascular macrophages and microglia in the CNS, which express low receptor densities of CD4, CCR5, and CXCR4, are exposed to HIV-1 after viral transport across the BBB. Previous studies have reported that HIV-1 variants isolated from the brains of HAD subjects at autopsy can infect macrophages (108,

109, 161, 233, 256, 298). Compartmentalized HIV-1 variants in the CSF were also reported to decay slowly with the initiation of therapy in some subjects with HIV-1-associated dementia, suggesting a longer-lived cell type as the origin of this virus (271). In addition, several reports have indicated that specific amino acid substitutions in the Env protein are associated with HAD and enhanced viral entry in macrophages (62, 64, 65, 108, 243, 256, 298). Although the properties of some compartmentalized HIV-1 variants have been reported in previous studies, it is still not known how extensive compartmentalization develops, or exactly which cell types in the CNS contribute to the production of compartmentalized virus in HAD subjects.

In this study we conducted an in depth analysis of HIV-1 populations in the CSF of HAD subjects by examining HIV-1 genetic compartmentalization and viral evolution between the peripheral blood and CSF using single genome amplification. We also examined the phenotypic characteristics of compartmentalized *env* genes from subjects with and without neurological disease to assess the cellular origin of the compartmentalized virus. Here we report the detection of extensive genetic compartmentalization between the blood and CSF viral populations in subjects with HIV-associated neurological disease, and clonal amplification of some CSF variants that are separated phylogenetically from plasma virus. In addition, we report that distinct cellular origins of compartmentalized HIV-1 define two classes of viral encephalitis, both of which are associated with neurological dysfunction and a clinical diagnosis of HIV-associated neurological disease.

## **MATERIALS AND METHODS**

### **Study subject population.**

All subjects used in this study were HIV-1-infected subjects that eventually initiated highly-active antiretroviral therapy. The subject samples used for viral genetic compartmentalization and envelope phenotype analyses were collected during previous studies carried out at the University of California at San Francisco. Subjects 4012, 4013, 5002, and 5003 were recruited from a study examining antiretroviral therapy responses in the CSF (289). Serial blood plasma and cerebrospinal fluid (CSF) samples were collected from subjects at baseline prior to the start of therapy. Plasma and CSF samples were collected longitudinally from subjects 7036 and 7115 for several years prior to the initiation of therapy. Plasma and CSF HIV-1 RNA concentrations were determined using the Amplicor HIV Monitor kit (Roche). Some of the subject sample characteristics have been previously reported (271). The studies were approved by the Committee for Human Research at the University of California at San Francisco, and all subjects provided written informed consent for the collection of samples.

### **Viral RNA isolation and single genome amplification.**

HIV-1 RNA was isolated from blood plasma and CSF samples (140  $\mu$ l) using the QIAmp Viral RNA kit (Qiagen). Samples with viral RNA levels less than 10,000 copies/ml were pelleted (0.5-1.0 ml) by centrifugation at 25,000 x g for 1.5 hours prior to RNA isolation in order to increase template number. Prior to RNA isolation, all CSF samples were centrifuged at 1,000 x g for 5 minutes to remove contaminating cellular debris. Viral RNA

was reverse transcribed using Superscript III Reverse Transcriptase (Invitrogen) with oligo(dT) as the primer per the manufacturer's instructions. Single genome amplification of the full-length HIV-1 *env* gene through the 3' U3 region was conducted as previously described (154, 220, 262). Briefly, cDNA was diluted to endpoint and nested PCR (67, 280) was conducted using the Platinum *Taq* High Fidelity polymerase (Invitrogen) as described by Salazar-Gonzalez *et al.* (262). The primers B5853 UP0 and LTR DN1 were used for the first round of PCR, and the primers B5957 UP1 and LTR DN1 were used for the second round of PCR (270). The SGA amplicons were sequenced from the start of V1 through the ectodomain of gp41 [Hxb2 numbering of positions 6600-8000].

#### **Phylogenetic and compartmentalization analyses.**

Phylogenetic analysis of cross-sectional and longitudinal plasma and CSF HIV sequences was carried out as stated below. Nucleotide sequences of the *env* genes were aligned using Clustal W (30, 299) or MAFFT software (152). Maximum likelihood phylogenetic trees were generated using PhyML (116) with the following parameters: HKY85 nucleotide substitution model, four substitution rate categories, estimation of the transition/transversion rate ratio, estimation of the proportion of invariant sites, and estimation of the gamma distribution parameter (115). Compartmentalization of CSF viral populations by sequence was determined using the Slatkin-Maddison test for compartmentalization (282) by HyPhy software (240) using 10,000 permutations. Pairwise distance was calculated for HIV-1 *env* sequences in the CSF-compartmentalized population for subjects with neurological disease using MEGA 4.1 software (162, 163, 296). All

sequences were subjected to quality control analysis to ensure that sequences from different subjects were not mislabeled.

### **Cells.**

293T and TZM-bl cells were cultured in Dulbecco's modified Eagle medium (DMEM) supplemented with 10% fetal bovine serum and 100 µg/ml of penicillin and streptomycin. 293-Affinofile cells (148) were maintained in DMEM supplemented with 10% dialyzed fetal bovine serum (12-14kD dialyzed; Atlanta biologicals) and 50 µg/ml blasticidin (D10F/B).

### **Construction of HIV-1 *env* clones.**

HIV-1 RNA was isolated from blood plasma and CSF samples, and the full-length *env* gene was amplified using the single genome amplification method as stated above. The SGA amplicons used in the cloning procedure were selected based on each subjects' phylogenetic tree structure and sequenced from the start of gp120 to the end of gp41. Since the SGA amplicons contained the full-length HIV-1 *env* gene through the 3' U3 region of the long terminal repeat, an additional PCR was conducted to amplify only the full-length HIV-1 *env* gene using the Phusion™ hot start high-fidelity DNA polymerase (Finnzymes) and the primers B5957F-TOPO (5'-CACCTTAGGCATCTCCTATGGCAGGAAGAAG-3') and B8904R-TOPO (5'-GTCTCGAGATACTGCTCCCACCC-3') following the manufacturer's instructions. HIV-1 *env* amplicons were then gel purified using the QIAquick gel extraction kit (Qiagen). The purified HIV-1 *env* genes were cloned into the pcDNA™3.1D/V5-His-TOPO® expression vector (Invitrogen) using the pcDNA™3.1 directional TOPO®

expression kit (Invitrogen) and MAX Efficiency® Stbl2™ competent cells (Invitrogen) as per the manufacturer's instructions. The cloned *env* genes were sequenced and screened to ensure that the original protein coding sequence was maintained.

### **Envelope-pseudotyped viruses.**

100mm x 20mm tissue culture dishes were coated with 10% poly-lysine in phosphate-buffered saline (PBS) and seeded with  $3 \times 10^6$  293T cells 24 hours prior to transfection. Envelope-pseudotyped luciferase reporter viruses were generated by co-transfection of 293 T cells with 3  $\mu$ g HIV-1 *env* expression vector and 3  $\mu$ g of the pNL4-3.LucR<sup>-</sup>E<sup>-</sup> plasmid (obtained from the NIH AIDS Research and Reference Reagent Program, Division of AIDS, NIAID, NIH) (37, 130) using the FuGENE® 6 transfection reagent and protocol (Roche). Five hours post-transfection the medium was changed and the cells were incubated at 37°C for an additional 48 hours. Viral supernatants were harvested using a 10 ml syringe, and filtered through a 0.45  $\mu$ m filter, and stored in aliquots at -80°C.

### **Coreceptor tropism analysis.**

One day prior to infection, TZM-bl cells were seeded onto 96-well black tissue culture plates ( $2 \times 10^5$  cells/well). Two hours prior to infection the coreceptor inhibitors TAK-779 (7, 60) and bicyclam JM-2987 (hydrobromide salt of AMD-3100) (19, 48, 132) (both obtained from the NIH AIDS Research and Reference Reagent Program, Division of AIDS, NIAID, NIH) were added at concentrations of 2.5  $\mu$ M and 5  $\mu$ M using the following conditions for each virus: no drug, TAK-779 only, AMD-3100 only, and both drugs. Cells were infected in the presence of drug using 50  $\mu$ l of viral supernatant per well and

spinoculated (2000 rpm) for 2 hours at 37°C. Infections were incubated for 48 hours at 37°C, and then the cells were washed twice with PBS and lysed with 50 µl of Reporter lysis buffer (Promega). Luciferase activity was assayed using the Luciferase assay system (Promega) on a Veritas microplate luminometer (Turner Biosystems). All infections and conditions were conducted in triplicate.

### **293-Affinofile cellular surface expression of CD4 and CCR5.**

Ninety-six-well plates were seeded with 293-Affinofile cells at a density of  $2.5 \times 10^5$  cells/well. Twenty-four hours later CD4 and CCR5 expression was induced with tetracycline and ponasterone A (ponA), respectively. Cells were induced in a matrix format for a total of 24 induction levels with varying amounts of tetracycline (0-0.1 µg/ml) and ponA (0-2 µM/ml). Induction was maintained for 18 hours at 37°C, the induction medium was then removed and cells were processed by quantitative flow cytometry. Cells were prepared for flow cytometry by staining at room temperature for 30 minutes with either phycoerythrin (PE)-conjugated anti-human CD4 antibody (clone Q4120, BD Biosciences) or PE-conjugated mouse anti-human CCR5 antibody (clone 2D7, BD Biosciences). Cells were then fixed with 4% paraformaldehyde, washed and analyzed by flow cytometry. CD4 and CCR5 receptor levels were quantified using *QuantiBRITE beads* (BD Biosciences).

### **Single-cycle infection of 293-Affinofile cells.**

Envelope-pseudotyped luciferase reporter viruses were initially titered on 293-Affinofile cells expressing the highest drug induction levels for CD4 (0.1 µg/ml tetracycline) and CCR5 (2 µM ponA) surface expression. The amount of pseudotyped virus used in the

single-cycle infection assay was normalized to  $10^6$  relative light units for infection at the highest drug levels tested. All pseudotyped viruses were used within the linear range of the assay, and all infection conditions were assayed in quadruplicate.

Two days prior to infection, 96-well black tissue culture plates were coated with 10% poly-lysine in PBS and seeded with 293-Affinofile cells ( $2.5 \times 10^5$  cells/well). Expression of CD4 and CCR5 was induced the following day by adding varying concentrations of tetracycline and ponasterone A as described above. Eighteen hours later, the induction medium was removed and fresh culture medium containing envelope-pseudotyped virus was gently added to the cells. The infection plates were spinoculated at 2000 rpm for 2 hours at  $37^\circ\text{C}$ , and incubated for an additional 48 hours at  $37^\circ\text{C}$ . Infection medium was then removed and the cells were washed twice with PBS and lysed with 50  $\mu\text{l}$  Reporter lysis buffer (Promega). Luciferase activity was assayed using the Luciferase assay system (Promega) on a Veritas microplate luminometer (Turner Biosystems).

## RESULTS

### **Extensive genetic compartmentalization between blood and CSF HIV-1 populations is correlated with HIV-1-associated dementia.**

Viral genetic compartmentalization was examined by conducting single genome amplification (SGA) on blood plasma and CSF samples from subjects with varying degrees of neurological disease (3 asymptomatic subjects, 1 MCMD subject, 7 HAD subjects; see Table 4.1). Compartmentalization in the CSF was determined based on the phylogenetic tree structure and the Slatkin-Maddison test for gene flow between populations. We found varying degrees of compartmentalization in the CSF of three neurologically asymptomatic subjects (Figure 4.1; subjects 4030, 4012, and 4021), which is consistent with reports from previous studies showing variable amounts of compartmentalized HIV-1 in the CSF of asymptomatic subjects (124, 126, 254). No compartmentalized variants were detected in the CSF of subject 4030, indicating extensive equilibration between the blood plasma and the CSF compartment. However, phylogenetic analysis of subject 4030 (Figure 4.1A) revealed an HIV-1 population in the blood plasma that was X4-like based on the V3 genotype, and an X4-like CSF variant (C16) that appeared to be a recombinant between X4- and R5-like variants detected in the peripheral blood (data not shown). In contrast, the phylogenetic tree of subject 4012 revealed a small clustering of CSF variants (Figure 4.1B), and we detected increased compartmentalization in the CSF of subject 4021 (Figure 4.1C).

Significant genetic compartmentalization was detected between the blood plasma and CSF HIV-1 populations of eight subjects with HIV-1-associated neurological disease (Table 4.1; Figure 4.2). Phylogenetic analysis revealed deep bifurcations and long branch-lengths

between the blood plasma and CSF viral populations, indicating that sustained HIV-1 replication is likely occurring in the CNS of subjects with neurological disease. Clonal amplification was identified for CSF variants that were separated phylogenetically from the plasma virus population in three subjects with HAD (subjects 4033, 5003, and 7036; Figure 4.2A), and this was associated with decreased *env* diversity in the CSF viral population (average pairwise distance within the compartmentalized population: 4033=0.007, 5003=0.003, 7036=0.002 nucleotide substitutions per site). In addition, HIV-1 populations in the CSF of subject 4051 were somewhat equilibrated with plasma virus based on the Slatkin-Maddison test ( $p=0.0908$ ), although a distinct sub-population of the CSF virus appeared to be compartmentalized based on the phylogenetic tree structure (Figure 4.2B). In addition, for two of these subjects (4033 and 5003), sequences from the population that was clonally amplified in the CSF also appeared in the blood, suggesting that there was a flow of viral genetic information from the CNS to the blood. Phylogenetic analysis also revealed significant compartmentalization between the plasma and CSF HIV-1 populations in four additional subjects with neurological disease (Figure 4.2C; subjects 4013, 4059, 5002, and 7115), which was associated with diverse *env* sequences in the CSF population (average pairwise distance within the compartmentalized population: 4013=0.023, 4059=0.029, 5002=0.017, 7115=0.02 nucleotide substitutions per site). These data indicate that significant genetic compartmentalization between the blood and CSF HIV-1 population is correlated with the development of neurological complications during HIV-1-infection.

### **Evolution of HIV-1 populations in the CSF prior to the development of HAD.**

In order to examine the evolution of compartmentalized HIV-1 variants in CNS/CSF of subjects with neurological disease, we conducted SGA on longitudinal plasma and CSF samples from two HAD subjects prior to the development of dementia (subjects 7036 and 7115). At the time of HAD diagnosis (2/18/2004), *env* sequences detected in the CSF of subject 7036 were considered compartmentalized based on the Slatkin-Maddison test ( $p < 0.0001$ ), and clonal amplification was also detected for some of the compartmentalized CSF variants (Figure 4.3). During our analysis of subject 7115, we detected clonal amplification in the CSF viral population two years prior to the development of dementia, although this amplified population was lost from the CSF population 6 months later. Phylogenetic analysis of *env* sequences from subject 7115 revealed a cluster of sequences derived from the CSF HIV-1 population, and at least one *env* sequence from each time-point was detected in this CSF cluster on the phylogenetic tree. The CSF viral population was not considered compartmentalized at the time of HAD diagnosis for subject 7115 (Slatkin-Maddison test,  $p = 0.3956$ ); however, one month after HAD diagnosis we detected significant compartmentalization between the blood and CSF viral populations (Figure 4.4; Slatkin-Maddison test,  $p < 0.0001$ ). These data suggest that an autonomously replicating HIV-1 population was maintained in the CNS of subject 7115 over the course of at least two years, and possibly led to the development of dementia. Additionally, significant compartmentalization in the CSF viral population seems to arise concurrently with the development of neurological complications, including HIV-1-associated dementia.

**Distinct cellular origins define two types of viral encephalitis.**

Perivascular macrophages and microglia are the two main cell types that express the CD4 receptor in the CNS and are purported to harbor replicating, compartmentalized HIV-1 variants (108, 109, 161, 233, 256, 298). We examined the phenotypes of 47 HIV-1 envelopes from the plasma and CSF viral populations of seven subjects with neurological disease, and from two asymptomatic subjects. Viral coreceptor usage and CD4 density dependence were assessed using HIV-1 *env* genes that were cloned and used to generate pseudotyped virus for the phenotype assays. The cloned *env* sequences are indicated with an asterisk in the subjects' phylogenetic trees in Figures 4.1 and 4.2. The HIV-1 envelope properties are listed in Table 4.2.

To determine envelope coreceptor usage, we infected TZM-bl cells with envelope-pseudotyped virus in the presence and absence of the CCR5 inhibitor TAK-779 (7, 60) and the CXCR4 inhibitor AMD-3100 (19, 48, 132). Most of the HIV-1 envelopes used the CCR5 coreceptor to enter cells; however, three envelopes used the CXCR4 coreceptor to enter cells (Figure 4.5 and Table 4.2). All three of the CXCR4-tropic envelopes (4030 P52, 4030 C16, and 5002 P10) were predicted based on the V3 genotypes and position-specific scoring matrix (PSSM) scores (145) (Table 4.2), including the CSF envelope variant from a neurologically asymptomatic subject (4030 C16). Thus, we conclude that for these subjects CXCR4-tropic viruses were not a significant feature of the viral population, especially in the CSF.

We examined the CD4 and CCR5 densities required for efficient virus entry into target cells in order to evaluate the cellular tropism of the plasma and CSF-derived HIV-1 envelopes. 293-Affinofile cells are a dual-inducible cell line where CD4 expression is controlled by tetracycline and CCR5 expression is controlled by ponasterone A (148). We

infected 293-Affinofile cells expressing different densities of CD4 and CCR5 in a matrix format using envelope-pseudotyped luciferase reporter virus, and measured luciferase activity to assess virus entry into cells. All HIV-1 envelopes had efficient entry into cells expressing a high density of CD4 on the cell surface (106,083 or 121,088 molecules/cell), and viral infection was also positively correlated with CCR5 surface expression at a high CD4 density, although in all cases infectivity varied only two-fold over the range of CCR5 densities tested (Figure 4.6 and data not shown).

We also examined the ability of HIV-1 envelopes to mediate entry into cells with low CD4 surface expression (1,315 or 2,630 molecules/cell) and found that some envelopes could efficiently enter cells expressing low CD4 density, whereas infection by other HIV-1 envelopes was dependent on high levels of CD4 surface expression. HIV-1 envelopes from the plasma and CSF of two asymptomatic subjects did not infect cells expressing low CD4 receptor densities, regardless of the CCR5 surface expression (Figure 4.7), indicating that these envelopes have a more T cell-tropic phenotype. Envelope phenotype characterization for subjects with HIV-associated neurological disease revealed two distinct classes of viral encephalitis (termed class 1 and class 2) associated with extensive genetic compartmentalization and the clinical diagnosis of dementia (Fisher's exact test,  $p=0.03$ ).

Class 1 viral encephalitis was linked to a dependence on high amounts of CD4 surface expression for viral attachment and entry into cells ( $n=3$  subjects). All of the envelopes derived from the blood plasma viral populations of subjects 4033, 5003, and 7036 required high CD4 densities for viral infection of 293-Affinofile cells (Figure 4.8A). In addition, HIV-1 envelopes derived from the CSF-compartmentalized population could not infect cells with low amounts of CD4 surface expression, indicating that the

compartmentalized variants in these subjects have a more T cell-tropic phenotype and likely did not originate from CNS macrophages (Figure 4.8A and Table 4.2).

Class 2 viral encephalitis was linked with the ability of compartmentalized CSF variants to use low densities of CD4 and CCR5 for cell attachment and entry (n=4 subjects). HIV-1 envelopes from the blood virus populations of subjects 4013, 4059, 5002, and 7115 required high CD4 surface expression for infection of 293-Affinofile cells. However, envelopes from the CSF-compartmentalized HIV-1 populations efficiently infected cells with low CD4 density, indicating that these compartmentalized envelopes have a macrophage-tropic phenotype (Figure 4.8B and Table 4.2). Two envelopes (4059 P21 and P28) from the plasma population of subject 4059 had some infectivity on low CD4 density cells, suggesting that some plasma variants in this subject have a more macrophage-tropic phenotype, although not to same degree as the compartmentalized CSF variants (Figure 4.8B). We also examined one CSF-derived envelope from subject 5002 that was not part of the compartmentalized viral population based on the phylogenetic tree structure (5002 C6). This CSF envelope variant was not able to infect cells with a low CD4 surface expression and had the same CD4 and CCR5 phenotype as the plasma HIV-1 variants, suggesting that the macrophage-tropic phenotype was specific to the compartmentalized HIV-1 variants in the CSF population. In addition, we analyzed CD4 counts as a measure of the degree of immunodeficiency for subjects with class 1 and class 2 viral encephalitis. The four subjects with class 2 viral encephalitis had significantly lower CD4 counts at the time that extensive compartmentalization was detected in the CSF compared to subjects with class 1 encephalitis ( $p=0.01$  using a two-tailed unpaired t-test). We also examined whether any HIV-1 genetic markers were associated with viral envelope phenotypes, and we found that a Q170K/R

amino acid substitution in the V1/V2 linker region of envelope was associated with the ability to infect low CD4 density cells (Figure 4.9;  $p=0.0002$  using a Fisher's exact test).

## **DISCUSSION**

HIV-1 replication in the central nervous system (CNS) is thought to occur in perivascular macrophages and microglia within the brain parenchyma (9, 161, 295). These local cells express low receptor densities of CD4 and CCR5 (177, 309), and can maintain productive HIV-1 infection (164, 241, 257). Brain-derived HIV-1 envelopes from subjects with encephalitis can have increased macrophage tropism and low CD4 dependence compared to envelopes obtained from lymph node tissue (63, 233, 256, 298). The development of HIV-1-associated dementia (HAD) has also been correlated with increased HIV-1 genetic compartmentalization between the CNS/CSF and the peripheral blood (64, 65, 126, 218, 236, 242, 254, 256, 291), suggesting that independent viral evolution in the CNS is linked with the clinical development of dementia. In the current study we have examined HIV-1 envelope genotypes and phenotypes associated with the clinical diagnosis of HAD. The goal of this work was to examine the viral characteristics associated with dementia, and to determine whether compartmentalized HIV-1 populations in the CSF of HAD subjects originate from local cells in the CNS.

In this study we used single genome amplification (SGA) to compare HIV-1 populations in the blood and CSF of chronically-infected subjects with varying degrees of neurological disease. Cross-sectional SGA analyses revealed significant compartmentalization in the CSF population associated with increased neurological disease. Our longitudinal SGA analyses of two HAD subjects also indicated that compartmentalized HIV-1 variants were maintained over a two year period as minor viral variants in the CSF population, and significant compartmentalization occurred concurrently with the

development of neurological disease. Finally, we examined compartmentalized HIV-1 envelope phenotypes from subjects with neurological disease and found that distinct cellular origins of compartmentalized virus define two classes of viral encephalitis associated with the clinical diagnosis of dementia.

Previously we had examined CSF-compartmentalized variant decay after the initiation of antiretroviral therapy in subjects with and without neurological disease (271). In this previous study, we found that compartmentalized HIV-1 variants in the CSF decay slowly after the initiation of HAART and originate from long-lived cells in some subjects with HAD (271). However, in a subset of HAD subjects we found that CSF-compartmentalized HIV-1 variants decay rapidly after the start of therapy, indicating that in these subjects the virus was originating from a short-lived cell type (271). In our current study, we used a subset of the same subject population and report that envelope phenotypes of compartmentalized HIV-1 variants in the CSF of HAD subjects revealed two classes of viral encephalitis. Class 1 viral encephalitis was associated with a high CD4 density-dependence of the compartmentalized virus for cell entry, while class 2 viral encephalitis was associated with the ability of CSF-compartmentalized HIV-1 variants to infect low CD4 density cells (Figure 4.8). The same subjects that displayed class 1 viral encephalitis (subjects 4033, 5003, and 7036) also had pleocytosis and CSF-compartmentalized HIV-1 variants that decayed rapidly after the initiation of therapy in our previous study (271). These data show that the compartmentalized virus in some HAD subjects is originating from a short-lived cell type and the envelopes have a T cell-tropic phenotype, indicating that the compartmentalized population is replicating in CD4<sup>+</sup> T cells (high CD4 surface expression), either within the CNS or the CSF. Conversely, the subject group that displayed class 2 viral

encephalitis (subjects 4013, 4059, 5002, and 7115) had CSF-compartmentalized HIV-1 variants that decayed slowly after the initiation of antiretroviral therapy (271). This indicates that the CSF-compartmentalized HIV-1 population in another group of neurologically symptomatic subjects is originating from a long-lived cell type, and the envelopes in this viral population have a macrophage-tropic phenotype, suggesting that the population is being maintained by autonomous viral replication in perivascular macrophages and/or microglia (low CD4 surface expression) within the CNS.

As noted above, we previously correlated the rapid decay of compartmentalized HIV-1 variants with high CSF pleocytosis (white blood cells in the CSF) in subjects with neurological disease (271). Increased amounts of infiltrating CD4<sup>+</sup> T cells would provide a reservoir for increased viral replication and population expansion, which correlates with the clonal amplification that we detected in the compartmentalized populations in some of these subjects. In addition, we know from our longitudinal analyses of HIV-1 evolution in subjects 7036 and 7115 that although compartmentalized HIV-1 variants are maintained as minor variants in the CSF population over several years, at some point a rapid expansion of specific CSF variants occurs which leads to significant genetic compartmentalization, and in these subjects this event was associated with clinical symptoms of neurological disease (Figures 4.3 and 4.4). It is possible that class 1-associated compartmentalized variants are maintained in perivascular macrophages and/or microglia in the CNS and amplified by infiltrating CD4<sup>+</sup> T cells; however, this scenario seems unlikely considering the T cell-tropic phenotype of these compartmentalized envelopes which indicates that these HIV-1 variants have been replicating in CD4<sup>+</sup> T cells.

The concept of extensively compartmentalized HIV-1 variants replicating in short-lived CD4<sup>+</sup> T cells in the CNS conflicts with current ideas about the origins of compartmentalized virus in the CNS. HIV-1 envelopes isolated from brain tissue of some subjects with dementia have macrophage-tropic phenotypes (63, 233, 256, 298), and are thought to persist and evolve in brain-resident macrophages. SIV studies of CNS infection detected only infiltrating SIV-specific CD8<sup>+</sup> T cells in the brains of infected monkeys, but found no CD4<sup>+</sup> T cells (188-190, 308). However, migration of CD4<sup>+</sup> T cells into the CNS is known to be important in the clearance of RNA virus infections in the CNS from both neurons and glial cells (110). Trafficking CD4<sup>+</sup> T cells have been reported in the CNS during infection of other neurotropic viruses, including rabies (74, 235, 258) and Sindbis virus (12). Additionally, a recent study reported that chronic brain infection by mouse hepatitis virus (strain JHM) resulted in long-term persistence of virus-specific CD4<sup>+</sup> and CD8<sup>+</sup> T cells in the CNS, and these cell populations were maintained by migration of peripheral virus-specific and naïve T cells into the CNS (325).

We propose that the presence of viral antigen, especially during periods of increased HIV-1 replication in the CNS/CSF compartment, would drive the migration of CD4<sup>+</sup> T cells into the CNS/CSF and lead to persistence and evolution of compartmentalized virus. The down-regulation of CD4 after infection with HIV-1 could explain the absence of CD4<sup>+</sup> T cells in the CNS of SIV-infected animals, in addition to rapid killing of these cells by the virus. Studies involving rabies virus have also shown regional brain tissue differences in BBB permeability and lymphocyte trafficking in the CNS, and increased CD4<sup>+</sup> T cell infiltration was observed in the cerebellum compared to the cerebral cortex (235, 258). CD4<sup>+</sup> T cell-driven replication of compartmentalized HIV-1 may occur in a specific anatomical

location with the CNS. Another possibility is that the majority of the T cell-driven compartmentalized virus replication and evolution is occurring in the CSF. Even under normal physiological conditions, the CSF contains ~3 leukocytes/ $\mu$ l and the majority of these cells are T cells, with an increased ratio of CD4<sup>+</sup> to CD8<sup>+</sup> T cells relative to the peripheral blood (248). Since we used the CSF as a surrogate for virus in the CNS, we cannot rule out the possibility that the T cell-tropic compartmentalized virus we measured for subjects 4033, 5003, and 7036 may be replicating in the CSF.

Slow decay of compartmentalized HIV-1 in the CSF was previously reported for a subset of neurologically symptomatic subjects after the initiation of HAART (68, 120, 271, 289). In addition, slow decay was associated with increased immunodeficiency and no/low CSF pleocytosis in these subjects (subjects 4013, 4059, 5002, and 7115) (271). We found that compartmentalized HIV-1 envelopes from subjects with slow viral decay also had a low CD4 density tropism (class 2 viral encephalitis), indicating that these variants are originating from longer-lived macrophages within the CNS. The detection of macrophage-tropic envelopes in the CSF population was also correlated with increased immunodeficiency based on peripheral CD4 counts. Decreased amounts of circulating CD4<sup>+</sup> T cells would result in reduced trafficking of CD4 cells into the CSF and brain tissue, which is consistent with the reduced CSF pleocytosis detected in these subjects (271).

The lack of CD4<sup>+</sup> T cells in these subjects (4013, 4059, 5002, and 7115) may explain the expansion of macrophage-tropic HIV-1 variants in the CNS during a period of increased viral replication. T cell-tropic and macrophage-tropic HIV-1 variants likely co-exist within a complex CNS viral population and are continuously evolving in isolation from the peripheral blood population. Increased HIV-1 replication would stimulate immune cell migration to the

CNS, and a common mechanism of immune control for viral CNS infections involves the migration of CD4<sup>+</sup> and CD8<sup>+</sup> T cells into the CNS to control and clear the infection (110). HIV-1-infected subjects with increased immunodeficiency lack substantial numbers of peripheral CD4<sup>+</sup> T cells, leading to the absence of these cells in the CNS. Furthermore, it has been proposed that events in the periphery may lead to increased CNS invasion of infected and uninfected monocytes, and differentiation of these cells into perivascular macrophages in the brain parenchyma (80). Supporting this idea, previous studies have reported an increase in the total number of brain perivascular macrophages in subjects with HIV (81, 82, 105) and in SIV-infected macaques with significant compartmentalization in the CSF (123). Increased numbers of perivascular macrophages would select for the outgrowth of macrophage-tropic HIV-1 variants from the CNS population during periods of increased immunodeficiency; however, we were not able to examine cell populations in the CNS due to the lack of brain tissue from our subject population.

Previous studies have reported that different amino acid substitutions in the Env protein are associated with macrophage tropism and dementia. Studies by Dunfee *et al.* (64, 65) have reported that the HIV Envs variant N283 and D386 were found more frequently in brain-derived *env* sequences from HAD subjects and had enhanced viral entry in macrophages (64). Another study identified amino acid residues on the CD4 binding loop flanks and residues in the V3 loop that conferred macrophage tropism to HIV-1 envelopes (62). Basic amino acid substitutions in the V1/V2 linker of HIV-1 envelope have also been reported in the CSF-compartmentalized populations of primary infection subjects (270). We found that a Q170K/R amino acid substitution in the V1/V2 linker region of envelope was associated with the ability to infect low CD4 density cells (Figure 4.9). A substitution from

glutamine to lysine is difficult and requires a C to A nucleotide transversion, which suggests that viral adaptation for low CD4 usage is enhancing the frequency of K170 in some envelopes. One possibility is that K170 enhances HIV-1 envelope binding to the sulfated polysaccharide heparan sulfate (HS) on the surface of macrophages. Studies mapping the HS domains of HIV-1 gp120 have reported an HS binding domain in the V1/V2 linker from amino acids 166 to 171 (43). Heparan sulfate is thought to enhance gp120 coreceptor binding (306), and one study reported that HS binding was necessary for efficient HIV-1 attachment to macrophages while CD4 binding was required for complete attachment and viral entry (264). Polyanionic compounds (such as HS) are known to bind to basic amino acid residues in proteins, and the K170 envelope variant may enhance HS binding to facilitate HIV-1 attachment and entry into low CD4 density cells. However, additional studies are necessary to discern the role K170 plays in HIV-1 attachment and entry.

In conclusion, our study defines two distinct classes of viral encephalitis, T cell-driven vs. macrophage-driven replication, leading to HIV-1 genetic compartmentalization in the CNS/CSF and the development of severe clinical neurological symptoms. Class 1 viral encephalitis was associated with compartmentalized HIV-1 variants with a high CD4 density dependence for cell entry. Neurologically symptomatic subjects with class 2 viral encephalitis had compartmentalized HIV-1 envelopes that displayed a low CD4 tropism. Future studies examining HIV-1 populations in paired blood, CSF, and brain tissue from HAD subjects with and without HIVE will help determine whether there are physiological differences in brain pathology between subjects with class 1 and class 2 viral encephalitis. This study illustrates the complex patterns of HIV-1 evolution in the CNS over the course of infection, and more studies will be required to understand the events leading up to extensive

compartmentalization in the CNS and clinical dementia. Our results suggest that increased HIV-1 replication and subsequent inflammation in the CNS/CSF compartment lead to clinical dementia, and the degree of immunodeficiency may define the cellular origin of the replicating compartmentalized virus.

## **ACKNOWLEDGEMENTS**

We thank Evelyn Lee for coordinating the clinical studies and materials, and the subjects for their participation. The following reagents were obtained through the NIH AIDS Research and Reference Reagent Program, Division of AIDS, NIAID, NIH: TAK-779, bicyclam JM-2987 (hydrobromide salt of AMD-3100), and pNL4-3.Luc.R-E- from Dr. Nathaniel Landau.

G. Schnell was supported in part by the NIH training grant T32-AI07001. S. Joseph was supported in part by NIH grant 5-30333-2311. This work was supported by the NIH award R01-MH67751 (to R.S.), the UNC Center for AIDS Research (NIH award P30-AI50410), the Lineberger Cancer Center core grant (NIH award P30-CA16086), NIH award K23-MH074466 and R01-MH81772 (to S.S.), NIH award R01-NS37660 (to R.W.P.), and NIH award UL1RR024131 (to UCSF).

**Table 4.1. Subject characteristics and CSF compartmentalization.**

| Subject ID | Sample date | Cell counts (cells/ $\mu$ l) |                      |                        | HIV-1 RNA (log <sub>10</sub> copies/ml) |      | CSF compartment <sup>c</sup> | Slatkin-Maddison <sup>d</sup> |
|------------|-------------|------------------------------|----------------------|------------------------|---|------|------------------------------|-------------------------------|
|            |             | CD4                          | CSF WBC <sup>a</sup> | ADC Stage <sup>b</sup> | Plasma                                  | CSF  |                              |                               |
| 4012       | 9/3/1997    | 295                          | 16                   | 0                      | 5.18                                    | 4.39 | Eq                           | p=0.1705                      |
| 4021       | 11/5/1998   | 215                          | 0                    | 0                      | 4.97                                    | 4.02 | Some Comp                    | p=0.002                       |
| 4030       | 9/16/1999   | 239                          | 4                    | 0                      | 4.86                                    | 4.06 | Eq                           | p=0.1516                      |
| 4013       | 11/17/1997  | 148                          | 10                   | 1                      | 4.62                                    | 4.75 | Comp                         | p<0.0001                      |
| 4033       | 1/12/2000   | 173                          | 28                   | 2                      | 4.83                                    | 5.23 | Comp, Amp                    | p=0.0021                      |
| 4051       | 8/20/2004   | 344                          | 12                   | 3                      | 5.61                                    | 5.41 | Some Comp                    | p=0.0908                      |
| 4059       | 8/16/2006   | 53                           | 1                    | 3                      | 5.31                                    | 5.08 | Comp                         | p<0.0001                      |
| 5002       | 10/17/1997  | 59                           | 4                    | 3                      | 4.24                                    | 5.32 | Comp                         | p<0.0001                      |
| 5003       | 11/3/1997   | 234                          | 46                   | 3                      | 3.31                                    | 4.33 | Comp, Amp                    | p<0.0001                      |
| 7036       | 10/31/2002  | 327                          | 20                   | 0                      | 4.67                                    | 3.89 | Uneq                         | p=0.0049                      |
|            | 4/28/2003   | 324                          | 30                   | 0                      | 4.97                                    | 4.41 | Eq                           | p=0.7113                      |
|            | 2/18/2004   | 267                          | 240                  | 2                      | 5.12                                    | 5.37 | Comp, Amp                    | p<0.0001                      |
| 7115       | 7/8/2002    | 145                          | 7                    | 0                      | 4.68                                    | 4.43 | Amp                          | p=0.0083                      |
|            | 12/3/2002   | 108                          | 24                   | 0                      | 4.76                                    | 4.85 | Some Comp                    | p=0.0256                      |
|            | 4/8/2004    | 50                           | 12                   | 2                      | 5.87                                    | 4.85 | Eq                           | p=0.3956                      |
|            | 5/11/2004   | 66                           | 6                    | 2                      | 3.46                                    | 4.63 | Comp                         | p<0.0001                      |
|            | 6/3/2004    | 150                          | 7                    | 3                      | 2.97                                    | 3.54 | n/a                          |                               |

<sup>a</sup>= CSF white blood cell counts (cells/ $\mu$ l)

<sup>b</sup>= ADC staging: (245).

<sup>c</sup>=HIV-1 population characteristics in the CSF compartment. Eq=equilibration with the blood plasma; Uneq=discordance between the CSF and blood plasma without substantial compartmentalization; Some Comp=a subpopulation of the CSF is compartmentalized; Comp=significant compartmentalization in the CSF; Amp=clonal amplification of variants detected in the CSF; n/a=not applicable. The classification of clonal amplification was determined by calculating the average overall pairwise distance (nucleotide substitutions per site) between *env* sequences in the compartmentalized HIV-1 population for subjects with neurological disease (subject 4013, 0.023; subject 4033, 0.007; subject 4051, 0.03; subject 4059, 0.029; subject 5002, 0.017; subject 5003, 0.003; subject 7036, sample date 2/18/2004, 0.002; subject 7115, sample date 7/8/2002, 0.002; subject 7115, sample date 5/11/2004, 0.02). A CSF HIV-1 population with an average pairwise distance <0.01 was considered to have clonal amplification.

<sup>d</sup>=Slatkin-Maddison test for gene flow between populations. A p-value <0.05 indicates statistically significant compartmentalization between the blood and CSF HIV-1 populations.

**Table 4.2. Cellular tropism characteristics of envelope-pseudotyped viruses.**

| Subject ID            | Sample date | Env clone | PSSM score <sup>a</sup> | Coreceptor phenotype | High CD4, low CCR5 <sup>b</sup> | High CD4, high CCR5 <sup>c</sup> | Low CD4, low CCR5 <sup>d</sup> | Low CD4, high CCR5 <sup>e</sup> | Comp. virus decay <sup>f</sup> |
|-----------------------|-------------|-----------|-------------------------|----------------------|---------------------------------|----------------------------------|--------------------------------|---------------------------------|--------------------------------|
| M-tropic <sup>g</sup> |             | Ba-L      | 0                       | R5                   | 51.8                            | 100                              | 14.3                           | 18.0                            |                                |
| T cell-tropic         |             | JR-CSF    | 0                       | R5                   | 66.5                            | 100                              | 0.3                            | 0.4                             |                                |
| 4012                  | 9/3/1997    | P1        | 0                       | R5                   | 52.7                            | 100                              | 1.7                            | 2.2                             | n/a                            |
|                       |             | P37       | 0                       | R5                   | 53.3                            | 100                              | 2.3                            | 3.2                             |                                |
|                       |             | C8        | 0                       | R5                   | 33.8                            | 100                              | 0.4                            | 0.7                             |                                |
|                       |             | C11       | 0                       | R5                   | 57.4                            | 100                              | 1.2                            | 1.3                             |                                |
| 4030                  | 9/16/1999   | P52       | 1                       | X4                   | 107.1                           | 100                              | 1.8                            | 1.2                             |                                |
|                       |             | P56       | 0                       | R5                   | 53.8                            | 100                              | 1.3                            | 1.4                             | n/a                            |
|                       |             | C11       | 0                       | R5                   | 52.6                            | 100                              | 0.6                            | 0.7                             |                                |
|                       |             | C16       | 1                       | X4                   | 112.9                           | 100                              | 4.1                            | 2.9                             |                                |
|                       |             | C23       | 0                       | R5                   | 54.4                            | 100                              | 3.0                            | 3.5                             |                                |
| 4033                  | 1/12/2000   | P9        | 0                       | R5                   | 63.7                            | 100                              | 3.5                            | 3.1                             | rapid                          |
|                       |             | P10       | 0                       | R5                   | 62.3                            | 100                              | 0.7                            | 0.5                             |                                |
|                       |             | P13       | 0                       | R5                   | 57.1                            | 100                              | 0.1                            | 0.1                             |                                |
|                       |             | C10       | 0                       | R5                   | 49.0                            | 100                              | 2.1                            | 3.0                             |                                |
|                       |             | C15       | 0                       | R5                   | 58.6                            | 100                              | 1.0                            | 1.1                             |                                |
|                       |             | C24       | 0                       | R5                   | 63.4                            | 100                              | 0.9                            | 1.1                             |                                |
| 5003                  | 11/3/1997   | P18       | 0                       | R5                   | 49.4                            | 100                              | 1.3                            | 1.6                             | rapid                          |
|                       |             | P33       | 0                       | R5                   | 54.2                            | 100                              | 1.3                            | 1.8                             |                                |
|                       |             | P44       | 0                       | R5                   | 57.9                            | 100                              | 0.1                            | 0.1                             |                                |
|                       |             | C4        | 0                       | R5                   | 47.3                            | 100                              | 0.9                            | 1.2                             |                                |
|                       |             | C18       | 0                       | R5                   | 37.8                            | 100                              | 0.5                            | 0.8                             |                                |
| 7036                  | 2/18/2004   | P9        | 0                       | R5                   | 52.4                            | 100                              | 0.1                            | 0.2                             | rapid                          |
|                       |             | C3        | 0                       | R5                   | 44.4                            | 100                              | 0.3                            | 0.5                             |                                |
|                       |             | C7        | 0                       | R5                   | 52.4                            | 100                              | 0.3                            | 0.4                             |                                |
|                       |             | C33       | 0                       | R5                   | 56.0                            | 100                              | 1.1                            | 1.2                             |                                |
| 4013                  | 11/17/1997  | P9        | 0                       | R5                   | 69.5                            | 100                              | 0.4                            | 0.4                             | slow                           |
|                       |             | P32       | 0                       | R5                   | 68.8                            | 100                              | 0.4                            | 0.4                             |                                |
|                       |             | P44       | 0                       | R5                   | 69.6                            | 100                              | 0.3                            | 0.3                             |                                |
|                       |             | C7        | 0                       | R5                   | 61.1                            | 100                              | 19.3                           | 22.9                            |                                |
|                       |             | C11       | 0                       | R5                   | 55.9                            | 100                              | 10.7                           | 10.8                            |                                |
|                       |             | C23       | 0                       | R5                   | 56.3                            | 100                              | 25.5                           | 28.4                            |                                |
| 4059                  | 8/16/2006   | P21       | 0                       | R5                   | 67.1                            | 100                              | 11.7                           | 13.6                            | slow                           |
|                       |             | P26       | 0                       | R5                   | 64.6                            | 100                              | 0.3                            | 0.4                             |                                |
|                       |             | P28       | 0                       | R5                   | 68.6                            | 100                              | 6.9                            | 7.9                             |                                |
|                       |             | C6        | 0                       | R5                   | 57.2                            | 100                              | 25.0                           | 34.9                            |                                |
|                       |             | C12       | 0                       | R5                   | 58.7                            | 100                              | 19.5                           | 23.6                            |                                |
|                       |             | C19       | 0                       | R5                   | 58.6                            | 100                              | 13.7                           | 17.4                            |                                |
| 5002                  | 10/17/1997  | P10       | 1                       | X4                   | 100.4                           | 100                              | 1.3                            | 1.0                             | slow                           |
|                       |             | P13       | 0                       | R5                   | 67.6                            | 100                              | 0.5                            | 0.4                             |                                |
|                       |             | P18       | 0                       | R5                   | 56.7                            | 100                              | 0.7                            | 0.9                             |                                |

|      |           |     |   |    |      |     |      |      |      |
|------|-----------|-----|---|----|------|-----|------|------|------|
|      |           | C1  | 0 | R5 | 56.7 | 100 | 19.9 | 26.1 |      |
|      |           | C13 | 0 | R5 | 49.9 | 100 | 12.6 | 19.1 |      |
|      |           | C6  | 0 | R5 | 47.9 | 100 | 1.7  | 2.1  |      |
| 7115 | 5/11/2004 | P6  | 0 | R5 | 43.5 | 100 | 0.05 | 0.07 | slow |
|      |           | P17 | 0 | R5 | 58.6 | 100 | 1.1  | 1.2  |      |
|      |           | C3  | 0 | R5 | 60.2 | 100 | 21.0 | 32.5 |      |
|      |           | C15 | 0 | R5 | 53.7 | 100 | 16.5 | 20.9 |      |
|      |           | C21 | 0 | R5 | 63.6 | 100 | 23.1 | 31.2 |      |

<sup>a</sup>=Position-specific scoring matrix score, ref. (145). (0 = R5-like sequence, 1 = X4-like sequence)

<sup>b</sup>=CD4 density: 106,083 molecules/cell, CCR5 density: 2,529 molecules/cell (subjects 4012, 4030, 5003, 7036, 7115; 5002 clones P13, C6, C13); CD4 density: 121,088 molecules/cell, CCR5 density: 6,156 (subjects 4013, 4033, 4059; 5002 clones P10, P18, C1)

<sup>c</sup>= CD4 density: 106,083 molecules/cell, CCR5 density: 53,498 molecules/cell (subjects 4012, 4030, 5003, 7036, 7115; 5002 clones P13, C6, C13); CD4 density: 121,088 molecules/cell, CCR5: 90,462 molecules/cell (subjects 4013, 4033, 4059; 5002 clones P10, P18, C1)

<sup>d</sup>= CD4 density: 1,315 molecules/cell, CCR5 density: 2,529 molecules/cell (subjects 4012, 4030, 5003, 7036, 7115; 5002 clones P13, C6, C13); CD4 density: 2,630 molecules/cell, CCR5 density: 6,156 molecules/cell (subjects 4013, 4033, 4059; 5002 clones P10, P18, C1)

<sup>e</sup>= CD4 density: 1,315 molecules/cell, CCR5 density: 53,498 molecules/cell (subjects 4012, 4030, 5003, 7036, 7115; 5002 clones P13, C6, C13); CD4 density: 2,630 molecules/cell, CCR5 density: 90,462 molecules/cell (subjects 4013, 4033, 4059; 5002 clones P10, P18, C1)

<sup>f</sup>= CSF-compartmentalized variant decay based on previously published data (271)

<sup>g</sup>=Macrophage-tropic control envelope



SGA amplicons were first aligned, and a maximum-likelihood phylogenetic tree was constructed using PhyML. Bootstrap numbers  $\geq 70$  are indicated at the appropriate nodes. Sequences obtained from the CSF are labeled with solid blue circles, and plasma sequences are labeled with solid red rectangles on the tree. Genetic distance between sequences is indicated by the distance scale bar at the bottom of the tree. HIV-1 *env* sequences that were selected for phenotypic analysis are indicated with asterisks.

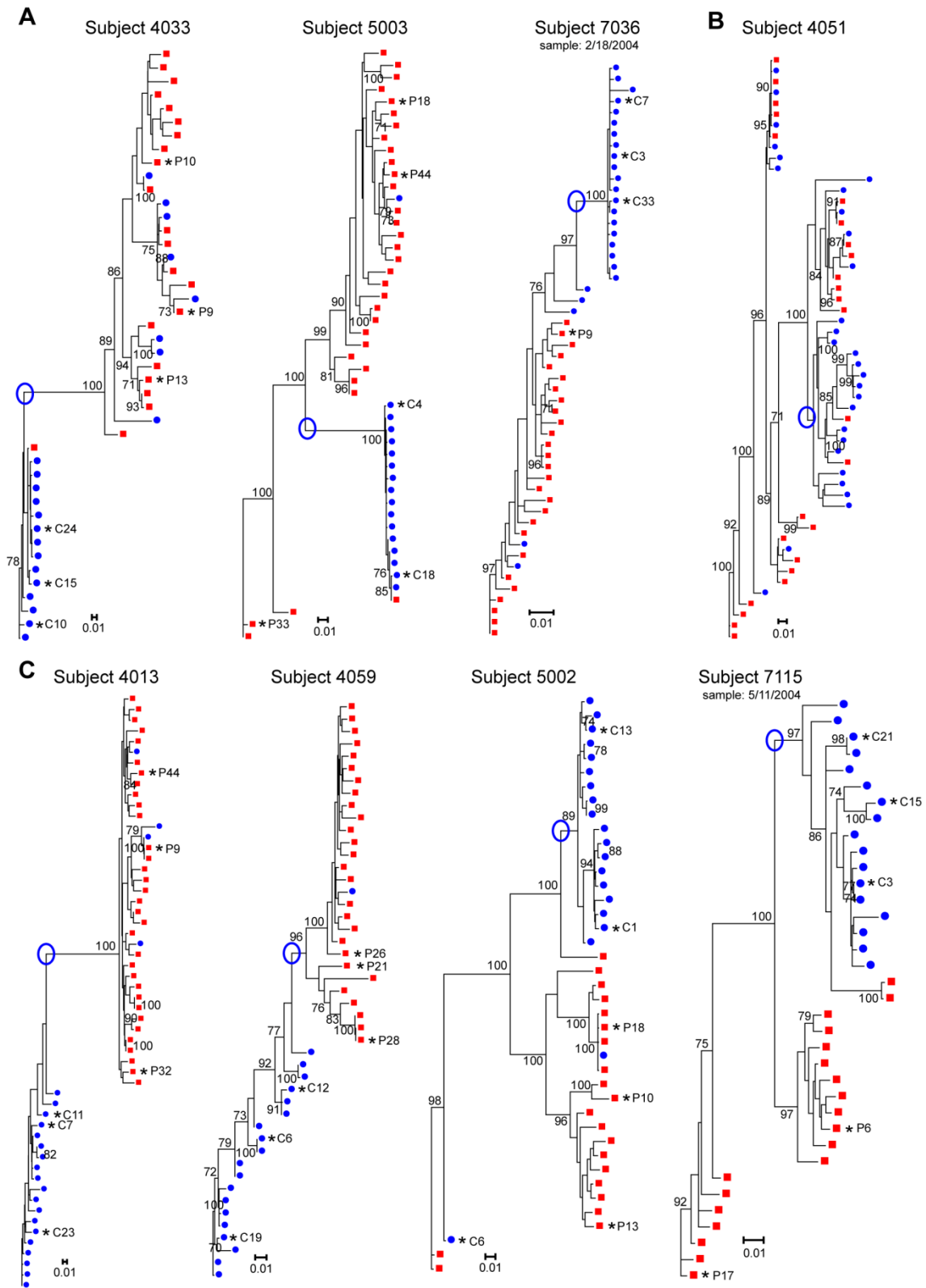


**Figure 4.2. Phylogenetic analysis of plasma and CSF HIV-1 populations for neurologically symptomatic subjects. (A) Phylogenetic trees of HIV-1 *env* sequences for**

subjects 4033, 5003, and 7036, which display significant compartmentalization and clonal amplification in the CSF HIV-1 population. (B) Phylogenetic tree of HIV-1 *env* sequences for subject 4051. A subset of the CSF population was considered compartmentalized. (C) Phylogenetic trees of HIV-1 *env* sequences for subjects 4013, 4059, 5002, and 7115, which display significant compartmentalization in the CSF HIV-1 population. The open blue circles illustrate the node of divergence for the compartmentalized CSF sequences. SGA amplicons were first aligned, and a maximum-likelihood phylogenetic tree was constructed using PhyML. Bootstrap numbers  $\geq 70$  are indicated at the appropriate nodes. Sequences obtained from the CSF are labeled with solid blue circles, and plasma sequences are labeled with solid red rectangles on the tree. Genetic distance between sequences is indicated by the distance scale bar at the bottom of the tree. HIV-1 *env* sequences that were selected for phenotypic analysis are indicated with asterisks.

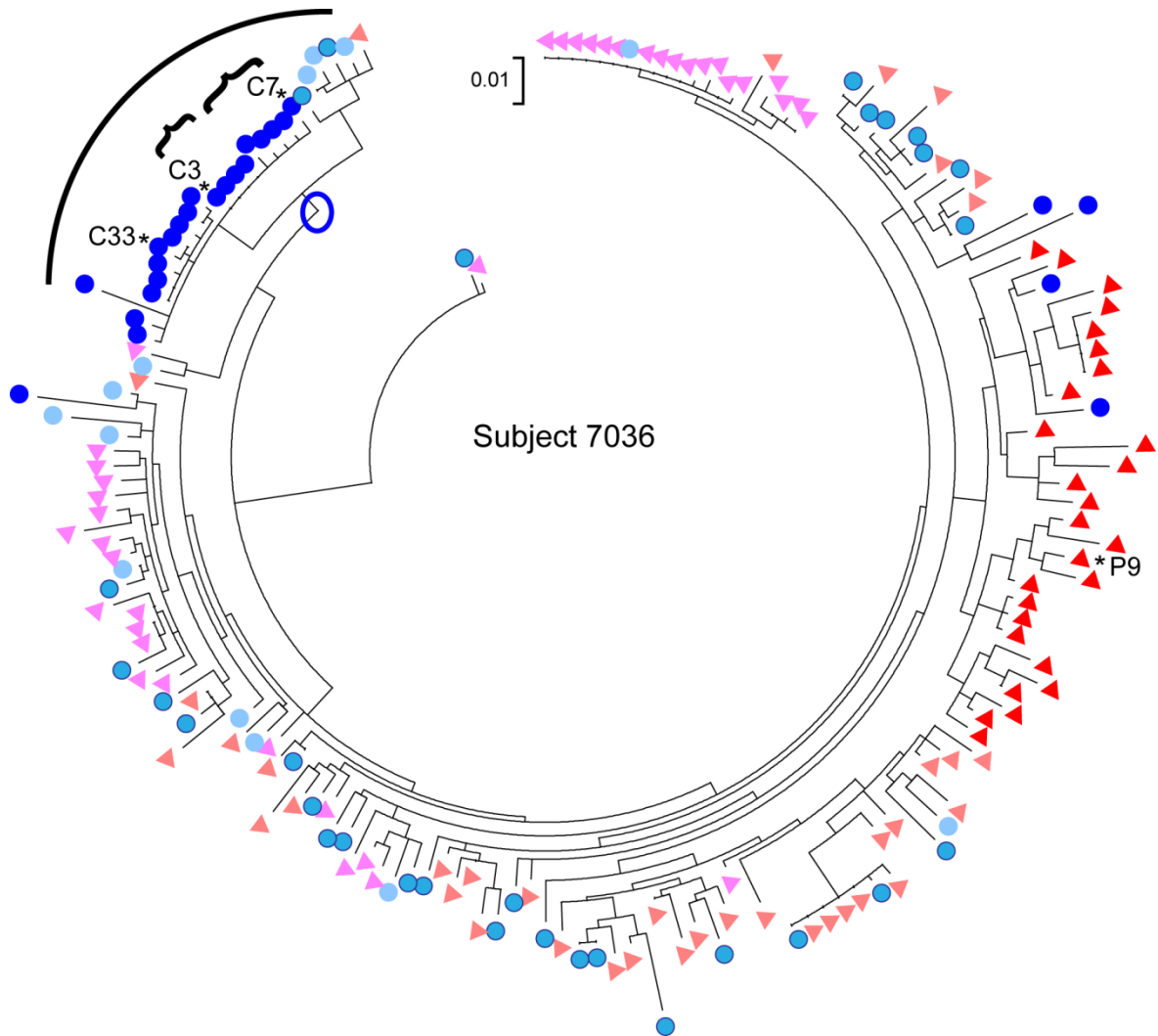


**Figure 4.3. Longitudinal phylogenetic analysis of subject 7036 HIV-1 populations.** Phylogenetic circle tree of plasma and CSF HIV-1 *env* sequences from sample dates 10/31/2002 (plasma=light pink triangle; CSF=pale blue circle), 4/28/2003 (plasma=dark salmon triangle; CSF=medium blue circle with dark outline), and 2/18/2004 (plasma=bright red triangle; CSF=royal blue circle). The compartmentalized *env* sequences in the CSF are indicated by the black curved line, and CSF sequences that were clonally amplified on 2/18/2004 are indicated by the black brackets. The open blue circle illustrates the node of divergence for the compartmentalized CSF sequences. Genetic distance between sequences is indicated by the scale bar. HIV-1 *env* sequences that were selected for phenotypic analysis are indicated with asterisks.

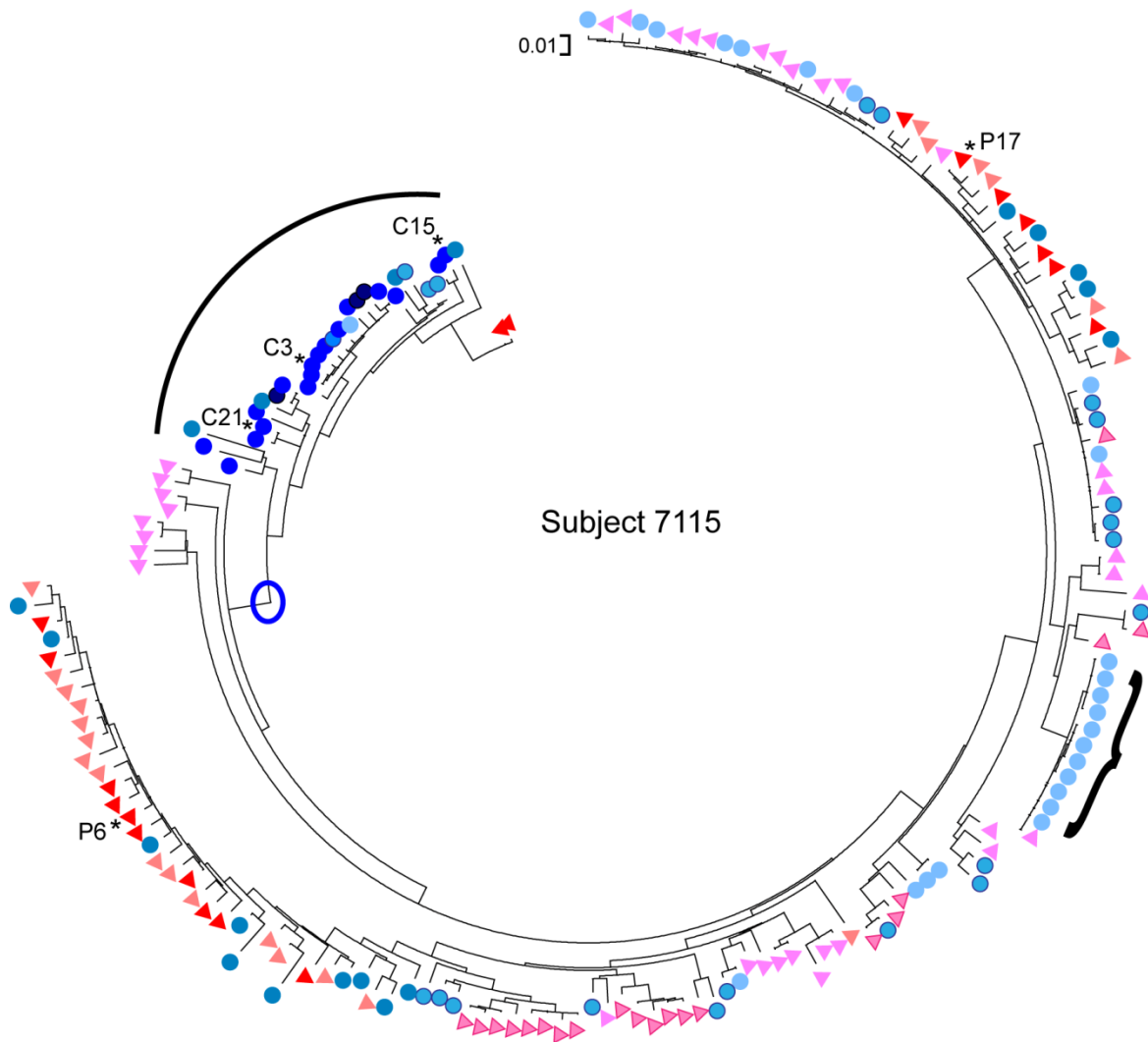


**Figure 4.4. Longitudinal phylogenetic analysis of subject 7115 HIV-1 populations.** Phylogenetic circle tree of plasma and CSF HIV-1 *env* sequences from sample dates 7/8/2002 (plasma=light pink triangle; CSF=pale blue circle), 12/3/2002 (plasma=pink triangle with dark pink outline; CSF=medium blue circle with dark outline), 4/8/2004 (plasma=light-red triangle; CSF=blue-gray circle), 5/11/2004 (plasma=bright red triangle; CSF=royal blue circle), and 6/3/2004 (CSF=navy blue circle with black outline). The compartmentalized *env* sequences in the CSF are indicated by the black curved line, and the open blue circle illustrates the node of divergence for the compartmentalized CSF sequences. CSF sequences that were clonally amplified on 7/8/2002 are indicated by the black brackets. Genetic distance between sequences is indicated by the scale bar. HIV-1 *env* sequences that were selected for phenotypic analysis are indicated with asterisks.

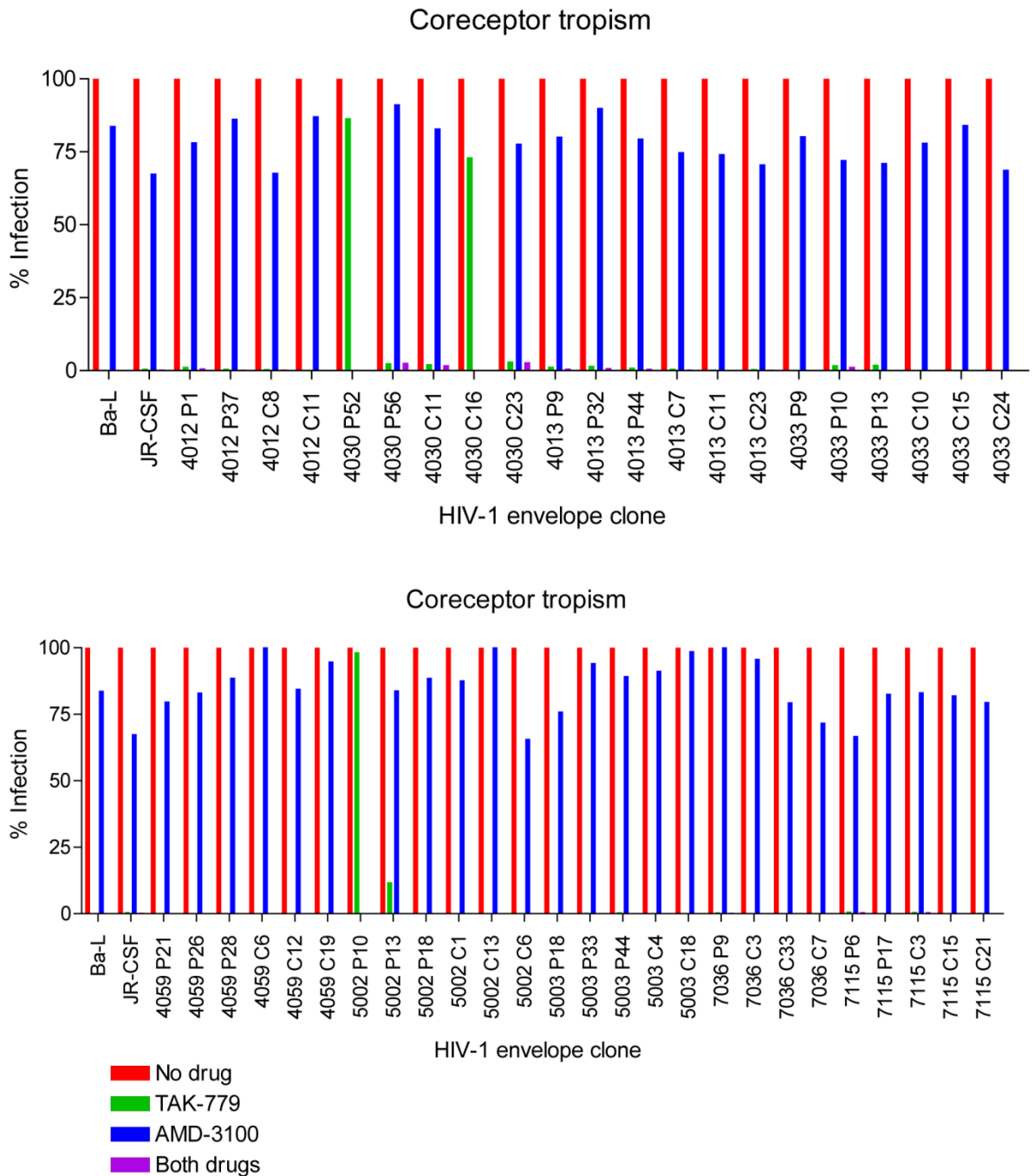


**Figure 4.5. Coreceptor tropism of HIV-1 envelope-pseudotyped reporter viruses.** TZM-bl cells were infected with pseudotyped virus in the presence of no drug (red bar), the CCR5 inhibitor TAK-779 only (green bar), the CXCR4 inhibitor AMD-3100 only (blue bar), or both drugs (purple bar). Infection was normalized for background, and luciferase activity for infection in the absence of drug was normalized to 100%. The Ba-L envelope was used as a macrophage-tropic control envelope, and the JR-CSF envelope was used as a T cell-tropic control envelope. A pseudotyped virus that was inhibited by TAK-779 but not by AMD-3100 was considered to use the CCR5 coreceptor for cell entry. A pseudotyped virus that

was inhibited by AMD-3100 but not by TAK-779 was considered to use the CXCR4 coreceptor for cell entry. Infection was inhibited for all pseudotyped viruses when both drugs were present. Results shown are from the average of three replicates.

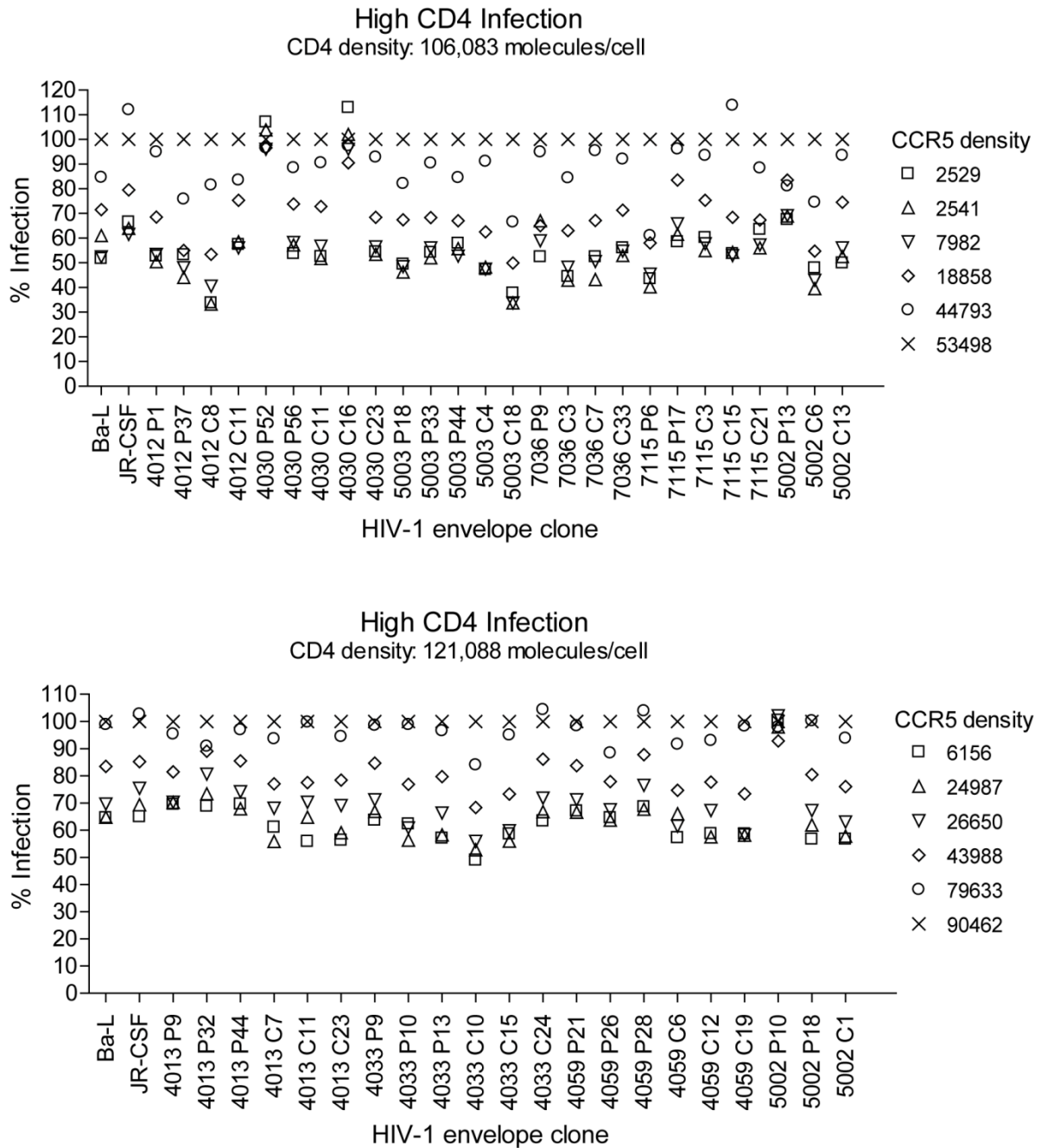


**Figure 4.6. HIV-1 envelopes from the plasma and CSF of all subjects efficiently infect cells with a high CD4 surface expression.** 293-Affinofile cells expressing high levels of CD4 (106,083 or 121,088 molecules/cell) and varying levels of CCR5 were infected with envelope-pseudotyped reporter viruses. Infection was normalized to 100% for each virus for luciferase activity on cells with the highest surface expression of CD4 and CCR5. The CCR5 densities are listed in units of molecules/cell. The Ba-L envelope was used as a macrophage-tropic control envelope, and the JR-CSF envelope was used as a T cell-tropic control envelope. Results shown are from the average of four replicates.

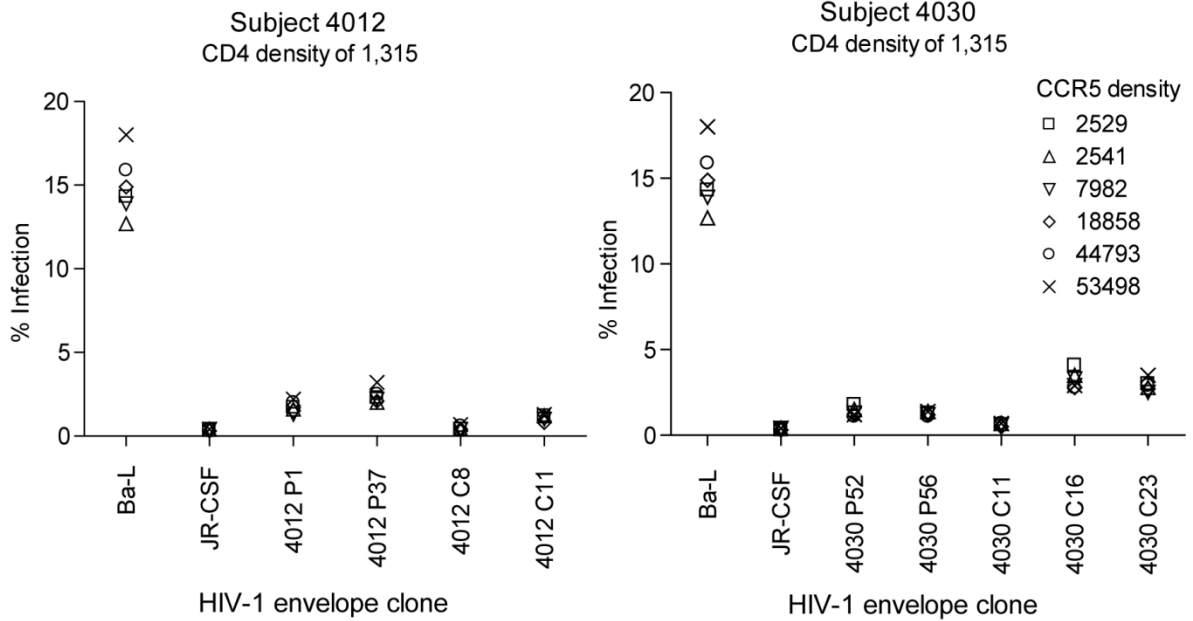


**Figure 4.7. HIV-1 envelopes from the plasma and CSF of neurologically asymptomatic subjects do not infect cells with a low CD4 surface expression.** 293-Affinofile cells expressing a low density of CD4 (1,315 molecules/cell) and varying levels of CCR5 were infected with envelope-pseudotyped reporter viruses. Infection was normalized to 100% for luciferase activity on cells with the highest surface expression of CD4 and CCR5. The CD4 and CCR5 densities are listed in units of molecules/cell. The Ba-L envelope was used as a macrophage-tropic control envelope, and the JR-CSF envelope was used as a T cell-tropic control envelope. Results shown are from the average of four replicates.

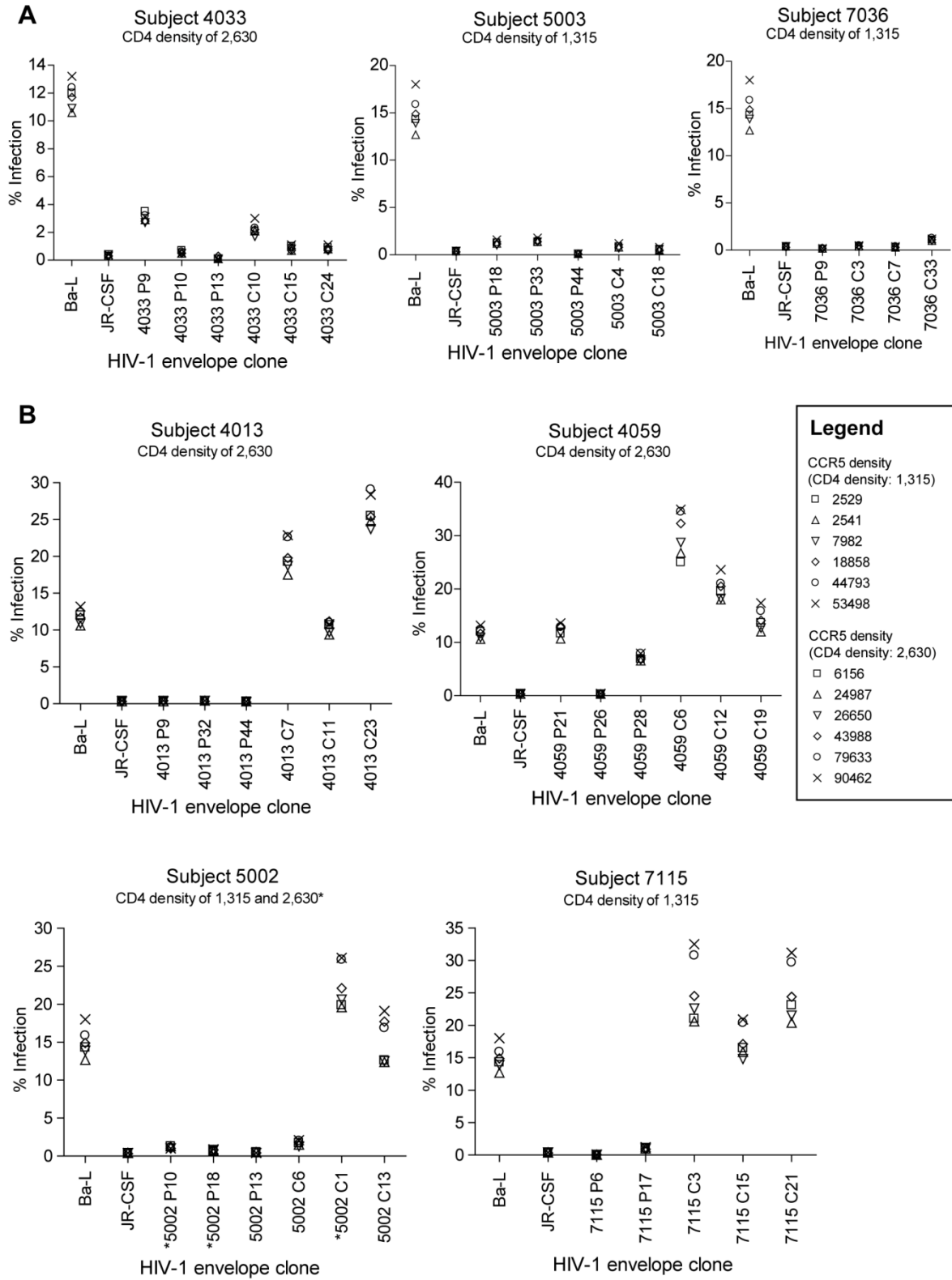


**Figure 4.8. HIV-1 envelopes from the plasma and CSF of neurologically symptomatic subjects differ in their ability to infect cells with a low CD4 surface expression. (A)**

Envelopes from the plasma and CSF-compartmentalized HIV-1 populations of some HAD subjects do not infect low CD4 density cells. **(B)** Envelopes from the CSF-compartmentalized HIV-1 population of some neurologically symptomatic subjects efficiently infect low CD4 density cells. Envelope clone 5002 C6 was selected from the non-compartmentalized viral population in the CSF. 293-Affinofile cells expressing a low density of CD4 (1,315 or 2,630 molecules/cell) and varying levels of CCR5 were infected with envelope-pseudotyped reporter viruses. Infection was normalized to 100% for luciferase activity on cells with the highest surface expression of CD4 and CCR5. The CD4 and CCR5 densities are listed in units of molecules/cell. The Ba-L envelope was used as a macrophage-tropic control envelope, and the JR-CSF envelope was used as a T cell-tropic control envelope. Results shown are from the average of four replicates.

|      |     |     |   |     |   |     |
|------|-----|-----|---|-----|---|-----|
|      |     | 161 |   | 170 |   | 180 |
|      |     |     |   | ↓   |   |     |
| HXB2 | env | I   | S | T   | S | I   |
|      |     | R   | G | K   | V | Q   |
|      |     | K   | E | Y   | A | F   |
|      |     | F   | Y | K   | L | D   |
| 4030 | C16 | -   | T | -   | V | -   |
|      |     | D   | R | -   | - | -   |
|      |     | S   | L | -   | R | P   |
| 4030 | C11 | -   | T | -   | G | -   |
|      |     | D   | - | -   | R | -   |
|      |     | L   | - | R   | - | -   |
| 4030 | C23 | -   | T | -   | - | -   |
|      |     | D   | R | -   | D | -   |
|      |     | L   | - | R   | - | -   |
| 4030 | P56 | -   | T | -   | - | -   |
|      |     | D   | R | -   | D | -   |
|      |     | L   | - | R   | - | -   |
| 4030 | P52 | -   | T | -   | V | -   |
|      |     | D   | R | -   | - | -   |
|      |     | S   | L | -   | R | P   |
| 4012 | C11 | -   | T | -   | N | -   |
|      |     | D   | R | -   | - | -   |
|      |     | L   | - | -   | - | -   |
| 4012 | C8  | -   | T | -   | N | -   |
|      |     | D   | R | -   | - | -   |
|      |     | L   | - | -   | - | -   |
| 4012 | P37 | -   | T | -   | N | -   |
|      |     | D   | R | -   | - | -   |
|      |     | L   | - | -   | - | -   |
| 4012 | P1  | -   | T | -   | N | -   |
|      |     | S   | D | R   | - | -   |
|      |     | L   | - | -   | - | -   |
| 5003 | C18 | -   | T | -   | R | -   |
|      |     | M   | R | -   | - | -   |
|      |     | -   | - | -   | - | -   |
| 5003 | C4  | -   | T | -   | R | -   |
|      |     | M   | R | -   | - | -   |
|      |     | -   | - | -   | - | -   |
| 5003 | P18 | V   | T | -   | V | -   |
|      |     | D   | M | R   | - | -   |
|      |     | L   | - | -   | - | -   |
| 5003 | P44 | V   | T | -   | V | -   |
|      |     | D   | M | R   | - | -   |
|      |     | L   | - | -   | - | -   |
| 5003 | P33 | V   | T | -   | M | -   |
|      |     | D   | M | R   | - | -   |
|      |     | L   | - | -   | - | -   |
| 5002 | P10 | V   | T | -   | H | -   |
|      |     | D   | E | S   | A | -   |
|      |     | N   | - | -   | - | -   |
| 5002 | P13 | V   | T | -   | H | -   |
|      |     | D   | S | A   | - | -   |
|      |     | N   | - | -   | - | -   |
| 5002 | P18 | V   | T | A   | H | -   |
|      |     | D   | F | T   | - | -   |
|      |     | V   | - | -   | - | -   |
| 5002 | C6  | V   | T | -   | H | -   |
|      |     | D   | S | T   | - | -   |
|      |     | T   | - | -   | - | -   |
| 7115 | P6  | -   | T | S   | G | -   |
|      |     | D   | R | -   | D | -   |
|      |     | -   | - | -   | - | -   |
| 7115 | P17 | -   | T | S   | G | -   |
|      |     | D   | R | -   | D | -   |
|      |     | -   | - | -   | - | -   |
| 7036 | C3  | V   | T | -   | L | -   |
|      |     | D   | E | -   | M | -   |
|      |     | -   | - | -   | - | -   |
| 7036 | C33 | V   | T | -   | L | -   |
|      |     | D   | E | -   | M | -   |
|      |     | -   | - | -   | - | -   |
| 7036 | C7  | V   | T | -   | L | -   |
|      |     | D   | E | -   | M | -   |
|      |     | -   | - | -   | - | -   |
| 7036 | P9  | V   | T | -   | N | -   |
|      |     | D   | G | T   | - | -   |
|      |     | L   | - | -   | - | -   |
| 4013 | P32 | V   | T | -   | D | -   |
|      |     | D   | K | -   | R | -   |
|      |     | L   | - | S   | - | -   |
| 4013 | P44 | V   | T | -   | D | -   |
|      |     | D   | K | -   | R | -   |
|      |     | L   | - | S   | - | -   |
| 4013 | P9  | V   | T | -   | I | -   |
|      |     | D   | K | -   | R | -   |
|      |     | L   | - | S   | - | -   |
| 4033 | C10 | -   | T | A   | - | R   |
|      |     | G   | N | -   | K | -   |
|      |     | L   | - | N   | - | -   |
| 4033 | C15 | -   | T | -   | R | G   |
|      |     | S   | - | K   | - | -   |
|      |     | L   | - | S   | - | -   |
| 4033 | C24 | -   | T | -   | R | G   |
|      |     | S   | - | K   | - | -   |
|      |     | L   | - | S   | - | -   |
| 4033 | P9  | V   | T | -   | N | -   |
|      |     | D   | K | -   | - | -   |
|      |     | L   | - | -   | - | -   |
| 4033 | P13 | -   | T | -   | N | -   |
|      |     | D   | K | -   | - | -   |
|      |     | L   | - | I   | - | -   |
| 4033 | P10 | V   | T | -   | N | -   |
|      |     | D   | K | -   | - | -   |
|      |     | L   | - | -   | - | -   |
| 4059 | P26 | V   | T | -   | N | E   |
|      |     | E   | N | -   | - | -   |
|      |     | K   | - | L   | L | -   |
| 4059 | P21 | V   | T | -   | N | E   |
|      |     | E   | N | -   | - | -   |
|      |     | K   | - | L   | L | -   |
| 4059 | P28 | V   | T | -   | N | E   |
|      |     | G   | T | -   | - | -   |
|      |     | K   | - | L   | L | -   |
| 4013 | C23 | -   | T | -   | N | -   |
|      |     | D   | R | -   | K | -   |
|      |     | L   | - | S   | - | -   |
| 4013 | C11 | -   | T | -   | N | -   |
|      |     | D   | R | -   | K | -   |
|      |     | L   | - | S   | - | -   |
| 4013 | C7  | -   | - | -   | N | -   |
|      |     | D   | R | -   | K | -   |
|      |     | L   | - | S   | - | -   |
| 5002 | C13 | -   | T | -   | H | L   |
|      |     | D   | Q | -   | K | -   |
|      |     | T   | - | N   | - | -   |
| 5002 | C1  | -   | T | -   | H | L   |
|      |     | D   | Q | -   | K | -   |
|      |     | T   | - | N   | - | -   |
| 4059 | C19 | V   | T | -   | N | E   |
|      |     | G   | N | -   | - | -   |
|      |     | R   | - | L   | L | -   |
| 4059 | C12 | V   | T | -   | N | E   |
|      |     | G   | N | -   | - | -   |
|      |     | K   | - | L   | L | -   |
| 4059 | C6  | V   | T | -   | N | E   |
|      |     | G   | N | -   | - | -   |
|      |     | K   | - | L   | L | -   |
| 7115 | C21 | V   | T | S   | G | -   |
|      |     | D   | - | -   | D | -   |
|      |     | -   | - | -   | - | -   |
| 7115 | C15 | V   | T | S   | G | -   |
|      |     | K   | D | -   | - | -   |
|      |     | D   | - | -   | - | -   |
| 7115 | C3  | -   | T | S   | G | -   |
|      |     | D   | - | -   | D | -   |
|      |     | L   | - | -   | - | -   |

**Figure 4.9. Lysine at position 170 in the HIV-1 envelope is associated with the ability to enter cells with a low CD4 surface expression.** HIV-1 Env sequences were aligned and

compared with the HXB2 Env. The amino acid sequences for HXB2 positions 161 to 180 are shown for each HIV-1 envelope that was phenotyped, and residues identical to the HXB2 reference sequence are displayed as dashes. Env position 170 is highlighted in yellow, and HIV-1 envelopes with the ability to infect low CD4 density cells are indicated by the black line.

## **CHAPTER V**

### **DISCUSSION AND FUTURE DIRECTIONS**

Neurological complications resulting from HIV-1 infection of the central nervous system (CNS) have been documented over the course of the AIDS epidemic. HIV-1-associated dementia (HAD) is a severe neurological disease resulting in both mental and motor impairment, and even milder cases of neurological dysfunction have a substantial impact on the quality of life for affected individuals. HIV-1 genetic compartmentalization has been detected in the brains of HAD subjects at autopsy (64, 65, 218, 242, 256), and in the cerebrospinal fluid (CSF) of HAD subjects sampled over the course of infection (126, 236, 254, 291). In addition, evidence from previous studies indicates that HIV-1 variants are replicating in perivascular macrophages and possibly microglia in the CNS (40, 82, 108, 109, 161, 233, 256, 295, 298, 315). However, after almost thirty years of research it is still unclear how HIV-1 induces neurological disease and why a subset of HIV-1-infected individuals develop HAD and others do not.

One of the main objectives for this dissertation was discerning the viral characteristics associated with CNS compartmentalization and clinical dementia. The projects outlined in this dissertation focused on characterizing HIV-1 genetic compartmentalization in the CNS/CSF over the course of HIV-1 infection, including when compartmentalization begins during the course of infection and how HIV-1 populations in the plasma and CSF evolve over time. I also defined the cellular origin of compartmentalized HIV-1 variants in the CSF, and examined the genotypic and phenotypic differences between compartmentalized and non-compartmentalized HIV-1 variants in subjects with HAD or no neurological symptoms.

In Chapter Two I assessed HIV-1 genetic compartmentalization between viral populations in the peripheral blood and CSF during primary HIV-1 infection. Using newer techniques such as single genome amplification and sequence analysis of the full length *env*

gene, I was able to show that compartmentalization can occur in the CSF of primary infection subjects in part through persistence of the putative transmitted parental variant, or via viral genetic adaptation to the CNS environment. I also found through longitudinal analyses that compartmentalization in the CSF can be resolved during infection, demonstrating the dynamic nature of HIV-1 infection in the CNS early after transmission. To my knowledge, this is the first study to report the detection of compartmentalized HIV-1 variants in the CSF of primary infection subjects. Now that I have generated full-length HIV-1 *env* variants from 11 primary infection subjects with and without compartmentalization in the CSF, it is important to continue these studies by cloning the *env* genes and examining differences in viral Env protein phenotypes.

Although differences exist between HIV-1 *env* genotypes in the blood and CSF populations of primary infection subjects with compartmentalization, it is possible that the envelope phenotypes do not differ this soon after HIV-1 transmission. Studies examining compartmentalized variants during chronic infection have reported differences in viral phenotypes between HIV-1 variants in the periphery and the CNS, including macrophage-tropic brain-derived envelopes and T cell-tropic lymph node-derived envelopes (108, 109, 233, 298). Current ideas postulate that macrophage tropism evolves later during the course of disease because macrophage-tropic envelopes have not been detected early during the course of infection. I found that genetic differences can occur between the peripheral and CNS HIV-1 populations during primary infection, and it is important to determine whether viral genetic adaptation in the CSF during primary HIV-1 infection correlates with viral phenotypic adaptation to the CNS environment, which would indicate enhanced HIV-1 replication in the brain.

The studies I conducted in Chapter Two also have implications for the clinical treatment of HIV-1 infection. Guidelines for the administration of antiretroviral drugs are not well defined for primary HIV-1 infection, and my results suggest that subjects with compartmentalization of viral variants in the CSF during primary infection should be considered for early antiretroviral therapy to reduce viral replication in the CNS. In order to understand the dynamic nature of HIV-1 infection in the CNS and the development of neuropathogenesis, HIV researchers will need to follow subjects from the early stages of primary infection through the chronic stage of disease. Compartmentalization late in infection likely indicates a loss of control of viral replication in the periphery and is associated with HAD (126). The detection of CSF-compartmentalized variants during primary HIV-1 infection may identify subjects that will have HIV-associated neurological problems later during infection; however, longitudinal studies will be necessary to answer this question and provide additional answers for clinicians regarding antiretroviral therapy during the early stages of infection.

The focus of Chapter Three was to examine the source of compartmentalized HIV-1 in the CNS of subjects with neurological disease and in neurologically-asymptomatic subjects who were initiating antiretroviral therapy. These studies used the heteroduplex tracking assay (HTA) to identify compartmentalized variants in the CSF and then measure the viral decay kinetics of individual variants after the initiation of antiretroviral therapy. In subjects with neurological disease, I found that compartmentalized variant decay kinetics were associated with the degree of CSF pleocytosis and immunodeficiency. Rapid decay of CSF-compartmentalized variants in HAD subjects was associated with high CSF pleocytosis, whereas slow decay measured for CSF-compartmentalized variants in subjects with

neurological disease was correlated with low peripheral CD4 cell count and reduced CSF pleocytosis. The longer half-lives I detected suggest that compartmentalized HIV-1 in the CSF of some neurologically symptomatic subjects may be originating from a long-lived cell type such as perivascular macrophages and microglia in the brain.

In Chapter Four I went a step further and examined the viral genotypes and phenotypes associated with the CSF-compartmentalized variants with differential decay rates. In this study I used SGA to generate full-length *env* genes from compartmentalized and non-compartmentalized variants in chronically-infected subjects with varying degrees of neurological disease. The cross-sectional SGA analyses revealed significant compartmentalization in the CSF population associated with increased neurological disease. Finally, the envelope phenotype characterization for subjects with HIV-associated neurological disease revealed two distinct classes of viral encephalitis (termed class 1 and class 2) associated with extensive genetic compartmentalization and the clinical diagnosis of dementia.

The new data generated from the studies in Chapter Four establish a cohesive new argument about the source of compartmentalized virus in the CNS of HAD subjects. I found that class 1 viral encephalitis was associated with a dependence on high CD4 density for infection of compartmentalized viruses (T cell-tropic), while class 2 viral encephalitis was associated with the ability of CSF-compartmentalized variants to infect low CD4 density cells (macrophage-tropic). These new phenotype data provide a link between compartmentalized virus decay kinetics and cell tropism. The subjects that displayed class 1 viral encephalitis (subjects 4033, 5003, and 7036) also had CSF-compartmentalized HIV-1 variants that decayed rapidly after the initiation of therapy (Chapter Three). These data

suggest that the compartmentalized virus in some HAD subjects is originating from a short-lived cell type and indicates that the compartmentalized population is most likely replicating in CD4<sup>+</sup> T cells in the CNS. The subject group that displayed class 2 viral encephalitis (subjects 4013, 4059, 5002, and 7115) also had CSF-compartmentalized HIV-1 variants that decayed slowly after the initiation of antiretroviral therapy (271). This indicates that the CSF-compartmentalized HIV-1 population in another group of neurologically symptomatic subjects is originating from a long-lived cell type and suggests that the population is being maintained by autonomous viral replication in perivascular macrophages and/or microglia within the CNS. The results described in Chapter Four also suggested that the degree of immunodeficiency may define the cellular origin of the compartmentalized virus since the four subjects with class 2 viral encephalitis had significantly lower peripheral CD4<sup>+</sup> T cell counts compared to subjects with class 1 encephalitis. Based on the data generated in Chapter Four, I have developed a simple model where compartmentalized HIV-1 variants are maintained in the CSF of HAD subjects by either T cell-driven viral replication (class 1 encephalitis) or macrophage-driven viral replication (class 2 encephalitis; see Figure 5.1).

Our studies illustrate a complex pattern of HIV-1 evolution in the CNS over the course of infection. Future longitudinal studies will need to focus on the events leading up to extensive compartmentalization in the CNS in order to understand how two distinct evolutionary pathways lead to clinical dementia. Currently in the literature it is generally accepted that viral replication in local CNS cells contributes to the development of neurological disease. One study by Harrington *et al.* (124) reported that compartmentalized HIV-1 variants in the CSF of neurologically asymptomatic subjects are originating from short-lived cells in the CNS. The studies presented in this dissertation have added to this

body of literature and demonstrated that viral replication maintained by both infiltrating CD4<sup>+</sup> T cells and local perivascular macrophages/microglia contributes to neurological disease.

Subjects diagnosed with HAD can be divided into two groups based on neuropathology detected in brain tissue. After years of research, it is apparent that some HAD subjects have a striking lack of pathology and tissue damage in the brain, while other HAD subjects have HIV-1 encephalitis characterized by pathological tissue damage and the presence of multinucleated giant cells of the macrophage/microglia origin (22, 23, 208). It is currently unknown why some subjects with severe dementia lack any brain pathology, and the absence of tissue damage in the CNS suggests that viral replication and inflammation in the CNS of these subjects is causing neuronal dysfunction rather than irreversible cell damage. Based on my recent findings, I propose that HIV-1-infected subjects with class 1 viral encephalitis will have little to no brain pathology, while subjects with class 2 viral encephalitis will have tissue damage and pathology commonly seen with HIVE. Future studies are necessary to test this hypothesis, and a comprehensive analysis examining HIV-1 populations in paired blood, CSF, and brain tissue from HAD subjects with and without HIVE will help determine whether there are differences in brain pathology between subjects with class 1 and class 2 viral encephalitis.

The discovery that viral replication within two distinct cell types can lead to clinical dementia is novel and indicates that in addition to macrophage-tropic variants, T cell-tropic HIV-1 variants are also able to persist in the CNS/CSF compartment and cause neurological dysfunction. Future studies may reveal differences in the clinical outcome between class 1 and class 2 encephalitis that could lead to different antiretroviral therapy regimens between

the two subject groups. If class 2 viral encephalitis is associated with HIVE and neuropathology, HAD subjects with macrophage-tropic compartmentalized variants may need more aggressive therapy regimens to fully suppress HIV-1 replication in the CNS. Conversely, T cell-tropic CSF-compartmentalized variants may be associated with better neurological recovery during therapy. In either case, the association between a specific encephalitis class and clinical neurological prognosis would be beneficial for both clinicians and HIV-infected patients. A genetic marker to distinguish T cell-tropic versus macrophage-tropic compartmentalized variants would be the simplest clinical test, although the commercially available phenotype assay could be altered to examine Env tropism differences since the compartmentalized populations in the CSF were dominated by either T cell-tropic or macrophage-tropic variants.

Future studies and experiments are necessary to conclusively determine the differences between class 1 and class 2 viral encephalitis associated with HIV-1 neurological disease. The studies presented in Chapter Four are limited by a small set of patient samples, so the addition of more paired blood and CSF samples from subjects with neurological disease will be necessary to increase the significance of the results. In addition, the studies discussed in this dissertation focused on neurological disease associated with only subtype B HIV-1 infections. HIV-1 subtype C is responsible for the most infections worldwide, so it is imperative that future studies examine CNS viral populations in subjects infected with subtype C HIV-1, although these studies are obviously more difficult to conduct due to the infrastructure limitations in Africa where subtype C is most prevalent. The findings regarding viral replication differences in the CNS during subtype B infection may translate to

subtype C infections in the CNS, but future experiments will be needed to answer this question.

Additional phenotype experiments need to be conducted using the Env-pseudotyped viruses generated in Chapter Four to elucidate the exact differences between low CD4 and high CD4 dependence for viral infection. Low CD4 usage by HIV-1 envelopes is associated with the ability to infect macrophages (63, 298). The phenotype experiments in Chapter Four were conducted in a human cell-line, so the next step is to examine the ability of the different envelopes to infect primary human monocyte-derived macrophages. I also need to determine when macrophage-tropic envelopes evolve during the course of HIV-1 infection in the CNS. I have generated full-length *env* genes from longitudinal plasma and CSF samples prior to the development of HAD for subject 7115. Low CD4-tropic envelopes were detected in the CSF population of subject 7115 after HAD diagnosis. I found that some of the CSF envelopes from earlier time points during infection had viral genotypes very similar to the low CD4-using envelopes. The phenotypes of these earlier CSF viruses need to be examined to determine when macrophage-tropic HIV-1 variants evolved prior to the development of dementia.

Envelope conformation differences also need to be investigated for T cell-tropic and macrophage-tropic HIV-1 envelopes. I postulate that HIV-1 envelopes with the ability to infect at low CD4 densities will have a more open and exposed CD4 binding pocket compared to envelopes with a high CD4 dependence. HIV-1 envelopes with the ability to use low CD4 densities are thought to have a greater CD4 affinity, allowing for envelope attachment on target cells with low CD4 surface expression. Future experiments need to compare the CD4 affinity differences between T cell-tropic and macrophage-tropic HIV-1

envelopes from the blood and CSF. One possible experiment would be to incubate envelope-pseudotyped viruses with varying amounts of soluble CD4 and then infect high CD4 density cells. HIV-1 envelopes with a greater affinity to CD4 will remain bound to the soluble CD4 molecules and infection will be inhibited.

Previous studies have also reported that brain-adapted HIV-1 envelopes have enhanced sensitivity to neutralizing antibodies (196, 284). An exposed CD4 binding pocket would result in increased neutralizing antibody sensitivity, which may explain why macrophage-tropic envelopes are not commonly found in the peripheral blood. The CNS is an immune-privileged site where antibodies are not common, and this creates an environment that is favorable for the evolution of macrophage-tropic HIV-1 variants. I can examine the neutralization sensitivity of different HIV-1 envelopes using heterologous antibodies targeting the V3 loop and the CD4 binding site of the envelope. HIV-1 envelopes with a more exposed CD4 binding pocket should have increased sensitivity to both V3 antibodies and antibodies targeting the CD4 binding site. In addition, serum samples were collected from all of the subjects used in our chronic infection studies. Thus, I will be able to analyze the sensitivity of different envelopes to autologous antibodies as well in future experiments.

Studies investigating the three-dimensional structure of HIV-1 envelope have been hindered by the constant variation in envelope conformation when it is not bound to the CD4 receptor. The crystal structure has only been solved for monomeric gp120 bound to the CD4 molecule with most of the variable loops truncated (165, 166), although more recently the structure of gp120 with the V3 loop attached was also solved (142). The structure has also been solved for an unliganded, fully glycosylated SIV gp120 monomer (missing the V1/V2 and V3 loops), which has provided a comparison for the HIV-1 gp120 structure (29). In

addition, the natural structure of gp160 is a trimer on the surface of virions; however, soluble gp120 is monomeric and does not form stable trimers. All of these setbacks in envelope structural biology have resulted in most studies using indirect measurements to identify differences in envelope conformations. Until the HIV field is able to solve the trimeric structure of envelope, there will continue to be holes not only in CNS HIV biology, but also in areas of HIV transmission and vaccine research.

Now that I have reported differences in HIV-1 envelope cell tropism for CNS variants, further studies are needed to examine the evolution of other HIV-1 genes in different cell types. The 3' LTR and Nef genes were amplified along with the full-length *env* genes during the SGA procedure in our studies. Some preliminary analyses have been conducted on the 3' LTR region of the HIV-1 genome, and LTR compartmentalization seems to correlate with the envelope compartmentalization pattern I reported in Chapter Four (W. Ince, unpublished observation). Previous studies have found that cellular transcription factors interact with specific domains located in the HIV-1 5' LTR and help drive transcription from the provirus (230). The cellular transcription factors that interact with the HIV-1 LTR are thought to be different based on whether HIV is replicating in a CD4<sup>+</sup> T cell versus a macrophage. Even though the LTR sequences I generated only contains the U3 region of the provirus LTR, functional studies will help determine any differences in cellular transcription factor binding sites between T cell-tropic versus macrophage-tropic HIV-1 variants. Longitudinal studies comparing both LTR and envelope evolution in the CNS will help identify which gene evolves towards macrophage-tropism first, although I predict that envelope evolution for entry into macrophages occurs prior to changes in the LTR.

Finally, replication and fitness differences need to be assessed for compartmentalized and non-compartmentalized HIV-1 variants in subjects with neurological disease. Full-length, replication competent HIV-1 clones should be generated for a subset of the envelopes that were tested in Chapter Four. In particular, a T cell-tropic variant and a macrophage-tropic variant from one subject should be compared to examine the kinetics of viral spread and replication in different cell types, and to examine relative fitness in competition experiments. Although the generation of full-length HIV-1 clones is extremely difficult due to the presence of nicks in the genomic RNA, it would be interesting to take this idea one step further by generating full-length virus clones of CSF-compartmentalized variants from different longitudinal time points pre- and post-HAD diagnosis. In the analysis of subject 7115, I found a viral population with macrophage-tropic envelope characteristics at one month post-HAD diagnosis, and similar viral genotypes were detected two years prior to the development of dementia as a minor portion of the CSF viral population. One possibility is that envelope macrophage tropism determinants evolve first, and then over time other portions of the HIV-1 genome evolve towards enhanced replication in cells of the monocyte/macrophage lineage. By studying full-length HIV-1 genomes I would be able to capture any replication advantages that may not be apparent from studies only focusing on envelope.

Neurological complications resulting from HIV-1 infection of the CNS will continue to be a problem for HIV-1-infected individuals, even in the era of HAART. HIV-1 infection and replication in the CNS are complex events, and a lot about this process is still unknown. Future longitudinal studies will need to focus on the evolutionary events leading up to significant HIV-1 compartmentalization in the CNS/CSF and the development of

neurological disease. New technologies and studies are required to solve the crystal structure of the HIV-1 gp160 trimer, and a complete understanding of the three-dimensional interactions of HIV-1 envelope with both the cellular receptors and neutralizing antibodies is necessary to generate an effective vaccine or therapy. Finally, further studies into the neuropathogenesis of HIV-1 may reveal that increased replication fitness combined with the degree of immunodeficiency explain the course of neurological disease during HIV-1 infection.

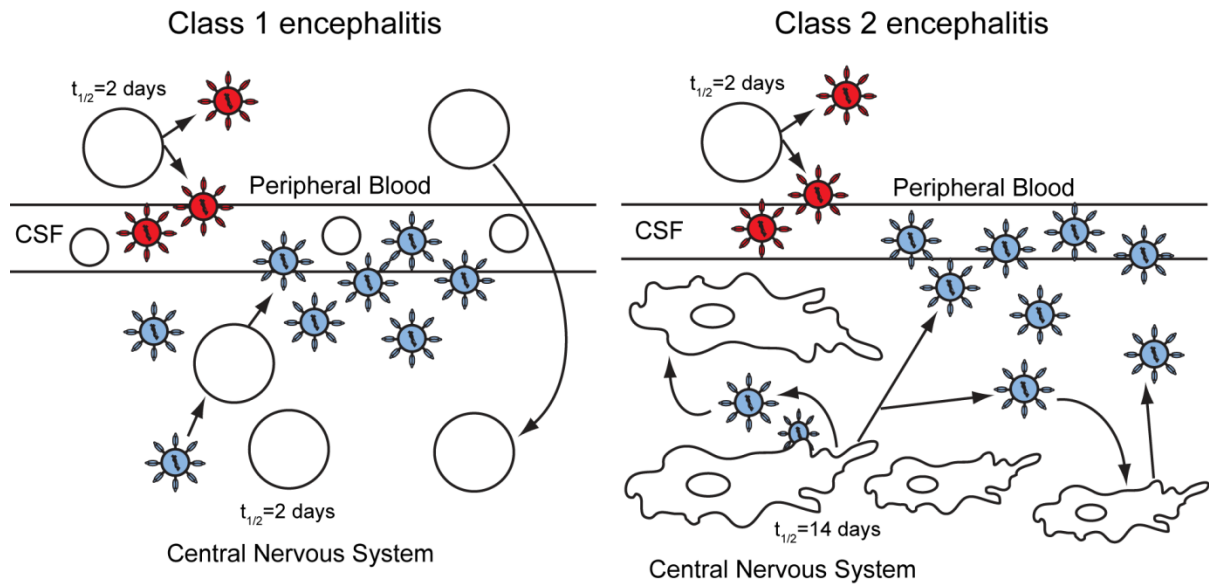


**Figure 5.1. Model of HIV-1 in the CNS during class 1 and class 2 viral encephalitis.**  $CD4^+$  T cells are represented by open circles, perivascular macrophages/microglia are represented by the irregularly shaped cells, red virus particles represent the blood plasma HIV-1 variants, and blue virus particles represent the CNS compartmentalized HIV-1 variants. Class 1 and class 2 viral encephalitis both occur in subjects with neurological disease that have significant CNS compartmentalization. Class 1 encephalitis is associated with high CSF pleocytosis, rapid decay of compartmentalized variants after the initiation of therapy, and a T cell-tropic phenotype of the compartmentalized variants. Class 2 encephalitis is associated with no/low CSF pleocytosis, increased immunodeficiency, slow decay of compartmentalized variants after the initiation of therapy, and a macrophage-tropic phenotype of the compartmentalized variants. We propose that the compartmentalized population in the CNS of subjects with class 1 encephalitis is T cell-tropic and HIV-1 replication maintained by T cells, while the CNS-compartmentalized population in subjects with class 2 encephalitis is macrophage-tropic and HIV-1 replication is maintained by long-lived perivascular macrophages and/or microglia in the CNS.

## APPENDIX

### IDENTIFICATION AND RECOVERY OF MINOR HIV-1 VARIANTS USING THE HETERODUPLEX TRACKING ASSAY AND BIOTINYLATED PROBES

Reprinted from: Schnell, G., W.L. Ince, and R. Swanstrom. 2008. Identification and Recovery of Minor HIV-1 Variants Using the Heteroduplex Tracking Assay and Biotinylated Probes. *Nucleic Acids Res* 36:e146.

## ABSTRACT

We describe a method to identify and recover minor human immunodeficiency virus type 1 (HIV-1) sequence variants from a complex population. The original heteroduplex tracking assay (HTA) was modified by incorporating a biotin tag into the probe to allow for direct sequence determination of the query strand. We used this approach to recover sequences from minor HIV-1 variants in the V3 region of the *env* gene, and to identify minor drug-resistant variants in *pro*. The biotin-HTA targeting of the V3 region of *env* allowed us to detect minor V3 variants, of which forty-five percent were classified as CXCR4-using viruses. In addition, the biotin-protease HTA was able to detect mixtures of wild type sequence and drug resistance mutations in four subjects that were not detected by bulk sequence analysis. The biotin-HTA is a robust assay that first separates genetic variants then allows direct sequence analysis of major and minor variants.

## INTRODUCTION

Genetically unstable organisms present a special challenge to therapeutic intervention. Genetic instability coupled with large population sizes leads to population diversity that can harbor advantageous mutations in the face of changing selective pressures. Our knowledge about genetic complexity is always limited by our ability to sample minor variants within the population. One example of this phenomenon is the human immunodeficiency virus type 1 (HIV-1), which maintains genetic diversity in its population that can impact evolution of escape from immune selection, drug resistance, and changes in target cell specificity (36).

Several approaches are available for sampling genetic complexity. Bulk sequence analysis of the total population suffers from limited sensitivity, and cannot reliably detect variants that comprise less than approximately 25% of the population (170, 220). A strategy of cloning a PCR product generated from a complex population followed by sequencing individual clones is limited by the number of clones analyzed, and the accurate detection of minor variants in the population requires a large sampling of clones (183, 220). Allele-specific PCR can detect variants in the 0.1-1% range, and although there is no information about linkage to other sequence variation (122, 222), further analysis of the allele-specific product can generate some linkage information (147). More recent pyrosequencing approaches offer deep sequencing capability, although the high error rate necessitates oversampling of sequences which reduces sensitivity, and bioinformatics approaches are necessary to handle the large data output (191).

An alternative approach to dissecting genetic diversity is the heteroduplex tracking assay (HTA). The HTA is a gel-based assay that separates viral variants based on sequence differences, and can resolve variants that comprise as little as 1-3% of the total viral population (49, 51, 52). In this assay, the desired genomic region is amplified by PCR, and a radioactively labeled probe is annealed to the PCR products. Heteroduplexes are generated between the probe and PCR products, and any insertions, deletions, or clustered mutations will result in a bend or kink in the DNA helix, conferring an altered migration through a non-denaturing polyacrylamide gel. However, this approach is limited in that it is not linked to direct sequence analysis.

In this report we describe a modification of the HTA strategy that couples the ability to separate genetic variants in a gel-based assay with direct sequence analysis of the separated variants. The ability to directly sequence the query strand of each heteroduplex in the gel was accomplished by adding a biotinylated-nucleotide tag to the radiolabeled probe strand. Using the biotinylated probe, we were able to purify the labeled heteroduplex and subsequently separate the query strand from the probe. The purified query strand was then subjected to PCR amplification and conventional sequence analysis. We used this approach to identify sequences from minor variants in the V3 region of the HIV-1 *env* gene that predict changes in target cell tropism, and to examine the heterogeneity of the *pro* gene population during the evolution of resistance to protease inhibitors.

## MATERIALS AND METHODS

### Plasma samples.

All plasma samples were obtained as excess tissue samples and with Institutional Review Board approval. Samples for the V3 studies were from subjects in a ritonavir efficacy study (27), and were provided by Dale Kempf (Abbott Laboratories) unlinked to personal identifiers. Samples for the protease studies were entry time-point plasma samples obtained from subjects in the ACTG 359 clinical trial (117).

### Plasmids and probes.

The V3 Mut-1 probe plasmid was generated using the V3<sub>JR-FL</sub> plasmid pJN27 developed by Nelson *et al.* (212). A BamHI restriction site located upstream of the probe insert in pJN27 was destroyed, and the EcoRI site located at the start of the probe sequence was mutated to a new BamHI site using the Quikchange site-directed mutagenesis strategy. The 5'-GATC-3' overhang after BamHI cleavage permits sequential labeling of the antisense strand in a fill-in reaction with biotin-labeled dGTP and <sup>35</sup>S-dATP. To limit PCR amplification of the probe sequence from the isolated heteroduplex, the upstream V3 PCR primer binding site in the pJN27 plasmid was mutated, reducing the efficiency of amplification by 1000 fold. The final sequence of the V3 Mut-1 probe at the upstream V3 boundary was 5'-GATCCGGCTTGAATCTGTAGAAATTAATTGTACACGACAAA...-3'. The final probe sequence at the downstream V3 boundary in the probe is 5'-...CATTGTAACATTAGTAGAGCAAAAAGCCGAATTAATTCTGCA-3'. Introduced

nucleotide changes are indicated by bolded and underlined letters, and plasmid sequence included in the V3 probe is shown in italics.

The pR-EBm protease probe plasmid was generated from the multiple-site-specific HTA probe pR-EB previously described by Resch, *et al.* (250). The site-directed mutagenesis procedure described above was used to generate the pR-EBm probe. The probe was modified for this study by introducing base mismatches in the upstream PCR primer binding site to limit amplification from the probe sequence from the isolated heteroduplex. Additionally, a BamHI site was introduced at the 3' end to accommodate biotin- and radio-labeling of the sense strand. The 5' probe sequence is 5'-

*TATGGATAACTAAAGGAAGCTCTATTAGATACT***TGGCT***...-3'*, and the 3' probe sequence is 5'-...TCAGATTGGTTGCACTTTAAATTTTCCATCG(*biotin-dGTP*)(*S*<sup>35</sup>-*dATP*)-3'. Introduced nucleotide changes are indicated by bolded, underlined letters, and plasmid sequence included in the probe is shown in italics.

### **Probe labeling.**

The V3 Mut-1 probe plasmid (10 µg) was digested with BamHI (60 µl total volume) followed by a fill-in reaction with 4 nmol Biotin-11-dGTP (PerkinElmer), 0.05 mCi [ $\alpha$ -<sup>35</sup>S]-dATP (1250 Ci/mmol; PerkinElmer), 20 units of the Klenow fragment of DNA polymerase I, and 0.6 µl of 1M DTT. The reaction was incubated for 15 minutes at room temperature followed by the addition of 1.4 µl 0.5M EDTA and heat inactivation for 15 minutes at 80°C. The excess nucleotides were then removed using the Qiagen PCR Purification kit (Qiagen), and the V3 Mut-1 probe was released from the vector by PstI digestion. The pR-EBm probe

plasmid was labeled using the same procedure, except that after purification the pR-EBm probe was released from the vector by NdeI digestion.

### **RNA isolation, RT-PCR, and heteroduplex tracking assay.**

Procedures for viral RNA isolation from plasma, RT-PCR, and the HTA were conducted as previously described (212, 250). Briefly, viral RNA was isolated from blood plasma (140 µl) using the QIAmp Viral RNA kit (Qiagen). Reverse transcription and PCR amplification of the 140 bp V3 amplicon were conducted with 5 µl of purified RNA (from 50 µl column elution volume) and the primers HIVV3F (Hxb2 7142-7171 [5'-GAATCTGTAGAAATTAATTGTACAAGACCC-3']) and HIVV3R (Hxb2 7239-7211 [5'-CCATTTTGCTCTACTAATGTTACAATGT-3']) by using the Qiagen One-Step RT-PCR kit (Qiagen) as per manufacturer's instructions. Amplification of a 247-bp region of *pro* was conducted using the procedure stated above and the primers PRAMPUP (Hxb2 2305-2334 [5'-AACTAAAGGAAGCTCTATTAGATACAGGAG-3']) and PRAMPDW (Hxb2 2551-2525 [5'-GGAAAATTTAAAGTGCAACCAATCTGA-3']). Heteroduplex annealing reactions consisted of 1 µl of 10x annealing buffer (159, 212), 0.1 µg biotinylated and radioactively-labeled probe, and 8 µl of unpurified PCR product. The reactions were denatured and the DNA was annealed at room temperature to allow heteroduplex formation. The heteroduplexes were separated by native polyacrylamide gel electrophoresis (as described in ref. 14 and 15), and the separated heteroduplexes were visualized by autoradiography. The relative abundance of each detected heteroduplex was determined by exposing the HTA gel to a phosphorimager screen, and the percent abundance of each variant was calculated using ImageQuant software (Molecular Dynamics).

### **Band extraction, DNA purification, and sequence analysis.**

The dried HTA gels were aligned with the exposed autoradiography film, and the desired labeled bands were excised from the gel. The gel fragment was transferred to a sterile 1.5 ml microcentrifuge tube. Crush & Soak buffer (120  $\mu$ l; 500 mM  $\text{NH}_4\text{OAc}$ , 0.1% SDS, 0.1 mM EDTA) was then added, and the tubes were incubated at 37°C overnight. After incubation, the tubes were centrifuged for 2 minutes at 14,000 rpm to pellet any gel fragments, and the supernatants were transferred to a 96-well PCR plate. Streptavidin-coated Dynabeads® (Invitrogen) (5  $\mu$ l per reaction) were washed twice then resuspended in the same volume in 2x B&W buffer (10 mM Tris-HCl [pH 7.5], 1 mM EDTA, 2M NaCl). The bead suspension was then aliquoted into a clean 96-well PCR plate (5  $\mu$ l per well). The plate containing the beads was placed on the magnet for 1 minute and the supernatant was removed. The plate was removed from the magnet, and the beads were resuspended in 80  $\mu$ l of 2x B&W buffer. An equal volume (80  $\mu$ l) of the gel-extracted heteroduplex product was then added to the beads. The plate was then incubated for 17 minutes at room temperature in a MixMate shaker (Eppendorf) at 700 rpm to prevent the beads from settling. After the incubation, the plate was placed on the magnet for 2 minutes, and the supernatant was removed and discarded. The beads were washed three times in 1x B&W buffer (20  $\mu$ l), and then washed twice in 1x SSC (pH 7.0; 50  $\mu$ l). After the last wash, the beads were resuspended in 20  $\mu$ l of freshly prepared 0.15M NaOH and incubated for 5 minutes at room temperature to denature the heteroduplexes. The plate was then placed on the magnet for 1 minute, and the supernatant containing the denatured query strand was transferred to a clean

96-well PCR plate. The supernatant was neutralized by adding 2.4  $\mu$ l of 10x TE (pH 7.5) and 2.4  $\mu$ l of 1.25M acetic acid.

The purified query strand DNA was then amplified with the Platinum Taq DNA Polymerase High Fidelity PCR kit (Invitrogen) as per the manufacturer's instructions, using 2  $\mu$ l DNA and the PCR primers described above. The V3 sequencing primers are V3SeqF (Hxb2 7147-7176 [5'-TGTAGAAATTAATTGTACAAGACCCAACAA-3']) and V3SeqR (Hxb2 7234-7205 [5'-TTTGCTCTACTAATGTTACAATGTGCTTGT-3']). The protease PCR primers described above were used to sequence the *pro* PCR products. Bulk sequencing was also conducted on the original PCR products amplified from viral RNA. GenBank accession numbers FJ347037-FJ347099.

## RESULTS

### **Biotinylated probes and HTA allow the identification and recovery of minor HIV-1 variants from a complex population.**

The HTA is capable of separating diverse genetic variants in a gel-based format (49, 51, 52, 159, 212, 250). We have modified the original HTA method to permit direct sequence determination of the query strand of the target heteroduplex and adapted the approach to a 96-well plate format. To accomplish direct sequencing of the query strand we incorporated a biotin tag into the probe strand (see Materials and Methods) to allow for the purification of the labeled heteroduplex followed by the separation of the query and probe strands (Figure A.1).

In this approach a query PCR product is generated, annealed to a radiolabeled/biotin-labeled probe, and the heteroduplexes are resolved by native polyacrylamide gel electrophoresis. Gel slices containing the labeled heteroduplexes are then excised from dried polyacrylamide gel using X-ray film that had been exposed to the gel as a guide. The excised gel slices are rehydrated and soaked overnight to recover heteroduplex DNA from the gel fragments. The biotin-tagged heteroduplexes are then purified away from the gel fragments and any unlabeled co-migrating DNA (i.e. heteroduplexes formed between the unlabeled PCR products) by binding the labeled heteroduplexes to streptavidin-coated magnetic Dynabeads®, followed by washing. The query DNA strand in the heteroduplex is then eluted from the probe DNA with dilute NaOH, which allows the probe strand to remain attached to the magnetic beads and thus removed from the solution. The purified query DNA strand is then used as the template in another round of PCR amplification, and the PCR

product is sequenced using standard technology. Below we describe the application of this approach to the sequence-based identification of HIV-1 variants that enter cells using the CXCR4 coreceptor, and of variants that encode drug resistance in subjects failing therapy with a protease inhibitor, in each case resolving these variants from genotypic mixtures.

**Minor X4 variants are identified and recovered using a biotinylated-V3 HTA probe.**

We analyzed the V3 region of *env* for 34 HIV-1-infected subjects with CD4<sup>+</sup> T cell counts less than 150 cells/ $\mu$ l to test the ability of our biotin-HTA method to detect and recover minor V3 variants in complex viral populations. Figure A.2A shows the separation of genotypic mixtures of the V3 region of the *env* gene in the HTA gel (211, 212). We were able to obtain V3 sequence from 63 of the 69 visible heteroduplexes in the polyacrylamide gels, and phosphorimager analysis was used to define the relative fraction of each variant. For these subjects the average number of variants was two variants per subject, and the number of variants ranged from 1 (12 subjects) up to 5 (1 subject).

We used the modified 11/25 rule (140, 249) and the position-specific scoring matrix (PSSM) (145) to predict the coreceptor usage of these V3 sequences based on the viral genotype. A total of 63 V3 sequences were generated for these 34 subjects, of which 48 corresponded to an R5-using genotype and 15 corresponded to an X4-using genotype (Figure A.2 and data not shown). The biotin-V3 HTA method recorded the presence of minor R5 or X4 V3 variants (defined as less than 30% of the total population) in 18 of the 34 subjects, and a total of 26 bands with a relative abundance of less than 30% were excised and sequenced. We obtained sequence for 20 of the bands while we failed to obtain sequence for 6 bands. The relative abundance of the 6 variants for which sequence was not obtained

ranged from 0.1% to 13% of the total population, with the failure to obtain usable sequence attributable to either very low abundance or near co-migration. Of the 20 minor V3 sequences we recovered, nine were classified as X4-using viruses. We were able to detect two of these minor X4 sequences as mixtures in bulk sequence analysis, while the other seven minor X4 variants were not detected by bulk sequence analysis due to low relative abundance. All of the V3 variants that were extracted from the gel and PCR amplified migrated to the same position in the gel as the original band amplified from viral RNA (data not shown). One limitation of this procedure is that major bands in the gel trail upwards, and PCR products of minor variants that migrate right above a major variant in the gel may contain a small amount of the major variant. However, in most cases (55 out of 69 variants) the V3 sequence obtained from the PCR products had clean peaks, and the major variant was not detected in the sequence analysis (data not shown). For the remaining fourteen variants that had multiple peaks present in the sequence analysis, and also displayed a large amount of the contaminating major variant, purified samples were re-amplified and purified again to obtain the target sequence. Using this enrichment method, we were able to determine the sequence of eight additional variants. Overall, we were able to obtain clear sequence for approximately 90% of all bands detected and approximately 75% of all detected bands representing less than 30% of the population, and the use of biotin-HTA resolved all mixtures seen with bulk sequence analysis.

In order to further examine the sensitivity and specificity of the biotin-HTA, several control experiments were conducted. First, we mixed together two V3 PCR products at varying ratios and then separated the mixtures using the biotin-V3 HTA. The bands were then excised from the gel, purified, and sequenced. In this control experiment we were able

to obtain sequence from a band that represented as little as 1.5% of the total population (Figure A.3A). Sequence was not obtained from the band representing 0.5% of the population; however, we did not reamplify the product in this case which can allow increased sensitivity of detection, as described above. To address specificity, single genome amplification (SGA) (262) of the *env* gene was conducted on blood plasma from subject 1314 in order to compare the relative abundance of variants determined using biotin-HTA to sampling of the viral population by sequencing individual viral templates. We generated and sequenced ten SGA amplicons and compared the V3 regions to the sequences identified using the biotin-V3 HTA. The ten amplicons represented two migration patterns in the V3-HTA, with seven of the amplicons having one migration rate (shown as amplicons 1.1 and 1.2 in Figure A.3B), and three of the amplicons having the other migration rate (labeled amplicon 2 in Figure A.3B). This closely approximated the ratio of 73% and 27% for these two bands as determined by V3-HTA (Figure A.3C), and this result is consistent with a similar control done previously with a V1/V2-HTA probe (159). The altered migration of heteroduplexes in the HTA is based on sequence differences between the strands, especially clustered mutations and insertion/deletions, with variable sensitivity to detect isolated point mutations. This feature can be seen in the sequence differences between the bands that were resolved by the biotin V3-HTA (amplicons 1 and 2, Figure A.3C), but the comigration of sequences that differed by only a few nucleotides (amplicons 1.1 and 1.2, Figure A.3C). In this case the level of variability in the isolated HTA band was revealed as a mixed peak in the sequence chromatogram when that band was isolated and sequenced (data not shown).

**Minor protease drug-resistant variants are detected using a biotinylated-protease HTA probe.**

We have applied the biotin-HTA to separate HIV-1 *pro* variants, encoding the viral protease, and to sequence these variants to detect mutations that confer resistance to protease inhibitors. The biotin-protease HTA is a modification of the previously described multiple site-specific HTA (MSS-HTA) (250) (see Materials and Methods) with the probe designed to query mutations at protease codon positions 46, 48, 54, 82, 84, and 90. We used both our own bulk sequence analysis and the biotin-protease HTA to screen nineteen subjects who had previously failed therapy that included the protease inhibitor IDV. A total of ten subjects had no primary resistance mutations by either method, although some had viral genotypes that included polymorphic mutations that can become enriched with therapy (277) (data not shown) (Stanford Database, <http://hivdb.stanford.edu/>). The remaining nine subjects all exhibited primary resistance mutations (Stanford database, <http://hivdb.stanford.edu/>). For three of these subjects we detected a homogeneous population by both methods (data not shown). The results of the biotin-HTA analysis and the bulk sequence analysis for the remaining 6 subjects are shown in Figure A.4.

Bulk sequence analysis was able to identify mutations in variants that comprised as little as 28% of the population (Figure A.4, subject 18, band 1), but also missed mutations that existed in variants making up as much as 45% of the population (Figure A.4; subject 4, band 1), perhaps due to poor incorporation of the chain terminating nucleotide at that position. In contrast, using the biotin-HTA approach we were able to identify primary resistance mutations at the query positions in 3 subjects (subject 4, band 1; subject 16, band 1; and subject 22, bands 1 and 2) that were not detected in bulk sequencing (Figure A.4).

Exclusive linkage between resistance mutations I54V and V82A was established in one subject (Figure A.4; subject 18, band 1). The least abundant variant we identified comprised 4% of the total population (Figure A.4B; subject 16, band 3), although this variant differed by only 1 synonymous change from the bulk sequence (data not shown). Resistance mutations were sometimes identified as mixtures in excised bands (Figure A.4; subject 4, band 1; subject 16, band 1; subject 18, band 4). This can result from either trailing of products from a major lower band, or, in the case of positions that the probe was not designed to query, the inability of the probe to distinguish between variants at that position (Figure A.4; subject 18, band 4; subject 19, bands 1-3). Despite existing as mixtures in these cases, resistance mutations were enriched, and therefore detected, in electrophoretically separated variants when they were otherwise not detected by bulk sequence analysis. One subject had a resistance mutation (subject 15, V82A – not shown) that was detected in a separate clinically approved bulk sequence analysis protocol but not in the HTA analysis, while three other subjects displayed resistance mutations that were detected by HTA but not by the clinically approved analysis (Figure A.4; subject 4, V82A; subject 16 and 18, I54V).

## DISCUSSION

The biotin-HTA allows for the detection and direct sequence analysis of multiple variants in a complex population. Using the biotin-HTA targeting the V3 region of *env*, we were able to detect and directly determine the sequence of 20 minor (less than 30% abundance) R5 and X4 viral variants, of which forty-five percent were classified as X4-using viruses. In addition, we used a biotin-protease HTA to detect and sequence specific drug resistance mutations in *pro* in nineteen subjects failing treatment with an HIV-1 protease inhibitor. Fifteen of the nineteen subjects had matching genotypes for the clinical screening data and the HTA analysis, while three subjects displayed resistance mutations that were detected by HTA but not by a clinically approved bulk sequence analysis.

An RNA heteroduplex generator-tracking assay (RNA-HTA) has been developed that uses a degradable RNA probe to allow direct sequence analysis of the query strand, which was tested by examining HIV-1 variants with drug-resistance mutations in the protease coding domain (151). Using this method, variants that comprised 1% of the total population were identified and subjected to sequence analysis. One drawback of the RNA-HTA method is that unlabeled DNA-DNA heteroduplexes generated from variants within the PCR product can comigrate with the labeled RNA-DNA heteroduplexes, going undetected in the gel but giving rise to sequence mixtures during the subsequent amplification and sequence analysis. Our biotin-HTA method introduces the ability to purify specifically the biotin/radiolabeled probe:PCR product heteroduplexes from unlabeled PCR product heteroduplexes that might migrate to the same location in the polyacrylamide gel. Similar to what Kapoor *et al.* saw in their studies (151), we also find that major variants trail upwards in the gel and can be

detected in the PCR products extracted from upper bands. In the case that an unreadable sequence is detected using the biotin-HTA procedure, it is possible to simply reamplify the now enriched mixture and run another biotin-HTA followed by sequence analysis.

In a control experiment we were able to obtain sequence information from a band that comprised 1.5% of the signal, and as seen previously (159), the HTA provides sampling that is similar to that obtained by other methods but has the advantage of being able to query many more templates than these other methods (Figure A.3). During the analysis of the subject samples, we were able to obtain the sequence of a variant that represented 0.5% of the total population (subject 1007, Figure A.2B) by running the extracted V3 PCR product on another biotin-HTA and re-amplifying the purified product, thus allowing for further enrichment of the minor variant. A useful comparison of the potential utility of the HTA is as follows. If one were to sequence 300 clones (assuming they are derived from independent templates in the PCR amplification), there is a 95% chance of detecting variants present at a 1% level. In this case detection of presence is more robust than the estimate of relative abundance; also, the amount of work essentially increases linearly as the number of clones analyzed increases. HTA is able to detect signals in the 1% range in the gel-based detection system. However, sampling quality can be significantly better since this approach is not limited by the number of templates sampled, i.e. sampling 300 templates is as easy as sampling 3000 templates. This allows the HTA approach to measure more accurately the relative abundance of even minor species in those circumstances where larger numbers of templates are available to be sampled, and to validate their abundance by comparing repeat amplifications.

Different HIV-1 entry inhibitors are being explored as possible drugs to block HIV-1 infection and to treat current infections. Several CCR5-inhibitors are approved or in development for the treatment of HIV-1 infection, including maraviroc (Pfizer) (59, 76) and vicriviroc (Schering Plough) (118, 293). CCR5-inhibitors work by binding the CCR5 coreceptor to block the entry of HIV-1. CXCR4-using viruses are naturally resistant to these CCR5-binding drugs and therefore this class of inhibitor is not indicated for subjects with X4 variants. In addition, coreceptor switching has been documented in several subjects using CCR5-inhibitors, although the level of CXCR4-emerging viruses was lower than expected (76, 313). In the subjects where CXCR4-using viruses emerged after treatment with a CCR5 inhibitor, phylogenetic analysis showed that these variants were a result of the outgrowth of a minor CXCR4-using variant that was present prior to the initiation of drug therapy (313). The biotin-V3 HTA that we have developed can detect and genotype minor V3 variants in the range of 1.5% of the total HIV-1 population, and could be used as an initial genotypic screen for CXCR4-using variants in people considering CCR5-inhibitor drug therapy.

Additionally, genotypic testing for the presence of resistance mutations is the standard-of-care for people initiating and failing therapy (Guidelines for the use of antiretroviral agents in HIV-1-infected adults and adolescents, U.S. D.H.H.S., <http://www.aidsinfo.nih.gov/ContentFiles/AdultandAdolescentGL.pdf>). The biotin-protease HTA provides an example where complex mixtures of sequences can be examined with greater sensitivity to detect resistance mutations. The biotin-HTA methods used here for the detection and direct sequence analysis of minor HIV-1 variants should be applicable to other complex viral and non-viral populations where increased sensitivity of detection of minor genetic variants is important.

## **ACKNOWLEDGEMENTS**

We thank Rushina Cholera for assistance in doing these experiments. We also thank Dale Kempf from Abbott and the ACTG 359 study team for making samples available for this study. National Institutes of Health (R37-AI44667 to R.S., T32-AI07001 to G.S., T32-GM07092 to W.I.).

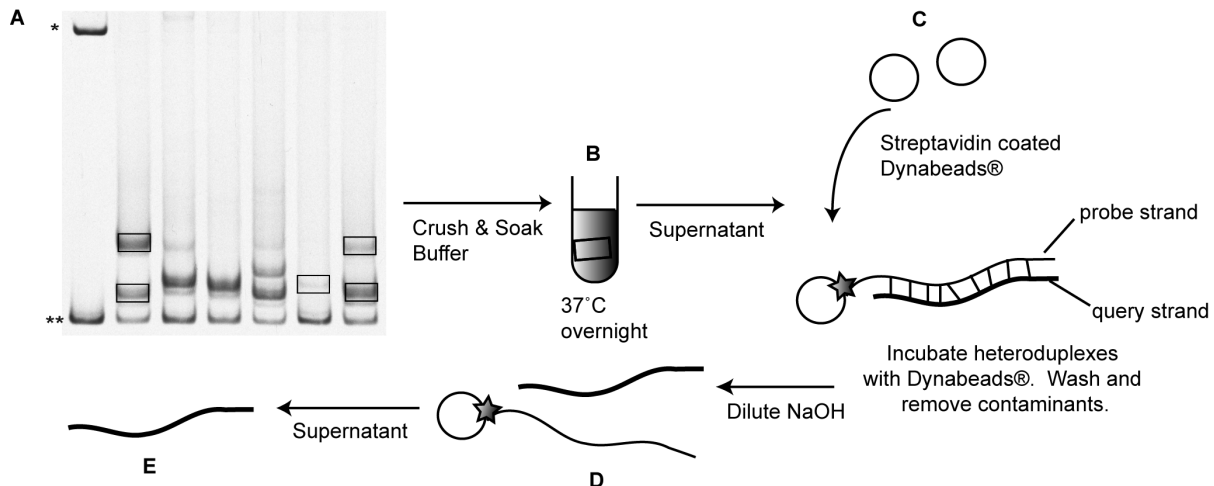


**Figure A.1. The biotin-HTA strategy.** (A) The region of interest is PCR amplified from the HIV-1 genome and mixed with a biotinylated probe to generate heteroduplexes between the probe and PCR product. The heteroduplexes are then separated by polyacrylamide gel electrophoresis based on DNA bending. The single-stranded probe band is denoted by the asterisk (\*), and the double-stranded probe band is denoted by double asterisks (\*\*). The labeled heteroduplexes are excised from the dried polyacrylamide gel. (B) The gel fragments are soaked overnight to recover heteroduplex DNA from the gel fragments. (C) The supernatant containing the biotin-tagged heteroduplexes is then incubated with streptavidin-coated magnetic Dynabeads®. The biotin-tagged heteroduplexes bind to the streptavidin-coated magnetic Dynabeads®, and contaminants are removed by washing. (D) The query DNA strand in the heteroduplex is eluted from the probe DNA with dilute NaOH, which allows the probe strand to remain attached to the magnetic beads. (E) The purified query strand is then used as template in another round of PCR amplification, and the PCR product is sequenced using standard technology.

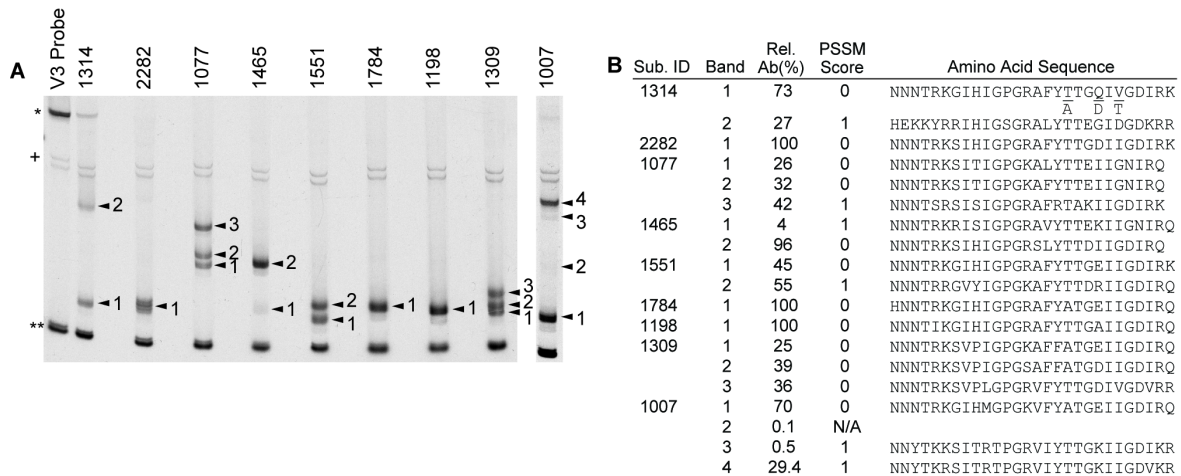


**Figure A.2. Identification and recovery of minor V3 variants using a biotinylated-V3 HTA.** (A) Biotin-V3 HTA gel for 9 representative subjects. The asterisk (\*) indicates the single-stranded probe band, double asterisks (\*\*) indicate the double-stranded probe band, the plus sign (+) indicates background bands, and arrowheads indicate shifted heteroduplex bands. (B) The numbered bands were extracted, purified, and sequenced to determine the V3 sequence of each band. It is important to note that the V3 PCR primers we used to amplify the V3 products extend into the first four and the last three amino acids of the V3 sequence, and the V3 sequences provided in Figure A.2 and GenBank (Acc. # FJ347037-FJ347099) do not include these amino acids. However, to accurately predict coreceptor usage using PSSM we added the JRFL consensus amino acid sequence to the beginning (CTRP) and end (AHC) of each V3 sequence. The relative abundance (Rel. Ab.) and PSSM score (0 = R5-like sequence, 1 = X4-like sequence, N/A = not applicable) for each sequence are listed in panel b.

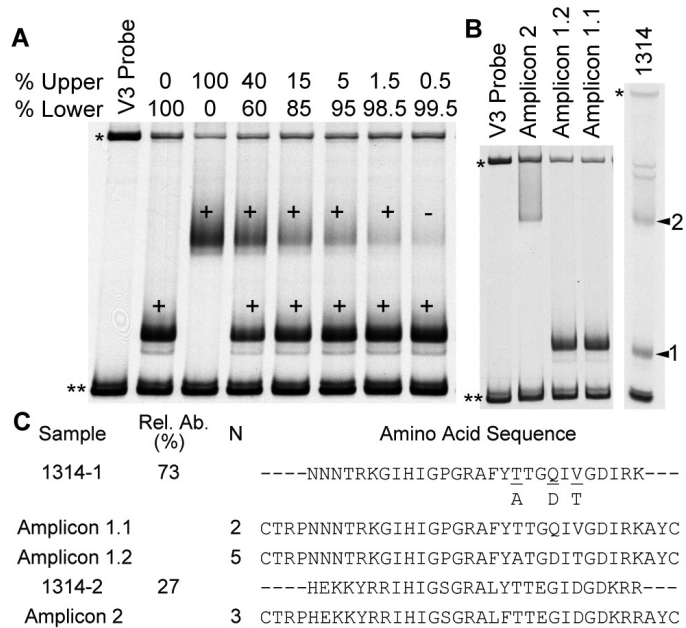
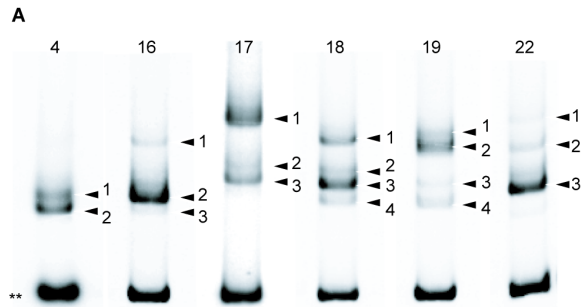


**Figure A.3. Examination of the sensitivity of the biotin-V3 HTA.** (A) Mixtures of two V3 PCR products were separated by the biotin-V3 HTA. The bands were cut from the gel, purified, and sequenced. The plus sign (+) indicates bands for which sequence was obtained, and the minus sign (-) indicates a band for which the sequence was not obtained. The asterisk (\*) indicates the single-stranded probe band, and double asterisks (\*\*) indicate the double-stranded probe band. (B, C) Single genome amplification (SGA) of the *env* gene was conducted on subject 1314. The migration of three different SGA-V3 PCR products and the original 1314 V3 PCR product are shown in panel b. The V3 amino acid sequence of the extracted bands and the SGA amplicons, the relative abundance (Rel. Ab.), and number of SGA amplicons (N) are listed in panel c.



**B**

| Subject ID |        | Protease Amino Acid Position |    |            |          |          |            |            |            |            |            |            |    |     | %  |
|------------|--------|------------------------------|----|------------|----------|----------|------------|------------|------------|------------|------------|------------|----|-----|----|
|            |        | 46                           | 48 | 54         | 60       | 62       | 63         | 71         | 72         | 73         | 77         | 82         | 84 | 90  |    |
| 4          | Bulk   | M                            | G  | I          | D        | I        | L          | A          | I          | G          | V          | V          | I  | L   |    |
|            | Band 1 | M                            | G  | I          | D        | I        | L          | A          | I          | G          | V          | <b>A/V</b> | I  | L   | 45 |
|            | Band 2 | M                            | G  | I          | D        | I        | L          | A          | I          | G          | V          | V          | I  | L   | 55 |
| 16         | Bulk   | L                            | G  | I          | D        | I        | P          | V          | I          | S          | V          | A          | I  | M   |    |
|            | Band 1 | L                            | G  | <b>I/V</b> | D        | I        | P          | V          | I          | S          | V          | A          | I  | M   | 10 |
|            | Band 2 | L                            | G  | I          | D        | I        | P          | V          | I          | S          | V          | A          | I  | M   | 87 |
|            | Band 3 | L                            | G  | I          | D        | I        | P          | V          | I          | S          | V          | A          | I  | M   | 4  |
| 17         | Bulk   | I                            | G  | I          | E        | V        | P          | A          | E          | C          | I          | V          | I  | L/M |    |
|            | Band 1 | I                            | G  | I          | E        | V        | P          | A          | E          | C          | I          | V          | I  | L   | 35 |
|            | Band 2 | I                            | G  | I          | E        | V        | P          | A          | E          | C          | I          | V          | I  | M   | 36 |
|            | Band 3 | I                            | G  | I          | E        | V        | P          | A          | E          | C          | I          | V          | I  | M   | 37 |
| 18         | Bulk   | I                            | G  | <b>I/V</b> | E        | V        | P          | V          | L          | <b>G/S</b> | V          | <b>V/A</b> | I  | L   |    |
|            | Band 1 | I                            | G  | V          | E        | V        | P          | V          | L          | G          | V          | A          | I  | L   | 28 |
|            | Band 2 | I                            | G  | I          | E        | V        | P          | V          | L          | S          | V          | V          | I  | L   | 14 |
|            | Band 3 | I                            | G  | I          | E        | V        | P          | V          | L          | S          | V          | V          | I  | L   | 48 |
|            | Band 4 | I                            | G  | I          | E        | V        | P          | <b>A/V</b> | <b>L/I</b> | G          | <b>V/I</b> | V          | I  | L   | 9  |
| 19         | Bulk   | L                            | G  | V          | D        | V        | L          | <b>A/V</b> | I          | G          | V          | A          | I  | L   |    |
|            | Band 1 | L                            | G  | V          | D        | V        | L          | <b>A/V</b> | I          | G          | V          | A          | I  | L   | 24 |
|            | Band 2 | L                            | G  | V          | D        | V        | <b>P/L</b> | <b>A/V</b> | I          | G          | V          | A          | I  | L   | 54 |
|            | Band 3 | L                            | G  | <b>I</b>   | D        | V        | <b>P/L</b> | A          | I          | G          | V          | A          | I  | L   | 8  |
|            | Band 4 | L                            | G  | <b>I</b>   | D        | V        | <b>P</b>   | A          | I          | G          | V          | A          | I  | L   | 14 |
| 22         | Bulk   | M                            | G  | I          | D        | V        | R          | A          | I          | G          | I          | F          | I  | L   |    |
|            | Band 1 | M                            | G  | <b>V</b>   | <b>D</b> | <b>I</b> | R          | A          | I          | G          | I          | F          | I  | L   | 5  |
|            | Band 2 | M                            | G  | <b>V</b>   | D        | V        | R          | A          | I          | G          | I          | F          | I  | L   | 13 |
|            | Band 3 | M                            | G  | I          | D        | V        | R          | A          | I          | G          | I          | F          | I  | L   | 76 |

**Figure A.4. Detection of minor protease inhibitor resistance mutations using a biotinylated-protease HTA. (A)** Protease-specific MSS-HTA gel for 6 representative subjects. Double asterisks (\*\*) indicate the double stranded probe band and arrowheads indicate shifted heteroduplex bands. **(B)** Numbered bands were extracted and sequenced to identify the predicted amino acid at the positions indicated. For each subject, the bulk PCR sequence is listed above the band sequences. Mixtures are indicated where identified by sequencing. The relative abundance of each band is listed in the right-most column as a percentage of the total. The amino acids inferred from the bulk sequence for subject 4 represent the wild-type consensus. Amino acid positions which the probe was designed to query are in bold (46, 48, 54, 82, 84, 90). Shaded amino acids represent positions at which heterogeneity was identified by HTA but not by bulk sequence analysis.

## REFERENCES

1. **Abbott, N.** 2002. Astrocyte-endothelial interactions and blood-brain barrier permeability. *J Anat* **200**:527.
2. **Abbott, N. J., L. Ronnback, and E. Hansson.** 2006. Astrocyte-endothelial interactions at the blood-brain barrier. *Nat Rev Neurosci* **7**:41-53.
3. **Abdulle, S., A. Mellgren, B. J. Brew, P. Cinque, L. Hagberg, R. W. Price, L. Rosengren, and M. Gisslen.** 2007. CSF neurofilament protein (NFL) -- a marker of active HIV-related neurodegeneration. *J Neurol* **254**:1026-32.
4. **Ances, B. M., and R. J. Ellis.** 2007. Dementia and neurocognitive disorders due to HIV-1 infection. *Semin Neurol* **27**:86-92.
5. **Ancuta, P., A. Kamat, K. J. Kunstman, E. Y. Kim, P. Autissier, A. Wurcel, T. Zaman, D. Stone, M. Mefford, S. Morgello, E. J. Singer, S. M. Wolinsky, and D. Gabuzda.** 2008. Microbial translocation is associated with increased monocyte activation and dementia in AIDS patients. *PLoS ONE* **3**:e2516.
6. **Arthos, J., C. Cicala, E. Martinelli, K. Macleod, D. Van Ryk, D. Wei, Z. Xiao, T. D. Veenstra, T. P. Conrad, R. A. Lempicki, S. McLaughlin, M. Pascuccio, R. Gopaul, J. McNally, C. C. Cruz, N. Censoplano, E. Chung, K. N. Reitano, S. Kottlilil, D. J. Goode, and A. S. Fauci.** 2008. HIV-1 envelope protein binds to and signals through integrin alpha4beta7, the gut mucosal homing receptor for peripheral T cells. *Nat Immunol* **9**:301-9.
7. **Baba, M., O. Nishimura, N. Kanzaki, M. Okamoto, H. Sawada, Y. Iizawa, M. Shiraishi, Y. Aramaki, K. Okonogi, Y. Ogawa, K. Meguro, and M. Fujino.** 1999. A small-molecule, nonpeptide CCR5 antagonist with highly potent and selective anti-HIV-1 activity. *Proc Natl Acad Sci U S A* **96**:5698-703.
8. **Bachis, A., F. Biggio, E. O. Major, and I. Mocchetti.** 2009. M- and T-tropic HIVs promote apoptosis in rat neurons. *J Neuroimmune Pharmacol* **4**:150-60.
9. **Bagasra, O., E. Lavi, L. Bobroski, K. Khalili, J. P. Pestaner, R. Tawadros, and R. J. Pomerantz.** 1996. Cellular reservoirs of HIV-1 in the central nervous system of infected individuals: identification by the combination of in situ polymerase chain reaction and immunohistochemistry. *AIDS* **10**:573-85.
10. **Banks, W. A., E. O. Freed, K. M. Wolf, S. M. Robinson, M. Franko, and V. B. Kumar.** 2001. Transport of human immunodeficiency virus type 1 pseudoviruses across the blood-brain barrier: role of envelope proteins and adsorptive endocytosis. *J Virol* **75**:4681-91.
11. **Bhaskaran, K., C. Mussini, A. Antinori, A. S. Walker, M. Dorrucchi, C. Sabin, A. Phillips, and K. Porter.** 2008. Changes in the incidence and predictors of human

- immunodeficiency virus-associated dementia in the era of highly active antiretroviral therapy. *Ann Neurol* **63**:213-21.
12. **Binder, G. K., and D. E. Griffin.** 2001. Interferon-gamma-mediated site-specific clearance of alphavirus from CNS neurons. *Science* **293**:303-6.
  13. **Blennow, K., P. Fredman, A. Wallin, C. G. Gottfries, I. Karlsson, G. Langstrom, I. Skoog, L. Svennerholm, and C. Wikkelso.** 1993. Protein analysis in cerebrospinal fluid. II. Reference values derived from healthy individuals 18-88 years of age. *Eur Neurol* **33**:129-33.
  14. **Boisse, L., M. J. Gill, and C. Power.** 2008. HIV infection of the central nervous system: clinical features and neuropathogenesis. *Neurol Clin* **26**:799-819.
  15. **Borrow, P., H. Lewicki, B. H. Hahn, G. M. Shaw, and M. B. Oldstone.** 1994. Virus-specific CD8<sup>+</sup> cytotoxic T-lymphocyte activity associated with control of viremia in primary human immunodeficiency virus type 1 infection. *J Virol* **68**:6103-10.
  16. **Boven, L. A., J. Middel, E. C. Breij, D. Schotte, J. Verhoef, C. Soderland, and H. S. Nottet.** 2000. Interactions between HIV-infected monocyte-derived macrophages and human brain microvascular endothelial cells result in increased expression of CC chemokines. *J Neurovirol* **6**:382-9.
  17. **Brabers, N. A., and H. S. Nottet.** 2006. Role of the pro-inflammatory cytokines TNF-alpha and IL-1beta in HIV-associated dementia. *Eur J Clin Invest* **36**:447-58.
  18. **Brew, B. J., R. B. Bhalla, M. Paul, H. Gallardo, J. C. McArthur, M. K. Schwartz, and R. W. Price.** 1990. Cerebrospinal fluid neopterin in human immunodeficiency virus type 1 infection. *Ann Neurol* **28**:556-60.
  19. **Bridger, G. J., R. T. Skerlj, D. Thornton, S. Padmanabhan, S. A. Martellucci, G. W. Henson, M. J. Abrams, N. Yamamoto, K. De Vreese, R. Pauwels, and et al.** 1995. Synthesis and structure-activity relationships of phenylenebis(methylene)-linked bis-tetraazamacrocycles that inhibit HIV replication. Effects of macrocyclic ring size and substituents on the aromatic linker. *J Med Chem* **38**:366-78.
  20. **Brzozka, K., S. Finke, and K. K. Conzelmann.** 2005. Identification of the rabies virus alpha/beta interferon antagonist: phosphoprotein P interferes with phosphorylation of interferon regulatory factor 3. *J Virol* **79**:7673-81.
  21. **Brzozka, K., S. Finke, and K. K. Conzelmann.** 2006. Inhibition of interferon signaling by rabies virus phosphoprotein P: activation-dependent binding of STAT1 and STAT2. *J Virol* **80**:2675-83.
  22. **Budka, H.** 1990. Human immunodeficiency virus (HIV) envelope and core proteins in CNS tissues of patients with the acquired immune deficiency syndrome (AIDS). *Acta Neuropathol* **79**:611-9.

23. **Budka, H.** 1986. Multinucleated giant cells in brain: a hallmark of the acquired immune deficiency syndrome (AIDS). *Acta Neuropathol* **69**:253-8.
24. **Budka, H.** 2005. The neuropathology of HIV-associated brain disease, p. 375-391. *In* H. E. Gendelman, I. Grant, I. P. Everall, S. A. Lipton, and S. Swindells (ed.), *The Neurology of AIDS*, vol. 2. Oxford University Press, Oxford.
25. **Budka, H., G. Costanzi, S. Cristina, A. Lechi, C. Parravicini, R. Trabattoni, and L. Vago.** 1987. Brain pathology induced by infection with the human immunodeficiency virus (HIV). A histological, immunocytochemical, and electron microscopical study of 100 autopsy cases. *Acta Neuropathol* **75**:185-98.
26. **Budka, H., C. A. Wiley, P. Kleihues, J. Artigas, A. K. Asbury, E. S. Cho, D. R. Cornblath, M. C. Dal Canto, U. DeGirolami, D. Dickson, and et al.** 1991. HIV-associated disease of the nervous system: review of nomenclature and proposal for neuropathology-based terminology. *Brain Pathol* **1**:143-52.
27. **Cameron, D. W., M. Heath-Chiozzi, S. Danner, C. Cohen, S. Kravcik, C. Maurath, E. Sun, D. Henry, R. Rode, A. Potthoff, and J. Leonard.** 1998. Randomised placebo-controlled trial of zidovudine in advanced HIV-1 disease. The Advanced HIV Disease Zidovudine Study Group. *Lancet* **351**:543-9.
28. **Chang, H. C., F. Samaniego, B. C. Nair, L. Buonaguro, and B. Ensoli.** 1997. HIV-1 Tat protein exits from cells via a leaderless secretory pathway and binds to extracellular matrix-associated heparan sulfate proteoglycans through its basic region. *AIDS* **11**:1421-31.
29. **Chen, B., E. M. Vogan, H. Gong, J. J. Skehel, D. C. Wiley, and S. C. Harrison.** 2005. Structure of an unliganded simian immunodeficiency virus gp120 core. *Nature* **433**:834-41.
30. **Chenna, R., H. Sugawara, T. Koike, R. Lopez, T. J. Gibson, D. G. Higgins, and J. D. Thompson.** 2003. Multiple sequence alignment with the Clustal series of programs. *Nucleic Acids Res* **31**:3497-500.
31. **Choe, H., M. Farzan, Y. Sun, N. Sullivan, B. Rollins, P. D. Ponath, L. Wu, C. R. Mackay, G. LaRosa, W. Newman, N. Gerard, C. Gerard, and J. Sodroski.** 1996. The beta-chemokine receptors CCR3 and CCR5 facilitate infection by primary HIV-1 isolates. *Cell* **85**:1135-48.
32. **Cinque, P., A. Bestetti, R. Marenzi, S. Sala, M. Gisslen, L. Hagberg, and R. W. Price.** 2005. Cerebrospinal fluid interferon-gamma-inducible protein 10 (IP-10, CXCL10) in HIV-1 infection. *J Neuroimmunol* **168**:154-63.
33. **Cinque, P., L. Vago, M. Mengozzi, V. Torri, D. Ceresa, E. Vicenzi, P. Transidico, A. Vagani, S. Sozzani, A. Mantovani, A. Lazzarin, and G. Poli.** 1998. Elevated cerebrospinal fluid levels of monocyte chemoattractant protein-1 correlate with HIV-1 encephalitis and local viral replication. *AIDS* **12**:1327-32.

34. **Clements, J. E., T. Babas, J. L. Mankowski, K. Suryanarayana, M. Piatak, Jr., P. M. Tarwater, J. D. Lifson, and M. C. Zink.** 2002. The central nervous system as a reservoir for simian immunodeficiency virus (SIV): steady-state levels of SIV DNA in brain from acute through asymptomatic infection. *J Infect Dis* **186**:905-13.
35. **Cocchi, F., A. L. DeVico, A. Garzino-Demo, A. Cara, R. C. Gallo, and P. Lusso.** 1996. The V3 domain of the HIV-1 gp120 envelope glycoprotein is critical for chemokine-mediated blockade of infection. *Nat Med* **2**:1244-7.
36. **Coffin, J. M.** 1995. HIV population dynamics in vivo: implications for genetic variation, pathogenesis, and therapy. *Science* **267**:483-9.
37. **Connor, R. I., B. K. Chen, S. Choe, and N. R. Landau.** 1995. Vpr is required for efficient replication of human immunodeficiency virus type-1 in mononuclear phagocytes. *Virology* **206**:935-44.
38. **Connor, R. I., H. Mohri, Y. Cao, and D. D. Ho.** 1993. Increased viral burden and cytopathicity correlate temporally with CD4+ T-lymphocyte decline and clinical progression in human immunodeficiency virus type 1-infected individuals. *J Virol* **67**:1772-7.
39. **Connor, R. I., K. E. Sheridan, D. Ceradini, S. Choe, and N. R. Landau.** 1997. Change in coreceptor use correlates with disease progression in HIV-1--infected individuals. *J Exp Med* **185**:621-8.
40. **Cosenza, M. A., M. L. Zhao, Q. Si, and S. C. Lee.** 2002. Human brain parenchymal microglia express CD14 and CD45 and are productively infected by HIV-1 in HIV-1 encephalitis. *Brain Pathol* **12**:442-55.
41. **Couderc, T., T. Barzu, F. Horaud, and R. Crainic.** 1990. Poliovirus permissivity and specific receptor expression on human endothelial cells. *Virology* **174**:95-102.
42. **Crowe, S., J. Mills, and M. S. McGrath.** 1987. Quantitative immunocytofluorographic analysis of CD4 surface antigen expression and HIV infection of human peripheral blood monocyte/macrophages. *AIDS Res Hum Retroviruses* **3**:135-45.
43. **Crublet, E., J. P. Andrieu, R. R. Vives, and H. Lortat-Jacob.** 2008. The HIV-1 envelope glycoprotein gp120 features four heparan sulfate binding domains, including the co-receptor binding site. *J Biol Chem* **283**:15193-200.
44. **Cullen, B. R.** 1998. Retroviruses as model systems for the study of nuclear RNA export pathways. *Virology* **249**:203-10.
45. **Daar, E. S., S. Little, J. Pitt, J. Santangelo, P. Ho, N. Harawa, P. Kerndt, J. V. Glorgi, J. Bai, P. Gaut, D. D. Richman, S. Mandel, and S. Nichols.** 2001. Diagnosis of primary HIV-1 infection. Los Angeles County Primary HIV Infection Recruitment Network. *Ann Intern Med* **134**:25-9.

46. **Dalgleish, A. G., P. C. Beverley, P. R. Clapham, D. H. Crawford, M. F. Greaves, and R. A. Weiss.** 1984. The CD4 (T4) antigen is an essential component of the receptor for the AIDS retrovirus. *Nature* **312**:763-7.
47. **de Boer, A. G., and P. J. Gaillard.** 2006. Blood-brain barrier dysfunction and recovery. *J Neural Transm* **113**:455-62.
48. **De Clercq, E., N. Yamamoto, R. Pauwels, J. Balzarini, M. Witvrouw, K. De Vreese, Z. Debyser, B. Rosenwirth, P. Peichl, R. Datema, and et al.** 1994. Highly potent and selective inhibition of human immunodeficiency virus by the bicyclam derivative JM3100. *Antimicrob Agents Chemother* **38**:668-74.
49. **Delwart, E. L., and C. J. Gordon.** 1997. Tracking changes in HIV-1 envelope quasispecies using DNA heteroduplex analysis. *Methods* **12**:348-54.
50. **Delwart, E. L., J. I. Mullins, P. Gupta, G. H. Learn, Jr., M. Holodniy, D. Katzenstein, B. D. Walker, and M. K. Singh.** 1998. Human immunodeficiency virus type 1 populations in blood and semen. *J Virol* **72**:617-23.
51. **Delwart, E. L., H. W. Sheppard, B. D. Walker, J. Goudsmit, and J. I. Mullins.** 1994. Human immunodeficiency virus type 1 evolution in vivo tracked by DNA heteroduplex mobility assays. *J Virol* **68**:6672-83.
52. **Delwart, E. L., E. G. Shpaer, J. Louwagie, F. E. McCutchan, M. Grez, H. Rubsamen-Waigmann, and J. I. Mullins.** 1993. Genetic relationships determined by a DNA heteroduplex mobility assay: analysis of HIV-1 env genes. *Science* **262**:1257-61.
53. **Deng, H., R. Liu, W. Ellmeier, S. Choe, D. Unutmaz, M. Burkhart, P. Di Marzio, S. Marmon, R. E. Sutton, C. M. Hill, C. B. Davis, S. C. Peiper, T. J. Schall, D. R. Littman, and N. R. Landau.** 1996. Identification of a major co-receptor for primary isolates of HIV-1. *Nature* **381**:661-6.
54. **Devadas, K., R. B. Lal, and S. Dhawan.** 2005. Immunology of HIV-1, p. 29-47. *In* H. E. Gendelman, I. Grant, I. P. Everall, S. A. Lipton, and S. Swindells (ed.), *The Neurology of AIDS*, vol. 2. Oxford University Press, Oxford.
55. **Dhawan, S., L. A. Toro, B. E. Jones, and M. S. Meltzer.** 1992. Interactions between HIV-infected monocytes and the extracellular matrix: HIV-infected monocytes secrete neutral metalloproteases that degrade basement membrane protein matrices. *J Leukoc Biol* **52**:244-8.
56. **Dhawan, S., B. S. Weeks, C. Soderland, H. W. Schnaper, L. A. Toro, S. P. Asthana, I. K. Hewlett, W. G. Stetler-Stevenson, S. S. Yamada, K. M. Yamada, and et al.** 1995. HIV-1 infection alters monocyte interactions with human microvascular endothelial cells. *J Immunol* **154**:422-32.

57. **Diesing, T. S., S. Swindells, H. Gelbard, and H. E. Gendelman.** 2002. HIV-1-associated dementia: a basic science and clinical perspective. *AIDS Read* **12**:358-68.
58. **Dietzschold, B., Rupprecht, C. E., Fu, Z. F., and H. Koprowski.** 1996. Rhabdoviruses, p. 1137-1159. *In* B. N. Fields, Knipe, D.M., Howley, P.M., et al. (ed.), *Fields Virology*, 3 ed, vol. 1. Lippincott-Raven Publishers, Philadelphia.
59. **Dorr, P., M. Westby, S. Dobbs, P. Griffin, B. Irvine, M. Macartney, J. Mori, G. Rickett, C. Smith-Burchnell, C. Napier, R. Webster, D. Armour, D. Price, B. Stammen, A. Wood, and M. Perros.** 2005. Maraviroc (UK-427,857), a potent, orally bioavailable, and selective small-molecule inhibitor of chemokine receptor CCR5 with broad-spectrum anti-human immunodeficiency virus type 1 activity. *Antimicrob Agents Chemother* **49**:4721-32.
60. **Dragic, T., A. Trkola, D. A. Thompson, E. G. Cormier, F. A. Kajumo, E. Maxwell, S. W. Lin, W. Ying, S. O. Smith, T. P. Sakmar, and J. P. Moore.** 2000. A binding pocket for a small molecule inhibitor of HIV-1 entry within the transmembrane helices of CCR5. *Proc Natl Acad Sci U S A* **97**:5639-44.
61. **Dreyer, E. B., P. K. Kaiser, J. T. Offermann, and S. A. Lipton.** 1990. HIV-1 coat protein neurotoxicity prevented by calcium channel antagonists. *Science* **248**:364-7.
62. **Duenas-Decamp, M. J., P. J. Peters, D. Burton, and P. R. Clapham.** 2009. Determinants flanking the CD4 binding loop modulate macrophage tropism of human immunodeficiency virus type 1 R5 envelopes. *J Virol* **83**:2575-83.
63. **Dunfee, R. L., E. R. Thomas, and D. Gabuzda.** 2009. Enhanced macrophage tropism of HIV in brain and lymphoid tissues is associated with sensitivity to the broadly neutralizing CD4 binding site antibody b12. *Retrovirology* **6**:69.
64. **Dunfee, R. L., E. R. Thomas, P. R. Gorry, J. Wang, J. Taylor, K. Kunstman, S. M. Wolinsky, and D. Gabuzda.** 2006. The HIV Env variant N283 enhances macrophage tropism and is associated with brain infection and dementia. *Proc Natl Acad Sci U S A* **103**:15160-5.
65. **Dunfee, R. L., E. R. Thomas, J. Wang, K. Kunstman, S. M. Wolinsky, and D. Gabuzda.** 2007. Loss of the N-linked glycosylation site at position 386 in the HIV envelope V4 region enhances macrophage tropism and is associated with dementia. *Virology* **367**:222-34.
66. **Earl, P. L., B. Moss, and R. W. Doms.** 1991. Folding, interaction with GRP78-BiP, assembly, and transport of the human immunodeficiency virus type 1 envelope protein. *J Virol* **65**:2047-55.
67. **Edmonson, P. F., and J. I. Mullins.** 1992. Efficient amplification of HIV half-genomes from tissue DNA. *Nucleic Acids Res* **20**:4933.

68. **Eggers, C., K. Hertogs, H. J. Sturenburg, J. van Lunzen, and H. J. Stellbrink.** 2003. Delayed central nervous system virus suppression during highly active antiretroviral therapy is associated with HIV encephalopathy, but not with viral drug resistance or poor central nervous system drug penetration. *AIDS* **17**:1897-906.
69. **Ellis, R. J., A. C. Gamst, E. Capparelli, S. A. Spector, K. Hsia, T. Wolfson, I. Abramson, I. Grant, and J. A. McCutchan.** 2000. Cerebrospinal fluid HIV RNA originates from both local CNS and systemic sources. *Neurology* **54**:927-36.
70. **Ellis, R. J., K. Hsia, S. A. Spector, J. A. Nelson, R. K. Heaton, M. R. Wallace, I. Abramson, J. H. Atkinson, I. Grant, and J. A. McCutchan.** 1997. Cerebrospinal fluid human immunodeficiency virus type 1 RNA levels are elevated in neurocognitively impaired individuals with acquired immunodeficiency syndrome. HIV Neurobehavioral Research Center Group. *Ann Neurol* **42**:679-88.
71. **Ellis, R. J., D. J. Moore, M. E. Childers, S. Letendre, J. A. McCutchan, T. Wolfson, S. A. Spector, K. Hsia, R. K. Heaton, and I. Grant.** 2002. Progression to neuropsychological impairment in human immunodeficiency virus infection predicted by elevated cerebrospinal fluid levels of human immunodeficiency virus RNA. *Arch Neurol* **59**:923-8.
72. **Engelhardt, B.** 2006. Molecular mechanisms involved in T cell migration across the blood-brain barrier. *J Neural Transm* **113**:477-85.
73. **Engelhardt, B., and R. M. Ransohoff.** 2005. The ins and outs of T-lymphocyte trafficking to the CNS: anatomical sites and molecular mechanisms. *Trends Immunol* **26**:485-95.
74. **Fabis, M. J., T. W. Phares, R. B. Kean, H. Koprowski, and D. C. Hooper.** 2008. Blood-brain barrier changes and cell invasion differ between therapeutic immune clearance of neurotrophic virus and CNS autoimmunity. *Proc Natl Acad Sci U S A* **105**:15511-6.
75. **Farina, C., F. Aloisi, and E. Meinl.** 2007. Astrocytes are active players in cerebral innate immunity. *Trends Immunol* **28**:138-45.
76. **Fatkenheuer, G., A. L. Pozniak, M. A. Johnson, A. Plettenberg, S. Staszewski, A. I. Hoepelman, M. S. Saag, F. D. Goebel, J. K. Rockstroh, B. J. Dezube, T. M. Jenkins, C. Medhurst, J. F. Sullivan, C. Ridgway, S. Abel, I. T. James, M. Youle, and E. van der Ryst.** 2005. Efficacy of short-term monotherapy with maraviroc, a new CCR5 antagonist, in patients infected with HIV-1. *Nat Med* **11**:1170-2.
77. **Fauci, A. S.** 1993. Multifactorial nature of human immunodeficiency virus disease: implications for therapy. *Science* **262**:1011-8.
78. **Feng, Y., C. C. Broder, P. E. Kennedy, and E. A. Berger.** 1996. HIV-1 entry cofactor: functional cDNA cloning of a seven-transmembrane, G protein-coupled receptor. *Science* **272**:872-7.

79. **Finke, S., and K. K. Conzelmann.** 2005. Replication strategies of rabies virus. *Virus Res* **111**:120-31.
80. **Fischer-Smith, T., C. Bell, S. Croul, M. Lewis, and J. Rappaport.** 2008. Monocyte/macrophage trafficking in acquired immunodeficiency syndrome encephalitis: lessons from human and nonhuman primate studies. *J Neurovirol* **14**:318-26.
81. **Fischer-Smith, T., S. Croul, A. Adeniyi, K. Rybicka, S. Morgello, K. Khalili, and J. Rappaport.** 2004. Macrophage/microglial accumulation and proliferating cell nuclear antigen expression in the central nervous system in human immunodeficiency virus encephalopathy. *Am J Pathol* **164**:2089-99.
82. **Fischer-Smith, T., S. Croul, A. E. Sverstiuk, C. Capini, D. L'Heureux, E. G. Regulier, M. W. Richardson, S. Amini, S. Morgello, K. Khalili, and J. Rappaport.** 2001. CNS invasion by CD14+/CD16+ peripheral blood-derived monocytes in HIV dementia: perivascular accumulation and reservoir of HIV infection. *J Neurovirol* **7**:528-41.
83. **Fishman, R. A.** June 1992. *Cerebrospinal Fluid in Diseases of the Nervous System*, 2 ed. W.B. Saunders Company.
84. **Foos, T. M., and J. Y. Wu.** 2002. The role of taurine in the central nervous system and the modulation of intracellular calcium homeostasis. *Neurochem Res* **27**:21-6.
85. **Fournier, J. G., M. Tardieu, P. Lebon, O. Robain, G. Ponsot, S. Rozenblatt, and M. Bouteille.** 1985. Detection of measles virus RNA in lymphocytes from peripheral blood and brain perivascular infiltrates of patients with subacute sclerosing panencephalitis. *N Engl J Med* **313**:910-5.
86. **Franzen, B., K. Duvefelt, C. Jonsson, B. Engelhardt, J. Ottervald, M. Wickman, Y. Yang, and I. Schuppe-Koistinen.** 2003. Gene and protein expression profiling of human cerebral endothelial cells activated with tumor necrosis factor-alpha. *Brain Res Mol Brain Res* **115**:130-46.
87. **Fredericksen, B. L., and M. Gale, Jr.** 2006. West Nile virus evades activation of interferon regulatory factor 3 through RIG-I-dependent and -independent pathways without antagonizing host defense signaling. *J Virol* **80**:2913-23.
88. **Freed, E. O., and M. A. Martin.** 2001. HIVs and Their Replication, p. 913-983. *In* D. M. Knipe and P. M. Howley (ed.), *Fundamental Virology*, vol. 4. Lippincott Williams and Wilkins, Philadelphia.
89. **Fuentes, M. E., S. K. Durham, M. R. Swerdel, A. C. Lewin, D. S. Barton, J. R. Megill, R. Bravo, and S. A. Lira.** 1995. Controlled recruitment of monocytes and macrophages to specific organs through transgenic expression of monocyte chemoattractant protein-1. *J Immunol* **155**:5769-76.

90. **Fullerton, S. M., G. A. Shirman, W. J. Strittmatter, and W. D. Matthew.** 2001. Impairment of the blood-nerve and blood-brain barriers in apolipoprotein e knockout mice. *Exp Neurol* **169**:13-22.
91. **Furuta, R. A., C. T. Wild, Y. Weng, and C. D. Weiss.** 1998. Capture of an early fusion-active conformation of HIV-1 gp41. *Nat Struct Biol* **5**:276-9.
92. **Gabuzda, D., and J. Wang.** 1999. Chemokine receptors and virus entry in the central nervous system. *J Neurovirol* **5**:643-58.
93. **Gallo, P., A. De Rossi, S. Sivieri, L. Chieco-Bianchi, and B. Tavalato.** 1994. M-CSF production by HIV-1-infected monocytes and its intrathecal synthesis. Implications for neurological HIV-1-related disease. *J Neuroimmunol* **51**:193-8.
94. **Gallo, P., K. Frei, C. Rordorf, J. Lazdins, B. Tavalato, and A. Fontana.** 1989. Human immunodeficiency virus type 1 (HIV-1) infection of the central nervous system: an evaluation of cytokines in cerebrospinal fluid. *J Neuroimmunol* **23**:109-16.
95. **Garcia-Sastre, A., and C. A. Biron.** 2006. Type 1 interferons and the virus-host relationship: a lesson in detente. *Science* **312**:879-82.
96. **Garcia, F., G. Niebla, J. Romeu, C. Vidal, M. Plana, M. Ortega, L. Ruiz, T. Gallart, B. Clotet, J. M. Miro, T. Pumarola, and J. M. Gatell.** 1999. Cerebrospinal fluid HIV-1 RNA levels in asymptomatic patients with early stage chronic HIV-1 infection: support for the hypothesis of local virus replication. *AIDS* **13**:1491-6.
97. **Garden, G. A.** 2002. Microglia in human immunodeficiency virus-associated neurodegeneration. *GLIA* **40**:240-51.
98. **Gartner, S.** 2000. HIV infection and dementia. *Science* **287**:602-4.
99. **Gee, J. R., and J. N. Keller.** 2005. Astrocytes: regulation of brain homeostasis via apolipoprotein E. *Int J Biochem Cell Biol* **37**:1145-50.
100. **Gelbard, H. A., H. S. Nottet, S. Swindells, M. Jett, K. A. Dzenko, P. Genis, R. White, L. Wang, Y. B. Choi, D. Zhang, and et al.** 1994. Platelet-activating factor: a candidate human immunodeficiency virus type 1-induced neurotoxin. *J Virol* **68**:4628-35.
101. **Genis, P., M. Jett, E. W. Bernton, T. Boyle, H. A. Gelbard, K. Dzenko, R. W. Keane, L. Resnick, Y. Mizrachi, D. J. Volsky, and et al.** 1992. Cytokines and arachidonic metabolites produced during human immunodeficiency virus (HIV)-infected macrophage-astroglia interactions: implications for the neuropathogenesis of HIV disease. *J Exp Med* **176**:1703-18.

102. **Ghorpade, A., B. Brichacek, and M. Bukrinsky.** 2005. The molecular biology of HIV-1, p. 17-28. *In* H. E. Gendelman, I. Grant, I. P. Everall, S. A. Lipton, and S. Swindells (ed.), *The Neurology of AIDS*, vol. 2. Oxford University Press, Oxford.
103. **Gisolf, E. H., R. H. Enting, S. Jurriaans, F. de Wolf, M. E. van der Ende, R. M. Hoetelmans, P. Portegies, and S. A. Danner.** 2000. Cerebrospinal fluid HIV-1 RNA during treatment with ritonavir/saquinavir or ritonavir/saquinavir/stavudine. *AIDS* **14**:1583-9.
104. **Gisslen, M., L. Hagberg, L. Rosengren, B. J. Brew, P. Cinque, S. Spudich, and R. W. Price.** 2007. Defining and evaluating HIV-related neurodegenerative disease and its treatment targets: a combinatorial approach to use of cerebrospinal fluid molecular biomarkers. *J Neuroimmune Pharmacol* **2**:112-9.
105. **Glass, J. D., H. Fedor, S. L. Wesselingh, and J. C. McArthur.** 1995. Immunocytochemical quantitation of human immunodeficiency virus in the brain: correlations with dementia. *Ann Neurol* **38**:755-62.
106. **Goff, S. P.** 2001. *Retroviridae: The Retroviruses and Their Replication*, p. 843-911. *In* D. M. Knipe and P. M. Howley (ed.), *Fundamental Virology*, vol. 4. Lippincott Williams and Wilkins, Philadelphia.
107. **Gonzalez-Scarano, F., and J. Martin-Garcia.** 2005. The neuropathogenesis of AIDS. *Nat Rev Immunol* **5**:69-81.
108. **Gorry, P. R., G. Bristol, J. A. Zack, K. Ritola, R. Swanstrom, C. J. Birch, J. E. Bell, N. Bannert, K. Crawford, H. Wang, D. Schols, E. De Clercq, K. Kunstman, S. M. Wolinsky, and D. Gabuzda.** 2001. Macrophage tropism of human immunodeficiency virus type 1 isolates from brain and lymphoid tissues predicts neurotropism independent of coreceptor specificity. *J Virol* **75**:10073-89.
109. **Gorry, P. R., J. Taylor, G. H. Holm, A. Mehle, T. Morgan, M. Cayabyab, M. Farzan, H. Wang, J. E. Bell, K. Kunstman, J. P. Moore, S. M. Wolinsky, and D. Gabuzda.** 2002. Increased CCR5 affinity and reduced CCR5/CD4 dependence of a neurovirulent primary human immunodeficiency virus type 1 isolate. *J Virol* **76**:6277-92.
110. **Griffin, D. E.** 2003. Immune responses to RNA-virus infections of the CNS. *Nat Rev Immunol* **3**:493-502.
111. **Grimaldi, L. M., G. V. Martino, D. M. Franciotta, R. Brustia, A. Castagna, R. Pristera, and A. Lazzarin.** 1991. Elevated alpha-tumor necrosis factor levels in spinal fluid from HIV-1-infected patients with central nervous system involvement. *Ann Neurol* **29**:21-5.
112. **Guillemin, G. J., and B. J. Brew.** 2004. Microglia, macrophages, perivascular macrophages, and pericytes: a review of function and identification. *J Leukoc Biol* **75**:388-97.

113. **Guillemin, G. J., J. Croitoru-Lamoury, D. Dormont, P. J. Armati, and B. J. Brew.** 2003. Quinolinic acid upregulates chemokine production and chemokine receptor expression in astrocytes. *GLIA* **41**:371-81.
114. **Guillemin, G. J., S. J. Kerr, and B. J. Brew.** 2005. Involvement of quinolinic acid in AIDS dementia complex. *Neurotox Res* **7**:103-23.
115. **Guindon, S., and O. Gascuel.** 2003. A simple, fast, and accurate algorithm to estimate large phylogenies by maximum likelihood. *Syst Biol* **52**:696-704.
116. **Guindon, S., F. Lethiec, P. Duroux, and O. Gascuel.** 2005. PHYML Online--a web server for fast maximum likelihood-based phylogenetic inference. *Nucleic Acids Res* **33**:W557-9.
117. **Gulick, R. M., X. J. Hu, S. A. Fiscus, C. V. Fletcher, R. Haubrich, H. Cheng, E. Acosta, S. W. Lagakos, R. Swanstrom, W. Freimuth, S. Snyder, C. Mills, M. Fischl, C. Pettinelli, and D. Katzenstein.** 2000. Randomized study of saquinavir with zidovudine or zalcitabine together with zalcitabine, didanosine, or both in human immunodeficiency virus-infected adults with virologic failure on zidovudine: AIDS Clinical Trials Group Study 359. *J Infect Dis* **182**:1375-84.
118. **Gulick, R. M., Z. Su, C. Flexner, M. D. Hughes, P. R. Skolnik, T. J. Wilkin, R. Gross, A. Krambrink, E. Coakley, W. L. Greaves, A. Zolopa, R. Reichman, C. Godfrey, M. Hirsch, and D. R. Kuritzkes.** 2007. Phase 2 study of the safety and efficacy of vicriviroc, a CCR5 inhibitor, in HIV-1-Infected, treatment-experienced patients: AIDS clinical trials group 5211. *J Infect Dis* **196**:304-12.
119. **Haas, D. W., L. A. Clough, B. W. Johnson, V. L. Harris, P. Spearman, G. R. Wilkinson, C. V. Fletcher, S. Fiscus, S. Raffanti, R. Donlon, J. McKinsey, J. Nicotera, D. Schmidt, R. E. Shoup, R. E. Kates, R. M. Lloyd, Jr., and B. Larder.** 2000. Evidence of a source of HIV type 1 within the central nervous system by ultraintensive sampling of cerebrospinal fluid and plasma. *AIDS Res Hum Retroviruses* **16**:1491-502.
120. **Haas, D. W., B. W. Johnson, P. Spearman, S. Raffanti, J. Nicotera, D. Schmidt, T. Hulgan, R. Shepard, and S. A. Fiscus.** 2003. Two phases of HIV RNA decay in CSF during initial days of multidrug therapy. *Neurology* **61**:1391-6.
121. **Haase, A. T.** 1986. Pathogenesis of lentivirus infections. *Nature* **322**:130-6.
122. **Halvas, E. K., G. M. Aldrovandi, P. Balfe, I. A. Beck, V. F. Boltz, J. M. Coffin, L. M. Frenkel, J. D. Hazelwood, V. A. Johnson, M. Kearney, A. Kovacs, D. R. Kuritzkes, K. J. Metzner, D. V. Nissley, M. Nowicki, S. Palmer, R. Ziermann, R. Y. Zhao, C. L. Jennings, J. Bremer, D. Brambilla, and J. W. Mellors.** 2006. Blinded, multicenter comparison of methods to detect a drug-resistant mutant of human immunodeficiency virus type 1 at low frequency. *J Clin Microbiol* **44**:2612-4.

123. **Harrington, P. R., M. J. Connell, R. B. Meeker, P. R. Johnson, and R. Swanstrom.** 2007. Dynamics of simian immunodeficiency virus populations in blood and cerebrospinal fluid over the full course of infection. *J Infect Dis* **196**:1058-67.
124. **Harrington, P. R., D. W. Haas, K. Ritola, and R. Swanstrom.** 2005. Compartmentalized human immunodeficiency virus type 1 present in cerebrospinal fluid is produced by short-lived cells. *J Virol* **79**:7959-66.
125. **Harrington, P. R., J. A. Nelson, K. M. Kitrinis, and R. Swanstrom.** 2007. Independent evolution of human immunodeficiency virus type 1 env V1/V2 and V4/V5 hypervariable regions during chronic infection. *J Virol* **81**:5413-7.
126. **Harrington, P. R., G. Schnell, S. L. Letendre, K. Ritola, K. Robertson, C. Hall, C. L. Burch, C. B. Jabara, D. T. Moore, R. J. Ellis, R. W. Price, and R. Swanstrom.** 2009. Cross-sectional characterization of HIV-1 env compartmentalization in cerebrospinal fluid over the full disease course. *AIDS* **23**:907-15.
127. **Haseloff, R. F., I. E. Blasig, H. C. Bauer, and H. Bauer.** 2005. In search of the astrocytic factor(s) modulating blood-brain barrier functions in brain capillary endothelial cells in vitro. *Cell Mol Neurobiol* **25**:25-39.
128. **Hatalski, C. G., W. F. Hickey, and W. I. Lipkin.** 1998. Humoral immunity in the central nervous system of Lewis rats infected with Borna disease virus. *J Neuroimmunol* **90**:128-36.
129. **Haughey, N. J., A. Nath, M. P. Mattson, J. T. Slevin, and J. D. Geiger.** 2001. HIV-1 Tat through phosphorylation of NMDA receptors potentiates glutamate excitotoxicity. *J Neurochem* **78**:457-67.
130. **He, J., S. Choe, R. Walker, P. Di Marzio, D. O. Morgan, and N. R. Landau.** 1995. Human immunodeficiency virus type 1 viral protein R (Vpr) arrests cells in the G2 phase of the cell cycle by inhibiting p34cdc2 activity. *J Virol* **69**:6705-11.
131. **Henderson, G. J., N. G. Hoffman, L. H. Ping, S. A. Fiscus, I. F. Hoffman, K. M. Kitrinis, T. Banda, F. E. Martinson, P. N. Kazembe, D. A. Chilongozi, M. S. Cohen, and R. Swanstrom.** 2004. HIV-1 populations in blood and breast milk are similar. *Virology* **330**:295-303.
132. **Hendrix, C. W., C. Flexner, R. T. MacFarland, C. Giandomenico, E. J. Fuchs, E. Redpath, G. Bridger, and G. W. Henson.** 2000. Pharmacokinetics and safety of AMD-3100, a novel antagonist of the CXCR-4 chemokine receptor, in human volunteers. *Antimicrob Agents Chemother* **44**:1667-73.
133. **Hesselgesser, J., M. Halks-Miller, V. DelVecchio, S. C. Peiper, J. Hoxie, D. L. Kolson, D. Taub, and R. Horuk.** 1997. CD4-independent association between HIV-1 gp120 and CXCR4: functional chemokine receptors are expressed in human neurons. *Curr Biol* **7**:112-21.

134. **Hickey, W. F., and H. Kimura.** 1988. Perivascular microglial cells of the CNS are bone marrow-derived and present antigen in vivo. *Science* **239**:290-2.
135. **Hickey, W. F., K. Vass, and H. Lassmann.** 1992. Bone marrow-derived elements in the central nervous system: an immunohistochemical and ultrastructural survey of rat chimeras. *J Neuropathol Exp Neurol* **51**:246-56.
136. **Hill, J. M., R. F. Mervis, R. Avidor, T. W. Moody, and D. E. Brenneman.** 1993. HIV envelope protein-induced neuronal damage and retardation of behavioral development in rat neonates. *Brain Res* **603**:222-33.
137. **Hintzen, R. Q., U. Fiszer, S. Fredrikson, M. Rep, C. H. Polman, R. A. van Lier, and H. Link.** 1995. Analysis of CD27 surface expression on T cell subsets in MS patients and control individuals. *J Neuroimmunol* **56**:99-105.
138. **Hlavacek, W. S., N. I. Stilianakis, D. W. Notermans, S. A. Danner, and A. S. Perelson.** 2000. Influence of follicular dendritic cells on decay of HIV during antiretroviral therapy. *Proc Natl Acad Sci U S A* **97**:10966-71.
139. **Ho, D. D., A. U. Neumann, A. S. Perelson, W. Chen, J. M. Leonard, and M. Markowitz.** 1995. Rapid turnover of plasma virions and CD4 lymphocytes in HIV-1 infection. *Nature* **373**:123-6.
140. **Hoffman, N. G., F. Seillier-Moiseiwitsch, J. Ahn, J. M. Walker, and R. Swanstrom.** 2002. Variability in the human immunodeficiency virus type 1 gp120 Env protein linked to phenotype-associated changes in the V3 loop. *J Virol* **76**:3852-64.
141. **Hooper, D. C., K. Morimoto, M. Bette, E. Weihe, H. Koprowski, and B. Dietzschold.** 1998. Collaboration of antibody and inflammation in clearance of rabies virus from the central nervous system. *J Virol* **72**:3711-9.
142. **Huang, C. C., M. Tang, M. Y. Zhang, S. Majeed, E. Montabana, R. L. Stanfield, D. S. Dimitrov, B. Korber, J. Sodroski, I. A. Wilson, R. Wyatt, and P. D. Kwong.** 2005. Structure of a V3-containing HIV-1 gp120 core. *Science* **310**:1025-8.
143. **Ince, W. L., P. R. Harrington, G. L. Schnell, M. Patel-Chhabra, C. L. Burch, P. Menezes, R. W. Price, J. J. Eron, Jr., and R. I. Swanstrom.** 2009. Major co-existing human immunodeficiency virus type 1 env gene subpopulations in the peripheral blood are produced by cells with similar turnover rates and show little evidence of genetic compartmentalization. *J Virol*:doi:10.1128/JVI.02486-08.
144. **Janeway, C. A., Travers, P., Walport, M., and M.J. Shlomchik.** 2005. *Immunobiology: the immune system in health and disease*, 6 ed. Garland Science Taylor & Francis Group, New York.
145. **Jensen, M. A., F. S. Li, A. B. van 't Wout, D. C. Nickle, D. Shriner, H. X. He, S. McLaughlin, R. Shankarappa, J. B. Margolick, and J. I. Mullins.** 2003. Improved

- coreceptor usage prediction and genotypic monitoring of R5-to-X4 transition by motif analysis of human immunodeficiency virus type 1 env V3 loop sequences. *J Virol* **77**:13376-88.
146. **Jevtovic, D., V. Vanovac, M. Veselinovic, D. Salemovic, J. Ranin, and E. Stefanova.** 2008. The incidence of and risk factors for HIV-associated cognitive-motor complex among patients on HAART. *Biomed Pharmacother.*
  147. **Johnson, J. A., J. F. Li, X. Wei, J. Lipscomb, D. Bennett, A. Brant, M. E. Cong, T. Spira, R. W. Shafer, and W. Heneine.** 2007. Simple PCR assays improve the sensitivity of HIV-1 subtype B drug resistance testing and allow linking of resistance mutations. *PLoS ONE* **2**:e638.
  148. **Johnston, S. H., M. A. Lobritz, S. Nguyen, K. Lassen, S. Delair, F. Posta, Y. J. Bryson, E. J. Arts, T. Chou, and B. Lee.** 2009. A quantitative affinity-profiling system that reveals distinct CD4/CCR5 usage patterns among human immunodeficiency virus type 1 and simian immunodeficiency virus strains. *J Virol* **83**:11016-26.
  149. **Jordan, B. D., B. A. Navia, C. Petito, E. S. Cho, and R. W. Price.** 1985. Neurological syndromes complicating AIDS. *Front Radiat Ther Oncol* **19**:82-7.
  150. **Kaplan, A. H., M. Manchester, and R. Swanstrom.** 1994. The activity of the protease of human immunodeficiency virus type 1 is initiated at the membrane of infected cells before the release of viral proteins and is required for release to occur with maximum efficiency. *J Virol* **68**:6782-6.
  151. **Kapoor, A., M. Jones, R. W. Shafer, S. Y. Rhee, P. Kazanjian, and E. L. Delwart.** 2004. Sequencing-based detection of low-frequency human immunodeficiency virus type 1 drug-resistant mutants by an RNA/DNA heteroduplex generator-tracking assay. *J Virol* **78**:7112-23.
  152. **Katoh, K., and H. Toh.** 2008. Recent developments in the MAFFT multiple sequence alignment program. *Brief Bioinform* **9**:286-98.
  153. **Kaul, M., and S. A. Lipton.** 1999. Chemokines and activated macrophages in HIV gp120-induced neuronal apoptosis. *Proc Natl Acad Sci U S A* **96**:8212-6.
  154. **Keele, B. F., E. E. Giorgi, J. F. Salazar-Gonzalez, J. M. Decker, K. T. Pham, M. G. Salazar, C. Sun, T. Grayson, S. Wang, H. Li, X. Wei, C. Jiang, J. L. Kirchherr, F. Gao, J. A. Anderson, L. H. Ping, R. Swanstrom, G. D. Tomaras, W. A. Blattner, P. A. Goepfert, J. M. Kilby, M. S. Saag, E. L. Delwart, M. P. Busch, M. S. Cohen, D. C. Montefiori, B. F. Haynes, B. Gaschen, G. S. Athreya, H. Y. Lee, N. Wood, C. Seoighe, A. S. Perelson, T. Bhattacharya, B. T. Korber, B. H. Hahn, and G. M. Shaw.** 2008. Identification and characterization of transmitted and early founder virus envelopes in primary HIV-1 infection. *Proc Natl Acad Sci U S A* **105**:7552-7.

155. **Kelder, W., J. C. McArthur, T. Nance-Sproson, D. McClernon, and D. E. Griffin.** 1998. Beta-chemokines MCP-1 and RANTES are selectively increased in cerebrospinal fluid of patients with human immunodeficiency virus-associated dementia. *Ann Neurol* **44**:831-5.
156. **Keller, B. C., B. L. Fredericksen, M. A. Samuel, R. E. Mock, P. W. Mason, M. S. Diamond, and M. Gale, Jr.** 2006. Resistance to alpha/beta interferon is a determinant of West Nile virus replication fitness and virulence. *J Virol* **80**:9424-34.
157. **Kim, J. H., J. H. Kim, J. A. Park, S. W. Lee, W. J. Kim, Y. S. Yu, and K. W. Kim.** 2006. Blood-neural barrier: intercellular communication at gliovascular interface. *J Biochem Mol Biol* **39**:339-45.
158. **Kitagawa, M., A. A. Lackner, D. J. Martfeld, M. B. Gardner, and S. Dandekar.** 1991. Simian immunodeficiency virus infection of macaque bone marrow macrophages correlates with disease progression in vivo. *Am J Pathol* **138**:921-30.
159. **Kitrinou, K. M., N. G. Hoffman, J. A. Nelson, and R. Swanstrom.** 2003. Turnover of env variable region 1 and 2 genotypes in subjects with late-stage human immunodeficiency virus type 1 infection. *J Virol* **77**:6811-22.
160. **Kivisakk, P., C. Trebst, Z. Liu, B. H. Tucky, T. L. Sorensen, R. A. Rudick, M. Mack, and R. M. Ransohoff.** 2002. T-cells in the cerebrospinal fluid express a similar repertoire of inflammatory chemokine receptors in the absence or presence of CNS inflammation: implications for CNS trafficking. *Clin Exp Immunol* **129**:510-8.
161. **Koenig, S., H. E. Gendelman, J. M. Orenstein, M. C. Dal Canto, G. H. Pezeshkpour, M. Yungbluth, F. Janotta, A. Aksamit, M. A. Martin, and A. S. Fauci.** 1986. Detection of AIDS virus in macrophages in brain tissue from AIDS patients with encephalopathy. *Science* **233**:1089-93.
162. **Kumar, S., M. Nei, J. Dudley, and K. Tamura.** 2008. MEGA: a biologist-centric software for evolutionary analysis of DNA and protein sequences. *Brief Bioinform* **9**:299-306.
163. **Kumar, S., K. Tamura, and M. Nei.** 1994. MEGA: Molecular Evolutionary Genetics Analysis software for microcomputers. *Comput Appl Biosci* **10**:189-91.
164. **Kure, K., J. F. Llena, W. D. Lyman, R. Soeiro, K. M. Weidenheim, A. Hirano, and D. W. Dickson.** 1991. Human immunodeficiency virus-1 infection of the nervous system: an autopsy study of 268 adult, pediatric, and fetal brains. *Hum Pathol* **22**:700-10.
165. **Kwong, P. D., R. Wyatt, S. Majeed, J. Robinson, R. W. Sweet, J. Sodroski, and W. A. Hendrickson.** 2000. Structures of HIV-1 gp120 envelope glycoproteins from laboratory-adapted and primary isolates. *Structure* **8**:1329-39.

166. **Kwong, P. D., R. Wyatt, J. Robinson, R. W. Sweet, J. Sodroski, and W. A. Hendrickson.** 1998. Structure of an HIV gp120 envelope glycoprotein in complex with the CD4 receptor and a neutralizing human antibody. *Nature* **393**:648-59.
167. **Lafrenie, R. M., L. M. Wahl, J. S. Epstein, I. K. Hewlett, K. M. Yamada, and S. Dhawan.** 1996. HIV-1-Tat modulates the function of monocytes and alters their interactions with microvessel endothelial cells. A mechanism of HIV pathogenesis. *J Immunol* **156**:1638-45.
168. **Lane, J. H., V. G. Sasseville, M. O. Smith, P. Vogel, D. R. Pauley, M. P. Heyes, and A. A. Lackner.** 1996. Neuroinvasion by simian immunodeficiency virus coincides with increased numbers of perivascular macrophages/microglia and intrathecal immune activation. *J Neurovirol* **2**:423-32.
169. **Lannuzel, A., P. M. Lledo, H. O. Lamghitnia, J. D. Vincent, and M. Tardieu.** 1995. HIV-1 envelope proteins gp120 and gp160 potentiate NMDA-induced  $[Ca^{2+}]_i$  increase, alter  $[Ca^{2+}]_i$  homeostasis and induce neurotoxicity in human embryonic neurons. *Eur J Neurosci* **7**:2285-93.
170. **Larder, B. A., A. Kohli, P. Kellam, S. D. Kemp, M. Kronick, and R. D. Henfrey.** 1993. Quantitative detection of HIV-1 drug resistance mutations by automated DNA sequencing. *Nature* **365**:671-3.
171. **Laskowitz, D. T., H. Fillit, N. Yeung, K. Toku, and M. P. Vitek.** 2006. Apolipoprotein E-derived peptides reduce CNS inflammation: implications for therapy of neurological disease. *Acta Neurol Scand Suppl* **185**:15-20.
172. **Lawson, L. J., V. H. Perry, and S. Gordon.** 1992. Turnover of resident microglia in the normal adult mouse brain. *Neuroscience* **48**:405-15.
173. **Lee, B., M. Sharron, L. J. Montaner, D. Weissman, and R. W. Doms.** 1999. Quantification of CD4, CCR5, and CXCR4 levels on lymphocyte subsets, dendritic cells, and differentially conditioned monocyte-derived macrophages. *Proc Natl Acad Sci U S A* **96**:5215-20.
174. **Lee, S. W., W. J. Kim, Y. K. Choi, H. S. Song, M. J. Son, I. H. Gelman, Y. J. Kim, and K. W. Kim.** 2003. SSeCKS regulates angiogenesis and tight junction formation in blood-brain barrier. *Nat Med* **9**:900-6.
175. **Letendre, S., J. Marquie-Beck, E. Capparelli, B. Best, D. Clifford, A. C. Collier, B. B. Gelman, J. C. McArthur, J. A. McCutchan, S. Morgello, D. Simpson, I. Grant, and R. J. Ellis.** 2008. Validation of the CNS Penetration-Effectiveness rank for quantifying antiretroviral penetration into the central nervous system. *Arch Neurol* **65**:65-70.
176. **Levine, B., J. M. Hardwick, B. D. Trapp, T. O. Crawford, R. C. Bollinger, and D. E. Griffin.** 1991. Antibody-mediated clearance of alphavirus infection from neurons. *Science* **254**:856-60.

177. **Lewin, S. R., S. Sonza, L. B. Irving, C. F. McDonald, J. Mills, and S. M. Crowe.** 1996. Surface CD4 is critical to in vitro HIV infection of human alveolar macrophages. *AIDS Res Hum Retroviruses* **12**:877-83.
178. **Liang, C., and M. A. Wainberg.** 2002. The role of Tat in HIV-1 replication: an activator and/or a suppressor? *AIDS Rev* **4**:41-9.
179. **Lindback, S., A. C. Karlsson, J. Mittler, A. Blaxhult, M. Carlsson, G. Briheim, A. Sonnerborg, and H. Gaines.** 2000. Viral dynamics in primary HIV-1 infection. Karolinska Institutet Primary HIV Infection Study Group. *AIDS* **14**:2283-91.
180. **Lindback, S., R. Thorstensson, A. C. Karlsson, M. von Sydow, L. Flamholz, A. Blaxhult, A. Sonnerborg, G. Biberfeld, and H. Gaines.** 2000. Diagnosis of primary HIV-1 infection and duration of follow-up after HIV exposure. Karolinska Institute Primary HIV Infection Study Group. *AIDS* **14**:2333-9.
181. **Lipton, S. A., N. J. Sucher, P. K. Kaiser, and E. B. Dreyer.** 1991. Synergistic effects of HIV coat protein and NMDA receptor-mediated neurotoxicity. *Neuron* **7**:111-8.
182. **Little, S. J., S. D. Frost, J. K. Wong, D. M. Smith, S. L. Pond, C. C. Ignacio, N. T. Parkin, C. J. Petropoulos, and D. D. Richman.** 2008. Persistence of transmitted drug resistance among subjects with primary human immunodeficiency virus infection. *J Virol* **82**:5510-8.
183. **Liu, S. L., A. G. Rodrigo, R. Shankarappa, G. H. Learn, L. Hsu, O. Davidov, L. P. Zhao, and J. I. Mullins.** 1996. HIV quasispecies and resampling. *Science* **273**:415-6.
184. **Liu, W. J., X. J. Wang, D. C. Clark, M. Lobigs, R. A. Hall, and A. A. Khromykh.** 2006. A single amino acid substitution in the West Nile virus nonstructural protein NS2A disables its ability to inhibit alpha/beta interferon induction and attenuates virus virulence in mice. *J Virol* **80**:2396-404.
185. **Liu, X., M. Jana, S. Dasgupta, S. Koka, J. He, C. Wood, and K. Pahan.** 2002. Human immunodeficiency virus type 1 (HIV-1) tat induces nitric-oxide synthase in human astroglia. *J Biol Chem* **277**:39312-9.
186. **Liu, Y., X. P. Tang, J. C. McArthur, J. Scott, and S. Gartner.** 2000. Analysis of human immunodeficiency virus type 1 gp160 sequences from a patient with HIV dementia: evidence for monocyte trafficking into brain. *J Neurovirol* **6 Suppl 1**:S70-81.
187. **Marcello, A., M. Zoppe, and M. Giacca.** 2001. Multiple modes of transcriptional regulation by the HIV-1 Tat transactivator. *IUBMB Life* **51**:175-81.
188. **Marcondes, M. C., T. H. Burdo, S. Sopper, S. Huitron-Resendiz, C. Lanigan, D. Watry, C. Flynn, M. Zandonatti, and H. S. Fox.** 2007. Enrichment and persistence

- of virus-specific CTL in the brain of simian immunodeficiency virus-infected monkeys is associated with a unique cytokine environment. *J Immunol* **178**:5812-9.
189. **Marcondes, M. C., E. M. Burudi, S. Huitron-Resendiz, M. Sanchez-Alavez, D. Watry, M. Zandonatti, S. J. Henriksen, and H. S. Fox.** 2001. Highly activated CD8(+) T cells in the brain correlate with early central nervous system dysfunction in simian immunodeficiency virus infection. *J Immunol* **167**:5429-38.
190. **Marcondes, M. C., C. A. Phillipson, and H. S. Fox.** 2003. Distinct clonal repertoire of brain CD8+ cells in simian immunodeficiency virus infection. *AIDS* **17**:1605-11.
191. **Margulies, M., M. Egholm, W. E. Altman, S. Attiya, J. S. Bader, L. A. Bembien, J. Berka, M. S. Braverman, Y. J. Chen, Z. Chen, S. B. Dewell, L. Du, J. M. Fierro, X. V. Gomes, B. C. Godwin, W. He, S. Helgesen, C. H. Ho, G. P. Irzyk, S. C. Jando, M. L. Alenquer, T. P. Jarvie, K. B. Jirage, J. B. Kim, J. R. Knight, J. R. Lanza, J. H. Leamon, S. M. Lefkowitz, M. Lei, J. Li, K. L. Lohman, H. Lu, V. B. Makhijani, K. E. McDade, M. P. McKenna, E. W. Myers, E. Nickerson, J. R. Nobile, R. Plant, B. P. Puc, M. T. Ronan, G. T. Roth, G. J. Sarkis, J. F. Simons, J. W. Simpson, M. Srinivasan, K. R. Tartaro, A. Tomasz, K. A. Vogt, G. A. Volkmer, S. H. Wang, Y. Wang, M. P. Weiner, P. Yu, R. F. Begley, and J. M. Rothberg.** 2005. Genome sequencing in microfabricated high-density picolitre reactors. *Nature* **437**:376-80.
192. **Marin, M., K. M. Rose, S. L. Kozak, and D. Kabat.** 2003. HIV-1 Vif protein binds the editing enzyme APOBEC3G and induces its degradation. *Nat Med* **9**:1398-403.
193. **Markiewicz, I., and B. Lukomska.** 2006. The role of astrocytes in the physiology and pathology of the central nervous system. *Acta Neurobiol Exp (Wars)* **66**:343-58.
194. **Marra, C. M., C. L. Maxwell, A. C. Collier, K. R. Robertson, and A. Imrie.** 2007. Interpreting cerebrospinal fluid pleocytosis in HIV in the era of potent antiretroviral therapy. *BMC Infect Dis* **7**:37.
195. **Martin, C., J. Albert, P. Hansson, P. Pehrsson, H. Link, and A. Sonnerborg.** 1998. Cerebrospinal fluid mononuclear cell counts influence CSF HIV-1 RNA levels. *J Acquir Immune Defic Syndr Hum Retrovirol* **17**:214-9.
196. **Martin, J., C. C. LaBranche, and F. Gonzalez-Scarano.** 2001. Differential CD4/CCR5 utilization, gp120 conformation, and neutralization sensitivity between envelopes from a microglia-adapted human immunodeficiency virus type 1 and its parental isolate. *J Virol* **75**:3568-80.
197. **Maslin, C. L., K. Kedzierska, N. L. Webster, W. A. Muller, and S. M. Crowe.** 2005. Transendothelial migration of monocytes: the underlying molecular mechanisms and consequences of HIV-1 infection. *Curr HIV Res* **3**:303-17.

198. **Meinl, E., M. Krumbholz, and R. Hohlfeld.** 2006. B lineage cells in the inflammatory central nervous system environment: migration, maintenance, local antibody production, and therapeutic modulation. *Ann Neurol* **59**:880-92.
199. **Mellgren, A., R. W. Price, L. Hagberg, L. Rosengren, B. J. Brew, and M. Gisslen.** 2007. Antiretroviral treatment reduces increased CSF neurofilament protein (NFL) in HIV-1 infection. *Neurology* **69**:1536-41.
200. **Methia, N., P. Andre, A. Hafezi-Moghadam, M. Economopoulos, K. L. Thomas, and D. D. Wagner.** 2001. ApoE deficiency compromises the blood brain barrier especially after injury. *Mol Med* **7**:810-5.
201. **Miller, D. W.** 2005. The blood-brain barrier as an immunocompetent organ, p. 115-124. *In* H. E. Gendelman, Grant, I., Everall, I.P., Lipton, S.A., and S. Swindells (ed.), *The Neurology of AIDS*, 2 ed. Oxford University Press, Oxford.
202. **Mintz, M.** 1994. Clinical comparison of adult and pediatric NeuroAIDS. *Adv Neuroimmunol* **4**:207-21.
203. **Monteiro de Almeida, S., S. Letendre, J. Zimmerman, S. Kolakowski, D. Lazzaretto, J. A. McCutchan, and R. Ellis.** 2006. Relationship of CSF leukocytosis to compartmentalized changes in MCP-1/CCL2 in the CSF of HIV-infected patients undergoing interruption of antiretroviral therapy. *J Neuroimmunol* **179**:180-5.
204. **Moses, A. V., F. E. Bloom, C. D. Pauza, and J. A. Nelson.** 1993. Human immunodeficiency virus infection of human brain capillary endothelial cells occurs via a CD4/galactosylceramide-independent mechanism. *Proc Natl Acad Sci U S A* **90**:10474-8.
205. **Moulard, M., and E. Decroly.** 2000. Maturation of HIV envelope glycoprotein precursors by cellular endoproteases. *Biochim Biophys Acta* **1469**:121-32.
206. **Murphy, G., A. Charlett, L. F. Jordan, N. Osner, O. N. Gill, and J. V. Parry.** 2004. HIV incidence appears constant in men who have sex with men despite widespread use of effective antiretroviral therapy. *AIDS* **18**:265-72.
207. **Murray, J. M., S. Emery, A. D. Kelleher, M. Law, J. Chen, D. J. Hazuda, B. Y. Nguyen, H. Tepler, and D. A. Cooper.** 2007. Antiretroviral therapy with the integrase inhibitor raltegravir alters decay kinetics of HIV, significantly reducing the second phase. *AIDS* **21**:2315-21.
208. **Navia, B. A., E. S. Cho, C. K. Petito, and R. W. Price.** 1986. The AIDS dementia complex: II. Neuropathology. *Ann Neurol* **19**:525-35.
209. **Navia, B. A., B. D. Jordan, and R. W. Price.** 1986. The AIDS dementia complex: I. Clinical features. *Ann Neurol* **19**:517-24.

210. **Navia, B. A., and R. W. Price.** 2005. An overview of the clinical and biological features of the AIDS dementia complex, p. 339-356. *In* H. E. Gendelman, I. Grant, I. P. Everall, S. A. Lipton, and S. Swindells (ed.), *The Neurology of AIDS*, vol. 2. Oxford University Press, Oxford.
211. **Nelson, J. A., F. Baribaud, T. Edwards, and R. Swanstrom.** 2000. Patterns of changes in human immunodeficiency virus type 1 V3 sequence populations late in infection. *J Virol* **74**:8494-501.
212. **Nelson, J. A., S. A. Fiscus, and R. Swanstrom.** 1997. Evolutionary variants of the human immunodeficiency virus type 1 V3 region characterized by using a heteroduplex tracking assay. *J Virol* **71**:8750-8.
213. **Neuenburg, J. K., H. R. Brodt, B. G. Herndier, M. Bickel, P. Bacchetti, R. W. Price, R. M. Grant, and W. Schlote.** 2002. HIV-related neuropathology, 1985 to 1999: rising prevalence of HIV encephalopathy in the era of highly active antiretroviral therapy. *J Acquir Immune Defic Syndr* **31**:171-7.
214. **Nottet, H. S.** 1999. Interactions between macrophages and brain microvascular endothelial cells: role in pathogenesis of HIV-1 infection and blood - brain barrier function. *J Neurovirol* **5**:659-69.
215. **Nottet, H. S., M. Jett, C. R. Flanagan, Q. H. Zhai, Y. Persidsky, A. Rizzino, E. W. Bernton, P. Genis, T. Baldwin, J. Schwartz, and et al.** 1995. A regulatory role for astrocytes in HIV-1 encephalitis. An overexpression of eicosanoids, platelet-activating factor, and tumor necrosis factor-alpha by activated HIV-1-infected monocytes is attenuated by primary human astrocytes. *J Immunol* **154**:3567-81.
216. **Nottet, H. S., Y. Persidsky, V. G. Sasseville, A. N. Nukuna, P. Bock, Q. H. Zhai, L. R. Sharer, R. D. McComb, S. Swindells, C. Soderland, and H. E. Gendelman.** 1996. Mechanisms for the transendothelial migration of HIV-1-infected monocytes into brain. *J Immunol* **156**:1284-95.
217. **Nuovo, G. J., and M. L. Alfieri.** 1996. AIDS dementia is associated with massive, activated HIV-1 infection and concomitant expression of several cytokines. *Mol Med* **2**:358-66.
218. **Ohagen, A., A. Devitt, K. J. Kunstman, P. R. Gorry, P. P. Rose, B. Korber, J. Taylor, R. Levy, R. L. Murphy, S. M. Wolinsky, and D. Gabuzda.** 2003. Genetic and functional analysis of full-length human immunodeficiency virus type 1 env genes derived from brain and blood of patients with AIDS. *J Virol* **77**:12336-45.
219. **Oster, W., A. Lindemann, S. Horn, R. Mertelsmann, and F. Herrmann.** 1987. Tumor necrosis factor (TNF)-alpha but not TNF-beta induces secretion of colony stimulating factor for macrophages (CSF-1) by human monocytes. *Blood* **70**:1700-3.
220. **Palmer, S., M. Kearney, F. Maldarelli, E. K. Halvas, C. J. Bixby, H. Bazmi, D. Rock, J. Falloon, R. T. Davey, Jr., R. L. Dewar, J. A. Metcalf, S. Hammer, J. W.**

- Mellors, and J. M. Coffin.** 2005. Multiple, linked human immunodeficiency virus type 1 drug resistance mutations in treatment-experienced patients are missed by standard genotype analysis. *J Clin Microbiol* **43**:406-13.
221. **Pantaleo, G., J. F. Demarest, H. Soudeyns, C. Graziosi, F. Denis, J. W. Adelsberger, P. Borrow, M. S. Saag, G. M. Shaw, R. P. Sekaly, and et al.** 1994. Major expansion of CD8+ T cells with a predominant V beta usage during the primary immune response to HIV. *Nature* **370**:463-7.
222. **Paredes, R., V. C. Marconi, T. B. Campbell, and D. R. Kuritzkes.** 2007. Systematic evaluation of allele-specific real-time PCR for the detection of minor HIV-1 variants with pol and env resistance mutations. *J Virol Methods* **146**:136-46.
223. **Parra, B., D. R. Hinton, N. W. Marten, C. C. Bergmann, M. T. Lin, C. S. Yang, and S. A. Stohlman.** 1999. IFN-gamma is required for viral clearance from central nervous system oligodendroglia. *J Immunol* **162**:1641-7.
224. **Patel, C. A., M. Mukhtar, and R. J. Pomerantz.** 2000. Human immunodeficiency virus type 1 Vpr induces apoptosis in human neuronal cells. *J Virol* **74**:9717-26.
225. **Patterson, C. E., J. K. Daley, and G. F. Rall.** 2002. Neuronal survival strategies in the face of RNA viral infection. *J Infect Dis* **186 Suppl 2**:S215-9.
226. **Paul, S., C. Ricour, C. Sommereyns, F. Sorgeloos, and T. Michiels.** 2007. Type I interferon response in the central nervous system. *Biochimie*.
227. **Pelkmans, L., J. Kartenbeck, and A. Helenius.** 2001. Caveolar endocytosis of simian virus 40 reveals a new two-step vesicular-transport pathway to the ER. *Nat Cell Biol* **3**:473-83.
228. **Peluso, R., A. Haase, L. Stowring, M. Edwards, and P. Ventura.** 1985. A Trojan Horse mechanism for the spread of visna virus in monocytes. *Virology* **147**:231-6.
229. **Pemberton, L. A., S. J. Kerr, G. Smythe, and B. J. Brew.** 1997. Quinolinic acid production by macrophages stimulated with IFN-gamma, TNF-alpha, and IFN-alpha. *J Interferon Cytokine Res* **17**:589-95.
230. **Pereira, L. A., K. Bentley, A. Peeters, M. J. Churchill, and N. J. Deacon.** 2000. A compilation of cellular transcription factor interactions with the HIV-1 LTR promoter. *Nucleic Acids Res* **28**:663-8.
231. **Perelson, A. S., A. U. Neumann, M. Markowitz, J. M. Leonard, and D. D. Ho.** 1996. HIV-1 dynamics in vivo: virion clearance rate, infected cell life-span, and viral generation time. *Science* **271**:1582-6.
232. **Persidsky, Y., and H. E. Gendelman.** 2003. Mononuclear phagocyte immunity and the neuropathogenesis of HIV-1 infection. *J Leukoc Biol* **74**:691-701.

233. **Peters, P. J., J. Bhattacharya, S. Hibbitts, M. T. Dittmar, G. Simmons, J. Bell, P. Simmonds, and P. R. Clapham.** 2004. Biological analysis of human immunodeficiency virus type 1 R5 envelopes amplified from brain and lymph node tissues of AIDS patients with neuropathology reveals two distinct tropism phenotypes and identifies envelopes in the brain that confer an enhanced tropism and fusigenicity for macrophages. *J Virol* **78**:6915-26.
234. **Peters, P. J., M. J. Duenas-Decamp, W. M. Sullivan, and P. R. Clapham.** 2007. Variation of macrophage tropism among HIV-1 R5 envelopes in brain and other tissues. *J Neuroimmune Pharmacol* **2**:32-41.
235. **Phares, T. W., R. B. Kean, T. Mikheeva, and D. C. Hooper.** 2006. Regional differences in blood-brain barrier permeability changes and inflammation in the apathogenic clearance of virus from the central nervous system. *J Immunol* **176**:7666-75.
236. **Pillai, S. K., S. L. Pond, Y. Liu, B. M. Good, M. C. Strain, R. J. Ellis, S. Letendre, D. M. Smith, H. F. Gunthard, I. Grant, T. D. Marcotte, J. A. McCutchan, D. D. Richman, and J. K. Wong.** 2006. Genetic attributes of cerebrospinal fluid-derived HIV-1 env. *Brain* **129**:1872-83.
237. **Poland, S. D., G. P. Rice, and G. A. Dekaban.** 1995. HIV-1 infection of human brain-derived microvascular endothelial cells in vitro. *J Acquir Immune Defic Syndr Hum Retrovirol* **8**:437-45.
238. **Polazzi, E., G. Levi, and L. Minghetti.** 1999. Human immunodeficiency virus type 1 Tat protein stimulates inducible nitric oxide synthase expression and nitric oxide production in microglial cultures. *J Neuropathol Exp Neurol* **58**:825-31.
239. **Pomerantz, R. J.** 2003. Reservoirs, sanctuaries, and residual disease: the hiding spots of HIV-1. *HIV Clin Trials* **4**:137-43.
240. **Pond, S. L., S. D. Frost, and S. V. Muse.** 2005. HyPhy: hypothesis testing using phylogenies. *Bioinformatics* **21**:676-9.
241. **Porwit, A., C. Parravicini, A. L. Petren, T. Barkhem, G. Costanzi, S. Josephs, and P. Biberfeld.** 1989. Cell association of HIV in AIDS-related encephalopathy and dementia. *APMIS* **97**:79-90.
242. **Power, C., J. C. McArthur, R. T. Johnson, D. E. Griffin, J. D. Glass, S. Perryman, and B. Chesebro.** 1994. Demented and nondemented patients with AIDS differ in brain-derived human immunodeficiency virus type 1 envelope sequences. *J Virol* **68**:4643-49.
243. **Power, C., J. C. McArthur, A. Nath, K. Wehrly, M. Mayne, J. Nishio, T. Langelier, R. T. Johnson, and B. Chesebro.** 1998. Neuronal death induced by brain-derived human immunodeficiency virus type 1 envelope genes differs between demented and nondemented AIDS patients. *J Virol* **72**:9045-53.

244. **Price, R. W., B. Brew, J. Sidtis, M. Rosenblum, A. C. Scheck, and P. Cleary.** 1988. The brain in AIDS: central nervous system HIV-1 infection and AIDS dementia complex. *Science* **239**:586-92.
245. **Price, R. W., and B. J. Brew.** 1988. The AIDS dementia complex. *J Infect Dis* **158**:1079-83.
246. **Price, R. W., E. E. Paxinos, R. M. Grant, B. Drews, A. Nilsson, R. Hoh, N. S. Hellmann, C. J. Petropoulos, and S. G. Deeks.** 2001. Cerebrospinal fluid response to structured treatment interruption after virological failure. *AIDS* **15**:1251-9.
247. **Ramsauer, M., D. Krause, and R. Dermietzel.** 2002. Angiogenesis of the blood-brain barrier in vitro and the function of cerebral pericytes. *Faseb J* **16**:1274-6.
248. **Ransohoff, R. M., P. Kivisakk, and G. Kidd.** 2003. Three or more routes for leukocyte migration into the central nervous system. *Nat Rev Immunol* **3**:569-81.
249. **Resch, W., N. Hoffman, and R. Swanstrom.** 2001. Improved success of phenotype prediction of the human immunodeficiency virus type 1 from envelope variable loop 3 sequence using neural networks. *Virology* **288**:51-62.
250. **Resch, W., N. Parkin, E. L. Stuelke, T. Watkins, and R. Swanstrom.** 2001. A multiple-site-specific heteroduplex tracking assay as a tool for the study of viral population dynamics. *Proc Natl Acad Sci U S A* **98**:176-81.
251. **Riddle, T. M., N. J. Shire, M. S. Sherman, K. F. Franco, H. W. Sheppard, and J. A. Nelson.** 2006. Sequential turnover of human immunodeficiency virus type 1 env throughout the course of infection. *J Virol* **80**:10591-9.
252. **Rieckmann, P., and B. Engelhardt.** 2003. Building up the blood-brain barrier. *Nat Med* **9**:828-9.
253. **Ritola, K., C. D. Pilcher, S. A. Fiscus, N. G. Hoffman, J. A. Nelson, K. M. Kitrinis, C. B. Hicks, J. J. Eron, Jr., and R. Swanstrom.** 2004. Multiple V1/V2 env variants are frequently present during primary infection with human immunodeficiency virus type 1. *J Virol* **78**:11208-18.
254. **Ritola, K., K. Robertson, S. A. Fiscus, C. Hall, and R. Swanstrom.** 2005. Increased human immunodeficiency virus type 1 (HIV-1) env compartmentalization in the presence of HIV-1-associated dementia. *J Virol* **79**:10830-4.
255. **Rizzuto, C. D., R. Wyatt, N. Hernandez-Ramos, Y. Sun, P. D. Kwong, W. A. Hendrickson, and J. Sodroski.** 1998. A conserved HIV gp120 glycoprotein structure involved in chemokine receptor binding. *Science* **280**:1949-53.
256. **Rossi, F., B. Querido, M. Nimmagadda, S. Cocklin, S. Navas-Martin, and J. Martin-Garcia.** 2008. The V1-V3 region of a brain-derived HIV-1 envelope

- glycoprotein determines macrophage tropism, low CD4 dependence, increased fusogenicity and altered sensitivity to entry inhibitors. *Retrovirology* **5**:89.
257. **Rostad, S. W., S. M. Sumi, C. M. Shaw, K. Olson, and J. K. McDougall.** 1987. Human immunodeficiency virus (HIV) infection in brains with AIDS-related leukoencephalopathy. *AIDS Res Hum Retroviruses* **3**:363-73.
258. **Roy, A., T. W. Phares, H. Koprowski, and D. C. Hooper.** 2007. Failure to open the blood-brain barrier and deliver immune effectors to central nervous system tissues leads to the lethal outcome of silver-haired bat rabies virus infection. *J Virol* **81**:1110-8.
259. **Ryzhova, E. V., P. Crino, L. Shawver, S. V. Westmoreland, A. A. Lackner, and F. Gonzalez-Scarano.** 2002. Simian immunodeficiency virus encephalitis: analysis of envelope sequences from individual brain multinucleated giant cells and tissue samples. *Virology* **297**:57-67.
260. **Sabri, F., K. Titanji, A. De Milito, and F. Chiodi.** 2003. Astrocyte activation and apoptosis: their roles in the neuropathology of HIV infection. *Brain Pathol* **13**:84-94.
261. **Sacktor, N., M. P. McDermott, K. Marder, G. Schifitto, O. A. Selnes, J. C. McArthur, Y. Stern, S. Albert, D. Palumbo, K. Kieburtz, J. A. De Marcaida, B. Cohen, and L. Epstein.** 2002. HIV-associated cognitive impairment before and after the advent of combination therapy. *J Neurovirol* **8**:136-42.
262. **Salazar-Gonzalez, J. F., E. Bailes, K. T. Pham, M. G. Salazar, M. B. Guffey, B. F. Keele, C. A. Derdeyn, P. Farmer, E. Hunter, S. Allen, O. Manigart, J. Mulenga, J. A. Anderson, R. Swanstrom, B. F. Haynes, G. S. Athreya, B. T. Korber, P. M. Sharp, G. M. Shaw, and B. H. Hahn.** 2008. Deciphering human immunodeficiency virus type 1 transmission and early envelope diversification by single-genome amplification and sequencing. *J Virol* **82**:3952-70.
263. **Samuel, M. A., and M. S. Diamond.** 2005. Alpha/beta interferon protects against lethal West Nile virus infection by restricting cellular tropism and enhancing neuronal survival. *J Virol* **79**:13350-61.
264. **Saphire, A. C., M. D. Bobardt, Z. Zhang, G. David, and P. A. Gallay.** 2001. Syndecans serve as attachment receptors for human immunodeficiency virus type 1 on macrophages. *J Virol* **75**:9187-200.
265. **Sasseville, V. G., W. A. Newman, A. A. Lackner, M. O. Smith, N. C. Lausen, D. Beall, and D. J. Ringler.** 1992. Elevated vascular cell adhesion molecule-1 in AIDS encephalitis induced by simian immunodeficiency virus. *Am J Pathol* **141**:1021-30.
266. **Sattentau, Q. J., and J. P. Moore.** 1991. Conformational changes induced in the human immunodeficiency virus envelope glycoprotein by soluble CD4 binding. *J Exp Med* **174**:407-15.

267. **Savio, T., and G. Levi.** 1993. Neurotoxicity of HIV coat protein gp120, NMDA receptors, and protein kinase C: a study with rat cerebellar granule cell cultures. *J Neurosci Res* **34**:265-72.
268. **Schmidtmayerova, H., H. S. Nottet, G. Nuovo, T. Raabe, C. R. Flanagan, L. Dubrovsky, H. E. Gendelman, A. Cerami, M. Bukrinsky, and B. Sherry.** 1996. Human immunodeficiency virus type 1 infection alters chemokine beta peptide expression in human monocytes: implications for recruitment of leukocytes into brain and lymph nodes. *Proc Natl Acad Sci U S A* **93**:700-4.
269. **Schnell, G., W. L. Ince, and R. Swanstrom.** 2008. Identification and recovery of minor HIV-1 variants using the heteroduplex tracking assay and biotinylated probes. *Nucleic Acids Res* **36**:e146.
270. **Schnell, G., R. W. Price, R. Swanstrom, and S. Spudich.** 2010. Compartmentalization and Clonal Amplification of HIV-1 Variants in the Cerebrospinal Fluid during Primary Infection. *J Virol* **84**:2395-407.
271. **Schnell, G., S. Spudich, P. Harrington, R. W. Price, and R. Swanstrom.** 2009. Compartmentalized human immunodeficiency virus type 1 originates from long-lived cells in some subjects with HIV-1-associated dementia. *PLoS Pathog* **5**:e1000395.
272. **Schrager, L. K., and M. P. D'Souza.** 1998. Cellular and anatomical reservoirs of HIV-1 in patients receiving potent antiretroviral combination therapy. *JAMA* **280**:67-71.
273. **Schroder, A. R., P. Shinn, H. Chen, C. Berry, J. R. Ecker, and F. Bushman.** 2002. HIV-1 integration in the human genome favors active genes and local hotspots. *Cell* **110**:521-9.
274. **Schroeter, M. L., K. Mertsch, H. Giese, S. Muller, A. Sporbert, B. Hickel, and I. E. Blasig.** 1999. Astrocytes enhance radical defence in capillary endothelial cells constituting the blood-brain barrier. *FEBS Lett* **449**:241-4.
275. **Sedaghat, A. R., J. B. Dinoso, L. Shen, C. O. Wilke, and R. F. Siliciano.** 2008. Decay dynamics of HIV-1 depend on the inhibited stages of the viral life cycle. *Proc Natl Acad Sci U S A* **105**:4832-7.
276. **Sevigny, J. J., S. M. Albert, M. P. McDermott, J. C. McArthur, N. Sacktor, K. Conant, G. Schifitto, O. A. Selnes, Y. Stern, D. R. McClernon, D. Palumbo, K. Kiebertz, G. Riggs, B. Cohen, L. G. Epstein, and K. Marder.** 2004. Evaluation of HIV RNA and markers of immune activation as predictors of HIV-associated dementia. *Neurology* **63**:2084-90.
277. **Shafer, R. W.** 2006. Rationale and uses of a public HIV drug-resistance database. *J Infect Dis* **194 Suppl 1**:S51-8.

278. **Shieh, J. T., A. V. Albright, M. Sharron, S. Gartner, J. Strizki, R. W. Doms, and F. Gonzalez-Scarano.** 1998. Chemokine receptor utilization by human immunodeficiency virus type 1 isolates that replicate in microglia. *J Virol* **72**:4243-9.
279. **Siliciano, J. D., J. Kajdas, D. Finzi, T. C. Quinn, K. Chadwick, J. B. Margolick, C. Kovacs, S. J. Gange, and R. F. Siliciano.** 2003. Long-term follow-up studies confirm the stability of the latent reservoir for HIV-1 in resting CD4<sup>+</sup> T cells. *Nat Med* **9**:727-8.
280. **Simmonds, P., P. Balfe, C. A. Ludlam, J. O. Bishop, and A. J. Brown.** 1990. Analysis of sequence diversity in hypervariable regions of the external glycoprotein of human immunodeficiency virus type 1. *J Virol* **64**:5840-50.
281. **Simon, V., and D. D. Ho.** 2003. HIV-1 dynamics in vivo: implications for therapy. *Nat Rev Microbiol* **1**:181-90.
282. **Slatkin, M., and W. P. Maddison.** 1989. A cladistic measure of gene flow inferred from the phylogenies of alleles. *Genetics* **123**:603-13.
283. **Smith, D. M., S. Zarate, H. Shao, S. K. Pillai, S. L. Letendre, J. K. Wong, D. D. Richman, S. D. Frost, and R. J. Ellis.** 2008. Pleocytosis is associated with disruption of HIV compartmentalization between blood and cerebral spinal fluid viral populations. *Virology*.
284. **Song, B., M. Cayabyab, N. Phan, L. Wang, M. K. Axthelm, N. L. Letvin, and J. G. Sodroski.** 2004. Neutralization sensitivity of a simian-human immunodeficiency virus (SHIV-HXBc2P 3.2N) isolated from an infected rhesus macaque with neurological disease. *Virology* **322**:168-81.
285. **Song, L., A. Nath, J. D. Geiger, A. Moore, and S. Hochman.** 2003. Human immunodeficiency virus type 1 Tat protein directly activates neuronal N-methyl-D-aspartate receptors at an allosteric zinc-sensitive site. *J Neurovirol* **9**:399-403.
286. **Spudich, S. S., A. C. Nilsson, N. D. Lollo, T. J. Liegler, C. J. Petropoulos, S. G. Deeks, E. E. Paxinos, and R. W. Price.** 2005. Cerebrospinal fluid HIV infection and pleocytosis: relation to systemic infection and antiretroviral treatment. *BMC Infect Dis* **5**:98.
287. **Stamatovic, S. M., O. B. Dimitrijevic, R. F. Keep, and A. V. Andjelkovic.** 2006. Protein kinase Calpha-RhoA cross-talk in CCL2-induced alterations in brain endothelial permeability. *J Biol Chem* **281**:8379-88.
288. **Stamatovic, S. M., P. Shakui, R. F. Keep, B. B. Moore, S. L. Kunkel, N. Van Rooijen, and A. V. Andjelkovic.** 2005. Monocyte chemoattractant protein-1 regulation of blood-brain barrier permeability. *J Cereb Blood Flow Metab* **25**:593-606.

289. **Staprans, S., N. Marlowe, D. Glidden, T. Novakovic-Agopian, R. M. Grant, M. Heyes, F. Aweeka, S. Deeks, and R. W. Price.** 1999. Time course of cerebrospinal fluid responses to antiretroviral therapy: evidence for variable compartmentalization of infection. *AIDS* **13**:1051-61.
290. **Stohlman, S. A., C. C. Bergmann, R. C. van der Veen, and D. R. Hinton.** 1995. Mouse hepatitis virus-specific cytotoxic T lymphocytes protect from lethal infection without eliminating virus from the central nervous system. *J Virol* **69**:684-94.
291. **Strain, M. C., S. Letendre, S. K. Pillai, T. Russell, C. C. Ignacio, H. F. Gunthard, B. Good, D. M. Smith, S. M. Wolinsky, M. Furtado, J. Marquie-Beck, J. Durelle, I. Grant, D. D. Richman, T. Marcotte, J. A. McCutchan, R. J. Ellis, and J. K. Wong.** 2005. Genetic composition of human immunodeficiency virus type 1 in cerebrospinal fluid and blood without treatment and during failing antiretroviral therapy. *J Virol* **79**:1772-88.
292. **Strizki, J. M., A. V. Albright, H. Sheng, M. O'Connor, L. Perrin, and F. Gonzalez-Scarano.** 1996. Infection of primary human microglia and monocyte-derived macrophages with human immunodeficiency virus type 1 isolates: evidence of differential tropism. *J Virol* **70**:7654-62.
293. **Strizki, J. M., C. Tremblay, S. Xu, L. Wojcik, N. Wagner, W. Gonsiorek, R. W. Hipkin, C. C. Chou, C. Pugliese-Sivo, Y. Xiao, J. R. Tagat, K. Cox, T. Priestley, S. Sorota, W. Huang, M. Hirsch, G. R. Reyes, and B. M. Baroudy.** 2005. Discovery and characterization of vicriviroc (SCH 417690), a CCR5 antagonist with potent activity against human immunodeficiency virus type 1. *Antimicrob Agents Chemother* **49**:4911-9.
294. **Svenningsson, A., O. Andersen, M. Edsbacke, and S. Stemme.** 1995. Lymphocyte phenotype and subset distribution in normal cerebrospinal fluid. *J Neuroimmunol* **63**:39-46.
295. **Takahashi, K., S. L. Wesselingh, D. E. Griffin, J. C. McArthur, R. T. Johnson, and J. D. Glass.** 1996. Localization of HIV-1 in human brain using polymerase chain reaction/in situ hybridization and immunocytochemistry. *Ann Neurol* **39**:705-11.
296. **Tamura, K., J. Dudley, M. Nei, and S. Kumar.** 2007. MEGA4: Molecular Evolutionary Genetics Analysis (MEGA) software version 4.0. *Mol Biol Evol* **24**:1596-9.
297. **Thali, M., J. P. Moore, C. Furman, M. Charles, D. D. Ho, J. Robinson, and J. Sodroski.** 1993. Characterization of conserved human immunodeficiency virus type 1 gp120 neutralization epitopes exposed upon gp120-CD4 binding. *J Virol* **67**:3978-88.
298. **Thomas, E. R., R. L. Dunfee, J. Stanton, D. Bogdan, J. Taylor, K. Kunstman, J. E. Bell, S. M. Wolinsky, and D. Gabuzda.** 2007. Macrophage entry mediated by HIV Envs from brain and lymphoid tissues is determined by the capacity to use low CD4 levels and overall efficiency of fusion. *Virology* **360**:105-19.

299. **Thompson, J. D., D. G. Higgins, and T. J. Gibson.** 1994. CLUSTAL W: improving the sensitivity of progressive multiple sequence alignment through sequence weighting, position-specific gap penalties and weight matrix choice. *Nucleic Acids Res* **22**:4673-80.
300. **Tschen, S. I., C. C. Bergmann, C. Ramakrishna, S. Morales, R. Atkinson, and S. A. Stohlman.** 2002. Recruitment kinetics and composition of antibody-secreting cells within the central nervous system following viral encephalomyelitis. *J Immunol* **168**:2922-9.
301. **Turchan-Cholewo, J., V. M. Dimayuga, S. Gupta, R. M. Gorospe, J. N. Keller, and A. J. Bruce-Keller.** 2009. NADPH oxidase drives cytokine and neurotoxin release from microglia and macrophages in response to HIV-Tat. *Antioxid Redox Signal* **11**:193-204.
302. **Unger, E. R., J. H. Sung, J. C. Manivel, M. L. Chenggis, B. R. Blazar, and W. Krivit.** 1993. Male donor-derived cells in the brains of female sex-mismatched bone marrow transplant recipients: a Y-chromosome specific in situ hybridization study. *J Neuropathol Exp Neurol* **52**:460-70.
303. **van Rossum, D., and U. K. Hanisch.** 2004. Microglia. *Metab Brain Dis* **19**:393-411.
304. **Vidy, A., M. Chelbi-Alix, and D. Blondel.** 2005. Rabies virus P protein interacts with STAT1 and inhibits interferon signal transduction pathways. *J Virol* **79**:14411-20.
305. **Vidy, A., J. El Bougrini, M. K. Chelbi-Alix, and D. Blondel.** 2007. The Nucleocytoplasmic Rabies Virus P Protein Counteracts Interferon Signaling by Inhibiting both Nuclear Accumulation and DNA Binding of STAT1. *J Virol* **81**:4255-63.
306. **Vives, R. R., A. Imberty, Q. J. Sattentau, and H. Lortat-Jacob.** 2005. Heparan sulfate targets the HIV-1 envelope glycoprotein gp120 coreceptor binding site. *J Biol Chem* **280**:21353-7.
307. **von Giesen, H. J., O. Adams, H. Koller, and G. Arendt.** 2005. Cerebrospinal fluid HIV viral load in different phases of HIV-associated brain disease. *J Neurol* **252**:801-7.
308. **von Herrath, M., M. B. Oldstone, and H. S. Fox.** 1995. Simian immunodeficiency virus (SIV)-specific CTL in cerebrospinal fluid and brains of SIV-infected rhesus macaques. *J Immunol* **154**:5582-9.
309. **Wang, J., K. Crawford, M. Yuan, H. Wang, P. R. Gorry, and D. Gabuzda.** 2002. Regulation of CC chemokine receptor 5 and CD4 expression and human immunodeficiency virus type 1 replication in human macrophages and microglia by T helper type 2 cytokines. *J Infect Dis* **185**:885-97.

310. **Watkins, B. A., H. H. Dorn, W. B. Kelly, R. C. Armstrong, B. J. Potts, F. Michaels, C. V. Kufta, and M. Dubois-Dalcq.** 1990. Specific tropism of HIV-1 for microglial cells in primary human brain cultures. *Science* **249**:549-53.
311. **Wei, X., S. K. Ghosh, M. E. Taylor, V. A. Johnson, E. A. Emini, P. Deutsch, J. D. Lifson, S. Bonhoeffer, M. A. Nowak, B. H. Hahn, and et al.** 1995. Viral dynamics in human immunodeficiency virus type 1 infection. *Nature* **373**:117-22.
312. **Weiss, J. M., S. A. Downie, W. D. Lyman, and J. W. Berman.** 1998. Astrocyte-derived monocyte-chemoattractant protein-1 directs the transmigration of leukocytes across a model of the human blood-brain barrier. *J Immunol* **161**:6896-903.
313. **Westby, M., M. Lewis, J. Whitcomb, M. Youle, A. L. Pozniak, I. T. James, T. M. Jenkins, M. Perros, and E. van der Ryst.** 2006. Emergence of CXCR4-using human immunodeficiency virus type 1 (HIV-1) variants in a minority of HIV-1-infected patients following treatment with the CCR5 antagonist maraviroc is from a pretreatment CXCR4-using virus reservoir. *J Virol* **80**:4909-20.
314. **Wiley, C. A., E. Masliah, M. Morey, C. Lemere, R. DeTeresa, M. Grafe, L. Hansen, and R. Terry.** 1991. Neocortical damage during HIV infection. *Ann Neurol* **29**:651-7.
315. **Wiley, C. A., R. D. Schrier, J. A. Nelson, P. W. Lampert, and M. B. Oldstone.** 1986. Cellular localization of human immunodeficiency virus infection within the brains of acquired immune deficiency syndrome patients. *Proc Natl Acad Sci U S A* **83**:7089-93.
316. **Willey, R. L., J. S. Bonifacino, B. J. Potts, M. A. Martin, and R. D. Klausner.** 1988. Biosynthesis, cleavage, and degradation of the human immunodeficiency virus 1 envelope glycoprotein gp160. *Proc Natl Acad Sci U S A* **85**:9580-4.
317. **Williams, K. C., S. Corey, S. V. Westmoreland, D. Pauley, H. Knight, C. deBakker, X. Alvarez, and A. A. Lackner.** 2001. Perivascular macrophages are the primary cell type productively infected by simian immunodeficiency virus in the brains of macaques: implications for the neuropathogenesis of AIDS. *J Exp Med* **193**:905-15.
318. **Wilson, J. R., P. F. de Sessions, M. A. Leon, and F. Scholle.** 2008. West Nile virus nonstructural protein 1 inhibits TLR3 signal transduction. *J Virol* **82**:8262-71.
319. **Wilt, S. G., E. Milward, J. M. Zhou, K. Nagasato, H. Patton, R. Rusten, D. E. Griffin, M. O'Connor, and M. Dubois-Dalcq.** 1995. In vitro evidence for a dual role of tumor necrosis factor-alpha in human immunodeficiency virus type 1 encephalopathy. *Ann Neurol* **37**:381-94.
320. **Xin, K. Q., K. Hamajima, S. Hattori, X. R. Cao, S. Kawamoto, and K. Okuda.** 1999. Evidence of HIV type 1 glycoprotein 120 binding to recombinant N-methyl-D-

- aspartate receptor subunits expressed in a baculovirus system. *AIDS Res Hum Retroviruses* **15**:1461-7.
321. **Xu, Y., J. Kulkosky, E. Acheampong, G. Nunnari, J. Sullivan, and R. J. Pomerantz.** 2004. HIV-1-mediated apoptosis of neuronal cells: Proximal molecular mechanisms of HIV-1-induced encephalopathy. *Proc Natl Acad Sci U S A* **101**:7070-5.
  322. **Yadav, A., and R. G. Collman.** 2009. CNS Inflammation and Macrophage/Microglial Biology Associated with HIV-1 Infection. *J Neuroimmune Pharmacol*.
  323. **Ylinen, L. M., Z. Keckesova, S. J. Wilson, S. Ranasinghe, and G. J. Towers.** 2005. Differential restriction of human immunodeficiency virus type 2 and simian immunodeficiency virus SIVmac by TRIM5alpha alleles. *J Virol* **79**:11580-7.
  324. **Zetola, N. M., and C. D. Pilcher.** 2007. Diagnosis and management of acute HIV infection. *Infect Dis Clin North Am* **21**:19-48, vii.
  325. **Zhao, J., and S. Perlman.** 2009. De novo recruitment of antigen-experienced and naive T cells contributes to the long-term maintenance of antiviral T cell populations in the persistently infected central nervous system. *J Immunol* **183**:5163-70.